SOURCES AND PATHWAYS FOR MERCURY TO MICHIGAN'S INLAND LAKES

By

Matthew James Parsons

A DISSERTATION

Submitted to
Michigan State University
in partial fulfillment of the requirements
for the degree of

DOCTOR OF PHILSOPHY

Geological Sciences

2011

ABSTRACT

SOURCES AND PATHWAYS FOR MERCURY TO MICHIGAN'S INLAND LAKES

By

Matthew James Parsons

Mercury has a unique geochemical cycle due to its ability to exist as a gas at Earth surface conditions. As a result Hg can be transported across a region (e.g., the Midwest) or across the globe. The importance of local watershed scale versus regional/global sources is still debated. The over-arching hypothesis driving this research is that local scale sources and watershed scale processes have more impacts on the rate of Hg accumulation in the aquatic environment than regional to global scale sources. To evaluate this hypothesis, ^{210}Pb dated mercury sediment chronologies were compared among inland lakes within the State of Michigan and investigated using the following approaches: 1) examine the spatial and temporal trends of Hg loading to the environment to discriminate regional and local scale processes, 2) use modern rates of recovery to identify those watershed attributes that influence the transport of Hg through the watershed and 3) use diagnostic ratios of polycyclic aromatic hydrocarbons (PAHs) to infer sources of Hg contamination.

Results of temporal and spatial analysis show that 1) mercury accumulation rates for many lakes are still increasing; 2) focusing corrected anthropogenic Hg inventories are similar to those determined from Great Lakes sediments suggesting a regional source and 3) anthropogenic accumulation rate profiles are similar by sub-region and share episodic accumulation events indicative of local scale sources.

Contemporary recovery rates were calculated for mercury based on concentration and accumulation rate profiles. These recovery rates were then compared to watershed attributes. Agricultural, forested and wetland attributes were all found to be significantly correlated. However, those cover types found along highly dynamic watershed flowpaths were found to be most significant.

Mercury and PAHs can share common sources and pathways resulting in similar environmental fates. Diagnostic ratios of PAHs are often used to differentiate source of these contaminants to the environment and may be useful to identify sources for Hg. Ratios of PAHs indicate that a variety of sources exist including biomass (e.g., grass or coal) and petroleum (e.g., vehicle or natural gas) combustion. Sources are unique on regional to sub-regional scales with biomass combustion a dominant source for lakes in the southeastern portion of the Lower Peninsula.

Deer Lake, an US EPA Area of Concern, in Michigan's Upper Peninsula was contaminated with Hg as a result of a mining related laboratory activities. Sediment cores collected from the lake revealed that the natural recovery remediation strategy employed was resulting in deposition of "clean" sediments and Hg concentrations should reflect those of nearby lakes in ca. 10y. Most recently a terrestrial pathway for Hg was identified using Al:Hg ratios which could hamper the process of delisting Deer Lake as an Area of Concern.

The results of this research support the hypothesis that local scale processes are more significant than regional to global sources for Hg to Michigan's lakes. This has important implications for the development of new environmental legislation limiting Hg output from coal-fired power plants and other energy generating facilities.

DEDICATION

This dissertation is dedicated to my wife Lindsey, son William and daughter Avery…the loves of my life

ACKNOWLEDGEMENTS

I would like to thank my advisor, David Long and my committee members Lina Patino, Tom Voice and Mantha Phanikumar for their advice and guidance. I would especially like to thank Sharon Yohn for preparing me for the toils of the grant and Ryan Vannier for taking over. The office staff of the Department of Geological whom without I'd still be figuring out where to park. Thanks to the Michigan Department of Environmental Quality who supported and funded this project with special thanks to Glen Schmidt our noble captain.

Finally, thanks to my family and friends who never doubted that I would finish…someday.

TABLE OF CONTENTS

LIST OF TABLES

LIST OF FIGURES

CHAPTER 1

INTRODUCTION

Mercury contamination and its subsequent methylation and bioaccumulation in aquatic food-webs has resulted in elevated levels of mercury in fish and resulted in statewide fish consumption advisories for the Great Lakes region, including inland lakes throughout the state of Michigan (Keeler *et al.*, 1994, Watras *et al.*, 1994). Fish consumption has been shown to be a primary pathway of mercury, and its more toxic form methylmercury, exposure to humans (Hightower and Moore, 2003). Toxicity issues related to methylmercury contaminated fish consumption was highlighted in the 1950's and 1960's with deaths in Minamata Bay and Niigata, Japan (Tsubaki and Irukayama, 1977). Although reported emissions of mercury have declined in the past decade (Engstrom and Swain, 1997, USEPA, 2008), the amount of river miles and lake acreage under fish consumption advisories have continued to increase (US EPA, 2004). The cause of which is two-fold:1) due to its geochemical cycle mercury can be transported long distances creating a contaminated water body in an otherwise pristine setting (Tseng *et al.*, 2004), and 2) waterbodies that were previously untested are being confirmed to contain fish that have Hg levels above regulatory limits (US EPA, 2004).

Mercury is ubiquitous in the environment, and is characterized by an atmospheric residence time of one year (Fitzgerald, 1989). As a result, Arctic region lakes (Hermanson, 1998) and Antarctic ice cores (Vandal *et al.*, 1993) are contaminated with mercury though they are far from anthropogenic sources. Anthropogenic sources of mercury to the environment include coal fired utilities, smelting activities, medical and municipal waste incineration, agricultural and paint fungicides, gold and silver mining activities, chlor-alkali facilities, and municipal waste streams (Jasinski, 1994). Many industrial applications for mercury have been

disallowed (e.g., agricultural fungicides) in the United States and substitutes are encouraged to be used (e.g., alcohol in thermometers) consequently consumption has decreased over the last three decades (Brooks, 2003); but mercury manometers, electronic switches and lamps, batteries, and dental amalgams continue to add to U.S. consumption. Even with consumption declines realized, all environmental records do not reflect a concomitant decline in mercury accumulation (Engstrom and Swain, 1997, Engstrom *et al.*, 1994, Lorey and Driscoll, 1999, Swain *et al.*, 1992b).

It is known that atmospheric deposition is the principle pathway for mercury contamination of inland lakes (Fitzgerald, 1989, Fitzgerald *et al.*, 1998, Mason *et al.*, 1994a, Watras *et al.*, 2000). However, the impact of global (e.g., China) versus regional (e.g., Midwest power plants) versus more local scale processes (e.g., increased runoff from agricultural fields) is still debated (Evers *et al.*, 2011). Determining the source for Hg to inland lakes has important implications for future environmental legislation (US EPA, 2011)which would seek to cap Hg emissions from power generating facilities in an attempt to further reduce Hg exposure. The environmental legacy of historic Hg emissions also plays an important role in any future legislative action since it is that Hg that now resides in soils that will continue to pose an exposure threat even when Hg emissions from all anthropogenic sources are reduced to zero (Mason *et al.*, 1994b). It will be important then to more fully understand the processes that result in Hg transport at the watershed scale.

A variety of approaches have been used to determine current and historical rates of contaminant loading to the environment including: atmospheric deposition studies, ombotrophic bogs, and lake sediment cores. Atmospheric deposition pathways have been studied to determine rates of mercury deposition (Glass and Sorensen, 1999, Landis and Keeler, 2002,

Landis *et al.*, 2002). Several Midwest states have been included in the National Atmospheric Deposition Program (NADP) providing a continuously updated data set for calibration of atmospheric cycling and deposition models (Illinois State Water Survey, 2008). The International Association of Deposition Networks (IADN) (Hillery *et al.*, 1998) has been collecting similar data for the last decade throughout the Great Lakes Region. Ombotrophic bogs throughout the world have also been used to determine current and historical rates of contaminant deposition (Benoit *et al.*, 1998, Bindler, 2003).

Lake sediment cores have been used to measure contaminant-loadings of atmospheric and terrestrial inputs (Callender and Rice, 2000, Engstrom and Swain, 1997, Swain *et al.*, 1992b, Yohn *et al.*, 2002b). Studies of lake sediment cores from the Midwest and Adirondacks have shown decreasing mercury accumulation rates attributed to a reduction in atmospheric deposition (Engstrom and Swain, 1997, Lorey and Driscoll, 1999, Swain *et al.*, 1992a). The Great Lakes region has been of particular interest in contaminant studies due to several industrialized areas within the basin and the revenue dollars it provides to Great Lakes states through recreation, tourism, and sport fishing. Sediment cores collected from Lake Superior had maximum concentrations of mercury in the surficial sediments for the majority of the samples collected (Rossmann, 1999). Approximately 70% of the mercury inventory was attributed to anthropogenic activity (Rossmann, 1999). Surficial sediment concentrations from Lake Michigan show a decline from historical data sets and estimate contributions from local sources to be approximately 50% of total mercury loadings (Rossmann, 2002).

Most regulatory actions have been intended to reduce loadings of mercury from atmospheric sources, such as the burning of fossil fuels and waste incineration facilities that create a regional signal which would be expected to consist of a uniform deposition or

accumulation rate across a broad spatial scale (Engstrom and Swain, 1997). However, local sources and processes acting on the watershed scale will not display uniform loading over large spatial scales. These sources and processes may become more important over time, as emissions from industrial activities are reduced, and therefore it is becoming increasingly important to understand local scale influences on mercury loadings to aquatic ecosystems.

Investigation of sediment cores of inland lakes can aid in determining regional and local signals of contaminant loadings. Previous work investigated the anthropogenic accumulation of lead and cadmium using multivariate statistics and metal ratios to determine current and legacy land use effects on anthropogenic accumulation rates of metals to inland lakes (Yohn *et al.*, 2003). Results showed that regional and local signals can be determined from temporal and spatial trends of anthropogenic metals. And the efficacy of environmental legislation, such as the Clean Air Act, on reducing regional signals of anthropogenic accumulation of lead can be tested (Yohn, 2003). For example, it has been demonstrated that the anthropogenic accumulation of lead and copper have not declined to background levels, as one would expect if a regional source was eliminated (Yohn *et al.*, 2002a). Therefore a different, possibly local, source may be contributing to the continued accumulation of anthropogenic chemicals.

Various sources can contribute to sediment deposition within lakes including terrestrial, atmospheric, and in-lake processes which mix with anthropogenic inputs (Yohn *et al.*, 2001) creating difficulty in elucidating source for a metal of interest. Heyvaert (2000) used titanium ratios to normalize mercury concentrations to correct for terrestrial inputs, a watershed correction factor. However, it may be more appropriate to look at background correction for mercury due its geochemical cycle (Strunk, 1991). Using background correction assumes that the majority of anthropogenic mercury deposited to the landscape occurs during atmospheric deposition and is

retained by soils and does not readily mobilize after deposition except during processes such as fire, clear cutting, urbanization, landscape disturbance (i.e., agricultural practices), and flooding.

Hypothesis and Approach

This study attempts to elucidate sources and pathways for Hg to inland lakes, and importance of local and regional scale sources. The over-arching hypothesis is that: local and watershed scale processes have more impact on the rate of Hg accumulation in the aquatic environment than regional to global scale sources.

Three approaches will be used to test this hypothesis, and they are:

1. examine the temporal changes of Hg accumulation over spatial scales. Local scale sources and watershed scale processes would be reflected in the sediment record as discontinuities in anthropogenic accumulation rates at multiple time periods and spatial scales and inventories across spatial scales,
2. use modern recovery rates of recovery to identify those watershed attributes that influence the movement of Hg through the watershed. Differences in processes amongst watersheds (e.g., agriculture v. forest) impact the rates of modern recovery from mercury contamination, and
3. use diagnostic ratios of polycyclic aromatic hydrocarbons (PAHs) as tracers of Hg contamination. Sources of PAHs can be differentiated using diagnostic ratios and Hg and PAHs share common sources and pathways thus PAH ratios can be used to infer sources of Hg.

Sediment was collected from inland lakes throughout the State of Michigan, dated with ^{210}Pb and analyzed for metals and organic contaminants to investigate this hypothesis. Results of analysis from individual lakes can be found in several year-end reports (Parsons *et al.*, 2004, Parsons *et al.*, 2006, Yohn *et al.*, 2001, Yohn *et al.*, 2002c, Yohn *et al.*, 2003) prepared for the Michigan Department of Environmental Quality as part of the Trends Monitoring Program: Sediments (Michigan, 2011). This dissertation is composed of five chapters beyond the introduction. Chapter 2 explores the use of anthropogenic accumulation rates and inventories examined at temporal and spatial scales, respectively, focusing on the identification of source regions. Chapter 3 investigates the use of geographic information system derived watershed attributes on the rate of recovery of inland lakes from Hg contamination. The fourth chapter uses diagnostic ratios of PAHs to infer sources of Hg; while the fifth, investigates the historic and modern sources of Hg to Deer Lake near Ishpeming, MI, a U.S. EPA Area of Concern (USEPA, 2007)using Hg:metal ratios and changes in metal profiles that are consistent with the known history of the lake. The final chapter offers a summary and suggestions for future work.

REFERENCES

REFERENCES

Benoit, J.M., Fitzgerald, W.F., Damman, A.W.H., 1998. The biogeochemistry of an ombrotrophic bog: Evaluation of use as an archive of atmospheric mercury deposition. Environmental Research 78, 118-133.

Bindler, R., 2003. Estimating the natural background atmospheric deposition rate of mercury utilizing ombrotrophic bogs in southern Sweden. Environmental Science and Technology 37, 40-46.

Brooks, W.E. United States Geological Survey. *Minerals Yearbook - Mercury*; Reston, VA: Government Printing Office, 2003.

Callender, E., Rice, K.C., 2000. The urban environmental gradient: Anthropogenic influences on the spatial and temporal distributions of lead and zinc in the environment. Environmental Science and Technology 24, 232-238.

Engstrom, D.R., Swain, E.B., 1997. Recent declines in atmospheric mercury deposition in the upper Midwest. Environmental Science and Technology 31, 960-967.

Engstrom, D.R., Swain, E.B., Henning, T.A., Brigham, M.E., Brezonik, P.L., 1994. Atmospheric Mercury Deposition to Lakes and Watersheds - a Quantitative Reconstruction from Multiple Sediment Cores. Environmental Chemistry of Lakes and Reservoirs 237, 33-66.

Evers, D.C., Wiener, J.G., Driscoll, C.T., Gay, D.A., Basu, N., Monson, B.A., Lambert, K.F., Morrison, H.A., Morgan, J.T., Williams, K.A., Soehl, A.G., 2011. Great Lakes Mercury Connections: The Extent and Effects of Mercury Pollution in the Great Lakes Region. Biodiversity Research Institute. Gorham, MA. Report BRI 2011-18, 44 pages. Available from: http://www.briloon.org/mercuryconnections/GreatLakes.

Fitzgerald, W.F., 1989. Atmospheric and oceanic cycling of mercury. Academic Press.

Fitzgerald, W.F., Engstrom, D.R., Mason, R.P., Nater, E.A., 1998. The case for atmospheric mercury contamination in remote areas. Environmental Science and Technology 32, 1-7.

Glass, G.E., Sorensen, J.A., 1999. Six-year trend (1990-1995) of wet mercury deposition in the Upper Midwest. USA. Environmental Science & Technology 33, 3303-3312.

Hermanson, M.H., 1998. Anthropogenic mercury deposition to arctic lake sediments. Water, Air, and Soil Pollution 101, 309-321.

Hightower, J., Moore, D., 2003. Mercury Levels in High-End Consumers of Fish. Environmental Health Perspectives 111, 604-608.

Hillery, B.R., Simcik, M.F., Basu, I., Hoff, R.M., Strachan, W.M.J., Burniston, D., Chan, C.H., Brice, K.A., Sweet, C.W., Hites, R.A., 1998. Atmospheric deposition of toxic pollutants

to the Great Lakes as measured by the integrated atmospheric deposition network. Environmental Science & Technology 32, 2216-2221.

National Atmospheric Deposition Program (NRSP-3), Illinois State Water Survey, NADP Program Office, 2204 Griffith Drive, Champaign, IL 61820, Available online at http://nadp.sws.uiuc.edu/mdn/. (Accessed: February 5, 1998).

Jasinski, S.M. *The Materials Flow of Mercury in the United States*; Government Printing Office, 1994.

Keeler, G.J., Hoyer, M.E., Lamborg, C.H., 1994. Mercury Pollution: Integration and Synthesis. In: Measurements of Atmospheric Mercury in the Great Lakes Basin.

Landis, M.S., Keeler, G.J., 2002. Atmospheric mercury deposition to Lake Michigan during the Lake Michigan Mass Balance Study. Environmental Science and Technology 36, 4518-4524.

Landis, M.S., Vette, A.F., Keeler, G.J., 2002. Atmospheric mercury in the Lake Michigan basin: Influence of the Chicago/Gary urban area. Environmental Science and Technology 36, 4508-4517.

Lorey, P., Driscoll, C.T., 1999. Historical trends in mercury deposition in Adirondack Lakes. Environmental Science and Technology 33, 718-722.

Mason, R.P., Fitzgerald, W.F., Morel, F.M., 1994a. The biogeochemical cycling of elemental mercury: anthropogenic influences. Geochimica at Cosmochimica Acta 58, 3191-3198.

Mason, R.P., Fitzgerald, W.F., Morel, F.M.M., 1994b. The Biogeochemical Cycling of Elemental Mercury - Anthropogenic Influences. Geochimica et Cosmochimica Acta 58, 3191-3198.

State of Michigan, 2011. Sediment Chemistry, Available online at http://www.michigan.gov/deq/0,4561,7-135-3313_3686_3728-32365--,00.html. (Accessed: September 5, 2011).

Parsons, M.J., Yohn, S.S., Long, D.T., Giesy, J.P., Bradley, P.W., 2004. Inland Lakes Sediment Trends: Sediment Analysis Results for Five Michigan Lakes. Lansing, MI. pages. Available from:

Parsons, M.J., Yohn, S.S., Long, D.T., Patino, L.C., Stone, K.A., 2006. Inland Lakes Sediment Trends: Mercury Sediment Analysis Results for 27 Michigan Lakes. Lansing, MI. 47 pages. Available from:

Rossmann, R., 1999. Horizontal and vertical distributions of mercury in 1983 Lake Superior sediments with estimates of storage and mass flux. Journal of Great Lakes Research 25, 683-696.

Rossmann, R., 2002. Lake Michigan 1994-1996 surficial sediment mercury. Journal of Great Lakes Research 28, 65-76.

Strunk, J.L. 1991. The extraction of mercury from sediment and the geochemical partitioning of mercury in sediments from Lake Superior. Thesis, Michigan State University. Dept. of Geology, 1991.,

Swain, E.B., Engstrom, D.R., Brigham, M.E., Henning, T.A., Brezonik, P.L., 1992a. Increasing Rates of Atmospheric Mercury Deposition in Midcontinental North-America. Science 257, 784-787.

Swain, E.B., Engstrom, D.R., Brigham, M.E., Henning, T.A., Brezonik, P.L., 1992b. increasing rates of atmospheric mercury deposition in Midcontinental North America. Science 257, 784-787.

Tseng, C.M., Lamborg, C., Fitzgerald, W.F., Engstrom, D.R., 2004. Cycling of dissolved elemental mercury in Arctic Alaskan lakes. Geochimica et Cosmochimica Acta 68, 1173-1184.

Tsubaki, T., Irukayama, K., 1977. Minamata Disease: Methylmercuy Poisoning in Minamata and Niigata, Japan. Elsevier.

U.S. EPA, 2004. National Listing of Fish Advisories, Available online at http://www.epa.gov/waterscience/fish/. (Accessed: September 25, 2011).

US EPA, 2011. Proposed Rule: National Emission Standards for Hazardous Air Pollutants From Coal- and Oil-Fired Electric Utility Steam Generating Units and Standards of Performance for Fossil-Fuel-Fired Electric Utility, Industrial-Commercial-Institutional, and Small Industrial-Commercial-Institutional Steam Generating Units. US EPA.Government Printing Office, Washington, D.C. 40 CFR Parts 60 and 63.

Deer Lake River Area of Concern, Available online at http://www.epa.gov/glnpo/aoc/drlake.html. (Accessed: January 30, 2008).

Toxic Release Inventory (TRI) Program, Available online at http://www.epa.gov/tri. (Accessed: January 30, 2008).

Vandal, G.M., Fitzgerald, W.F., Boutron, C.F., Candelone, J.P., 1993. Variations in Mercury Deposition to Antarctica over the Past 34,000 Years. Nature 362, 621-623.

Watras, C.J., Bloom, N.S., Hudson, J.M., Gherini, S., Munson, R., Claas, S.A., Marrison, K.A., Hurely, J., Wiener, J.G., Fitzgerald, W.F., Mason, R., Vandal, G., Powell, D., Rada, R., Rislov, L., Winfrey, M., Elder, J., Krabbenhoft, D., Andren, A.W., Babiarz, C., Porcella, D.B., Huckabee, J.W., 1994. Sources and fates of mercury and methylmercury in Wisconsin lakes. In: C.J. Watras, J.W. Huckabee (Eds.), Mercury Pollution: Intergration and Synthesis. CRC Press, Ann Arbor, pp. 153-179.

Watras, C.J., Morrison, K.A., Hudson, R.J., Frost, T.M., Kratz, T.K., 2000. Decreasing mercury in northern Wisconsin: temporal trends in bulk precipitation and a precipitation-dominated lake. Environmental Science and Technology 34, 4051-4057.

Yohn, S.S., 2003. Regional versus local influences on lead and cadmium loading in the Great Lakes region. Applied Geochemistry In press.

Yohn, S.S., Long, D.T., Fett, J.D., Patino, L., Giesy, J.P., Kannan, K., 2002a. Assessing environmental change through chemical-sediment chronologies from inland lakes. Lakes Reserv Res Manage 7, 217-230.

Yohn, S.S., Long, D.T., Fett, J.D., Patino, L.C., Giesy, J.P., Kannan, K., 2002b. Assessing environmental change through chemical-sediment chronologies from inland lakes. Lakes & Reservoirs: Research and Management 7, 217-230.

Yohn, S.S., Long, D.T., Giesy, J.P., Fett, J.D., Kannan, K., 2001. Inland lakes sediment trends: sediment analysis results for two Michigan Lakes. Lansing, MI. 49 pages. Available from:

Yohn, S.S., Long, D.T., Giesy, J.P., Scholle, L.K., Patino, L.C., Fett, J.D., Kannan, K., 2002c. Inland lakes sediment trends: sediment analysis results for five Michigan Lakes. East Lansing. 64 pages. Available from:

Yohn, S.S., Long, D.T., Giesy, J.P., Scholle, L.K., Patino, L.C., Parsons, M., Kannan, K., 2003. Inland Lakes Sediment Trends: sediment analysis results for six Michigan Lakes. East Lansing. 66 pages. Available from: http://www.deq.state.mi.us/documents/deq-wb-swas-sedimenttrend0203finalreport.pdf.

CHAPTER 2
SPATIAL AND TEMPORAL TRENDS OF MERCURY LOADINGS TO MICHIGAN INLAND LAKES

Abstract

Several studies of chronologies of mercury (Hg) in inland lake sediments have demonstrated that Hg accumulation had decreased in recent decades. However, episodic mercury accumulation events were recorded in some of these lakes, but not investigated in detail. Recent decreases had been attributed to the reduction of regional Hg consumption and secondary removal during process waste treatment. In addition to regional sources, local sources, including watershed disturbance, might significantly contribute to Hg loading. Here, mercury chronologies of Hg loadings based on dated sediment cores are presented for 26 inland, Michigan lakes. Although spatial trends of anthropogenic inventories suggest a regional pattern dominated by human activities, sub-regional to local scale sources are also found to be significant. Temporal trends show episodic Hg accumulation events superimposed on a more general, long-term trend. Episodic increases common to lakes suggest a common source or processes common to lakes. Episodic increases unique to a lake indicate a more local scale source. Similar Hg profiles from lakes that are geographically proximal provide evidence for sub-regional to regional scale sources. Local sources and pathways for mercury to inland lakes need to be more fully understood to effectively reduce Hg loading to the environment.

Introduction

Mercury (Hg) concentrations greater than historical levels, as recorded in sediment cores, have been observed in the high northern latitudes (Bindler *et al.*, 2001, Gobeil *et al.*, 1999, Hermanson, 1998), New England (Kamman and Engstrom, 2002,

Lorey and Driscoll, 1999), the Midwestern United States (Engstrom and Swain, 1997, Swain *et al.*, 1992), Western United States (Gray *et al.*, 2005, Menounou and Presley, 2003), and Europe (Wihlborg and Danielsson, 2006, Yang and Rose, 2003). Although regulatory controls have attempted to limit mercury emissions (1997), the number of river miles and fresh water lakes in which Hg concentrations exceed regulatory guidelines continue to increase. The reasons for this increase have been attributed to monitoring efforts extending to water bodies that were previously untested (2004), or increased releases from human activities and subsequent deposition in remote areas (Fitzgerald *et al.*, 1998). Consumption of contaminated fish has been shown to be a principle exposure route of methylmercury to humans (Hightower and Moore, 2003, 1997). As a result of elevated health risks, several Midwestern states have advised consumers to reduce consumption of fish from all of the Great Lakes and all Michigan inland lakes due to potential Hg exposure (2004).

Freshwater sediments retain mercury transported to the lake system (Engstrom *et al.*, 1994) and when coupled with dating techniques, sediments can record the history of mercury loadings over time. Dated sediment cores have been used to investigate the historic accumulation of Hg in sediments of the North American Great Lakes (Long *et al.*, 1995) and inland lakes (Engstrom and Swain, 1997, Kamman and Engstrom, 2002, Lorey and Driscoll, 1999, Swain *et al.*, 1992). While analysis of Great Lakes sediment provides significant information about deposition of Hg on larger spatial scales, it is difficult to determine local watershed scale contribution to Hg loadings. Investigating inland lakes across a region allows examination of both regional- and, local, including

watershed scale, contribution to Hg accumulation. Earlier determinations of sediment chronologies have demonstrated that Hg loadings in some areas of the United States (USA) such as the Western United States (Gray *et al.*, 2005, Menounou and Presley, 2003), Midwestern United States (Engstrom and Swain, 1997, Swain *et al.*, 1992), New England (Kamman and Engstrom, 2002, Perry *et al.*, 2005), the Adirondack region of New York (Lorey and Driscoll, 1999), and Europe (Wihlborg and Danielsson, 2006, Yang and Rose, 2003) have decreased in recent years. However, several of the lakes included in previous studies had recent increases in Hg accumulation.

The results reported in this paper are part of a larger study, "Inland Lakes Trends Monitoring Program: Sediments," to determine trends of organic and inorganic contaminant accumulation in Michigan's inland lakes (2006). Here the chronologies of Hg loading into lakes were determined from 26 ^{210}Pb-dated, confirmed by ^{137}Cs and stable Pb, sediment cores from inland lakes throughout Michigan. Anthropogenic inventories of Hg loadings to lakes were investigated at several spatial scales, and Hg accumulation rates, examined temporally to test the hypothesis that local-scale sources of Hg significantly contribute to Hg accumulation in inland lakes. Understanding local scale sources for Hg will become increasingly important in assessing the efficacy of control measures for regional sources.

Methods

During the summers of 1999 through 2004, 26 lake sediment cores were collected aboard the U.S. Environmental Protection Agency (EPA) R/V *Mudpuppy* or Michigan

Department of Environmental Quality (MDEQ) M/V *Nibi* (Figure 2.1). Lakes were selected to cover all regions of the state and varied in their watershed (area) and hydrological characteristics, such as whether they were headwater or seepage lakes. An MC-400 Lake/Shelf multi-corer was used to extract four simultaneous cores for ^{210}Pb-dating and analysis of Hg and other metals. The core was sectioned on shore shortly after retrieval at 0.5-1.0 cm intervals for the first 5-8 cm and 1 cm intervals for the remainder of the core; core lengths varied from 50-60 cm. Sectioning of the

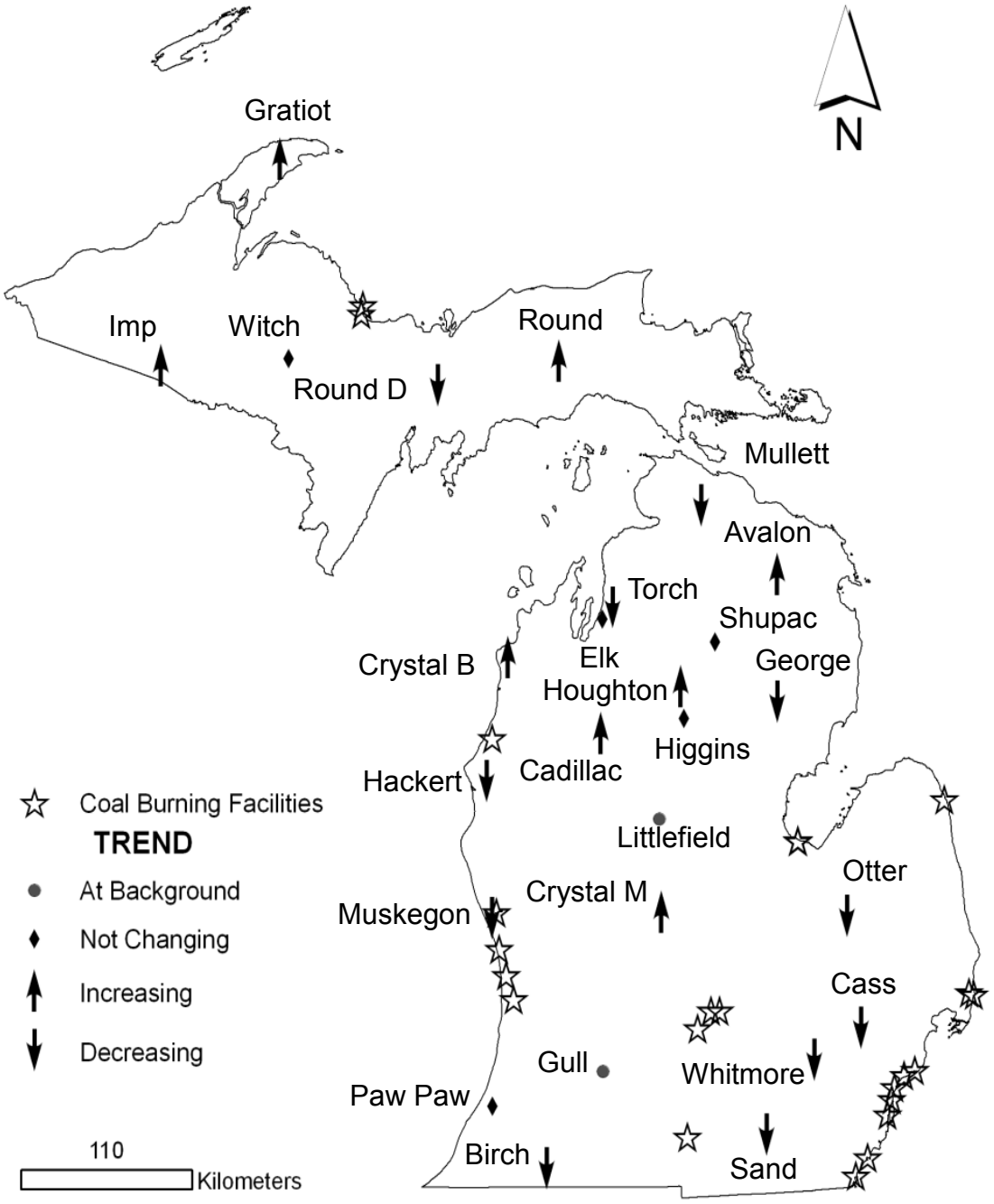

Figure 2.1. Inland lake trends monitoring program: sediments study lakes, trends of Hg loading over the last decade, and coal burning power plants. An up-arrow indicates accumulation rates had increased toward the surface, a down-arrow indicates accumulation rates had decreased. Solid triangles mean that accumulation rates were elevated but are not increasing or decreasing. Solid circles indicate that accumulation rates had returned to pre-industrial rates. Open stars represent coal burning power plants greater than 25 MW generating capacity as of 2005.

cores used for determining Hg concentrations and ^{210}Pb was conducted at the same stratigraphic resolution. More detailed descriptions of the sectioning protocols and results of ^{210}Pb are presented elsewhere (Yohn *et al.*, 2002a, Yohn *et al.*, 2001, Yohn *et al.*, 2002b, Yohn *et al.*, 2003). Specific dating related information and methodology can be found in Appendix B.

Sediment Focusing. Sediment focusing is the movement of fine grained materials from erosional to depositional zones of a lake basin, and can be quantified by calculating a focusing factor, which is the ratio of observed to expected ^{210}Pb inventory. The observed ^{210}Pb inventory is the product of sediment dry mass and excess ^{210}Pb summed over all core sections. The expected inventory of ^{210}Pb for this study region is 0.574 Bq/cm^2 (Golden *et al.*, 1993). Accounting for sediment focusing allows comparison of inventories and accumulation rates among lakes (Golden *et al.*, 1993).

Calculations. Anthropogenic Hg concentration was calculated by subtracting the long-term geochemical background Hg concentration from the total concentration. The background concentration was defined as that average concentration from the deepest core section to the point where concentrations began to increase that could be associated with human activities, primarily after colonization of the area by Europeans. This point was determined graphically by determining where the concentration increased significantly. Anthropogenic inventories, the mass of chemical in a sediment core due to

human inputs, were calculated as the product of anthropogenic Hg concentration and sediment dry mass for each individual core section. Results for each core section were then summed over the entire core to determine the inventory. The anthropogenic accumulation rate was calculated as the product of the sedimentation rate and the anthropogenic Hg concentration. Inventories and accumulation rates were corrected for sediment focusing.

Sedimentation rates in lakes vary considerably, and when sedimentation rates are great, bottom sections of the sediment core will not contain background concentrations of Hg. Therefore, it was necessary to estimate the focusing-corrected background accumulation rate (FCBGAR). These estimates were based on results of a backward stepwise multivariate regression model taking into account physical variables and surficial soil properties of the watershed. This model assumes that soil properties have not significantly changed since the pre-industrial period and soil properties that control the mobility of Hg do not vary among watersheds. Physical variables entered into the model included: lake area, watershed area, and watershed:lake area ratio (WS:LA). Soil properties were determined via dasymetric mapping of STATSGO (USDA) soil characteristics using ArcInfo (ESRI, 1998) and included: cation-exchange capacity, %organic matter, %clay, carbonate as $CaCO_3$, kfact and kffact, which is a slope adjusted kfact value. Parameters for variables to enter the model included tolerance greater than 0.6 and probability to enter/leave less than 0.15. The final model (n=14, Adjusted r^2 = 0.66) is presented in equation 1; variables were significant at $p<0.05$ (one-tail t-statistic), tolerances were greater than 0.75, and residuals were randomly distributed.

$$FCBGAR = 5.016 + 0.225\,\%ORG + 0.015\,WA - 0.091\,LA, \quad (1)$$

where: *%ORG* is the percent organic matter in soil, *WA* is the watershed area and *LA* is the area of the lake. The average (± SD) modeled FCBGAR was 7.9 (3.7) μg Hg/m^2/yr, whereas the average of the observed FCBGAR was 6.0 (3.5) μg Hg/m^2/yr. The intercept, which would represent the FCBGAR in the hypothetical absence of the variables above, was reasonably close to the median FCBGAR of the observed values, 5.8 μg Hg/m^2/yr. Thus, the predicted FCBGAR values were used to approximate anthropogenic accumulation rates for lakes that did not reach geochemical background Hg concentrations. Background estimations were not used to calculate anthropogenic inventories due to the temporal variation of mercury accumulation; however, these estimates would not change the accumulation rate profile.

Previous models have used *WA* and *LA* to predict Hg accumulation and organic matter has been demonstrated to play a significant role in the cycling of mercury in the watershed (Lorey and Driscoll, 1999, Swain *et al.*, 1992) . Although the positive relationship between *WA* and FCBGAR was expected, the negative relationship between *LA* and FCBGAR was not anticipated. Removal of *LA* from the model consistently resulted in poorer estimates, lower adjusted r^2, of FCBGAR. Greater inputs of Hg would be expected for large lakes and thus background values would reflect this relationship. We suspect that the *LA* variable may in part explain differences in sedimentation rates

observed in the larger lakes. Observed background Hg concentrations and sedimentation rates, both of which would result in a low FCBGAR, were both least for larger lakes. Organic matter is important in the biogeochemical cycling of Hg in soils (Grigal, 2003, Meili, 1991). Greater concentrations of organic matter in soils effectively retain Hg and other metals. More effective retention in soils might lead to greater concentrations during runoff events resulting in the transport of Hg from the watershed (Scherbatskoy *et al.*, 1998).

Quantification of Mercury. Total Hg concentrations were determined in lyphophilized sediment by use of a Lumex Thermal Decomposition Atomic Absorption Spectrometer in accordance with EPA Method 7473 (USEPA, 1998). Calibration of the instrument and in-run validation were performed using standard reference material (SRM) 1515 Apple Leaves or SRM1633b Coal Fly Ash; detection limits were 0.69 ng Hg/g, dw and 0.58 ng Hg/g, dw, respectively. In-run SRM validation measurements were consistently within the range specified.

Results and Discussion

Anthropogenic Inventories. Anthropogenic inventories are an accounting of the long-term loading of a contaminant to a lake. Analysis of the spatial patterns of inventories among lakes can reveal patterns of source in a region. For the purposes of this discussion a region has been defined as the entire state of Michigan whereas sub-regions are smaller areas within the region, such as southeast Michigan. A regional pattern of deposition is indicated if inventories decrease along some gradient, such as

population density or industrial development. The source for the pattern of deposition may be common to all lakes, a common source, or similar watershed processes occurring at different rates, a source common to all lakes. For example, Pb inventories in these study lakes decrease from the South to the North, implying a regional source (Yohn *et al.*, 2004). Lead from the use of leaded gasoline is the most commonly accepted cause for this trend; greater lead inventories in the southern, more populated and industrialized portion of the state trend toward lesser inventories in the northern, less populated, portions of the state. A regional source may also be present if inventories are similar among lakes within a sub-region. Focusing-corrected copper inventories were found to be similar among depositional basins of Lake Michigan. (Kolak *et al.*, 1998). This suggests a regional source for copper entering Lake Michigan.

Recent measurements of atmospheric deposition of Hg for the Great Lakes region have demonstrated a South to the North gradient (Keeler and Dvonch, 2005). If this general South to North trend has been persistent over time then inventories plotted along this spatial gradient should follow a similar pattern, evidence of a regional source. Results of focusing-corrected anthropogenic Hg inventories for 18 Michigan lakes (Figure 2.2) were plotted along a South to North gradient to investigate the possibility of a regional source. Mercury inventories varied among lakes, ranging from 0.3 μg Hg/cm^2 in Round Lake to 1.6 μg Hg/cm^2 in Houghton Lake (Figure 2.2). Anthropogenic Hg inventories were found to vary slightly in Lakes Michigan (0.08 – 0.17 μg Hg/cm^2) and Superior (0.02 – 0.15 μg Hg/cm^2), with anthropogenic inventories decreasing from the South to the North (Long *et al.*, 1995). If the range of inventories determined in the

Great Lakes represents a regional estimate of Hg loading for this region (both the Upper and Lower Peninsulas of Michigan), then deviations from these patterns suggest the influence of sub-regional to local scale sources. Most anthropogenic inventories from inland lakes are consistent with a regional source; however, notable exceptions include, Higgins, Houghton and Gull lakes.

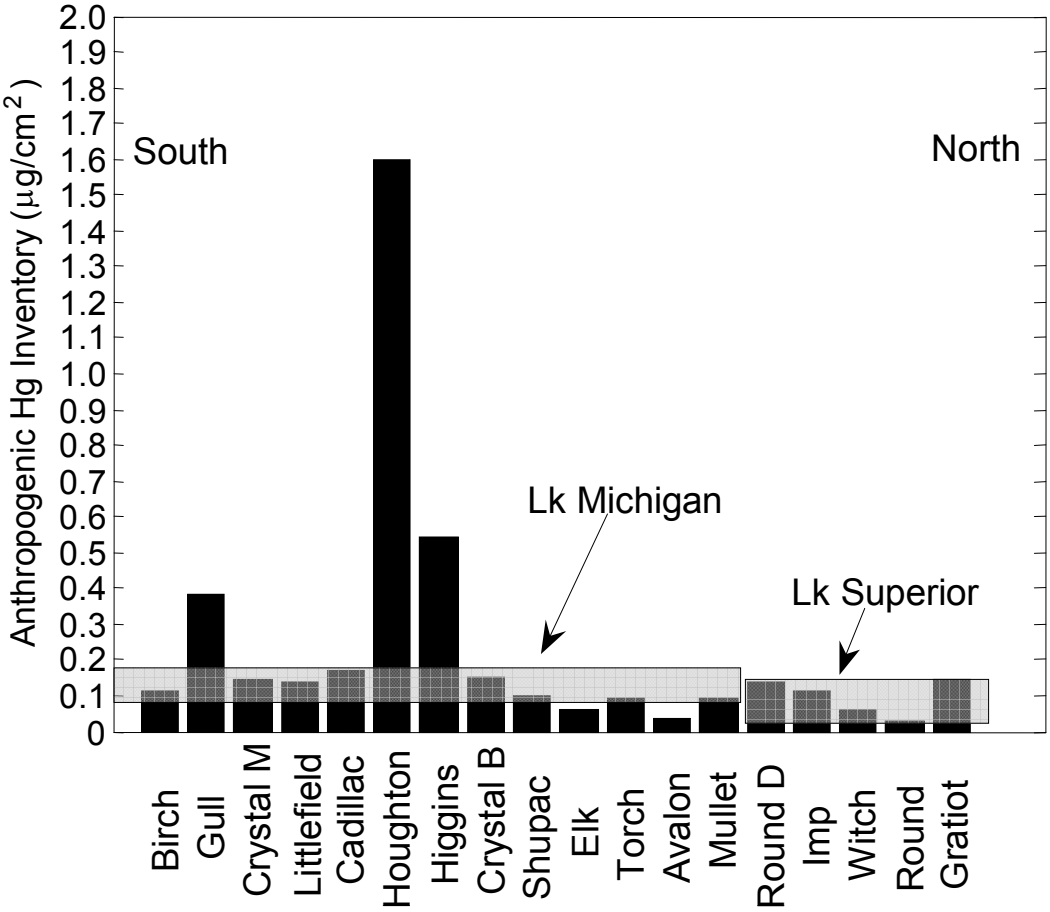

Figure 2.2. Focusing-corrected anthropogenic Hg inventories from 18 inland Michigan lakes. Inventories are plotted along a south to north gradient. The boxes represent the range of anthropogenic inventories for Lake Michigan and Lake Superior (Long *et al.*, 1995).

The relative importance of local sources can be determined by comparing the anthropogenic inventories of lakes from the same geographic region because these lakes would be expected to have similar loadings due to long range atmospheric loading so that differences could be attributed to more local sources. Lakes Higgins and Houghton, in the central Lower Peninsula, and Elk and Torch lakes, in the NW Lower Peninsula, are examples of geographically proximal lakes. Anthropogenic inventories differ among these pairs of lakes indicating that local, likely watershed-scale, sources were contributing to Hg loadings. Crystal M and Littlefield lakes lie within the central portion of the state and have similar anthropogenic inventories. Inventories for these lakes are within the range of those from Lake Michigan suggesting that Hg loading in this area is most likely due to regional sources of Hg. The differences among the Upper Peninsula lakes, Gratiot, Imp, Round D, and Round, imply that local sources contribute significantly to Hg loadings; however, these lakes are within the range of anthropogenic inventories found in Lake Superior. Portions of the Upper Peninsula are more mineralized than other areas of the state and have undergone intense mining, which may have lead to increased export of Hg from the watershed (Kerfoot *et al.*, 1999, Kerfoot *et al.*, 2004).

Temporal Trends. In general, anthropogenic accumulation began in the late 1800s and reached nominal peak values during the 1950s to 1980s depending on the lake (Figures 1.3-1.7). Episodic events have been superimposed on this general trend. These events may be unique to a lake or may be common among many lakes in a sub-region. Episodic increases common among lakes indicate that they resulted from increased accumulation and not post-depositional mobilization or spatial variability within the

sediments. Episodic increases that are common among lakes may be due to a common source or watershed processes that are common to all lakes. Profiles are grouped by sub-region to highlight accumulation rate patterns. Profiles for all of the other lakes that were studied can be found in Appendix B.

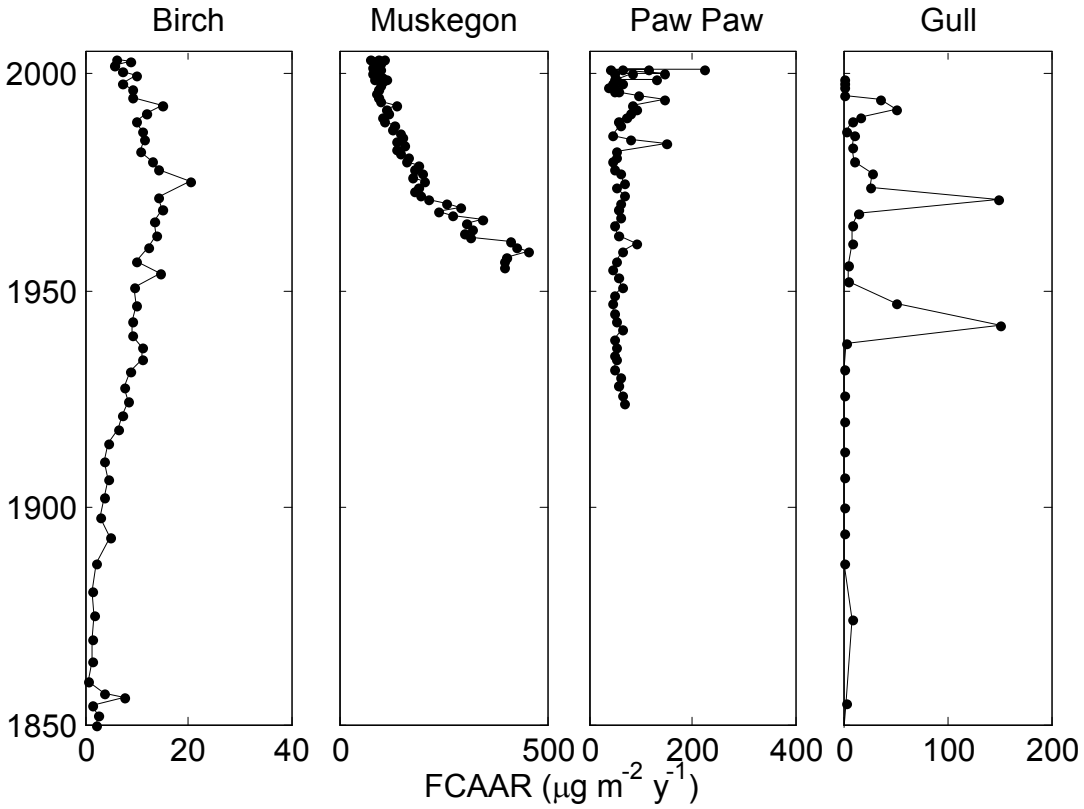

Figure 2.3. ^{210}Pb dated focusing-corrected anthropogenic accumulation rates for four southwestern Michigan lakes, dates older than 1850 were truncated to highlight more recent loading. Note the change in scale of the x-axis.

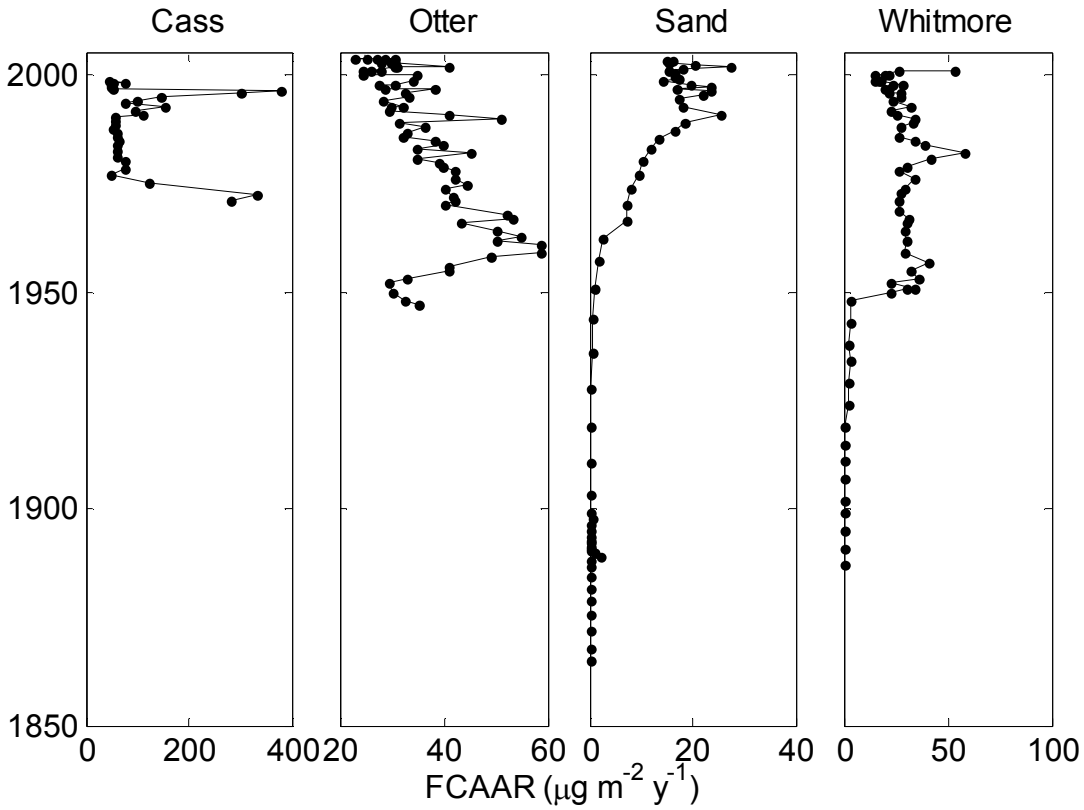

Figure 2.4. ^{210}Pb dated focusing-corrected anthropogenic accumulation rates for 4 southeastern Michigan lakes. Note the change in scale of the x-axis.

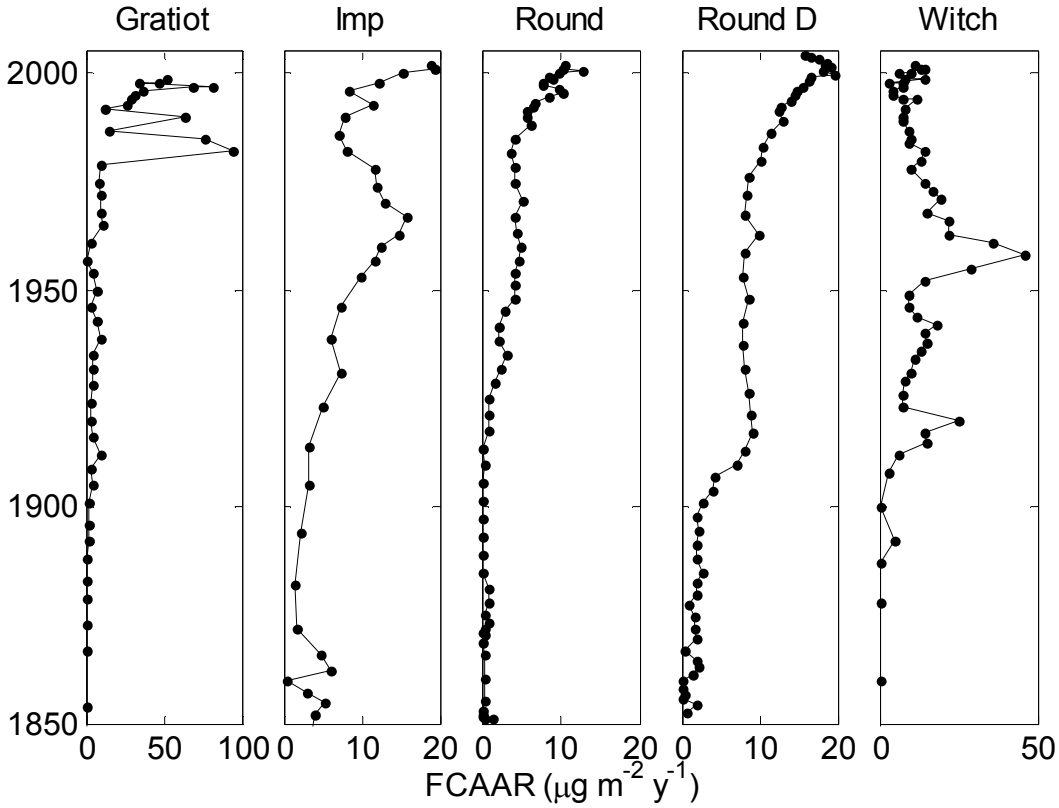

Figure 2.5. ^{210}Pb dated focusing-corrected anthropogenic accumulation rates for five Upper Peninsula of Michigan lakes, dates older than 1850 were truncated to highlight more recent loading. Note the change in scale of the x-axis.

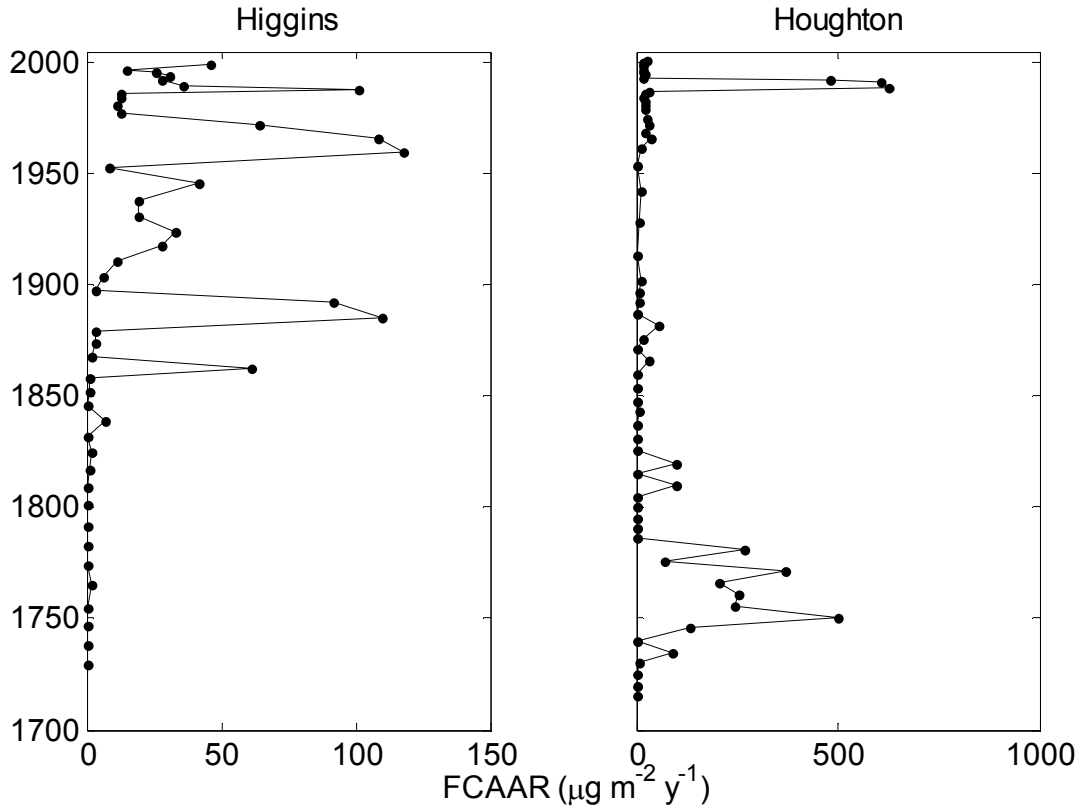

Figure 2.6. ^{210}Pb dated focusing-corrected anthropogenic Hg accumulation rates for two north-central Michigan lakes. Note the change in scale of the x-axis.

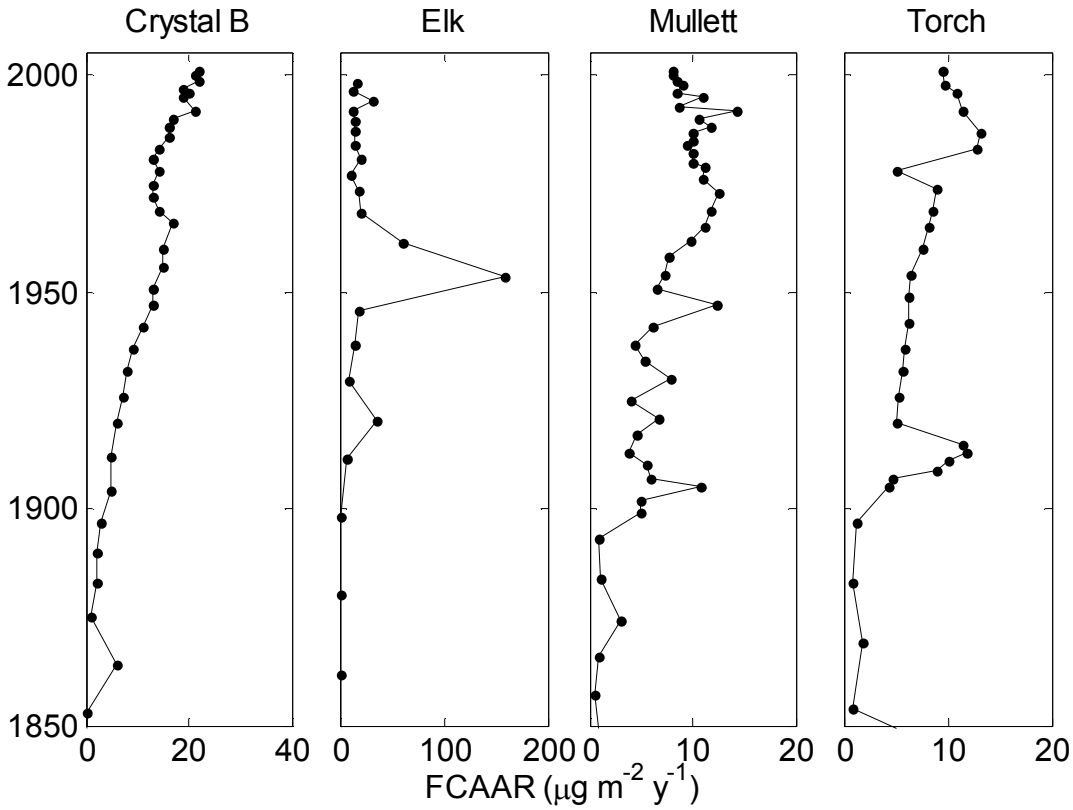

Figure 2.7. ^{210}Pb dated focusing-corrected anthropogenic accumulation rates for four northwestern Michigan lakes, dates older than 1850 were truncated to highlight more recent loading. Note the change in scale of the x-axis.

Anthropogenic Hg profiles from lakes in southwestern Michigan reflect the proximity to industrialized areas and also include several episodic accumulation events (Figure 2.3). The proximity of this sub-region to the Chicago, IL/Gary, IN area suggests that these lakes should reflect the impact of Hg from this highly industrialized region. It has been suggested previously that the Chicago/Gary area is a source of Hg to southern Lake Michigan (Landis and Keeler, 2002, Landis *et al.*, 2002) and it has been proposed that the Chicago/Gary industrial complex was a major source for lead, cadmium and zinc to these study lakes (Yohn, 2004). The similarity, excluding episodic accumulation events, of the loading profiles observed for Gull and Birch lakes implies a source of Hg common to both lakes was present until the early 1990s, although the onset of the anthropogenic Hg accumulation occurred earlier in Birch Lake. The recent recovery of Gull Lake to a rate of anthropogenic loading that is near zero is notable, since this was observed in only 2 of the 26 study lakes studied (see Littlefield Lake, Figure S1 in Appendix B). Accumulation rates in Birch and Muskegon lakes decreased toward the surface whereas the rates in Lake Paw Paw have increased. The uniqueness of the accumulation rates observed near the surface of the core from Lake Paw Paw and the unique episodic events (ca 1960 and 1984) suggests a local source. Paw Paw Lake was dated with a linear dating model using a single sedimentation rate (see Appendix B, Table S1). Meaning, in Paw Paw Lake, episodic events were due to increased Hg concentration on the sediment and not increased sediment delivery. Episodic events that were common among all southwestern lakes include a peak in the early 1990s and early

to mid 1970s. Great anthropogenic Hg accumulation rates in Paw Paw and Muskegon lakes suggest that local-scale sources are significant contributors of Hg to these lakes.

Southeastern Michigan is a highly populated and industrialized area of the state. This area also has the highest number of coal-fired utilities in the State; although all of these facilities lie to the east of the study lakes (Figure 2.1). Winds are generally westerly or southerly in this region. Mercury accumulation rates are greater in lakes from this sub-region which may be a consequence of greater atmospheric deposition in this region compared to less urban regions of Michigan (2005). Mercury in the cores from Whitmore, Cass, and Otter lakes exhibit large anthropogenic accumulation rates with peak rates that were amongst the greatest measured for all of the lakes studied (Figure 2.4). Lakes Otter and Whitmore, which are situated in the northern part of this sub-region, exhibit rapid increases in anthropogenic Hg accumulation during the latter part of the 1940s into the early 1950s. This implies a common source or a source that is common to both lakes of Hg loading to both lakes during that period. Furthermore, several of the episodic increases in Hg loading occurred simultaneously among these lakes, suggesting a source of Hg loading common to both lakes. Episodic events in the early and mid 1990s are common among all of the southeastern lakes. During the early 2000s, episodic events occurred in Sand and Otter Lakes. When accumulation profiles in these lakes were compared to those observed in the surficial portion of the core from Whitmore Lake it is possible that Whitmore Lake is currently experiencing a spike in Hg accumulation. If Whitmore Lake were revisited, the most recent sediments should show a decline in accumulation rate. Dating-model error, measurement error and field methodologies all contribute to possible errors in sediment core chronologies. However,

the observation that so many episodic events "line-up" among lakes suggests that the events are real. Similar to Paw Paw and Muskegon lakes, the accumulation rates in Cass Lake were anomalously great; these rates suggest a unique source or a sub-regional source in close proximity to the lake. Recently, decreases in Hg loading have been observed among all of the lakes in the southeastern sub-region (Figure 2.1), generally from maximal loading rates, in anthropogenic Hg accumulation. Sediment cores from lakes in urban areas of Minneapolis, MN have demonstrated that loading rates of Hg have decreased in recent years (Engstrom and Swain, 1997). The hypothesis stated for the decreased Hg loading to urban Minneapolis lakes is that limited growth in already built-up areas has slowed the potential for new sources of Hg to the lakes. This also adequately explains the recent declines observed for southeastern Michigan (suburban Detroit and Flint) lakes in our study; although the reasons for episodic increases are unclear at this time.

Rates of anthropogenic Hg loading to five Upper Peninsula (UP) lakes, Gratiot, Imp, Round D, Round, and Witch, appears to be sub-regional in nature (Figure 2.5). Other than the episodic accumulation events, this conclusion is further supported by the similarity of profiles in the eastern portion of the UP (Round D and Round) compared to those in the western UP (Imp and Witch). Both Round D and Round lakes appear to have reached a steady state accumulation rate shortly after reaching maxima in the early 1900s and 1950s respectively. Then, during the late 1970s, Hg accumulation rates in both lakes increased and followed similar trajectories. Witch and Imp lakes both reached maximal Hg accumulation rates in the 1960s followed by a steady decline until the 1990s. After 1990, both Imp and Witch lakes exhibited greater accumulation rates until 2000, followed

by a more recent decrease. Except for a unique accumulation rate profile in more recent times, certain episodic increases in Hg accumulation during the 1910s, 1940s, and 1980s in Gratiot Lake were common to other western UP lakes, suggesting that Gratiot Lake would be included in this sub-region. The episodic events after 1975 in Gratiot were superimposed on a generally increasing trend. The extent of these events suggests that the source was local, most likely watershed, in scale.

Anthropogenic Hg accumulation rate profiles from Lakes Higgins and Houghton in the north-central portion of the Lower Peninsula of Michigan exhibit simultaneous occurrence of episodic increases (Figure 2.6). A notable deviation was observed during the mid to late 18th century in Houghton Lake. Reasons for not observing this phenomenon in other Michigan lakes that contain sediment of adequate age to record the disturbance are not yet clear, but may be due to the unique geography of the Houghton Lake area. Higgins Lake lies 14 km due north of Houghton Lake, and their watersheds share a common boundary. Houghton Lake lies at or near the headwaters of three major river systems, two of which flow into Lake Michigan (Muskegon and Manistee rivers) and one into Lake Huron (Au Sable River). Native Americans commonly used rivers as efficient transportation corridors from West to East (Quimby, 1962) and the advantage of efficient travel may have led to early settlement. Native American tribes during this period were known to travel inland over 100 km from the Lake Michigan shoreline (Quimby, 1962). Other metals, such as, aluminum (Al), zinc and cadmium, do show an accumulation rate increase during this period suggesting a terrestrial input (Yohn *et al.*, 2003). The disturbance that led to the increase of these metals is unclear, but may be due to the early trading and land-clearing activities in the region.

Prior to 1930, the Hg accumulation rate profiles of 4 northwestern Michigan lakes, Elk, Torch, Crystal B and Mullett were similar (Figure 2.7), which suggests a regional to sub-regional source of Hg. After the 1930s, lakes Mullett and Torch appear to have been influenced by a more sub-regional source, whereas Elk and Crystal lakes show the effects of more local sources. Loading rates of Al to Elk Lake decreased during the mid-20th century episodic Hg increase. These two observations, taken together, suggest that the source was a point source or local atmospheric deposition rather than terrestrial (Long *et al.*, 2000). Mercury accumulation rates in Crystal B Lake were found to be increasing towards the sediment water interface, which is unique for this sub-region, suggesting a local source.

While it is clear that some episodic accumulation events are due to local-scale sources it is unclear at this time the reasons for these events. Possible sources being considered include: waste incinerators (Liu *et al.*, 2007), fuel combustion (Lynam and Keeler, 2006), dental office waste (Drummond *et al.*, 2003), forest fire (Turetsky *et al.*, 2006), clear-cutting of forest (Porvari *et al.*, 2003), pulp and paper mills (Hynynen *et al.*, 2004), and cement manufacturing (Pacyna *et al.*, 2006).

Recent Trends. Hg concentration profiles in sediments from several lakes have recorded recent increases in Hg loading (Engstrom and Swain, 1997, Lorey and Driscoll, 1999, Perry *et al.*, 2005, Swain *et al.*, 1992). Over the last decade in Michigan, 8 of the 26 lake profiles showed anthropogenic Hg accumulation rates that increased toward the surface, 11 showed trends that indicate anthropogenic loading had declined, 5 showed elevated accumulation rates but no clear increasing or decreasing trend, and 2 had

anthropogenic accumulation rates at background levels (Figure 2.1). Considering the lakes experiencing increased loading, the lack of a spatial trend suggests that the source was not regional in scale. Lakes that are increasing are not located in areas of the state that have a high density of coal-fired power plants (Figure 2.1), further evidence of the importance of local-scale sources of Hg to these lakes. In addition, these results are inconsistent with a decrease in Hg emissions (Engstrom and Swain, 1997). Possible local sources include: mobilization from watershed soils, industry, and agriculture. The increase observed in sediment cores from Adirondack lakes have been attributed to a decrease in the retention of Hg by watershed soils (Lorey and Driscoll, 1999). Some researchers have attributed the increase recorded in western Minnesota lakes to Hg-laden soils delivered from agricultural fields (Engstrom and Swain, 1997). At this time it is unclear as to why we observe increased accumulation rates in more recent periods but one or all of the above may have contributed.

REFERENCES

REFERENCES

Michigan Department of Environmental Quality, 2007. Sediment Chemistry, Available online at http://www.michigan.gov/deq/0,1607,7-135-3313_3686_3728-32365--,00.html. (Accessed: January 15, 2007).

Bindler, R., Renberg, I., Appleby, P.G., Anderson, N.J., Rose, N.L., 2001. Mercury accumulation rates and spatial patterns in lake sediments from west Greenland: A coast to ice margin transect. Environmental Science and Technology 35, 1736-1741.

Drummond, J.L., Cailas, M.D., Croke, K., 2003. Mercury generation potential from dental waste amalgam. Journal of Dentistry 31, 493-501.

Engstrom, D.R., Swain, E.B., 1997. Recent declines in atmospheric mercury deposition in the upper Midwest. Environmental Science and Technology 31, 960-967.

Engstrom, D.R., Swain, E.B., Henning, T.A., Brigham, M.E., Brezonik, P.L., 1994. Atmospheric Mercury Deposition to Lakes and Watersheds - a Quantitative Reconstruction from Multiple Sediment Cores. In: Environmental Chemistry of Lakes and Reservoirs. pp. 33-66.

ARC/INFO, Environmental Systems Research Institute, 1998. ARC/INFO

Fitzgerald, W.F., Engstrom, D.R., Mason, R.P., Nater, E.A., 1998. The case for atmospheric mercury contamination in remote areas. Environmental Science and Technology 32, 1-7.

Gobeil, C., MacDonald, R.W., Smith, J.M., 1999. Mercury profiles in sediments of the Arctic Ocean basin. Environmental Science and Technology 33, 4194-4198.

Golden, K.A., Wong, C.S., Jeremiason, J.D., Eisenreich, S.J., Sanders, M.G., Hallgren, J., Swackhammer, D.L., Engstrom, D.R., Long, D.T., 1993. Accumulation and preliminary inventory of organochlorines in Great Lakes sediments. Water Science and Technology 28, 19-31.

Gray, J.E., Fey, D.L., Holmes, C.W., Lasorsa, B.K., 2005. Historical deposition and fluxes of mercury in Narraguinnep Reservoir, southwestern Colorado, USA. Applied Geochemistry 20, 207-220.

Grigal, D.F., 2003. Mercury sequestration in forests and peatlands: A review. Journal of Environmental Quality 32, 393-405.

Hermanson, M.H., 1998. Anthropogenic mercury deposition to arctic lake sediments. Water, Air, and Soil Pollution 101, 309-321.

Hightower, J., Moore, D., 2003. Mercury Levels in High-End Consumers of Fish. Environmental Health Perspectives 111, 604-608.

Hynynen, J., Palomaki, A., Merilainen, J.J., Witick, A., Mantykoski, K., 2004. Pollution history and recovery of a boreal lake exposed to a heavy bleached pulping effluent load. Journal of Paleolimnology 32, 351-374.

Kamman, N.C., Engstrom, D.R., 2002. Historical and present fluxes of mercury to Vermont and New Hampshire lakes inferred from Pb-210 dated sediment cores. Atmospheric Environment 36, 1599-1609.

Keeler, G.J., Dvonch, J.T., 2005. Atmospheric mercury: A decade of observations in the Great Lakes. In: N. Pirrone, K. Mahaffey (Eds.), Dynamics of Mercury Pollution on Regional and Global Scales: Atmospheric Processes and Human Exposures around the World. Kluwer Ltd., Norwell, MA.

Kerfoot, W.C., Harting, S., Rossmann, R., Robbins, J.A., 1999. Anthropogenic copper inventories and mercury profiles from Lake Superior: Evidence for mining impacts. Journal of Great Lakes Research 25, 663-682.

Kerfoot, W.C., Harting, S.L., Jeong, J., Robbins, J.A., Rossmann, R., 2004. Local, regional, and global implications of elemental mercury in metal (copper, silver, gold, and zinc) ores: Insights from Lake Superior sediments. Journal of Great Lakes Research 30, 162-184.

Kolak, J.J., Long, D.T., Beals, T.M., Eisenreich, S.J., Swackhamer, D.L., 1998. Anthropogenic inventories and historical and present accumulation rates of copper in Great Lakes sediments. Applied Geochemistry 13, 59-75.

Landis, M.S., Keeler, G.J., 2002. Atmospheric mercury deposition to Lake Michigan during the Lake Michigan Mass Balance Study. Environmental Science and Technology 36, 4518-4524.

Landis, M.S., Vette, A.F., Keeler, G.J., 2002. Atmospheric mercury in the Lake Michigan basin: Influence of the Chicago/Gary urban area. Environmental Science and Technology 36, 4508-4517.

Liu, B., Keeler, G.J., Dvonch, J.T., Barres, J.A., Lynam, M.M., Marsik, F.J., Morgan, J.T., 2007. Temporal variability of mercury speciation in urban air. Atmospheric Environment 41, 1911-1923.

Long, D.T., Eisenreich, S.J., Swackhammer, D.L. *Volume III - Metal Concentrations in Sediments of the Great Lakes*; Government Printing Office, 1995.

Long, D.T., Simpson, S.S., Geisey, J.P., Fett, J.D., 2000. Inland lakes sediment trends: sediment analysis results for five Michigan Lakes. Lansing, MI. 17 pages.

Available from: http://www.deq.state.mi.us/documents/deq-swq-gleas-9900sedtrendreport.pdf.

Lorey, P., Driscoll, C.T., 1999. Historical trends of mercury deposition in Adirondack lakes. Environmental Science and Technology 33, 718-722.

Lynam, M.M., Keeler, G.J., 2005. Automated speciated mercury measurements in Michigan. Environmental Science and Technology 39, 9253-9262.

Lynam, M.M., Keeler, G.J., 2006. Source-receptor relationships for atmospheric mercury in urban Detroit, Michigan. Atmospheric Environment 40, 3144-3155.

Meili, M., 1991. The Coupling of Mercury and Organic-Matter in the Biogeochemical Cycle - Towards a Mechanistic Model for the Boreal Forest Zone. Water, Air, and Soil Pollution 56, 333-347.

Menounou, N., Presley, B.J., 2003. Mercury and other trace elements in sediment cores from central texas lakes. Archives of Environmental Contamination and Toxicology 45, 11-29.

Pacyna, E.G., Pacyna, J.M., Fudala, J., Strzelecka-Jastrzab, E., Hlawiczka, S., Panasiuk, D., 2006. Mercury emissions to the atmosphere from anthropogenic sources in Europe in 2000 and their scenarios until 2020. Science of the Total Environment 370, 147-156.

Perry, E., Norton, S.A., Kamman, N.C., Lorey, P.M., Driscoll, C.T., 2005. Deconstruction of Historic Mercury Accumulation in Lake Sediments, Northeastern United States. Ecotoxicology 14, 85-99.

Porvari, P., Verta, M., Munthe, J., Haapanen, M., 2003. Forestry practices increase mercury and methyl mercury output from boreal forest catchments. Environmental Science and Technology 37, 2389-2393.

Quimby, G.I., 1962. A Year with a Chippewa Family, 1763-1764. Ethnohistory 9, 217-239.

Scherbatskoy, T., Shanley, J.B., Keeler, G.J., 1998. Factors controlling mercury transport in an upland forested catchment. Water Air and Soil Pollution 105, 427-438.

Swain, E.B., Engstrom, D.R., Brigham, M.E., Henning, T.A., Brezonik, P.L., 1992. Increasing Rates of Atmospheric Mercury Deposition in Midcontinental North-America. Science 257, 784-787.

Turetsky, M.R., Harden, J.W., Friedli, H.R., Flannigan, M., Payne, N., Crock, J., Radke, L., 2006. Wildfires threaten mercury stocks in northern soils. Geophysical Research Letters 33.

U.S. EPA, 2004. National Listing of Fish Advisories, Available online at http://www.epa.gov/waterscience/fish/. (Accessed: September 25, 2011).

State Soil Geographic (STATSGO) Database for Michigan, Available online at http://www.ncgc.nrcs.usda.gov/products/datasets/statsgo/index.html. (Accessed: September 25, 2011).

USEPA. Office of Solid Wastes. *Mercury in solids and solutions by thermal decomposition, amalgamation, and atomic absorption spectrophotometry*; Government Printing Office, 1998.

USEPA. Office of Research and Development Office of Air Quality Planning and Standards. *Mercury Study Report to Congress*; Washington, DC: Government Printing Office, 1997.

Wihlborg, P., Danielsson, A., 2006. Half a century of mercury contamination in Lake Vanern (Sweden). Water, Air, and Soil Pollution 170, 285-300.

Yang, H.D., Rose, N.L., 2003. Distribution of mercury in six lake sediment cores across the UK. Science of the Total Environment 304, 391-404.

Yohn, S., Long, D., Fett, J., Patino, L., 2004. Regional versus local influences on lead and cadmium loading to the Great Lakes region. Applied Geochemistry 19, 1157-1175.

Yohn, S.S. 2004. Natural and Anthropogenic Factors Influencing Spatial and Temporal Patterns of Metal Accumulation in Inland Lakes. Thesis, Michigan State University, East Lansing, MI.

Yohn, S.S., Long, D.T., Fett, J.D., Patino, L., Giesy, J.P., Kannan, K., 2002a. Assessing environmental change through chemical-sediment chronologies from inland lakes. Lakes Reserv Res Manage 7, 217-230.

Yohn, S.S., Long, D.T., Giesy, J.P., Fett, J.D., Kannan, K., 2001. Inland lakes sediment trends: sediment analysis results for two Michigan Lakes. Lansing, MI. 49 pages. Available from:

Yohn, S.S., Long, D.T., Giesy, J.P., Scholle, L.K., Patino, L.C., Fett, J.D., Kannan, K., 2002b. Inland lakes sediment trends: sediment analysis results for five Michigan Lakes. East Lansing. 64 pages. Available from:

Yohn, S.S., Long, D.T., Giesy, J.P., Scholle, L.K., Patino, L.C., Parsons, M., Kannan, K., 2003. Inland Lakes Sediment Trends: sediment analysis results for six Michigan Lakes. East Lansing. 66 pages. Available from: http://www.deq.state.mi.us/documents/deq-wb-swas-sedimenttrend0203finalreport.pdf.

CHAPTER 3
A REGIONAL ANALYSIS ON THE EFFECTS OF WATERSHED ATTRIBUTES ON THE RECOVERY OF INLAND LAKES FROM MERCURY ENRICHMENT.

Abstract

Sediments from inland lakes record recent declines in mercury (Hg) loading to the environment. The rate of decline or recovery rate varies among lakes which we hypothesize to be due to differences in how watershed attributes influence the transport of Hg through the watershed. Sediment cores were collected, dated using lead-210, and analyzed for Hg from 13 inland lakes throughout the State of Michigan to test this hypothesis. Slopes of linear recovery calculated from the most recent declines in concentration and accumulation rate were compared to watershed attributes using Pearson's correlation coefficient. Agricultural, forested and wetland attributes were all important determinants of recovery rate. However, the strongest correlations were found for land cover types along highly conductive watershed flow paths or within close proximity to the lake. These results highlight the importance of watershed attributes and the transport of Hg from the catchment to the lake. However, this work also emphasizes the importance of location within the watershed as an important determinant of contemporary recovery.

Introduction

How aquatic systems are recovering from man-caused stresses continues to be a critical question for both researchers and natural resource managers. Of particular concern is recovery from mercury (Hg) contamination because organic forms bioaccumulate in aquatic food webs and consumption of tainted fishes can impact human health (Hightower and Moore, 2003, USEPA, 1997). Environmental archives (e.g., sediment chronologies) have been shown to be reliable recorders of anthropogenic activities and have demonstrated the efficacy of

environmental legislation (Bindler *et al.*, 2001, Engstrom and Swain, 1997, Kamman and Engstrom, 2002, Long *et al.*, 2010, Lorey and Driscoll, 1999, Swain *et al.*, 1992). However for Hg, sediment concentrations and fluxes for most lakes are still elevated above geochemical background values (Bindler *et al.*, 2001, Engstrom *et al.*, 2007, Kamman and Engstrom, 2002, Parsons *et al.*, 2007, Swain *et al.*, 1992) This condition is in part due to continued Hg emissions and the transport of previously deposited Hg, so called "legacy Hg", from the watershed to the aquatic ecosystem due to natural processes that might be exacerbated by human disturbances. However, as anthropogenic Hg emissions continue to decrease, which some have suggested for the Great Lakes region (Evers *et al.*, 2011, Keeler and Dvonch, 2005), one might hypothesize that transport through the watershed might play an ever more important role in the rates of recovery of ecosystems from Hg contamination. The activities that result in differences in Hg transport through the watershed will need to better defined, especially if those activities result in a slower recovery

Sediment profiles of heavy metals (e.g., Cd, Cu, Pb, Zn and Hg) when influenced by human activities consist of three primary temporal phases, the first being a time which can be considered geochemical background, or reference condition, which in the State of Michigan occurs prior to European settlement, ca. 1850. Throughout inland lakes of Michigan the next phase recognized in sediment profiles is the onset of deforestation. This is followed by the increased production and consumption of heavy metals during the industrial revolution (Long *et al.*, 2010) which is evidenced by rapidly increasing sediment concentrations and fluxes starting in the late 19^{th} century. The final phase occurs after the passage of environmental legislation, i.e., Clean Air Act (US EPA, 2008), when the loading of metals to the environment significantly decreased. This final, or recovery, phase is evidenced by decreasing sediment concentrations

and fluxes. The rate of recovery, defined here as the slope of decreasing concentrations or fluxes, can differ among lakes which may be due in part to proximity to local sources, but also due to differences in watershed attributes or differing rates of landscape disturbance.

Export rates of Hg from watersheds have been shown to be influenced by land use (Babiarz *et al.*, 1998, Hurley *et al.*, 1995b). Although the transport of Hg through the watershed is not fully understood some generalizations can be made. All catchments are sinks for atmospherically deposited Hg and rates of retention can be greater than 90% (Aastrup *et al.*, 1991, Harris *et al.*, 2007). Those landscapes that experience higher rates of erosion (e.g., agricultural) would be expected to have a higher probability to export rather than retain Hg (Munthe *et al.*, 2007a). Urban areas, in the absence of local emitters, have been suggested to export less Hg then most other land use types due to a lack of activities that disturb the landscape (Engstrom and Swain, 1997). Forests have been shown to be sinks for Hg; but can release Hg during storm events (Munthe *et al.*, 2007b), forest fires (Turetsky *et al.*, 2006), and logging (Munthe and Hultberg, 2004, Porvari *et al.*, 2003). There does not appear to be a consensus about the effects of wetlands on Hg export. Some have shown that wetland type or presence does not influence Hg export (St. Louis *et al.*, 1996), while others have found that Hg is less likely to be retained when wetlands are present (Hurley *et al.*, 1995a, Mierle and Ingram, 1991).

Both sediment concentration and accumulation rate chronologies are commonly used to represent system state due to the unique information they provide about environmental condition. Concentration profiles provide information about environmental exposure that may be useful to natural resource managers and differences with respect to watershed concentrations that aid in

determining the state of recovery of the system from disturbance (see Long et al., 2010). Knowledge of the accumulation rates can be important since concentration can be diluted or amplified depending upon the changes in flux of allochthonous and autochthonous materials. For example, if the flux of Hg to sediment were fixed, consequences of an increase in lake productivity (e.g., increased calcium carbonate deposition) would dilute the Hg concentration recorded in the sediment. However, the Hg accumulation rate would remain unchanged since the increase in sedimentation rate would offset the decrease in Hg concentration. Likewise if the source of the terrestrial input would for some reason change, e.g., logging activities strip native top soil, see (Long *et al.*, 2010), and the atmospheric flux of Hg is again fixed then the concentration might be expected to decrease. The Hg accumulation rate would increase; however, since the flux of soil material would be expected to be much greater than under previous conditions. Under this set of circumstances the definition of recovery is confounded since concentrations are decreasing, an indication of recovery, but accumulation rate is increasing. A study of system recovery then must compare concentrations and accumulation rates since each can provide alternative interpretations or additional information about movement of Hg through the watershed.

Sediment cores used for this study were collected from 14 inland lakes throughout the State of Michigan (Figure 3.1) as part of a larger Inland Lakes Trends Monitoring Program funded by the Michigan Department of Natural Resources and Environment. Lakes included in this study vary in watershed land use from highly urban landscapes in southeast Michigan to the remote, highly forested region, of Michigan's Upper Peninsula (Table 3.1). Slopes of the concentrations and flux declines were compared against watershed attributes in order to

investigate the relationship between the recovery of inland lakes from anthropogenic Hg contamination and watershed land use.

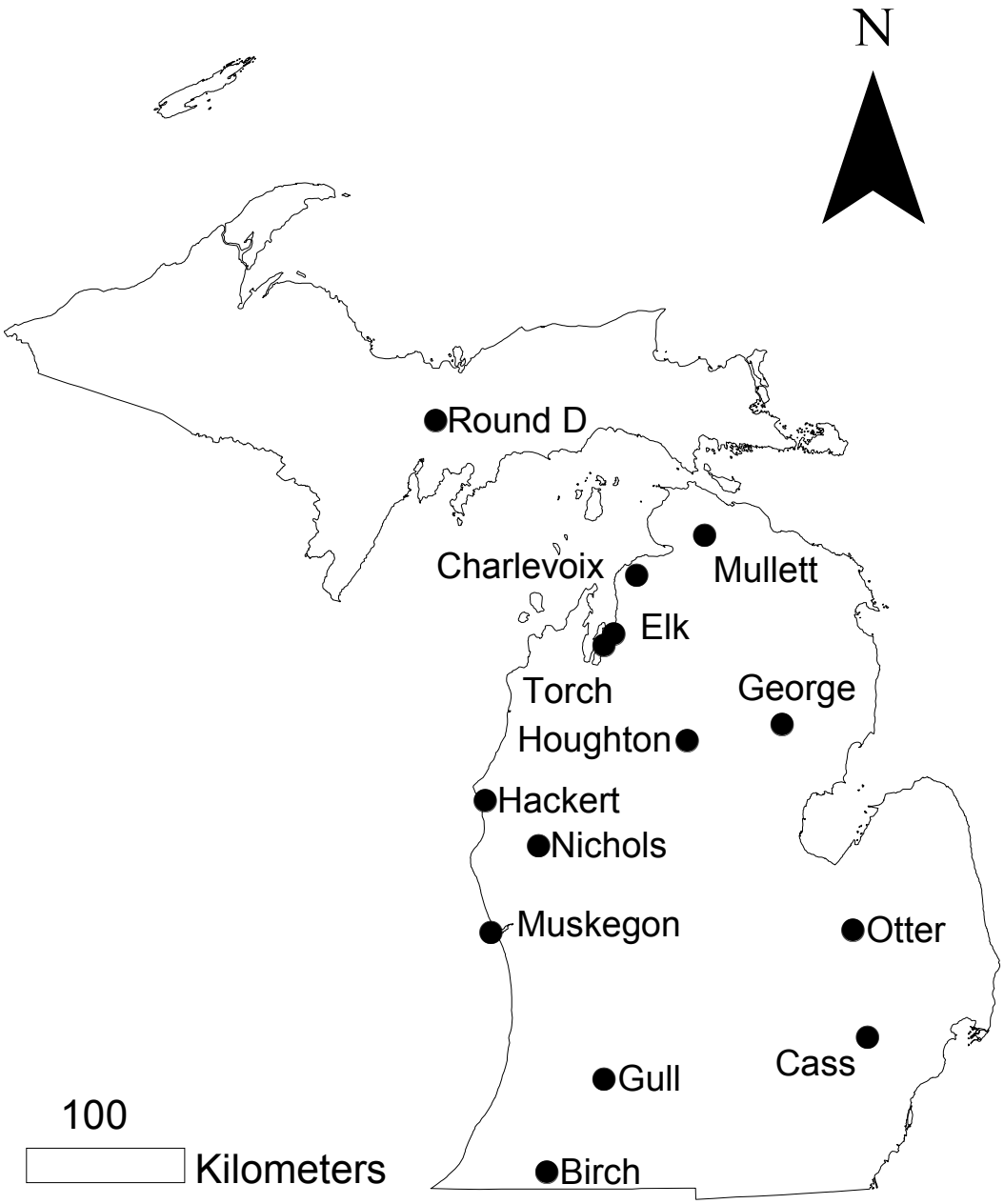

Figure 3.1. Location of study lakes.

Methods

Core collection and recovery estimates. Sediment cores were collected using an Ocean Instruments MC-400 from the deepest portion of the lake from the MDNRE *R/V Nibi* or US EPA *R/V Mudpuppy* between 1999 and 2007. Sediment cores were sectioned on shore at 0.5 to 1.0 cm increments and stored on ice in acid-cleaned polypropylene jars during. In the laboratory, samples for mercury analysis were transferred to Whirl-Pak bags and lyophilized. Mercury analysis was performed using a Lumex Mercury Analyzer following US EPA Method 7473 (USEPA, 1998). Samples for radiometric dating were submitted to the Freshwater Institute at the University of Manitoba. The radionuclide ^{210}Pb was measured in every slice to determine sedimentation rates and assign dates and cesium-137 (^{137}Cs) was measured in select slices to determine peak activities. Cesium-137 analyses were performed by direct counting of 5-10 g of sediment on a γ-spectrometer (Ge-Li) semiconductor detector. Samples of 1-3 g were analyzed for ^{210}Pb and radium-226 by leaching in 6N hydrochloric acid in the presence of a polonium-209 tracer, autoplating on a silver disk, and counting the disk on an α-spectrometer, determining ^{210}Pb via its polonium-210 daughter product. Sediment slice ages were estimated using the constant rate of supply (CRS) (Appleby and Oldfield, 1978), constant flux:constant sedimentation (CF:CS) (Golden *et al.*, 1993), or segmented CF:CS model (Heyvaert *et al.*, 2000). Assigned dates were verified using peak activities of ^{137}Cs (Appleby, 2001) and stable Pb (Alfaro-De la Torre and Tessier, 2002).

Recovery rates for concentration and accumulation rates were determined by calculating the slope of the most recent decreasing trend of Hg, measured from the most recent peak or change in slope trajectory. To avoid inclusion of episodic or short term increases (Figure 3.2) in the calculation of slope the Hg profile was first smoothed using *smooth* command in Matlab (Mathworks, 1994 - 2008). Slopes were compared to watershed attributes using Pearson's product-moment correlation coefficient (r) which assumes a normal distribution and where necessary data were transformed to meet this assumption. Statistical analyses were performed in the statistical environment R (The R Foundation for Statistical Computing, 2008). Outliers, as indicated by statistical boxplots, were removed so that these data did not overly influence the results. Only statistically significant results ($p \leq 0.10$) are reported. In the case of zeros in the dataset and the requirement to transform the data a constant was added to each original value equivalent to the value of the first quartile squared divided by the value of the third quartile.

Determination of watershed attributes. Land use data were obtained from the 2001 IFMAP/GAP Lower and Upper Peninsula datasets (Michigan Department of Natural Resources, 2003) for each watershed. Land use was classified using the upper-most level Anderson classification and resulted in 7 land use types: urban (URB), agriculture (AG), forest (FOR), barren (BAR), upland (UPL), water (WAT) and wetland (WET). Lowland forests originally included as wetland were reclassified as forested land use. Flow inverted (FLI) and flow inverted squared (FLI2) land use values, for the watershed and within 100 m of the lake shoreline, were calculated by determining the flow length (i.e., the pathway a drop of water would take to the lake when dropped on the watershed) using the FLOWLENGTH command in ArcGIS (ESRI, 1998). The inverse (1/flowlength) and inverse squared ($1/\text{flowlength}^2$) of the

flowlength were then multiplied by the land use with the 30 m^2 grid cell of individual land use coverages assigned a 1, for presence, or 0 for absence. This method has the potential to provide information about land use in close proximity or along highly conductive flow paths that would not be represented by other measures. All land use variables were also calculated for a 100 m buffer around the lake shoreline and converted to proportions for this analysis. By convention land use type will precede FLI and FLI2 to indicate these transformations (e.g., AG.FLI is read flow length inverted agriculture). Likewise land use calculated within the buffer is given the suffix M (e.g., AG.FLI.M is read flow length inverted agriculture in the 100 m buffer).

Sulfate deposition (SD), used here as a proxy for coal combustion (Yohn, 2004), was estimated for the region by using inverse distance weighting of the 1990-2009 average sulfate deposition values for 19 National Atmospheric Deposition Program stations around the Great Lakes region (Illinois State Water Survey, 2008). Soil erodibility, expressed here as the k-factor (K.F) and slope corrected k-factor (K.FF), was estimated using dasymetric mapping techniques using the State Soil Geographic Database (STATSGO) (USDA, 1994).

Four physical variables were investigated along with land cover attributes: latitude, watershed area (WA), calculated with the lake removed, lake area (LA), and WA:LA. Watersheds were delineated from National Elevation Dataset (NED) 1 arc second digital elevation models (DEM), available from the USGS seamless website (USGS, 2008), using the watershed command in ESRI ArcGIS (ESRI, 1998). Others have shown that WA:LA is an important determinant for sediment Hg fluxes (Swain *et al.*, 1992). Latitude was investigated as a proxy for atmospheric deposition rates which have been shown to decrease from the South to the North in this region (Keeler and Dvonch, 2005). Since latitude only captures a regional trend Hg emissions estimates were included to detect possible correlations to local sources that may be

unique to a sub-region or an individual lake. Mercury emissions were calculated using the 2002 U.S. EPA Hg emissions estimates for the State of Michigan (USEPA, 2006) for 50 and 100 km buffers around the lake. A complete list of the watershed characteristics for lakes in this study can be found in Table 1.

Table 3.1. Watershed attributes of study lakes: watershed area (WA), lake area (LA), watershed to lake area ratio (WA:LA), urban (URB), agriculture (AG), forest (FOR), upland (UP), barren (BAR), and wetland (WET).

Lake	Concentration Recovery Rate (μg/kg/y)	Flux Recovery Rate ($\mu g/m^2/y/y$)	Latitude	WA (km^2)	LA (km^2)	WA:LA
Birch	-2.7	-0.22	41.8669	16.9	1.2	14.2
Cass	-1.9	-1.14	42.6036	38.7	5.2	7.5
Charlevoix	-1	-0.57	45.2632	765.1	69.8	11
Elk	-1.5	-0.25	44.8690	85.8	31.3	2.7
George	-5.6	-1.45	44.3997	5.1	0.8	6.3
Gull	-1.3	-0.47	42.3963	55.3	8.2	6.8
Hackert	-4.3	-0.57	43.9827	1.6	0.5	3.2
Houghton	-4.5	-0.55	44.3203	382.7	81.2	4.7
Mullett	-0.3	-0.09	45.4850	1239.5	70.3	17.6
Muskegon	-4.5	-2.74	43.2333	884.7	16.8	52.7
Nichols	-6.5	-0.41	43.7292	0.9	0.7	1.3
Otter	-1.8	-0.52	43.2164	0.5	0.3	1.5
Round D	-7.8	-1.13	46.1462	6.8	1.8	3.8
Torch	-1.6	-0.27	44.9326	120.8	76	1.6

Lake	URB	AG	FOR	UP	BAR	WET
Birch	6.40%	48.30%	27.80%	7.80%	0.10%	4.40%
Cass	24.80%	0.50%	37.50%	18.90%	0.10%	11.00%
Charlevoix	3.40%	17.30%	61.00%	14.80%	0.30%	2.30%
Elk	4.20%	20.40%	53.60%	18.60%	0.20%	1.80%
George	5.00%	6.30%	59.90%	17.40%	0.20%	9.40%
Gull	5.60%	59.80%	21.00%	6.10%	0.10%	4.90%
Hackert	5.90%	33.80%	42.30%	10.20%	0.20%	4.30%
Houghton	3.70%	0.80%	62.20%	14.60%	0.20%	16.40%
Mullett	2.80%	7.20%	68.10%	17.70%	0.20%	3.20%
Muskegon	7.00%	17.20%	47.40%	18.00%	0.40%	7.00%
Nichols	0.90%	0.00%	86.40%	2.00%	0.20%	5.40%
Otter	8.30%	4.80%	49.60%	16.70%	0.00%	17.90%
Round D	0.20%	0.00%	78.60%	3.40%	0.10%	15.40%
Torch	4.20%	18.60%	54.30%	19.40%	0.20%	1.50%

Table 3.1 (cont'd).

Lake	SD (kg/ha/y)	K.F	K.FF	URB.M	AG.M
Birch	17.7	0.17	0.09	23.10%	3.70%
Cass	14.3	0.22	0.11	17.30%	0.00%
Charlevoix	11.8	0.17	0.19	1.60%	3.00%
Elk	13	0.19	0.27	6.50%	7.10%
George	12.2	0.22	0.04	12.80%	0.00%
Gull	16.5	0.26	0.12	20.30%	1.00%
Hackert	15.1	0.26	0.03	11.20%	14.60%
Houghton	13.5	0.13	0.06	40.60%	0.00%
Mullett	11.5	0.16	0.14	13.30%	0.80%
Muskegon	16.7	0.21	0.1	31.20%	0.20%
Nichols	15.2	0.17	0.09	3.00%	0.00%
Otter	12	0.21	0.1	9.60%	0.00%
Round D	8	0.15	0.14	0.00%	0.00%
Torch	12.6	0.19	0.29	7.90%	2.90%

Lake	FOR.M	UP.M	BAR.M	WET.M	FOR.M
Birch	40.20%	10.00%	0.00%	21.20%	40.20%
Cass	42.60%	9.80%	0.00%	9.00%	42.60%
Charlevoix	47.00%	15.30%	7.60%	11.90%	47.00%
Elk	46.20%	10.20%	0.20%	9.00%	46.20%
George	41.50%	14.10%	0.30%	8.10%	41.50%
Gull	45.00%	12.20%	0.00%	11.00%	45.00%
Hackert	42.70%	10.00%	0.20%	6.80%	42.70%
Houghton	19.70%	8.60%	0.40%	9.00%	19.70%
Mullett	43.70%	8.00%	0.00%	16.20%	43.70%
Muskegon	5.30%	16.50%	8.40%	11.10%	5.30%
Nichols	87.00%	3.70%	0.00%	2.20%	87.00%
Otter	45.60%	14.90%	0.00%	23.70%	45.60%
Round D	71.90%	4.10%	0.10%	3.20%	71.90%
Torch	44.80%	12.20%	0.40%	7.00%	44.80%

Table 3.1 (cont'd)

Lake	URB.FLI	AG.FLI	FOR.FLI	UP.FLI	BAR.FLI
Birch	14.20%	28.40%	38.20%	9.70%	0.00%
Cass	19.30%	0.10%	41.60%	14.00%	0.00%
Charlevoix	11.60%	11.60%	51.70%	15.00%	2.20%
Elk	6.70%	17.10%	49.00%	14.40%	0.20%
George	11.40%	2.20%	57.20%	16.70%	0.10%
Gull	12.80%	23.90%	39.20%	11.20%	0.00%
Hackert	9.00%	21.40%	46.60%	10.40%	0.10%
Houghton	23.60%	0.80%	42.60%	11.70%	0.60%
Mullett	8.20%	5.60%	60.80%	13.90%	0.10%
Muskegon	26.80%	3.30%	25.60%	17.80%	4.50%
Nichols	0.30%	0.00%	89.80%	2.60%	0.00%
Otter	9.50%	2.20%	48.60%	18.10%	0.00%
Round D	0.20%	0.00%	80.90%	2.00%	0.10%
Torch	7.90%	7.90%	54.90%	16.30%	0.30%

Lake	WET.FLI	URB.FLI2	AG.FLI2	FOR.FLI2	UP.FLI2
Birch	8.20%	20.00%	6.50%	42.20%	11.70%
Cass	10.90%	15.50%	0.00%	40.50%	9.10%
Charlevoix	5.00%	15.60%	4.00%	43.50%	13.60%
Elk	5.30%	4.50%	9.30%	50.60%	9.20%
George	7.20%	11.30%	0.20%	51.40%	14.40%
Gull	6.70%	14.30%	3.10%	43.30%	16.20%
Hackert	4.90%	10.20%	15.10%	46.10%	8.90%
Houghton	15.10%	36.40%	0.10%	27.20%	10.20%
Mullett	6.80%	9.90%	1.80%	52.90%	9.50%
Muskegon	9.30%	22.20%	0.20%	8.50%	17.10%
Nichols	3.60%	0.00%	0.00%	91.40%	3.20%
Otter	18.90%	7.10%	0.60%	45.70%	20.90%
Round D	5.90%	0.00%	0.00%	69.40%	1.60%
Torch	3.70%	6.30%	3.30%	49.80%	13.50%

Table 3.1 (cont'd).

Lake	BAR.FLI2	WET.FLI2	URB.FLI.M	AG.FLI.M	FOR.FLI.M
Birch	0.00%	19.00%	23.90%	3.30%	43.80%
Cass	0.00%	11.50%	18.00%	0.00%	40.30%
Charlevoix	6.00%	8.60%	17.90%	3.10%	41.60%
Elk	0.20%	8.90%	6.20%	7.80%	50.90%
George	0.00%	8.60%	15.10%	0.00%	47.40%
Gull	0.00%	10.10%	18.60%	1.30%	45.40%
Hackert	0.10%	5.50%	11.80%	14.80%	45.50%
Houghton	0.50%	10.80%	43.40%	0.00%	23.30%
Mullett	0.00%	12.20%	13.70%	1.10%	49.90%
Muskegon	7.30%	12.40%	28.10%	0.20%	5.30%
Nichols	0.00%	1.80%	0.50%	0.00%	90.70%
Otter	0.00%	21.20%	9.00%	0.00%	47.80%
Round D	0.10%	4.30%	0.00%	0.00%	69.40%
Torch	0.40%	6.80%	8.20%	2.90%	48.00%

Lake	UP.FLI.M	BAR.FLI.M	WET.FLI.M	URB.FLI2.M	AG.FLI2.M
Birch	11.50%	0.00%	17.10%	23.20%	2.20%
Cass	9.20%	0.00%	10.20%	17.30%	0.00%
Charlevoix	13.80%	6.10%	8.90%	18.50%	2.80%
Elk	9.30%	0.10%	9.20%	5.30%	7.50%
George	15.50%	0.00%	8.90%	13.40%	0.00%
Gull	14.80%	0.00%	9.60%	16.00%	1.20%
Hackert	9.50%	0.20%	5.40%	11.50%	13.40%
Houghton	9.70%	0.40%	8.70%	40.90%	0.00%
Mullett	8.90%	0.00%	12.90%	11.70%	1.10%
Muskegon	17.80%	7.20%	12.40%	26.10%	0.20%
Nichols	3.50%	0.00%	2.10%	0.00%	0.00%
Otter	18.30%	0.00%	21.20%	7.60%	0.00%
Round D	2.40%	0.20%	4.20%	0.00%	0.00%
Torch	12.80%	0.30%	7.00%	7.40%	2.60%

Table 3.1 (cont'd).

Lake	FOR.FLI2.M	UP.FLI2.M	BAR.FLI2.M	WET.FLI2.M	Hg.50 (Lbs/y)	Hg.100 (Lbs/y)
Birch	40.60%	11.70%	0.00%	21.70%	67	178.6
Cass	38.40%	7.90%	0.00%	11.40%	1025.9	3127.7
Charlevoix	38.60%	13.30%	7.00%	9.40%	77.8	118.5
Elk	49.60%	7.70%	0.20%	9.80%	78.9	123.2
George	47.50%	13.30%	0.00%	9.20%	1.2	864
Gull	41.10%	16.60%	0.00%	10.90%	77.8	404
Hackert	45.30%	8.40%	0.10%	5.70%	56.5	222.4
Houghton	23.70%	9.40%	0.40%	9.20%	22.1	129.1
Mullett	50.00%	8.40%	0.00%	13.20%	21	110
Muskegon	4.60%	16.70%	6.90%	13.10%	170.2	255.5
Nichols	91.60%	3.40%	0.00%	1.40%	30.8	317.7
Otter	44.90%	20.90%	0.00%	21.80%	353.7	1306.2
Round D	64.50%	1.70%	0.10%	4.50%	30.6	74.7
Torch	46.30%	12.20%	0.40%	7.70%	78.9	119.6

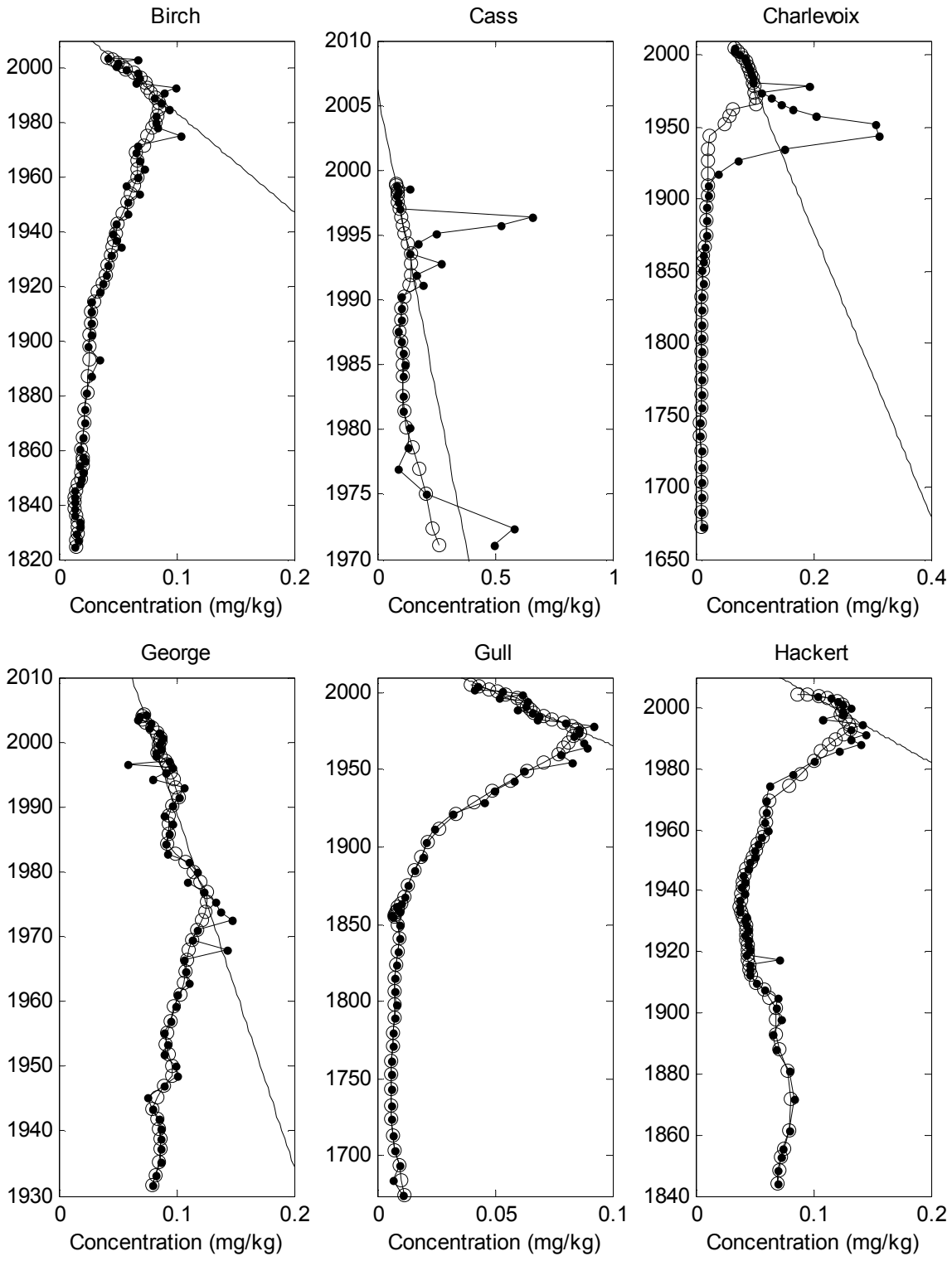

Figure 3.2: Mercury concentration profiles (solid markers), results of profile smoothing (open markers) and recovery rate (solid line) for study lakes.

Figure 3.2 (cont'd)

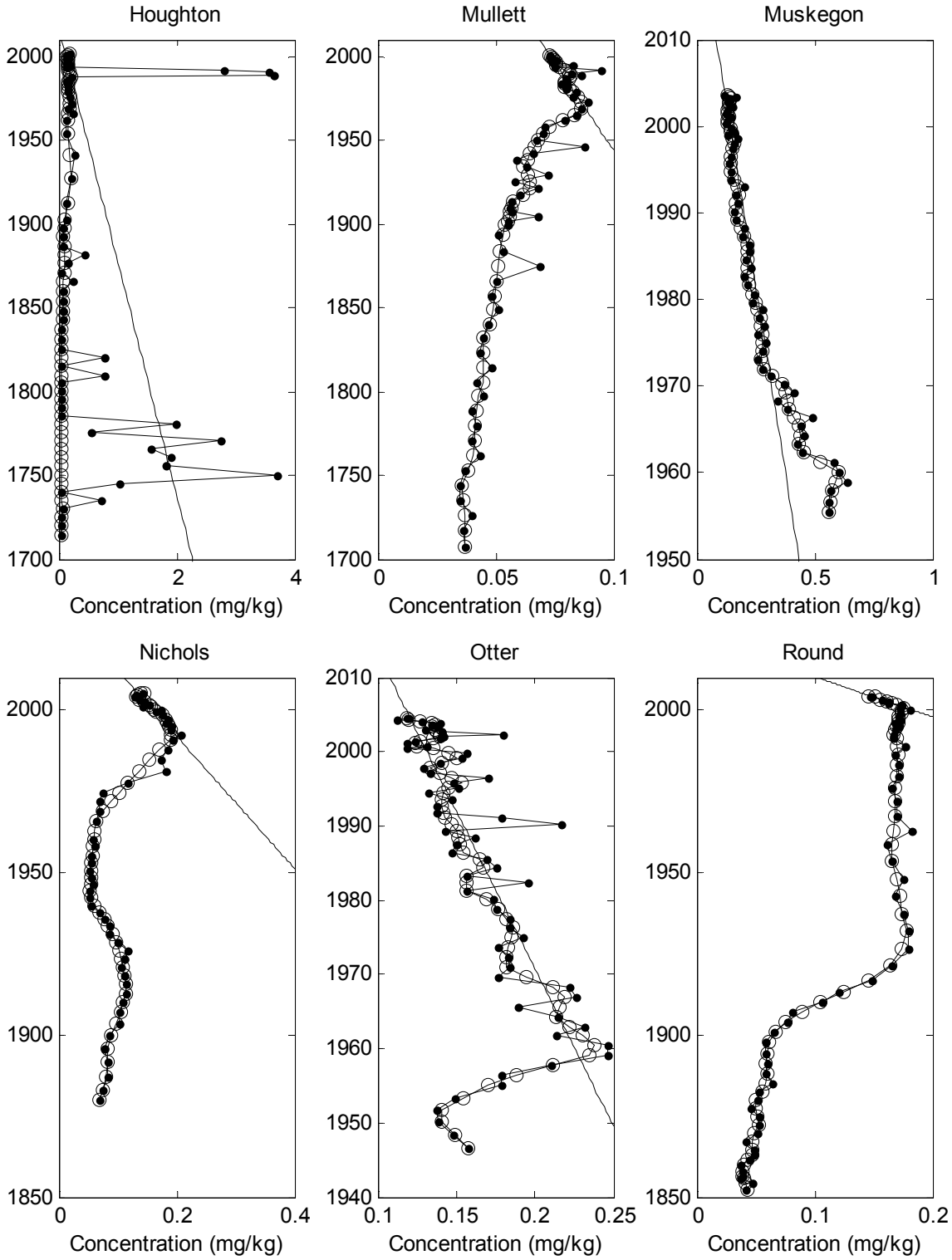

Figure 3.2 (cont'd)

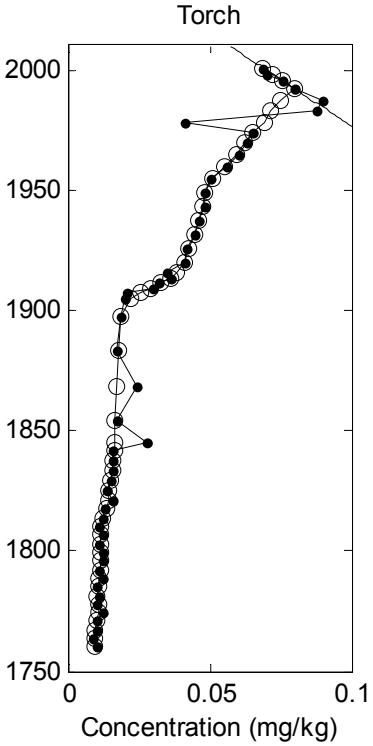

Results and Discussion

Using sediment chronologies to define recovery. The geochemistry of lake sediment is determined by three primary sources of material 1) what is deposited, wet or dry, from the atmosphere, 2) autocthonous production e.g., calcium carbonate deposition and 3) erosional inputs from the catchment. Groundwater input could also be considered a source, but for this discussion it is ignored since inputs of Hg would be small compared to the other three. This makes the sediment archive a composite of these sources and a recorder of differences in the rates at which material is delivered to the system. The recovery portion of the sediment archive is then a reflection of decreases in deposition and watershed export, autocthonous production is not considered since Hg would not be supplied by this process but rather its geochemical form altered. Although it is sometimes difficult to differentiate between atmospheric deposition and catchment export, it could be assumed that atmospheric deposition has not changed in the last

decade, or longer, as has been shown for this region (Prestbo and Gay, 2009) or that atmospheric deposition across the region would not vary enough to be reflected in sediment archives. Differences in the recovery slope are then mostly influenced by variation in watershed processes. A recovery slope closer to zero (plotting Hg on the abscissa and age on the ordinate) would be indicative of efficient removal of Hg from the landscape leading to the slow decline observed in the Hg profile. This could be from watershed activities that denude the landscape e.g., agriculture or watershed processes that lead to the rapid release of Hg. Conversely, a steep recovery slope suggests that Hg is being retained within the watershed quite possibly a result of a lack of activities that disturb the landscape or watershed attributes that tend to retain Hg.

Patterns of watershed attributes. The areal extent of the watersheds in this study ranged from 0.95 to more than 1300 km^2 with the majority falling below 200 km^2 (Table 1). Ratios of watershed area to lake area varied between 1.1 and 53 with most less than 10. Watersheds with a higher percentage of URB are located in the southeastern Lower Peninsula; those high in AG along the western half of the Lower Peninsula. Highly forested catchments are found in the northern Lower and Upper Peninsula and those in the southwest Lower Peninsula are the least forested. Soil erodibility values, K.F and K.FF, were generally low, less than 0.2 for most watersheds, indicative of clay soils found throughout the state. Sulfate deposition decreased from the South to the North which follows the general population and industrialization trend for the State, with the exception that sulfate deposition was higher in the southwest than the southeast Lower Peninsula(Yohn, 2004). This is likely an indication of the importance of the large Chicago, IL/Gary, IN industrial complex located near southwest Michigan.

Patterns of concentration recovery rates. Concentration recovery rates varied from -0.30 to -7.8 μg Hg kg^{-1} y^{-1} with the more positive values indicating a slower recovery rate, i.e., max and reference concentrations being equal a return to reference conditions would take more time. In lakes Gull, Houghton and Elk recovery rates were calculated from the mid-1960s until present. In other lakes the recovery rate had not changed for the last 10 y prior to sampling. One exception was Round D lake which exhibited a sharp decline in concentration around 2000, in this case the most recent slope, which contained 8 sediment slices, was used (Figure 3.2). This suggests that the choice of using the 2001 land use data set rather than an earlier data set was justified. Round D and Nichols lakes have the fastest rate of recovery while Charlevoix and Mullett lakes are recovering much more slowly (8-26 times slower, respectively). Lakes with very rapid concentration recovery rates have small watersheds that are primarily forested with very little urban or agricultural land uses. Differences in land use distribution between the slowest and fastest recovery rates appear at first glance to be a greater percentage of agricultural land use in watersheds of lakes with slower rates of recovery (Table 1). Similar rates of recovery were found for some lakes within close proximity of each other. This may be due to comparable rates of atmospheric deposition for these systems or could be due to a similar distribution of land use and rates of disturbances within their watersheds. For example, Elk and Torch lakes, located in northwest Lower Peninsula of Michigan have similar land use distributions within their, primarily forested, watersheds (Table 1) and similar concentration recovery rates. The rate of recovery for Gull Lake, located in the southwestern portion of the Lower Peninsula, is similar to the northwestern Lower Peninsula lakes. However, it has a very different land use distribution within it's, primarily agricultural, watershed and different rates of atmospheric deposition of Hg would be expected between these two areas of the State (Keeler and Dvonch, 2005). Others have

shown agricultural land-use to export Hg more rapidly than forested landscapes (Babiarz *et al.*, 1998, Hurley *et al.*, 1995a), but this does not help to explain why Gull Lake was similar to the northwestern Lower Peninsula lakes.

Patterns of flux recovery rates. Rates of flux recovery ranged from -0.09 to -2.7 μg Hg m^{-2} y^{-1} y^{-1} where more positive values again represent a slower rate of recovery. Much like the slopes of concentration recovery, flux recovery slopes had not changed 10 y prior to sampling the lake. Unlike concentration recovery; however, flux recovery rates were most rapid for Muskegon and George whereas Birch and Mullett lakes were the slowest. Common among the concentration and flux recovery rates was that Mullett had the slowest rate of recovery and that George had a high rate of recovery. Lake Charlevoix which did have a slow concentration recovery was amongst the more rapid flux recovery lakes. Lakes with more rapid flux recovery rates tended to have a higher percentage of URB while those with slower rates had higher AG land cover within a 100 m buffer of the lake. As with concentration recovery, lakes that are in close proximity to one another tended to have similar flux recovery rates, e.g., Torch and Elk.

Factors influencing concentration recovery rates. Watershed area, WA:LA, SD, LAT, soil erosion factors, and Hg emissions were not found to be significantly correlated to the rate of concentration recovery. This might have been expected if the rate of recovery is dependent upon land use and rate of disturbance of watershed soils rather than atmospheric deposition and proximity to local emission sources.

The strongest correlation of the concentration recovery rate to land use was found for agricultural land, but only along watershed flowpaths (LN AG.FLI2: $r = -0.75$, $p \leq 0.004$;

Hackert removed as outlier)) (Figure 3.3), the inverse relationship indicates that as AG.FLI2 increases the rate of concentration recovery slows. Other measures of agriculture within the watershed were also found to be significant but more poorly correlated, (AG.FLI: $r = -0.62$, $p = 0.025$; Birch, Gull and Hackert removed as outliers) and (LN AG: $r = -0.54$, $p = 0.087$; Birch and Gull removed as outliers). The association of slowed concentration recovery to AG found here is consistent with others that have found agricultural land use to be an important determinant for Hg accumulation (Balogh *et al.*, 1998, Engstrom *et al.*, 2007). However, these results suggest that where these activities are located within the landscape to be more explanatory than total areal extent.

Wetlands within the watershed were found to be moderately positively correlated (WET: $r = 0.65$, $p = 0.02$) to concentration recovery. The positive relationship means that lakes with greater areal extent of wetlands showed faster rates of recovery. Conversely, wetlands within the 100 m buffer of the shoreline were found to be negatively correlated (WET.M: $r = -0.61$, $p = 0.005$, Birch and Otter removed as outliers). What this demonstrates is that the proximity of the wetland to the lake shoreline plays an important role in the cycling of Hg in the watershed. Wetlands have been reported to be sources of methyl-Hg, but there is disagreement in the literature if they act as sinks (St. Louis *et al.*, 1996) or sources (Hurley *et al.*, 1995b, Mierle and Ingram, 1991) for total Hg. We interpret the contradiction between WET and WET.M to mean that wetlands on the landscape can act to sequester Hg, but when they are located close to the lake they can slowly release Hg, thus slowing the rate of recovery.

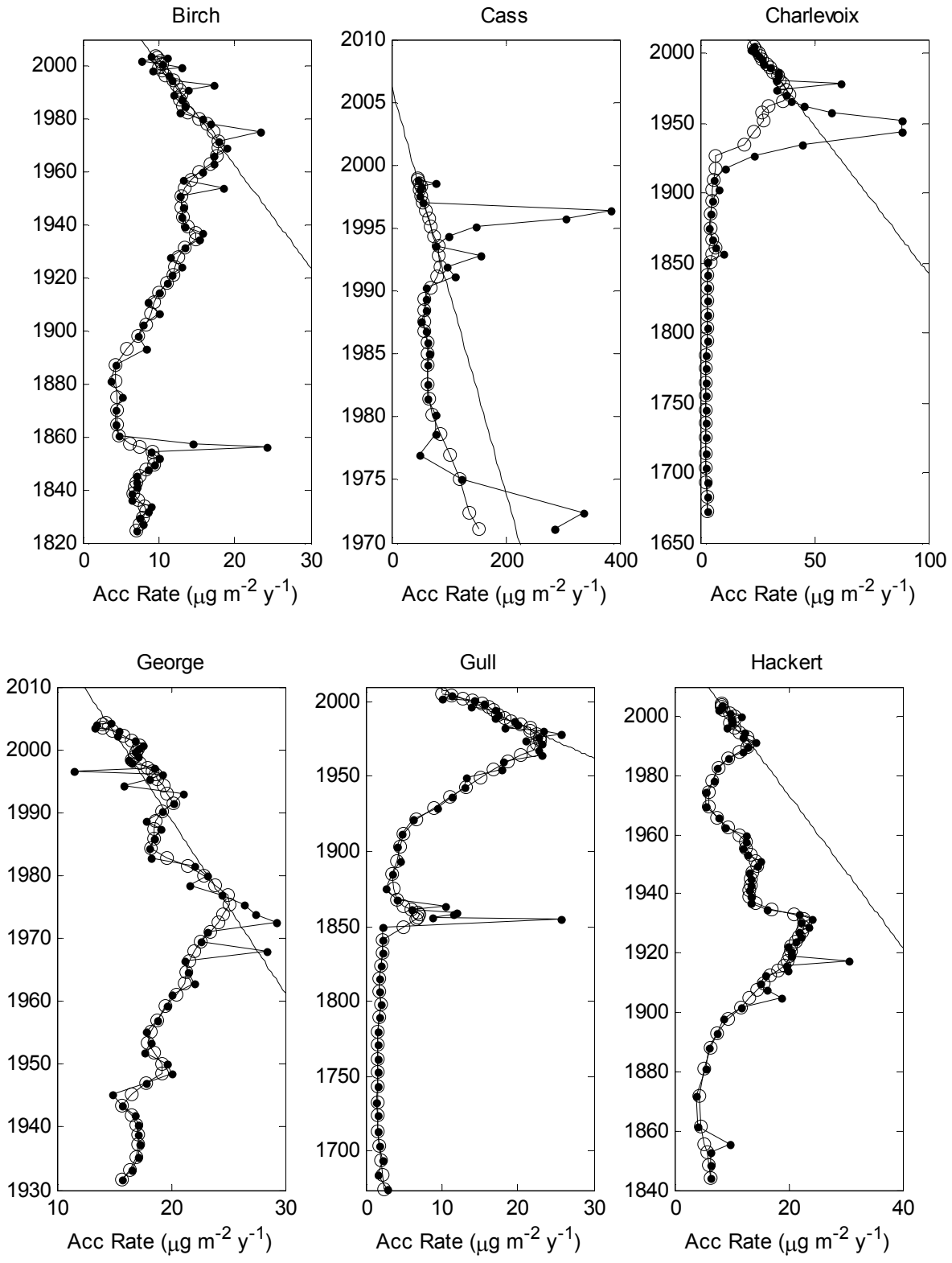

Figure 3.3. Mercury accumulation rate (Acc Rate) profiles (solid markers), results of profile smoothing (open markers) and recovery rate (solid line) for study lakes.

Figure 3.3 (cont'd)

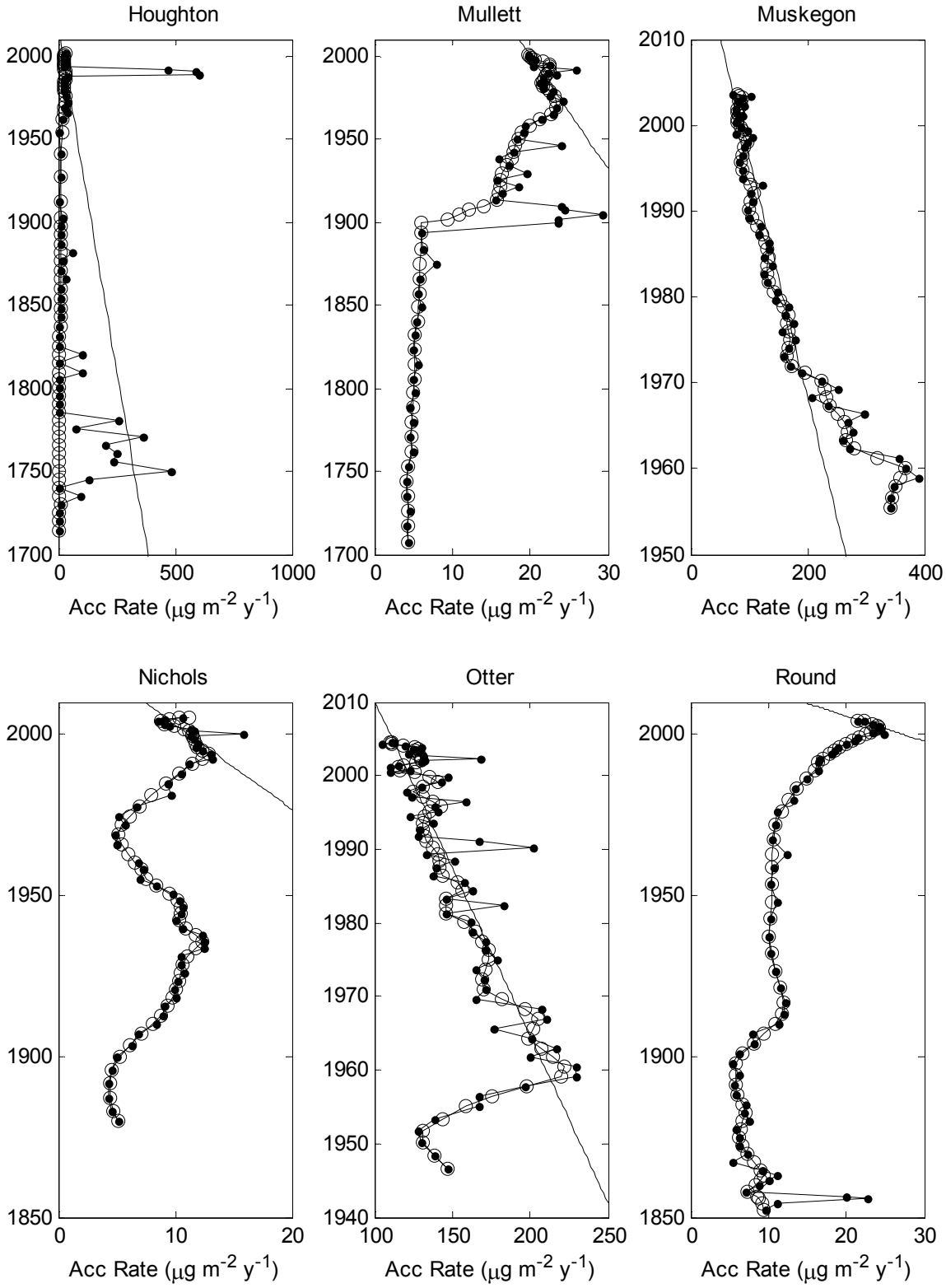

Figure 3.3 (cont'd)

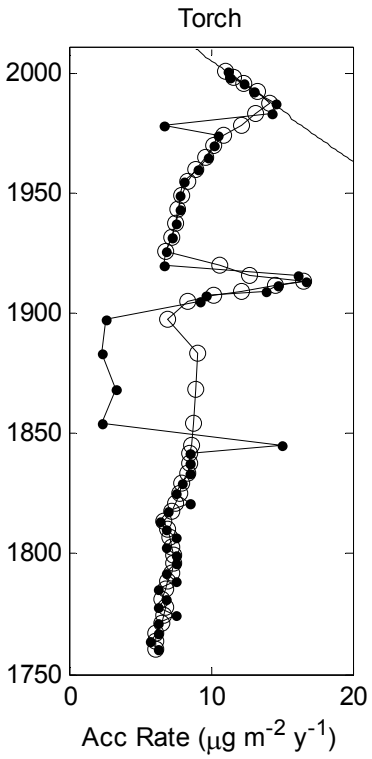

Forested land cover types along hydrodynamic flowpaths were also found to be significantly correlated to concentration recovery (FOR.FLI: r = -0.67, p = 0.02, Nichols and Round D removed as outliers; FOR.FLI2: r = -0.64, p = 0.06, Nichols, Round D, Houghton, and Muskegon removed as outliers). This result was not expected since forests have been found to be net sinks of Hg (Aastrup *et al.*, 1991, Engstrom and Swain, 1997, Harris *et al.*, 2007); if Hg is efficiently being sequestered then a more rapid recovery would be expected for highly forested landscapes. These results suggest that Hg is being released from forests along hydronamic flowpaths; however, thus slowing concentration recovery. This may be due to the ease of which run-off containing Hg laden particles can reach the lake using the high conductivity flowpaths and the fact that mercury concentrations are generally elevated in the litter and organic soils of forests due to the accumulation of Hg over decadal or longer time spans (Obrist *et al.*, 2011).

Factors influencing flux recovery rates. As with concentration recovery, none of the physical attributes of the watersheds, e.g., WA, were correlated to flux recovery rates and neither were soil erodibility, Hg emissions or sulfate deposition.

The relationships found to be significant for flux recovery were quite similar to those of concentration recovery. Percentage wetlands within the watershed was found to have the greatest correlation (Ln WET: $r = 0.68$, $p = 0.01$). As with concentration recovery, a proximity measure for wetlands was also found to be significantly correlated to flux recovery, WET.FLI (Ln WET.FLI: $r = -0.69$, $p = -0.02$; Houghton and Otter removed as outliers). The reasons for the relationships found for wetland variables correlated to flux recovery are similar to those for concentration recovery. Wetlands within the watershed act as traps for Hg leading to a faster recovery as WET increases; whereas, wetlands along the highly conductive flowpaths of the watershed tend to supply Hg to the lake, resulting in slower recovery. Proximity measures of forest cover types were also found to be significant (FOR.FLI: $r = -0.60$, $p = 0.05$; Nichols and Round D removed as outliers, FOR.FLI2: $r = -0.60$, $p = 0.09$; Round D, Nichols, Houghton, and Muskegon removed as outliers). Similar to the results found for concentration recovery, flux recovery became slower as the percentage of forest along hydronamic flowpaths increased. The arguments made for the relationship between concentration recovery and forest land cover are the same as those that can be made for flux recovery.

Noticeably absent from the analysis of flux recovery was the agricultural land cover types. This was not expected since agricultural land cover is generally associated with erosion of

the top soil layers leading to the export of contaminant laden particles (Balogh *et al.*, 1998, Engstrom *et al.*, 2007). It would have been anticipated then that increases in agricultural land cover would have led to a decreased rate of flux recovery. The reasons for the absence are unclear, but may be related to how drastically sedimentation rates are changed within highly agricultural watersheds compared to those lakes in highly forested landscapes and the changes in soil matrix that occurs as a result of erosional processes (Engstrom *et al.*, 2007).

Surprisingly, watershed attributes such as WA:LA, urban land cover, and Hg emissions were not identified as significant determinants of flux or concentration recovery. The ratio of watershed to lake area has well been established as a predictor of Hg accumulation rates (Kamman and Engstrom, 2002, Lorey and Driscoll, 1999, Swain *et al.*, 1992). The model suggests that as WA:LA increased Hg accumulation rate is predicted to rise due to the greater surface area for atmospheric deposition and potential for export to the lake. It was expected then that lakes with a larger WA:LA would have slower rates of recovery since the soil pool available for export is greater. However, this relationship appears to break down when lakes are not in close proximity to each other or the group of lakes is diverse (Drevnick *et al.*, 2011, Muir *et al.*, 2009) as would be the case for lakes in this study (Figure 3.1, Table 3.1).

Urban landscapes have been suggested to export less Hg than other land cover types in recent decades due to decreases in atmospheric deposition and the lack of watershed disturbance (Engstrom and Swain, 1997). It would then be anticipated that URB would be correlated to the rate of recovery with those lakes high in urban land cover having faster recovery rates. Our data, although representing a broad range of watershed characteristics, had a maximum urban land

cover of 25% (Cass Lake) with most lakes less than 10%. Interestingly, Cass Lake had one of the fastest flux recovery rates which may be a reflection of greater urban land cover. However, the lack of distribution and representation of true "urban" lakes (URB > 50%) may be contributing to the lack of significant correlation.

It was hypothesized that recovery rates would be slower in lakes that had high emission rates, but emissions were not found to be significantly correlated regardless of the radius chosen. Other variables used to represent atmospheric deposition, e.g., SD and LAT, were also found unimportant. The lack of relationship could be related to the atmospheric transport of Hg and the possibility that Hg is being deposited far from the source; although, many studies have shown that the majority of Hg deposited derives from local to regional scale sources (Donahue *et al.*, 2006, Keeler *et al.*, 2006, Menounou and Presley, 2003). It has been shown that only a portion of the Hg deposited to the catchment is immediately transported to lake with most of the watershed load being made up of "legacy" Hg (Harris *et al.*, 2007). This means that it may have been more appropriate to use estimates from earlier decades rather than current emissions. However, if the pattern of Hg emissions has not changed greatly, a likely scenario, then this analysis would have resulted in similar outcomes. If the majority of Hg is retained in the watershed, mostly sorbed to soil organic matter (Grigal, 2003, Meili, 1991, Obrist *et al.*, 2011, Schuster, 1991, Skyllberg *et al.*, 2000), it is then those activities within the catchment that disturb the soil Hg pool that control export and therefore recovery. That is not to say that atmospheric emission and deposition of Hg are unimportant but rather the relative impact of these activities compared to watershed processes is small when comparing lakes within a region.

Although this analysis singles out certain watershed attributes that influence recovery from Hg enrichment it is likely that it is a combination of factors that in coordination determine the shape of Hg profiles and the trajectory of recovery. That being said, this work has important implications for natural resource and watershed managers in that the locations of activities and processes within the watershed were found to be significant which may help investigators identify areas of interest in future catchment studies of Hg cycling.

REFERENCES

REFERENCES

Aastrup, M., Johnson, J., Bringmark, E., Bringmark, L., Iverfeldt, A., 1991. Occurrence and Transport of Mercury within a Small Catchment-Area. Water Air and Soil Pollution 56, 155-167.

Alfaro-De la Torre, M.C., Tessier, A., 2002. Cadmium deposition and mobility in the sediments of an acidic oligotrophic lake. Geochimica et Cosmochimica Acta 66, 3549-3562.

Appleby, P.G., 2001. Chronostratigraphic Techniques in Recent Sediments. In: W. M. Last, J. P. Smol (Eds.), Tracking Environmental Change Using Lake Sediments. Kluwer Academic Publishers, Boston, pp. 171-205.

Appleby, P.G., Oldfield, F., 1978. The calculation of ^{210}Pb dates assuming a constant rate of supply of unsupported ^{210}Pb to the sediment. Catena 5, 1-8.

Babiarz, C.L., Hurley, J.P., Benoit, J.M., Shafer, M.M., Andren, A.W., Webb, D.A., 1998. Seasonal influences on partitioning and transport of total and methylmercury in rivers from contrasting watersheds. Biogeochemistry 41, 237-257.

Balogh, S.J., Meyer, M.L., Johnson, D.K., 1998. Transport of mercury in three contrasting river basins. Environmental Science & Technology 32, 456-462.

Bindler, R., Renberg, I., Appleby, P.G., Anderson, N.J., Rose, N.L., 2001. Mercury accumulation rates and spatial patterns in lake sediments from west Greenland: A coast to ice margin transect. Environmental Science and Technology 35, 1736-1741.

Donahue, W.F., Allen, E.W., Schindler, D.W., 2006. Impacts of coal-fired power plants on trace metals and polycyclic aromatic hydrocarbons (PAHs) in lake sediments in central Alberta, Canada. Journal of Paleolimnology 35, 111-128.

Drevnick, P.E., Engstrom, D.R., Driscoll, C.T., Swain, E.B., Balogh, S.J., Kamman, N.C., Long, D.T., Muir, D.C.G., Parsons, M.J., Rolfhus, K.R., Rossmann, R., 2011. Spatial and Temporal Patterns of Mercury Accumulation in Lacustrine Sediments across the Laurentian Great Lakes Region. Environmental Pollution In Press.

Engstrom, D.R., Balogh, S.J., Swain, E.B., 2007. History of mercury inputs to Minnesota lakes: Influences of watershed disturbance and localized atmospheric deposition. Limnology and Oceanography 52, 2467-2483.

Engstrom, D.R., Swain, E.B., 1997. Recent declines in atmospheric mercury deposition in the upper Midwest. Environmental Science and Technology 31, 960-967.

ARC/INFO, Environmental Systems Research Institute, 1998. ARC/INFO

Evers, D.C., Wiener, J.G., Driscoll, C.T., Gay, D.A., Basu, N., Monson, B.A., Lambert, K.F., Morrison, H.A., Morgan, J.T., Williams, K.A., Soehl, A.G., 2011. Great Lakes Mercury

Connections: The Extent and Effects of Mercury Pollution in the Great Lakes Region. Biodiversity Research Institute. Gorham, MA. Report BRI 2011-18, 44 pages. Available from: http://www.briloon.org/mercuryconnections/GreatLakes.

Golden, K.A., Wong, C.S., Jeremiason, J.D., Eisenreich, S.J., Sanders, M.G., Hallgren, J., Swackhammer, D.L., Engstrom, D.R., Long, D.T., 1993. Accumulation and preliminary inventory of organochlorines in Great Lakes sediments. Water Science and Technology 28, 19-31.

Grigal, D.F., 2003. Mercury sequestration in forests and peatlands: A review. Journal of Environmental Quality 32, 393-405.

Harris, R.C., Rudd, J.W.M., Amyot, M., Babiarz, C.L., Beaty, K.G., Blanchfield, P.J., Bodaly, R.A., Branfireun, B.A., Gilmour, C.C., Graydon, J.A., Heyes, A., Hintelmann, H., Hurley, J.P., Kelly, C.A., Krabbenhoft, D.P., Lindberg, S.E., Mason, R.P., Paterson, M.J., Podemski, C.L., Robinson, A., Sandilands, K.A., Southworth, G.R., Louis, V.L.S., Tate, M.T., 2007. Whole-ecosystem study shows rapid fish-mercury response to changes in mercury deposition. Proceedings of the National Academy of Sciences of the United States of America 104, 16586-16591.

Heyvaert, A.C., Reuter, J.E., Slotton, D.G., Goldman, C.R., 2000. Paleolimnological reconstruction of historical atmospheric lead and mercury deposition at Lake Tahoe, California-Nevada. Environmental Science and Technology 34, 3588-3597.

Hightower, J., Moore, D., 2003. Mercury Levels in High-End Consumers of Fish. Environmental Health Perspectives 111, 604-608.

Hurley, J.P., Benoit, J.M., Babiarz, C.L., Shafer, M.M., Andren, A.W., Sullivan, J.R., Hammond, R., Webb, D.A., 1995a. Influences of Watershed Characteristics on Mercury Levels in Wisconsin Rivers. Environmental Science & Technology 29, 1867-1875.

Hurley, P.J., Benoit, J.M., Babiarz, C.L., Shafer, M.M., Andren, A.W., Sullivan, J.R., Hammond, R., Webb, D.A., 1995b. Influences of watershed characteristics on mercury levels in Wisconsin rivers. Environmental Science and Technology 29, 1867-1875.

National Atmospheric Deposition Program (NRSP-3), Illinois State Water Survey, NADP Program Office, 2204 Griffith Drive, Champaign, IL 61820, Available online at http://nadp.sws.uiuc.edu/mdn/. (Accessed: February 5, 1998).

Kamman, N.C., Engstrom, D.R., 2002. Historical and present fluxes of mercury to Vermont and New Hampshire lakes inferred from Pb-210 dated sediment cores. Atmospheric Environment 36, 1599-1609.

Keeler, G.J., Dvonch, J.T., 2005. Atmospheric mercury: A decade of observations in the Great Lakes. In: N. Pirrone, K. Mahaffey (Eds.), Dynamics of Mercury Pollution on Regional

and Global Scales: Atmospheric Processes and Human Exposures around the World. Kluwer Ltd., Norwell, MA.

Keeler, G.J., Landis, M.S., Norris, G.A., Christianson, E.M., Dvonch, J.T., 2006. Sources of mercury wet deposition in Eastern Ohio, USA. Environmental Science & Technology 40, 5874-5881.

Long, D.T., Parsons, M.J., Yansa, C.H., Yohn, S.S., McLean, C.E., Vannier, R.G., 2010. Assessing the response of watersheds to catastrophic (logging) and possible secular (global temperature change) perturbations using sediment-chemical chronologies. Applied Geochemistry 25, 143-158.

Lorey, P., Driscoll, C.T., 1999. Historical trends in mercury deposition in Adirondack Lakes. Environmental Science and Technology 33, 718-722.

Matlab, The Mathworks, 1994 - 2008. Matlab Student 7.0.1.

Meili, M., 1991. The Coupling of Mercury and Organic-Matter in the Biogeochemical Cycle - Towards a Mechanistic Model for the Boreal Forest Zone. Water, Air, and Soil Pollution 56, 333-347.

Menounou, N., Presley, B.J., 2003. Mercury and other trace elements in sediment cores from central texas lakes. Archives of Environmental Contamination and Toxicology 45, 11-29.

Michigan Department of Natural Resources, 2003. IFMAP/GAP land cover. In: MDNR (Ed.), Lansing, MI,

Mierle, G., Ingram, R., 1991. The Role of Humic Substances in the Mobilization of Mercury from Watersheds. Water Air and Soil Pollution 56, 349-357.

Muir, D.C.G., Wang, X., Yang, F., Nguyen, N., Jackson, T.A., Evans, M.S., Douglas, M., Kock, G., Lamoureux, S., Pienitz, R., Smol, J.P., Vincent, W.F., Dastoor, A., 2009. Spatial Trends and Historical Deposition of Mercury in Eastern and Northern Canada Inferred from Lake Sediment Cores. Environmental Science & Technology 43, 4802-4809.

Munthe, J., Bodaly, R.A., Branfireun, B.A., Driscoll, C.T., Gilmour, C.C., Harris, R., Horvat, M., Lucotte, M., Malm, O., 2007a. Recovery of mercury-contaminated fisheries. Ambio 36, 33-44.

Munthe, J., Hellsten, S., Zetterberg, T., 2007b. Mobilization of mercury and methylmercury from forest soils after a severe storm-fell event. Ambio 36, 111-113.

Munthe, J., Hultberg, H., 2004. Mercury and methylmercury in runoff from a forested catchment: concentrations, fluxes, and their response to manipultions. Water Air and Soil Pollution: Focus 4, 607-618.

Obrist, D., Johnson, D.W., Lindberg, S.E., Luo, Y., Hararuk, O., Bracho, R., Battles, J.J., Dail, D.B., Edmonds, R.L., Monson, R.K., Ollinger, S.V., Pallardy, S.G., Pregitzer, K.S., Todd, D.E., 2011. Mercury Distribution Across 14 US Forests. Part I: Spatial Patterns of Concentrations in Biomass, Litter, and Soils. Environmental Science & Technology 45, 3974-3981.

Parsons, M.J., Long, D.T., Yohn, S.S., Giesy, J.P., 2007. Spatial and Temporal Trends of Mercury Loadings to Michigan Inland Lakes. Environmental Science and Technology 41, 5634-5640.

Porvari, P., Verta, M., Munthe, J., Haapanen, M., 2003. Forestry practices increase mercury and methyl mercury output from boreal forest catchments. Environmental Science & Technology 37, 2389-2393.

Prestbo, E.M., Gay, D.A., 2009. Wet deposition of mercury in the US and Canada, 1996-2005: Results and analysis of the NADP mercury deposition network (MDN). Atmospheric Environment 43, 4223-4233.

Schuster, E., 1991. The Behavior of Mercury in the Soil with Special Emphasis on Complexation and Adsorption Processes - A Review of the Literature. Water Air and Soil Pollution 56, 667-680.

Skyllberg, U., Xia, K., Bloom, P.R., Nater, E.A., Bleam, W.F., 2000. Binding of mercury(II) to reduced sulfur in soil organic matter along upland-peat soil transects. Journal of Environmental Quality 29, 855-865.

St. Louis, V.L., Rudd, J.W.M., Kelly, C.A., Beaty, K.G., Flett, R.J., Roulet, N.T., 1996. Production and loss of methylmercury and loss of total mercury from boreal forest catchments containing different types of wetlands. Environmental Science & Technology 30, 2719-2729.

Swain, E.B., Engstrom, D.R., Brigham, M.E., Henning, T.A., Brezonik, P.L., 1992. Increasing Rates of Atmospheric Mercury Deposition in Midcontinental North-America. Science 257, 784-787.

R version 2.6.2, 2008. R version 2.6.2

Turetsky, M.R., Harden, J.W., Friedli, H.R., Flannigan, M., Payne, N., Crock, J., Radke, L., 2006. Wildfires threaten mercury stocks in northern soils. Geophysical Research Letters 33.

US EPA, 2008. Air Pollution Prevention and Control. US EPA.Government Printing Office, Washington, D.C.

State Soil Geographic (STATSGO) Database for Michigan, Available online at http://www.ncgc.nrcs.usda.gov/products/datasets/statsgo/index.html. (Accessed: September 25, 2011).

USEPA. Office of Solid Wastes. *Mercury in solids and solutions by thermal decomposition, amalgamation, and atomic absorption spectrophotometry*; Government Printing Office, 1998.

USEPA. Office of Research and Development Office of Air Quality Planning and Standards. *Mercury Study Report to Congress*; Washington, DC: Government Printing Office, 1997.

US EPA, 2010. National Emissions Inventory, Available online at http://www.epa.gov/ttn/chief/index.html. (Accessed: June 1, 2010).

United States Geological Survey, The National Map Seamless Server, Available online at http://seamless.usgs.gov/index.php. (Accessed: September 25, 2011).

Yohn, S.S. 2004. Natural and Anthropogenic Factors Influencing Spatial and Temporal Patterns of Metal Accumulation in Inland Lakes. Thesis, Michigan State University, East Lansing, MI.

CHAPTER 4
INFERRING SOURCES FOR MERCURY TO INLAND LAKES USING SEDIMENT CHRONOLOGIES OF POLYCYCLIC AROMATIC HYDROCARBONS

Abstract

Sediment chronologies from inland lakes suggest the influence of local to sub-regional scale sources for Hg. However, source apportionment using sediment chronologies is difficult due to the mixing of sources and pathways. Mercury and polycyclic aromatic hydrocarbons (PAH) concentration profiles often share common sources and pathway into the environment. Therefore, sediment cores from seven inland lakes of Michigan were collected for the measurement of PAHs and Hg and dated using ^{210}Pb. To infer sources of PAHs and Hg, assuming common source, diagnostic ratios of kinetic and thermodynamic PAH isomers were used. Ratios indicate the existence of modern combustion sources to each lake and historic combustion sources to lakes near cement kilns and an iron foundry. Coal combustion sources were identified for two lakes near urban centers. Whereas a petroleum combustion source was identified for a lake that has a coal fired power plant along its shoreline. These results therefore have implications for the cycling of Hg on local to regional scales.

Introduction

Several studies have shown that much of the anthropogenic mercury (Hg) emitted to the atmosphere is a result of the combustion of coal and petroleum products (Bindler, 2003, Fitzgerald, 1989, Kamman and Engstrom, 2002, Keeler *et al.*, 2006, Landis *et al.*, 2002, Lindberg *et al.*, 2007, Long *et al.*, 1995, Menounou and Presley, 2003, Pacyna *et al.*, 2006, Watras *et al.*, 1994). As a result of its physical properties Hg can reside in the atmosphere for up to a year resulting in global transport (Fitzgerald *et al.*, 1998). For example, several studies have

shown that Hg emitted in Asia has reached the North American continent (Boutron *et al.*, 1998, Durnford *et al.*, 2010, Jaffe *et al.*, 2005, Jaffe and Strode, 2008, Obrist *et al.*, 2008, Reidmiller *et al.*, 2009, Valente *et al.*, 2007). Still others have demonstrated that much of the Hg emitted to the atmosphere can be attributed to local and regional sources (Donahue *et al.*, 2006, Keeler *et al.*, 2006). As current environmental legislation (US EPA, 2011) attempts to reduce Hg release determining the source, especially the distinction between local, regional and global, becomes of impending importance. Environmental archives of Hg (e.g., sediment and ice cores) have been used by others to elucidate the likely source of Hg by comparing the record to national production and consumption records (Engstrom and Swain, 1997) and event-based markers (e.g., major volcanic eruptions) (Schuster *et al.*, 2002). However, it is difficult to recognize the potential of local sources using these methods since only national trends are used or, in the case of ice cores, no local sources exist. The study of source apportionment has been approached using atmospheric deposition collectors and multivariate statistical techniques providing evidence of local to global scale sources (Dvonch *et al.*, 1999, Dvonch *et al.*, 1998, Keeler *et al.*, 2006). Their use is limited; however, due to the lack of atmospheric collectors and the uneven distribution of collectors throughout a region, nation or the world (Evers *et al.*, 2011).

Inland lakes are widely distributed and when many lakes can be sampled across a broad region have the potential to discriminate between local and regional sources. However, since sediments incorporate both direct atmospheric sources and watershed processes the interpretation of source can become difficult. This may be overcome if an independent marker could be used to infer source. Polycyclic aromatic hydrocarbons (PAHs) are primarily formed during the incomplete combustion of petroleum products and organic material (e.g., vegetation) (Hites *et*

al., 1977). Due to their volatility PAHs can remain in the atmosphere after emission which can result in long distance transport (Killin *et al.*, 2004, Sofowote *et al.*, 2011, Usenko *et al.*, 2010), but can also be deposited nearer the source as a result of their particle reactivity (Barrick and Prahl, 1987). Because they are particle reactive sediment chronologies can be used to infer the record of their release to the environment (Hites *et al.*, 1977). There are a variety of activities that result in a release of PAHs into the environment (e.g., coal combustion and vehicular exhaust) and the sedimentary record is a mixture of all sources which can make source apportionment difficult. Sources of PAHs can be natural (e.g., oil seeps, bitumens, and forest fires) or anthropogenic (fossil fuels and combustion) (Yunker and Macdonald, 2003, Yunker *et al.*, 2002). Unique diagnostic ratios of PAHs have been shown to be useful in the identification of types of sources (Howe *et al.*, 2004, Simcik *et al.*, 1999, Sofowote *et al.*, 2010, Yunker and Macdonald, 2003, Zheng *et al.*, 2011).

There have been many studies that measured metals and PAHs in the environment (Di Leonardo *et al.*, 2009, Donahue *et al.*, 2006, Gnandi *et al.*, 2011, Mzoughi and Chouba, 2011). However, few of these studies investigated the correlations in environmental loading between them even though there is strong evidence that they might share common sources and pathways. For example, the sum of PAHs measured in aerosols from the North Sea was found to be significantly correlated to lead and other heavy metals (Chester *et al.*, 1993). In a study designed to investigate the impact of vehicular emissions on roadways a multivariate statistical analysis showed that Hg tended to cluster with the PAHs rather than the other trace metals, such as lead and zinc (Zechmeister *et al.*, 2006) which could be an indication of the shared combustion source and pathway for Hg and PAHs in vehicular exhaust. In New Orleans, LA, USA it was found that

PAH ratios indicated a pyrolytic source and that the PAHs were moderately correlated to trace metals (Wang *et al.*, 2004).

A significant problem with the use of diagnostic ratios of PAHs is the differential degradation of individual PAHs which are driven by differences in vapor pressure and resistance to photolytic decay (Yunker *et al.*, 1999, Zhang *et al.*, 2005). Differences in the rate of degradation are greatest amongst the lower molecular weight PAHs, e.g., anthracene, making the use of diagnostic ratios that compare lower molecular weight PAHs troublesome. Corrections for differential degradation can be made when meteorological and source data are available (Zhang *et al.*, 2005); however, in most cases, and is the case in this study, these data are unavailable. To overcome this issue most studies of PAHs in the environment use multiple diagnostic ratios of PAHs (Yunker and Macdonald, 2003).

This work is a portion of the larger Michigan Department of Natural Resources and Environment Sediment Trends Monitoring Program (Michigan, 2011b). Lakes for this study were chosen to investigate the hypothesis that Hg is derived mainly from local to regional scales sources. If true then diagnostic ratios should identify local to regional scale sources or show a lack of impact from global scale combustion sources.

Materials and Methods

A detailed description of core collection (Parsons *et al.*, 2007), ^{210}Pb dating (Parsons *et al.*, 2007), Hg (Parsons *et al.*, 2007) and PAH analysis (Kannan *et al.*, 2005) can be found elsewhere. Briefly, cores were collected aboard the MDNRE R/V *Nibi* or US EPA R/V *Mudpuppy* using an Ocean Instruments MC-400 and sectioned on-shore immediately after collection. Separate cores

were used for ^{210}Pb dating, metals and organic analyses. Sectioning of the Hg and ^{210}Pb core was performed at equal intervals, 0.5 cm increments for the first 8 cm and 1 cm intervals thereafter. The entire organics core was sectioned at 1 cm intervals. Due to the limited quantity of sediment collected at 1-cm intervals, equal amounts of sediment were combined from successive sediment samples starting from the top of the core.

Table 4.1. PAH parameters and abbreviations.

Mass	**Compound**	**Abbreviation**
152	Acenaphthylene	Ayl
154	Acenaphthene	Aen
166	Fluorene	F
178	Phenanthrene	Ph
	Anthracence	An
202	Pyrene	Py
	Fluoranthene	Fl
228	Chrysene	Ch
	Benz[*a*]anthracene	BaA
252	Benzo[*b*]fluoranthene	BF
	Benzo[*j*]fluoranthene	BF
	Benzo[*k*]fluoranthene	BF
276	Benzo[*ghi*]perylene	BghiP
	Indeno[1,2,3-*cd*]pyrene	IP
278	Dibenz[a,h]anthracene	DhA

Mercury analysis was performed using an Ohio Lumex Hg Analyzer according to EPA Method 7473. Measurements of ^{210}Pb were made by Paul Wilkinson at the University of Winnipeg's Freshwater Institute; ^{137}Cs was measured to verify age estimates. The US EPA's 16 priority PAHs were analyzed using gas chromatography-mass spectrometry. Sediments for organics analysis were Soxhlet extracted then treated with activated copper. Extracts were passed through 10 g of activated Florisil (60-100 mesh; Sigma, St. Louis, MO) and the fraction eluted with 100 mL of 20% dichloromethane in hexane and then concentrated. Results of PAHs

are reported here as ng/g dry weight. Total PAHs (ΣPAH) is defined here as the sum of all 16 US EPA priority PAHs, Table 1.

Since the organics core was not sectioned at the same intervals as the ^{210}Pb core dates for the organic core were estimated by calculating the local polynomial regression of depth versus age using the *loess* command in the statistical package R (The R Foundation for Statistical Computing, 2008). Mercury concentrations were then estimated by interpolation using the estimated dates from the regression analysis.

Results and Discussion

Patterns of PAH and Hg. Lakes chosen for this study (Figure 4.1) had at least a moderately high correlation (Pearson's $r > 0.7$, Table 1) between ΣPAH and Hg possibly indicating a common source for these contaminants. The pattern of peak and surficial ΣPAH loosely follows the South to North industrialization and population trend, a pattern which was also found for peak lead (Pb) concentrations for this region (Yohn *et al.*, 2004). The higher surficial and peak ΣPAH concentrations in Muskegon and Otter suggest a more local than regional source which was found for Pb. Peak and surficial ΣPAHs were greatest in Otter and lowest in Avalon Lake. The year of peak ΣPAH concentration occurred earliest in Avalon, 1915, and Round lakes, 1929, whereas peak concentration was observed in the surficial sediments of Crystal Lake. The timing of peak ΣPAHs in Avalon and Round are not consistent with the peak in atmospheric deposition described by others (Barrick and Prahl, 1987, Fernandez *et al.*, 2000, Lima *et al.*, 2003, Wakeham *et al.*, 1980, Yunker and Macdonald, 2003); peaks in ΣPAH near the turn of the last century have been attributed to the burning of wood, e.g., forest fires and home heating

(Fernandez *et al.*, 2000). Crystal Lake showed a peak in the middle of the last century (Figure 4.2c) consistent with an anthropogenic combustion source, but had higher concentrations in the surficial sediment which may be evidence of newer sources. The year of peak ΣPAH concentrations corresponded to the year of peak Hg concentration in Round Lake. Muskegon, Otter and Sand lakes had peak ΣPAH years similar to that of Hg; whereas, Avalon, Birch and Crystal lakes peak ΣPAH and Hg concentrations did not occur in the same year. Surficial Hg concentrations were lowest in Avalon and greatest in Round and there is a positive correlation between surficial Hg and ΣPAHs concentrations. Lakes with greatest PAH and Hg concentrations tend to be located near urban centers of the State; Muskegon near the City of Muskegon, Otter near the City of Flint, and Sand near the City of Detroit. The exception being Round, located in the Michigan's Upper Peninsula, which could be described as a remote lake lacking significant urban development other than sparse shoreline housing.

Table 4.2. ΣPAHs (ng/g dry wt) and Hg (mg/kg dry wt) concentration in the surficial sediments and at maximum. The first column shows the Pearson's correlation coefficient between Hg and ΣPAH.

Lake	r	ΣPAHs (surficial)	ΣPAHs (peak)	ΣPAH Peak Year	Hg (surficial)	Hg (peak)	Hg Peak Year
Avalon	0.75	949	1612	1915	0.050	0.052	1971
Birch	0.86	1224	2093	1957	0.068	0.095	1977
Crystal	0.90	1707	1707	2006	0.082	0.084	1990
Muskegon	0.70	2844	4663	1978	0.16	0.37	1973
Otter	0.76	3323	8046	1958	0.12	0.25	1960
Round	0.92	1888	1977	1929	0.17	0.18	1929
Sand	0.92	1849	2932	1982	0.095	0.12	1988

Prior to the rise of ΣPAHs in the late 1800s and early 1900s mass 252 PAH dominate the core profile in Avalon, Birch, Crystal and Round Lakes (Figure 4.2a-c & 4.2f). This is in contrast to what has been found for the Fraser River Basin (Yunker *et al.*, 2002) where the mass 178 and 202 PAHs were dominant. This may suggest a petrogenic origin for the mass 252 PAHs to these

lakes (Yunker *et al.*, 1993). In Sand Lake (Figure 4.2g) mass 178 and 202 were greater than the other PAHs which is consistent with the burning of grass, hardwood and softwoods (Fine *et al.*, 2001, Jenkins *et al.*, 1996, Masclet *et al.*, 1995). Masses 228 and 276 were for the most part the least prevalent PAH prior to 1900 in all lakes which, a reflection of the lack of fossil fuel combustion in the region at the time (Yunker and Macdonald, 2003).

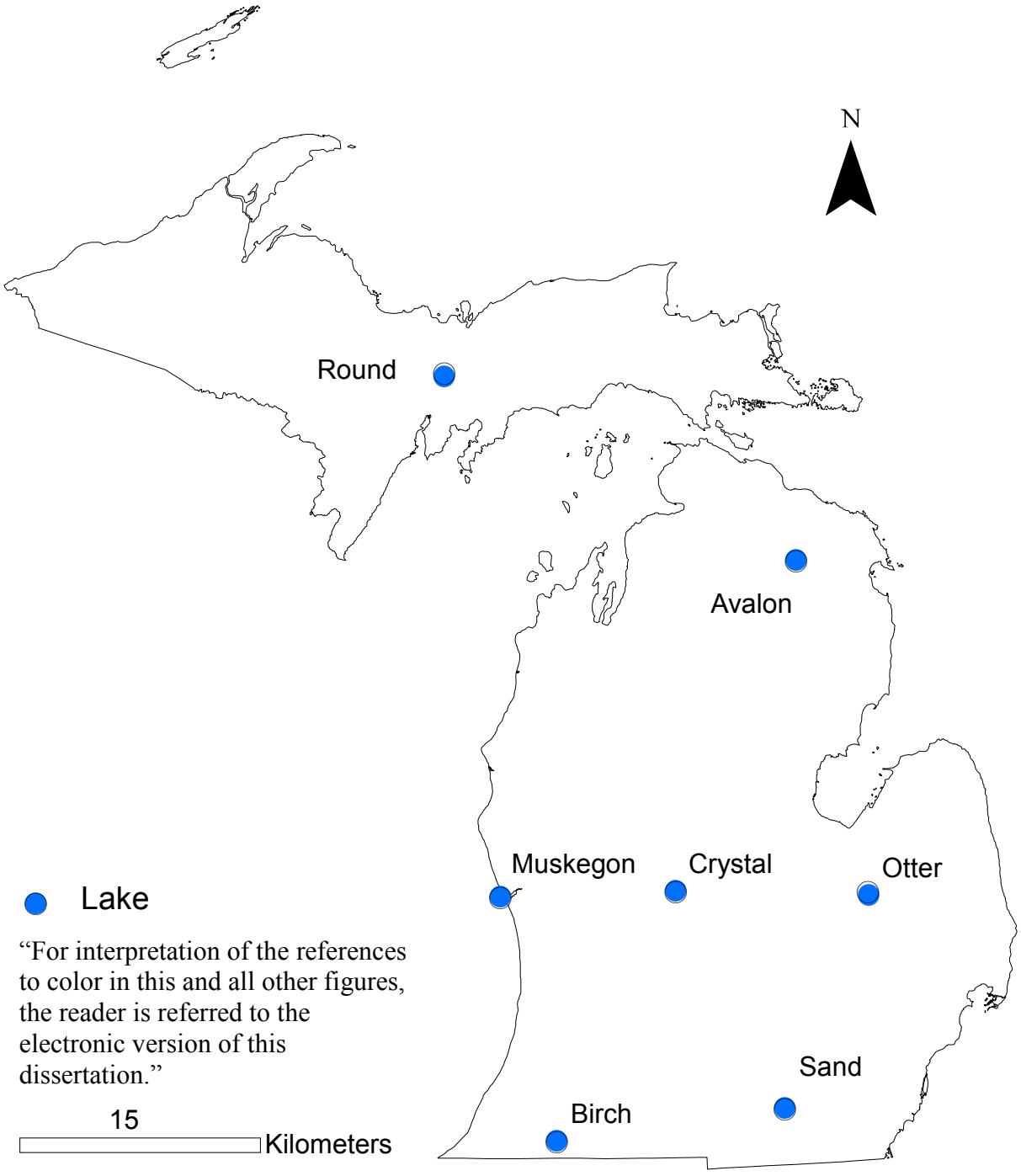

Figure 4.1. Study lakes.

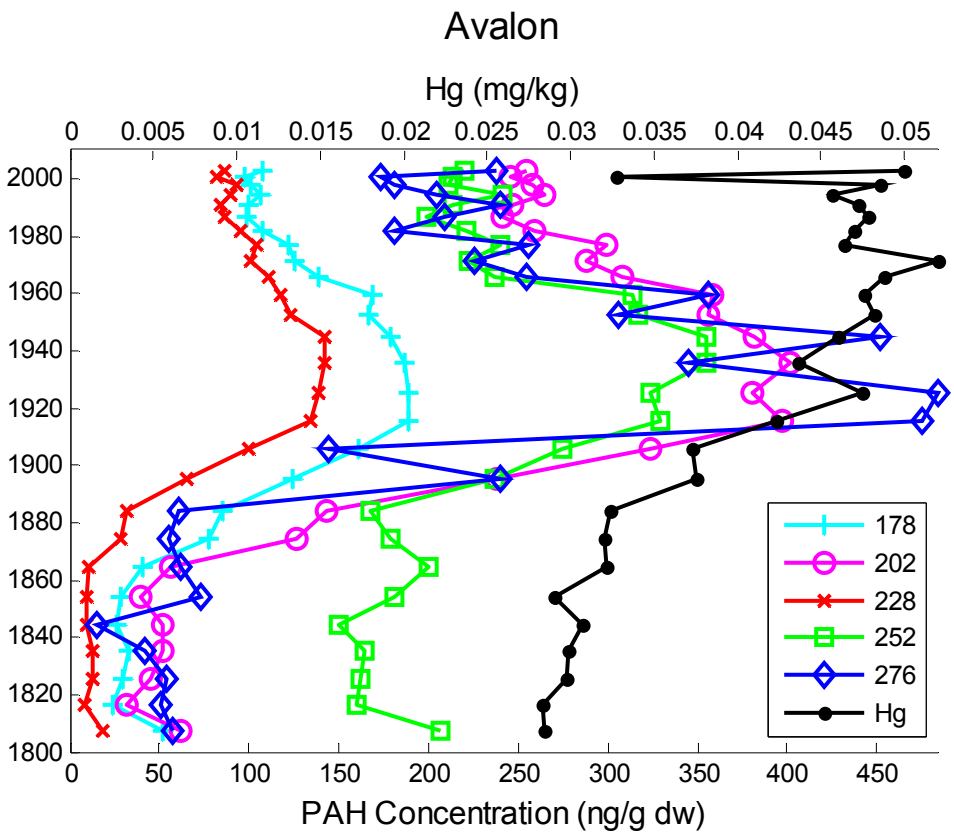

Figure 4.2a. Concentration profiles of Hg and PAH isomer groups for Avalon Lake.

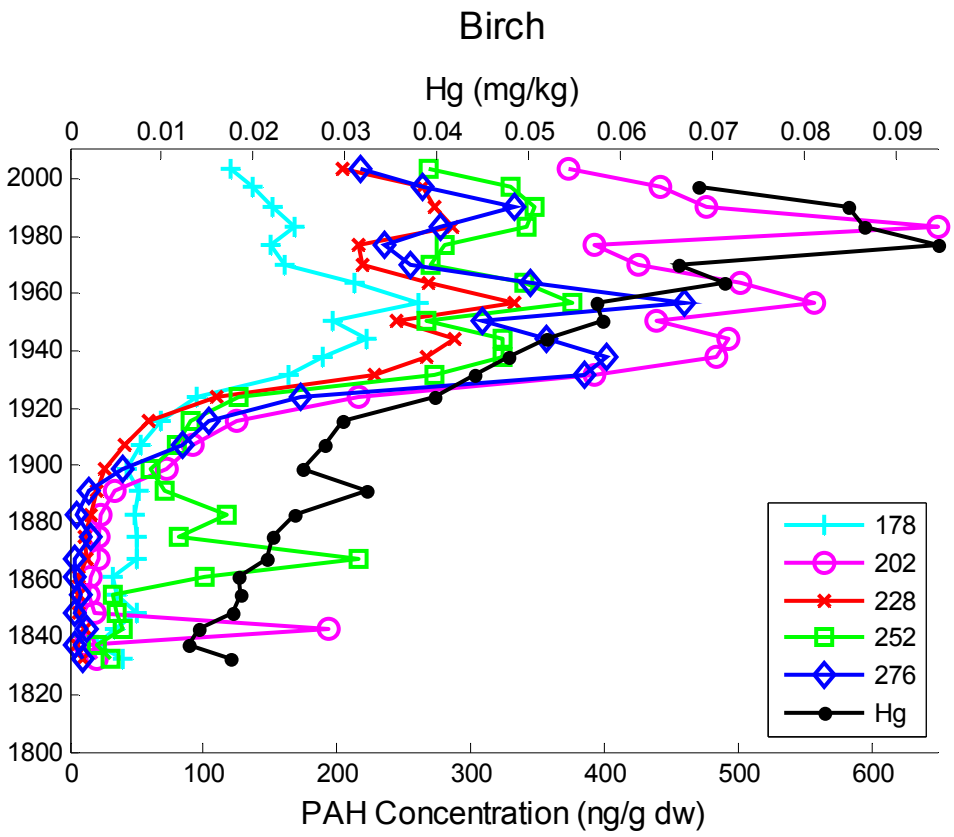

Figure 4.2b. Concentration profiles of Hg and PAH isomer groups for Birch Lake.

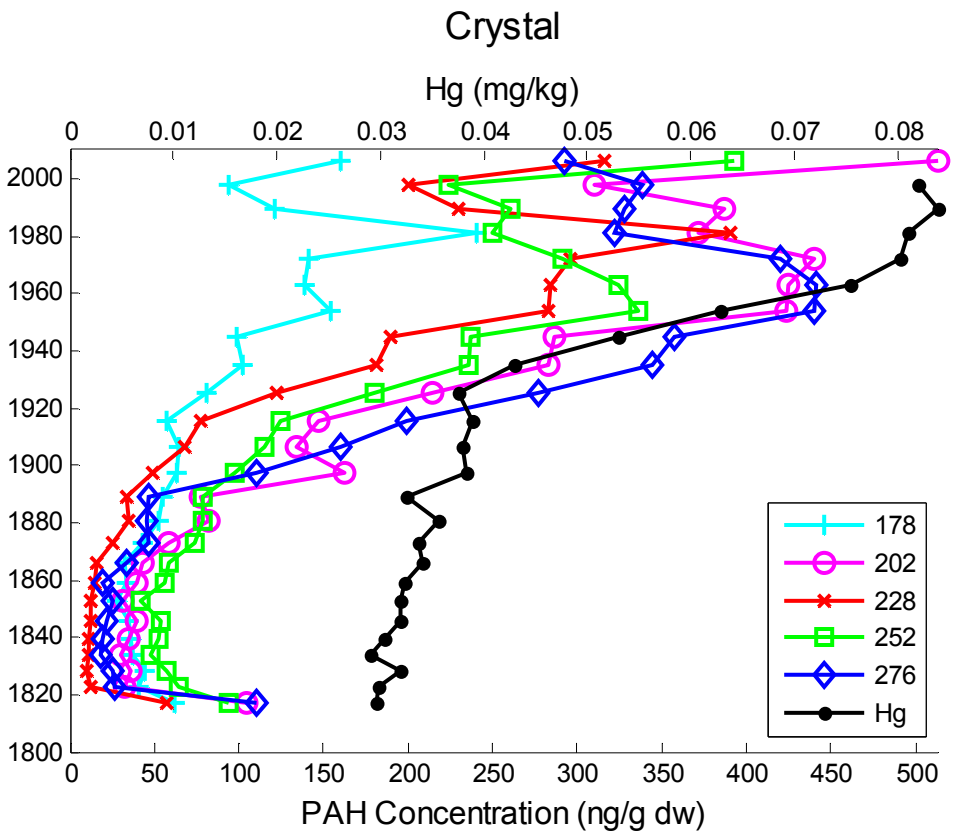

Figure 4.2c. Concentration profiles of Hg and PAH isomer groups for Crystal Lake.

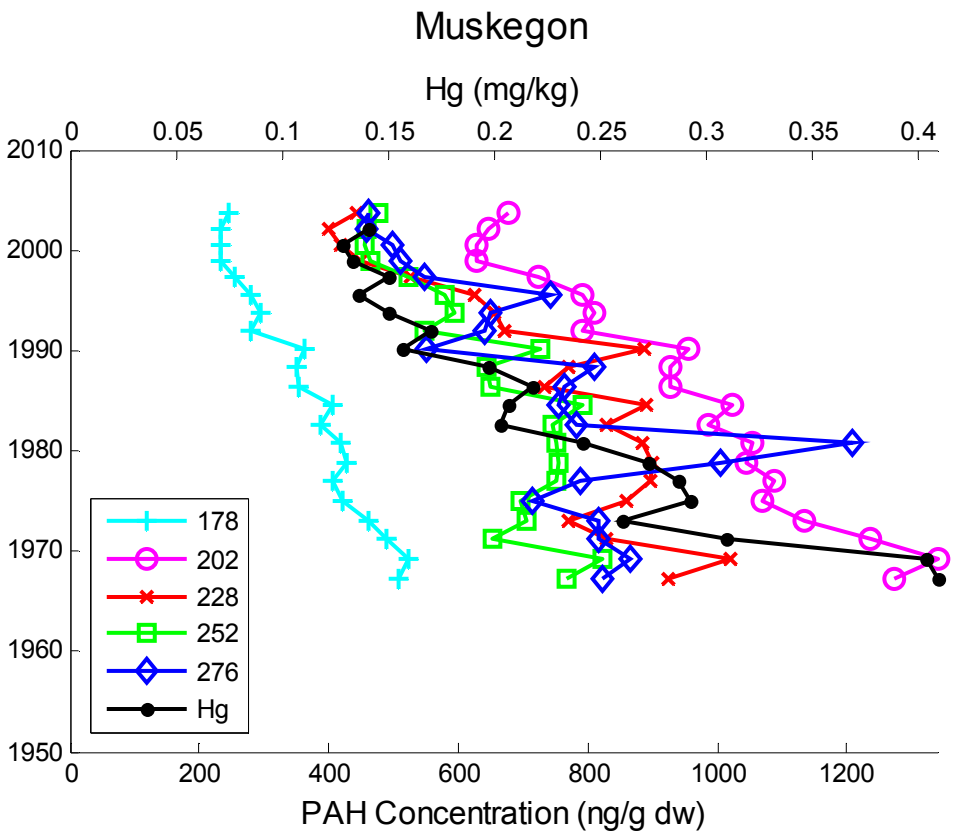

Figure 4.2d. Concentration profiles of Hg and PAH isomer groups for Muskegon Lake.

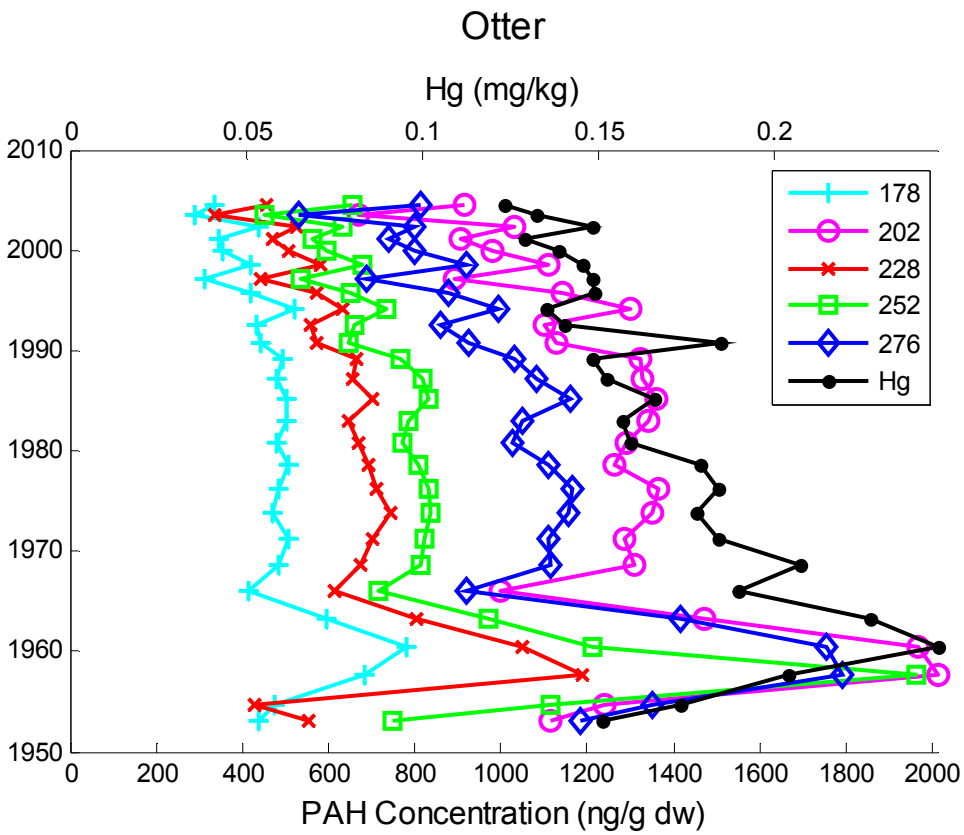

Figure 4.2e. Concentration profiles of Hg and PAH isomer groups for Otter Lake.

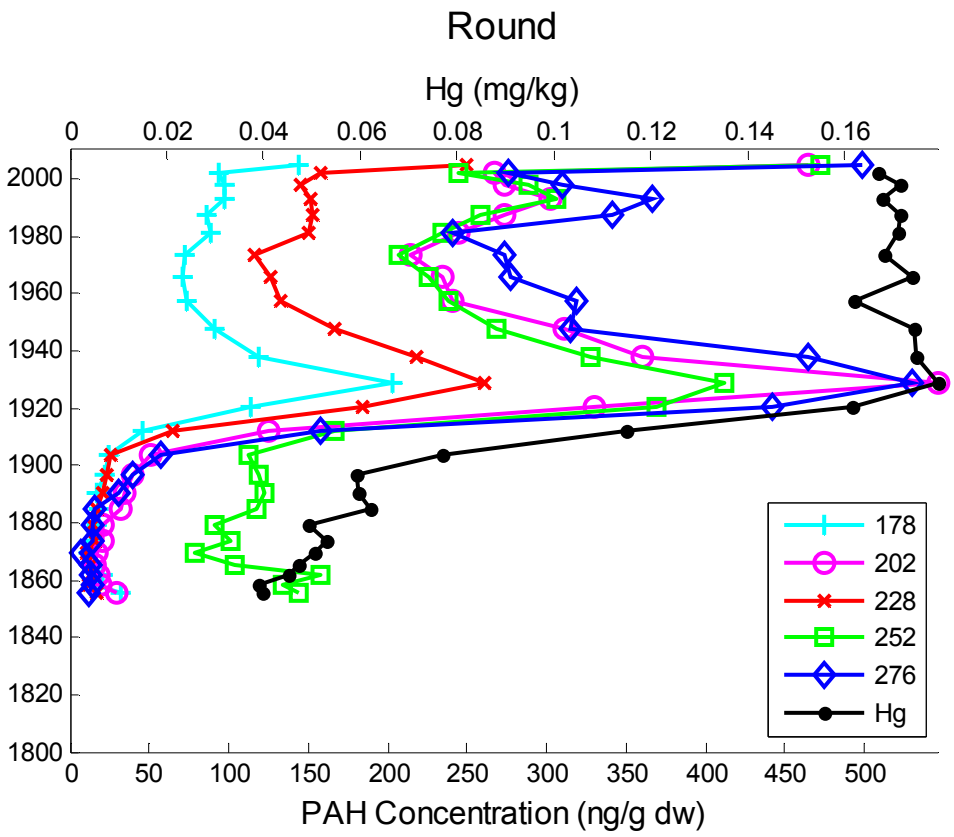

Figure 4.2f. Concentration profiles of Hg and PAH isomer groups for Round Lake.

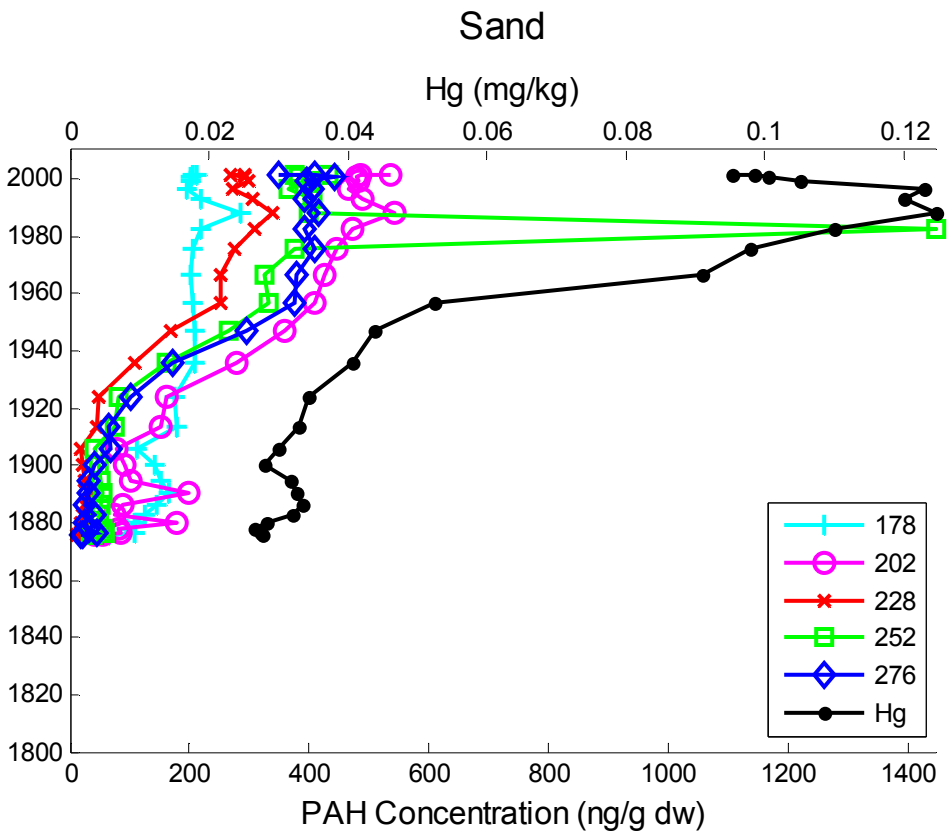

Figure 4.2g. Concentration profiles of Hg and PAH isomer groups for Sand Lake.

After the turn of the last century until recent times the masses 202, 252 and 276 PAHs were dominant in most lakes. In Avalon, Round and Sand lakes all three of these mass groups were elevated to near equal concentrations after their respective peaks (Avalon and Round) or after 1940 (Sand). Mass 202 was greater after the ΣPAH peak in Avalon and after 1920 in Sand Lake; whereas, mass 276 was greatest among PAH mass groups after ca. 1920 in Round Lake. Birch was similar to Avalon and Sand lakes, but mass 202 was clearly the major constituent after the peak in ΣPAH around ca. 1960. During the mid-century ΣPAH peak, 1950-1970, the masses 202 and 276 were dominant in Crystal Lake. The mass 202 PAHs were the major constituent in Muskegon and Otter throughout the entire core (Figures 4.2d & 4.2e, respectively). Profiles of PAHs from the Strait of Georgia also showed mass 202 to be the major constituent (Yunker and Macdonald, 2003) and is associated with sources from urbanized or industrialized areas (Lipiatou and Saliot, 1991, Yunker *et al.*, 1993). These sources include the burning of gasoline, diesel and coal which have also been shown to be important sources for masses 202, 252, and to a lesser extent 228 and 276 (Oros and Simoneit, 2000, Rogge *et al.*, 1993, Wang *et al.*, 1999).

The significant correlation between the ΣPAH and Hg concentration profiles in these lakes implies that throughout the lakes history a common influence on their concentrations. However, there are several instances of coincident increases and decreases that can be either unique or shared among the PAH mass groups. In Avalon Lake the slight concentration increase across all mass groups during the mid-1990s may be related to the coincident increase in Hg concentration during the same period. Curiously Hg does not peak until more recent times, ca. 1970, in Avalon while those of the PAH mass groups peaked much earlier, ca. 1920, and have since declined. The Huron Portland Cement Company started near the town of Alpena (located

about 20 miles to the east of Avalon Lake) around the turn of the 19th century and by 1910 was the largest cement plant in the world (NOAA, 2011). Cement kilns have long been recognized as contributors of Hg to the environment (Munthe *et al.*, 2007), that combined with the increased demand for cement due to the construction of the first concrete roads in Michigan (Morrison, 1945) could be a likely reason for the earlier than expected peak of PAHs in Avalon Lake. In Birch Lake the peak of Hg in ca. 1980 followed by decline until present is mimicked by most mass groups. The trajectory of increase in Hg after 1920 in Crystal Lake closely resembles that of mass groups 202 and 276 than the other groups. This would be consistent with an urbanization of the watershed and the combustion of grasses for the clearing of agricultural land (Fine *et al.*, 2001, Jenkins *et al.*, 1996, Masclet *et al.*, 1995). Whereas the increase in Hg between 1830 and 1890 more closely resembles the increases in masses 252 and 202. The profiles of Hg from Muskegon and Otter lakes resembles all of the PAH masses suggesting a common influence for all mass groups and Hg. In Round Lake the profiles of Hg and the PAH masses were quite similar from 1860 until the 1920s when Hg becomes nearly constant.

Diagnostic PAH Ratios. The ratio of PAH isomers are used to identify sources. However, their use as a diagnostic tool to differentiate sources can be confounded by differences in volatility, water solubility, and adsorption (Zhang *et al.*, 2005). These attributes can cause differential environmental transport and thus alter ratios. To deal with this problem researchers generally limit studies to PAHs with multiple isomers with interpretive support using multiple diagnostic ratios (Wang *et al.*, 2004, Yunker and Macdonald, 2003, Yunker *et al.*, 2002). The isomer ratios compare the least stable, or kinetic, isomer to the more stable, thermodynamic, isomer. When combustion sources are predominant the least stable isomer is enhanced (Yunker and

Macdonald, 1995) thus, the PAH mass groups with the greatest range in stabilities between the isomers have more potential to differentiate between petroleum and combustion sources (Yunker *et al.*, 2002). The PAH molecular masses with the greatest range of stability, in order of most potential for discrimination to least, are 276, 202, 252 and 178 (Yunker *et al.*, 2002). Examples of specific diagnostic ratios include the following. A ratio of anthracene to phenanthrene plus anthracene (An/178) less than 0.1 indicates a dominance of petroleum, e.g., naturally occurring oil seeps or unburned gasoline, while ratios greater than 0.10 indicates combustion processes (Yunker *et al.*, 2002). Fluoranthene to fluoranthene plus pyrene (Fl/Fl + Py) less than 0.40 indicates petroleum, a value between 0.40 and 0.50 reflects liquid fossil fuels and ratios greater than 0.50 are characteristic of grass, wood or coal combustion. Ratios of Benzo[a]anthracene to benzo[a]anthracene plus chrysene (BaA/228) tend to be less than 0.20 for petroleum sources, between 0.20 and 0.35 can indicate petroleum or combustion sources, and greater than 0.35 for combustion sources. Values of the indeno[1,2,3-cd]pyrene to indeno[1,2,3-cd]pyrene plus benzo[ghi]perylene (IP/IP + Bghi) ratio less than 0.20 are likely representative of petroleum whereas those values greater than 0.5 imply grass, wood and coal combustion, while those values in between 0.20 and 0.50 are characteristic of liquid fossil fuel combustion.

Prior to ca. 1930 Avalon, Birch and Sand lakes showed a predominance of petroleum sources (Figure 4.3a-b & 4.3g); whereas, Crystal and Round (Figure 4.3c & 4.3f, respectively) lakes showed influence from combustion sources as indicated by the An/178 ratio. Muskegon and Otter (Figure 4.3d & 4.3e, respectively) lakes show evidence of only combustion sources, likely due to the short time period covered by the sediment cores and industrial sources within proximity of these lakes. The Fl/Fl+Py ratio reveals grass/wood/coal combustion for nearly all

sediment slices in all lakes except for Muskegon where fossil fuel combustion was found to be important prior to the early 1980s while afterwards a predominant source could not be identified. In Birch, Crystal, Round and Sand lakes the ratio of BaA/228 is lower at the base of the sediment cores, indicative of petroleum sources, then increases towards petroleum combustion ratios between 1880 and 1900 except for Sand Lake where the transition was later, ca. 1930. Conversely in Avalon Lake, the BaA/228 ratio suggests combustion sources throughout much of the core. In Otter Lake a combustion source was identified for the entire core; whereas a mixture of petroleum and combustion sources were found for Muskegon Lake. The sources indicated by the ratio of IP/IP+Bghi were mixed between grass/wood/coal combustion and fossil fuel combustion. In Crystal, Round and Sand lakes the older portions of the core are characterized by grass/wood/coal combustion sources. Round and Sand showed grass/wood/coal combustion important recently in contrast to Crystal which like Muskegon Lake was dominated by fossil fuel combustion. Avalon and Birch lakes IP/IP+Bghi ratios varied between fossil fuel and grass/wood/coal combustion source. Conversely, Otter Lake seems dominated by grass/wood/coal combustion.

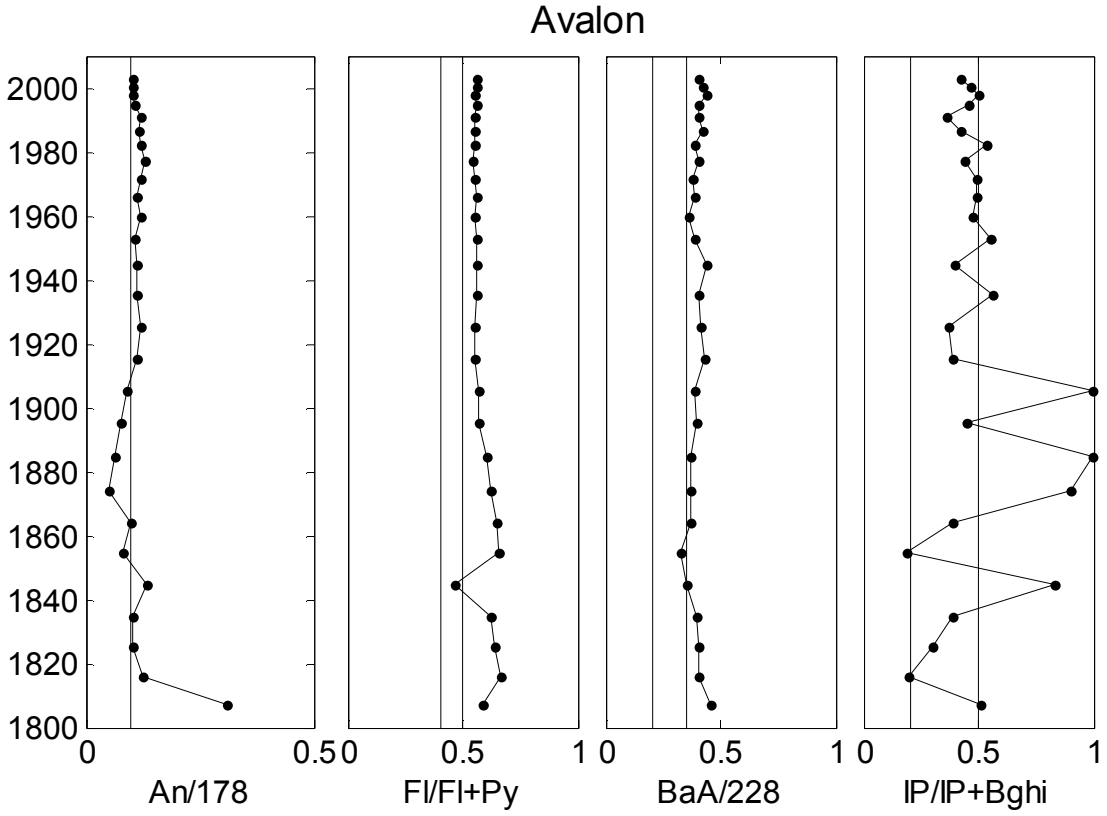

Figure 4.3a. Selected ratios of PAH isomers in sediment of Avalon Lake. Vertical lines represent specific PAH diagnostic ratios used to distinguish source, see text for specific examples.

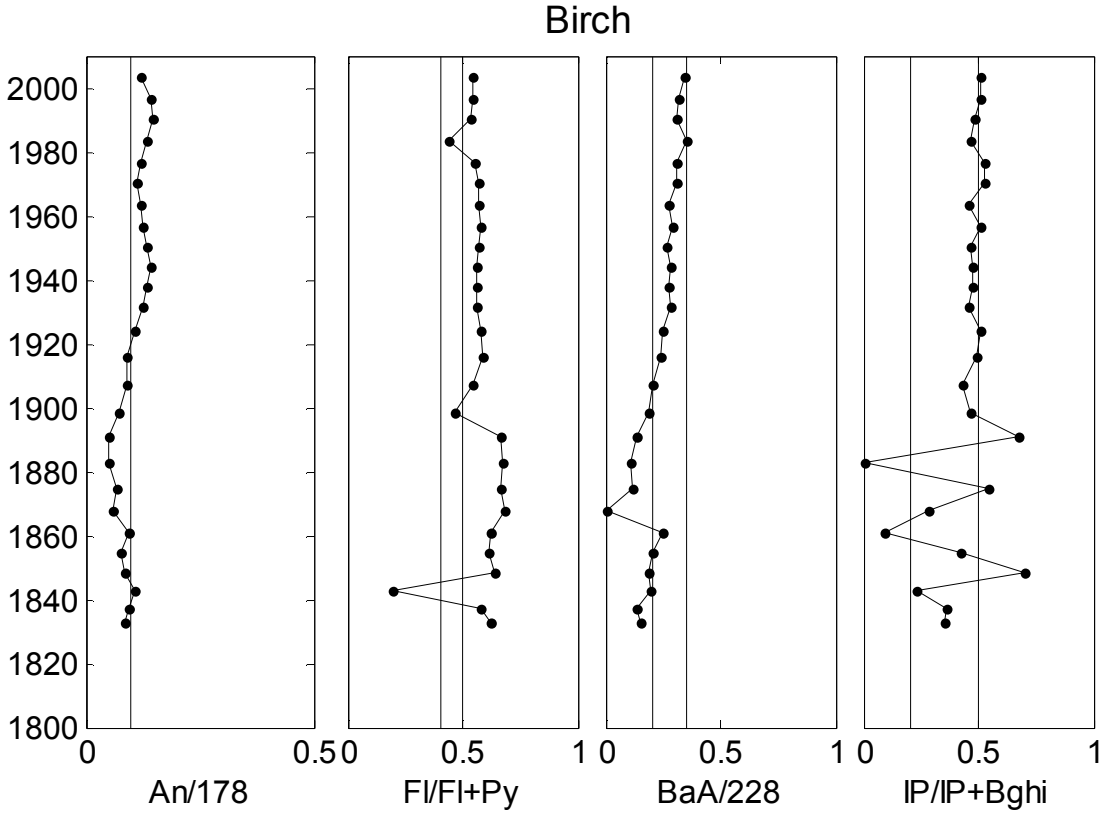

Figure 4.3b. Selected ratios of PAH isomers in sediment of Birch Lake. Vertical lines represent specific PAH diagnostic ratios used to distinguish source, see text for specific examples.

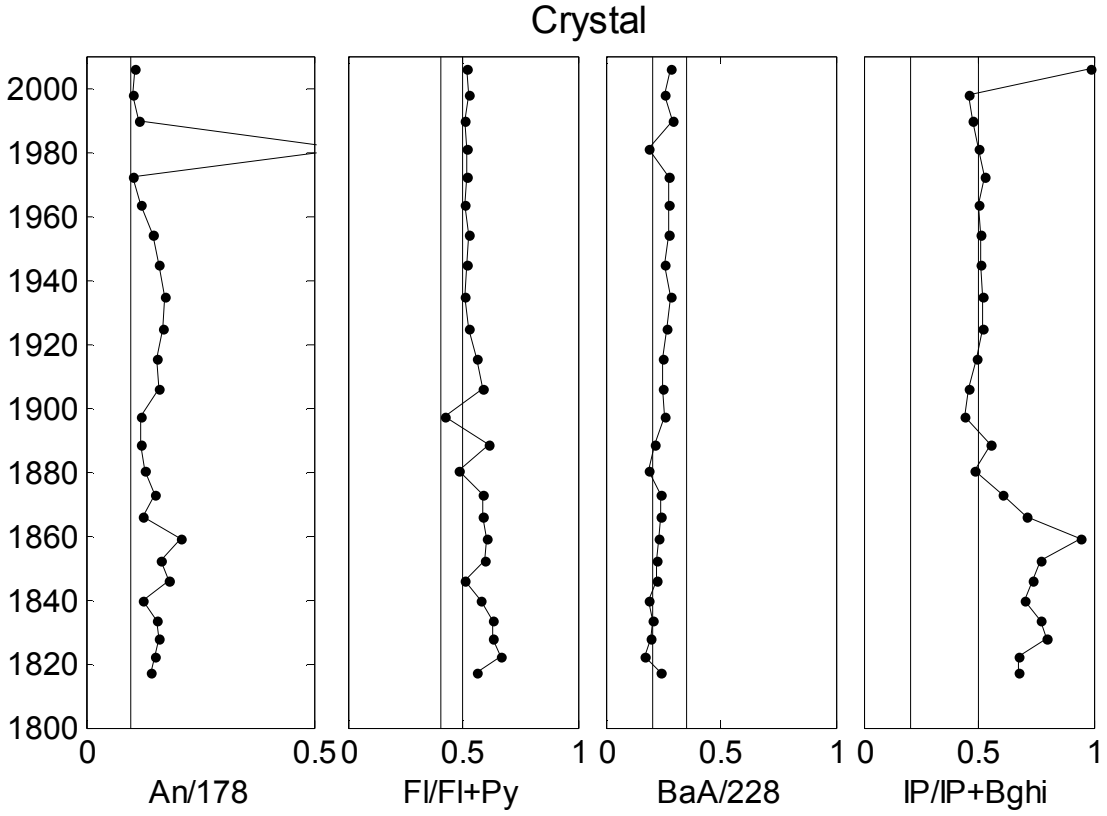

Figure 4.3c. Selected ratios of PAH isomers in sediment of Crystal Lake. Vertical lines represent specific PAH diagnostic ratios used to distinguish source, see text for specific examples.

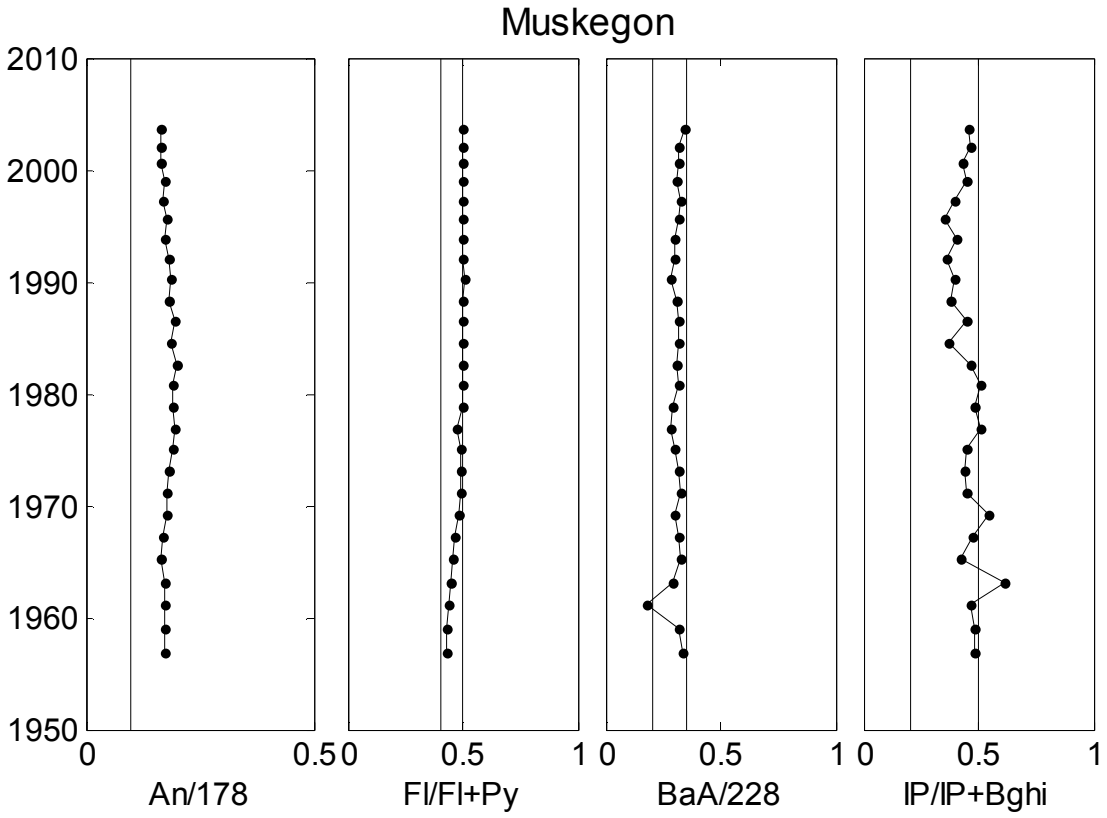

Figure 4.3d. Selected ratios of PAH isomers in sediment of Muskegon Lake. Vertical lines represent specific PAH diagnostic ratios used to distinguish source, see text for specific examples.

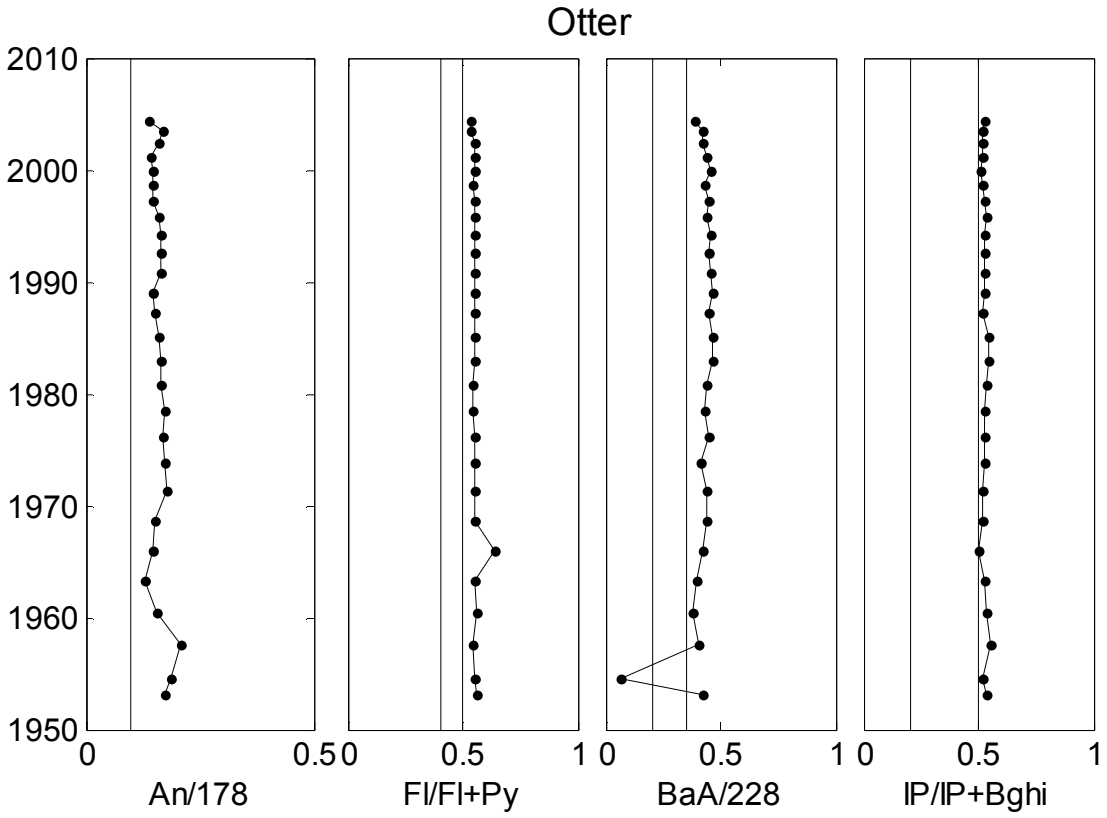

Figure 4.3e. Selected ratios of PAH isomers in sediment of Otter Lake. Vertical lines represent specific PAH diagnostic ratios used to distinguish source, see text for specific examples.

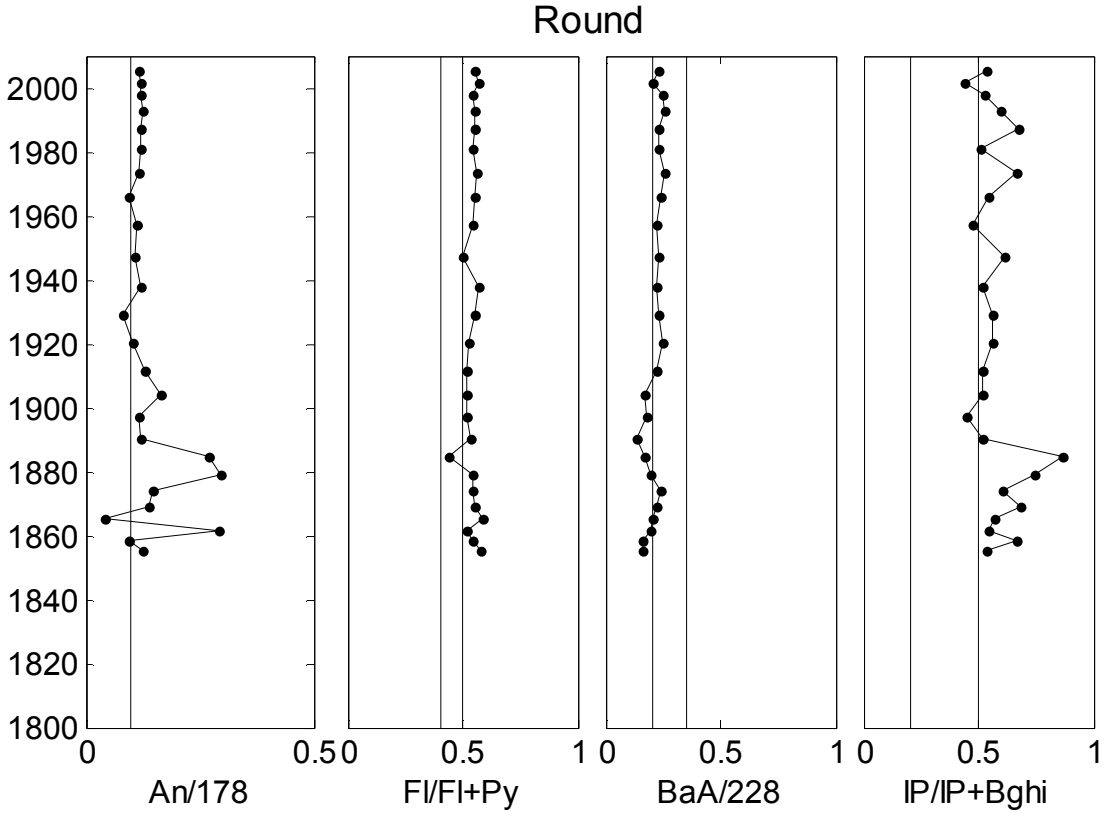

Figure 4.3f. Selected ratios of PAH isomers in sediment of Round Lake. Vertical lines represent specific PAH diagnostic ratios used to distinguish source, see text for specific examples.

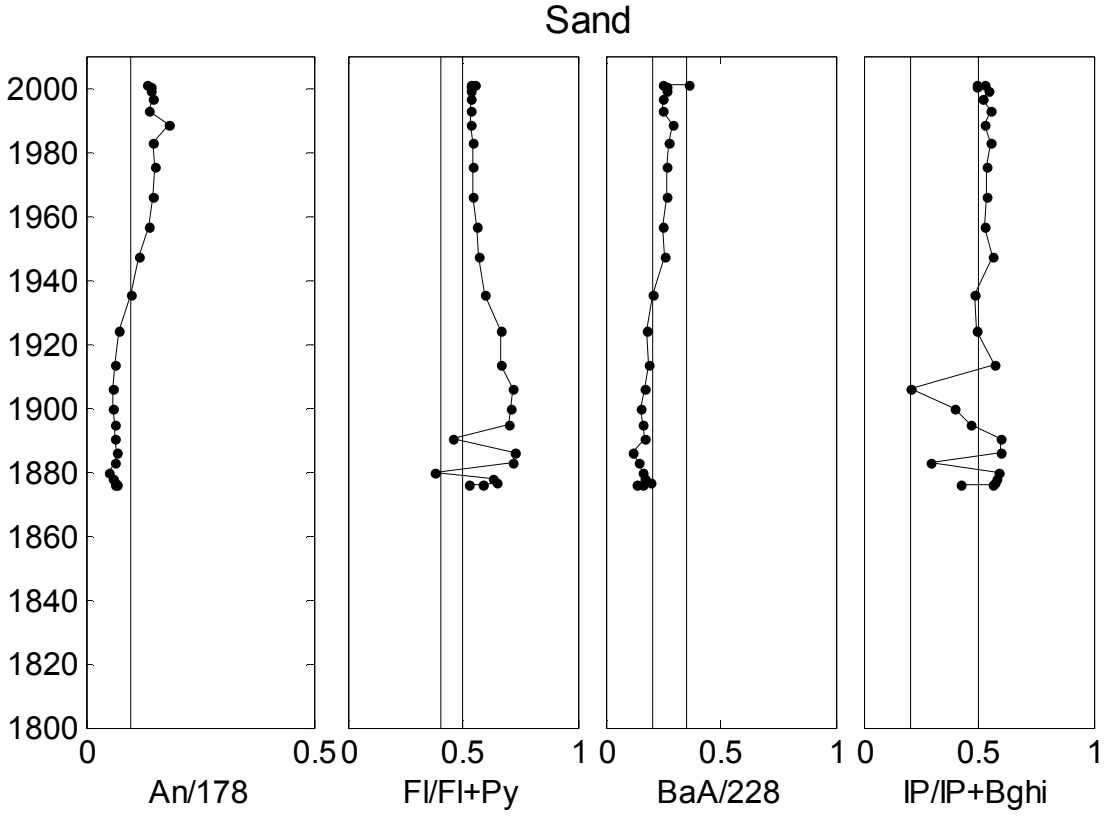

Figure 4.3g. Selected ratios of PAH isomers in sediment of Sand Lake. Vertical lines represent specific PAH diagnostic ratios used to distinguish source, see text for specific examples.

In Avalon Lake the sediment ratios of Fl/Fl+Py and IP/IP+Bghi do not indicate the same source for PAHs. The Fl/Fl+Py ratio can be interpreted as being from a combustion source which is consistent with the PAH profile plots that revealed the cement plant in Alpena as the most likely source for both Hg and PAHs. The conflict then is likely a result of sources mixing. Flouranthene can be enriched in particulate transported long distances (Yunker and Macdonald, 2003) resulting in the higher Fl/Fl+Py ratios observed in Avalon Lake while the more local source of IP would be from the combustion of fossil fuels, possibly the power generating station located due west of the lake (Figure 4.4) which combusts natural gas or local vehicle traffic. The latter is unlikely however since this area of the State is lightly populated. Although both natural gas combustion and cement production are sources of Hg it is likely that cement production would be more dominant in this case since the IP/IP+Bghi ratio hovers between fossil fuel and biomass combustion and the Fl/Fl+Py clearly indicates biomass combustion. The cause for the decoupling of the Hg profile from that of the PAH profile is unclear. Decreases in PAH could be a result of decreased demand for cement coupled with new sources of limestone or coal fly ash used in the production that had a higher Hg content resulting in further increases of Hg between 1920 and 1980.

The cause of concurrent peaks of Hg and PAHs in the sediments of Birch Lake in the 1990s could not be clearly identified using indicator ratios or profile plots. However, similar to Avalon Lake, PAH ratios do not indicate the same source. The ratio of Fl/Fl+Py indicates a combustion source while that of IP/IP+Bghi varies between fossil fuel sources and biomass combustion. The mixture of sources is confirmed by the BaA/228 ratios which transition from petroleum deep in the core towards combustion and petroleum sources coincident with the

stabilization of the Fl/Fl+Py and IP/IP+Bghi ratios. Since Birch Lake is located in a highly agricultural landscape it is likely that the combustion source identified by the increased Fl is from the increased combustion of coal from the greater Chicago, IL/Gary, IN area. The State Line Power Plant along the Indiana/Illinois border, to the southwest of Birch Lake, was built in the 1920s (Indiana, 2011) concurrent with the transition of the An/178 ratio from petroleum to combustion and a change in the rate of Hg increase. During the peak of PAHs in the late 1980s into the 1990s mass group 202 and 252 are dominant consistent with results found for areas downwind of industrialized and urbanized areas (Yunker and MacDonald, 2003).

In Crystal Lake between 1820 and 1880 the Fl/Fl+Py and IP/IP+Bghi ratios indicate biomass combustion, consistent with the burning and clearing of forest that occurred in this region (Long *et al.*, 2010). After about 1930, both of these indicator ratios become stabilized near the ratio discriminating between fossil fuel and biomass combustion. This is likely the result of sources mixing since Crystal Lake is within close proximity of several natural gas consumers and immediately east of several coal fired power plants (Figure 4.4).

Muskegon Lake is located within a large metropolitan area and has a coal fired power plant, along with other industrial activities, on its shoreline. One might assume that the PAH diagnostic ratios would be dominated by a coal signal. However, the Fl/Fl+Py and IP/IP+Bghi ratios both indicated fossil fuel combustion as the dominant source rather than coal. Ratios indicating fossil fuel combustion could be due to a vehicular source which would be likely for this urbanized region; vehicle emissions were found to contribute just under 10% of PAH load to southern Lake Michigan (Simcik *et al.*, 1999) but, it is unlikely that a vehicular source could

result in the concentrations of Hg in the lake sediments (Parsons *et al.*, 2007). Therefore, a potential source could be the natural gas and fuel oil electricity generating stations located in southeast Wisconsin, about 90 miles west and west-southwest of Muskegon Lake, for example the Milwaukee County Power Plant has burned natural gas or #2 fuel oil for electricity generation since 1970 (Resources, 2011).

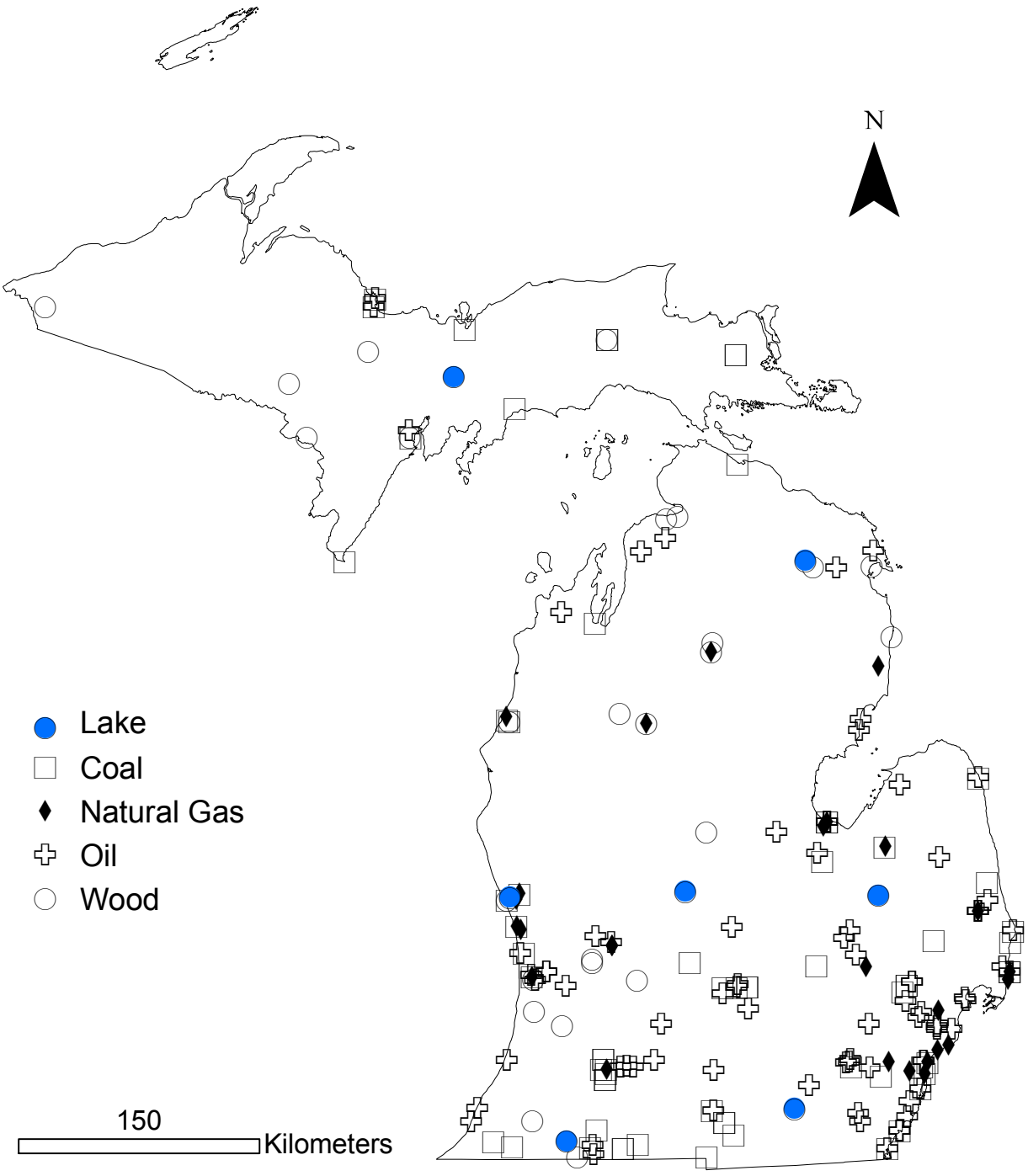

Figure 4.4. Industrial and utility energy emitters according to the 2002 Mercury Emissions Inventory for the State of Michigan.

The diagnostic ratios from Otter Lake reveal a dominant source for PAHs is from biomass combustion. Mercury and PAHs concentrations are highly correlated suggest a common source for these contaminants; the proximity of Otter Lake to the coal fired power plants (Figure 4.4) combined with diagnostic ratio data could indicate a common source, the combustion of coal for power production.

In Round Lake, ratios of Fl/Fl+Py and IP/IP+Bghi indicate a biomass combustion source throughout much of the core. Combustion sources in this area would likely be limited to the burning of grasses and forests prior to 1900. Round Lake, located in the middle of the Upper Peninsula, is not currently in close proximity to any industrial sources (Figure 4.4). A major industrial activity in Upper Peninsula is mining; however, most historic mining related activities have been located to the northwest on the Keewenaw Peninsula. The town of Fayette, approximately 80 km south of the lake, would have been the closest industrial source. Located on the shores of Little Bay De Noc between 1867 and 1891, Fayette was a major iron ore smelter and used local timber to fuel the process (Michigan, 2011a). The peak of Hg and PAHs occurred during the late 1920s into the 1930s, similar to Avalon Lake. And much like Avalon the higher mass PAHs were predominant during the peak. This would be consistent with a biomass combustion source (Yunker and Macdonald, 2003) during the industrial period of the town and until recent times. Ratios tend to show biomass combustion after about 1900, which may be an indication of the mining related activities occurring in Michigan's Upper Peninsula at the turn of the last century or the clearing of forests for agriculature or timber. The Hg profile was similar to those of the PAHs until the peak and then became decoupled. The decoupling occurs at the time of decline in the mining industry, due to the economic factors and maturity of the mines, in

the region. Diagnostic ratios after the peak ca. 1920 are consistent with the combustion of biomass (e.g., coal) a likely source for Hg to Round Lake.

Sand Lake is located near the City of Detroit. Prior to 1900 Fl/Fl + Py and IP/IP + Bghi ratios in the sediment indicate biomass combustion, consistent with biomass burning during intense clear cutting of forests. Mercury also shows an increase prior to 1900 which is likely due to the erodibility of forest cleared watersheds (Long *et al.*, 2010). After 1900, Hg and PAH start to increase which is most likely due to the the installation of the cement kiln in Cement City due west of Sand Lake (Figure 4.5). The kiln was shut down in the early 1960s (Morrison, 1945). After ca. 1940, the ratios of Fl/Fl + Py and IP/IP + Bghi were consistent with a biomass combustion source. The predominance of the mass group 202 after 1920 suggests burning of grass, hardwood and softwood; although it is usually accompanied by the mass group 178 (Fine *et al.*, 2001, Jenkins *et al.*, 1996, Masclet *et al.*, 1995). The presence of the mass group 202 may be related to the use of marl at the Cement City cement manufacturer, which would contain remnants of grasses and softwoods washed in from the marl source watershed. The slope of Hg and PAH concentration profiles are similar between 1900 and 1950. After 1950, concentrations of both contaminants continue to increase; however, Hg does so at a much higher rate. This may be due to the decommissioning of the cement kiln and commissioning of 2 major coal-fired power plants to the east of Sand Lake in the City of Detroit. The coincident peak and decline of Hg and PAH in the 1980s and 1990s implies a common source or influence and would be consistent with the implementation of abatement technologies required by the Clean Air Act.

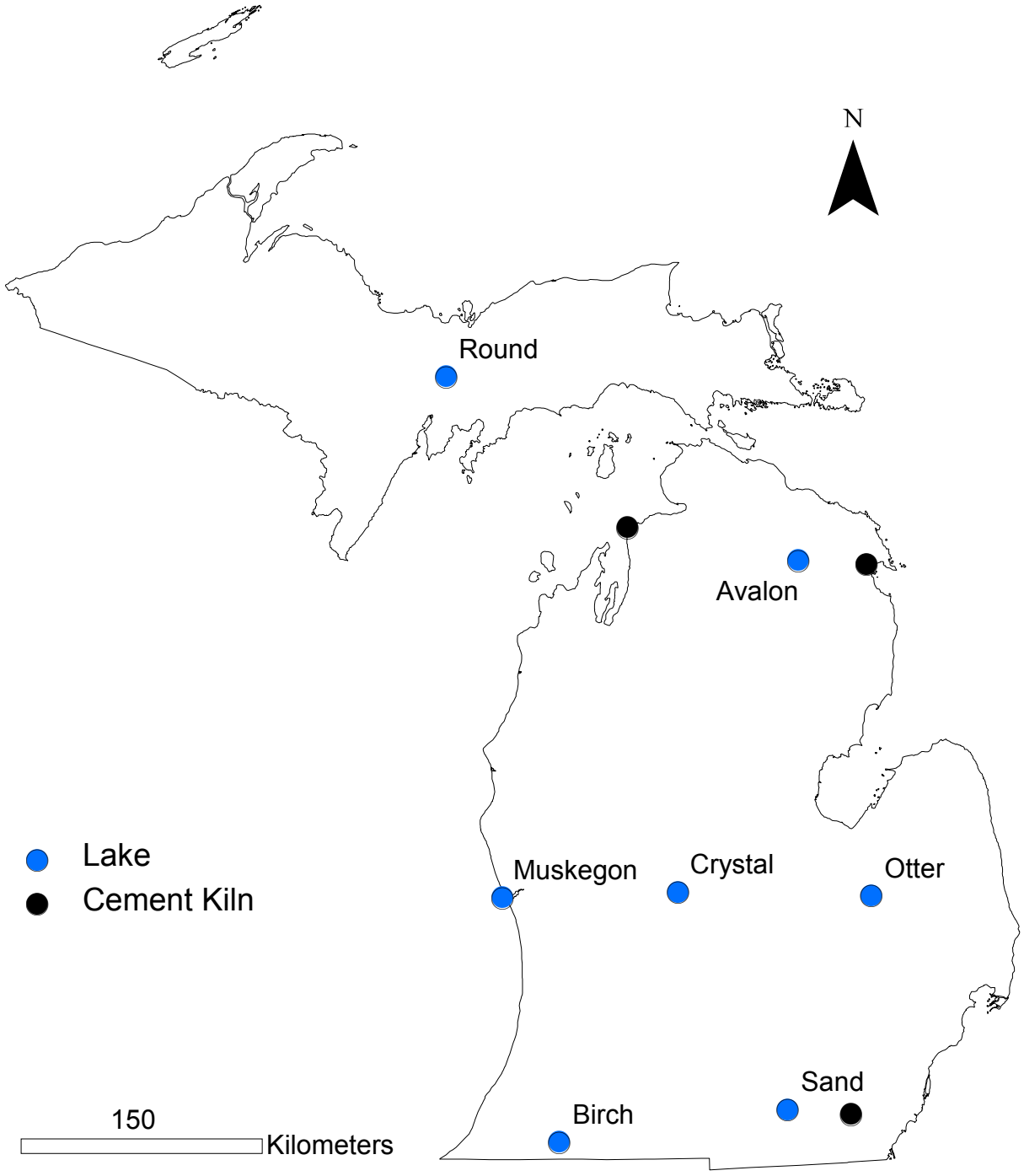

Figure 4.5. Current cement kilns in the State of Michigan. The historic cement kiln located in Cement City, MI is not shown but would have been located approximately 20 km due west of Sand Lake.

Sediment chronologies of contaminants reflect activities within the watershed and atmospheric sources that could be located within or outside of the watershed. This makes the identification of sources challenging since the concentration recorded in the sediment profile contains potential information from all sources. Earlier research attempts to assign sources based on sediment chronologies have successfully used production and consumption records of contaminants (Engstrom and Swain, 1997, Lockhart *et al.*, 2000). This work compliments those studies and helps to confirm sources identified using production/consumption methods. Furthermore, this approach has demonstrated that sources for PAHs, both historic and modern, to inland lakes throughout the State of Michigan vary by region. Assuming that PAHs and Hg share common sources and pathways, then identifying these local to regional scale sources has important implications for legislation seeking to limit the release of Hg to environment. Furthermore, some of the historic sources of Hg may have not been identified using traditional methods (e.g., cement kilns, Avalon and Sand lakes, and mining related activities, Round Lake). A modern coal combustion source was found to be significant for lakes in the southern portion of the State and in some cases can be correlated to plant start-ups. A coal combustion source could not be identified for Muskegon Lake which has a coal-fired power plant on its shoreline, which provides further insight into the local scale transport of Hg. This approach is limited; however, to the availability and quality of PAH data and can be enhanced by including those PAHs identified by others to have more discriminatory power (e.g., retene see (Yunker and Macdonald, 2003)).

REFERENCES

REFERENCES

Barrick, R.C., Prahl, F.G., 1987. Hydrocarbon Geochemistry of the Puget Sound Region .3. Polycyclic Aromatic-Hydrocarbons in Sediments. Estuarine Coastal and Shelf Science 25, 175-191.

Bindler, R., 2003. Estimating the natural background atmospheric deposition rate of mercury utilizing ombrotrophic bogs in southern Sweden. Environmental Science and Technology 37, 40-46.

Boutron, C.F., Vandal, G.M., Fitzgerald, W.F., Ferrari, C.P., 1998. A forty year record of mercury in central Greenland snow. Geophysical Research Letters 25, 3315-3318.

Chester, R., Bradshaw, G.F., Ottley, C.J., Harrison, R.M., Merrett, J.L., Preston, M.R., Rendell, A.R., Kane, M.M., Jickells, T.D., 1993. The atmospheric distributions of Trace-Metals, Trace Organics and Nitrogen Species Over the North-Sea. Philosophical Transactions of the Royal Society of London Series a-Mathematical Physical and Engineering Sciences 343, 543-556.

Di Leonardo, R., Vizzini, S., Bellanca, A., Mazzola, A., 2009. Sedimentary record of anthropogenic contaminants (trace metals and PAHs) and organic matter in a Mediterranean coastal area (Gulf of Palermo, Italy). Journal of Marine Systems 78, 136-145.

Donahue, W.F., Allen, E.W., Schindler, D.W., 2006. Impacts of coal-fired power plants on trace metals and polycyclic aromatic hydrocarbons (PAHs) in lake sediments in central Alberta, Canada. Journal of Paleolimnology 35, 111-128.

Durnford, D., Dastoor, A., Figueras-Nieto, D., Ryjkov, A., 2010. Long range transport of mercury to the Arctic and across Canada. Atmospheric Chemistry and Physics 10, 6063-6086.

Dvonch, J.T., Graney, J.R., Keeler, G.J., Stevens, R.K., 1999. Use of elemental tracers to source apportion mercury in South Florida precipitation. Environmental Science & Technology 33, 4522-4527.

Dvonch, J.T., Graney, J.R., Marsik, F.J., Keeler, G.J., Stevens, R.K., 1998. An investigation of source-receptor relationships for mercury in south Florida using event precipitation data. Science of the Total Environment 213, 95-108.

Engstrom, D.R., Swain, E.B., 1997. Recent declines in atmospheric mercury deposition in the upper Midwest. Environmental Science and Technology 31, 960-967.

Evers, D.C., Wiener, J.G., Driscoll, C.T., Gay, D.A., Basu, N., Monson, B.A., Lambert, K.F., Morrison, H.A., Morgan, J.T., Williams, K.A., Soehl, A.G., 2011. Great Lakes Mercury Connections: The Extent and Effects of Mercury Pollution in the Great Lakes Region.

Biodiversity Research Institute. Gorham, MA. Report BRI 2011-18, 44 pages. Available from: http://www.briloon.org/mercuryconnections/GreatLakes.

Fernandez, P., Vilanova, R.M., Martinez, C., Appleby, P., Grimalt, J.O., 2000. The historical record of atmospheric pyrolytic pollution over Europe registered in the sedimentary PAH from remote mountain lakes. Environmental Science & Technology 34, 1906-1913.

Fine, P.M., Cass, G.R., Simoneit, B.R.T., 2001. Chemical characterization of fine particle emissions from fireplace combustion of woods grown in the northeastern United States. Environmental Science & Technology 35, 2665-2675.

Fitzgerald, W.F., 1989. Atmospheric and oceanic cycling of mercury. Academic Press.

Fitzgerald, W.F., Engstrom, D.R., Mason, R.P., Nater, E.A., 1998. The case for atmospheric mercury contamination in remote areas. Environmental Science & Technology 32, 1-7.

Gnandi, K., Bandowe, B.A.M., Deheyn, D.D., Porrachia, M., Kersten, M., Wilcke, W., 2011. Polycyclic aromatic hydrocarbons and trace metal contamination of coastal sediment and biota from Togo. Journal of Environmental Monitoring 13, 2033-2041.

Hites, R.A., Laflamme, R.E., Farrington, J.W., 1977. Sedimentary Polycyclic Aromatic-Hydrocarbons - Historical Record. Science 198, 829-831.

Howe, T.S., Billings, S., Stolzberg, R.J., 2004. Sources of polycyclic aromatic hydrocarbons and hexachlorobenzene in spruce needles of eastern Alaska. Environmental Science & Technology 38, 3294-3298.

City of Hammond Indiana, 2011. History of State Line Generating Plant, Available online at http://www.hammondindiana.com/history/stateline.htm. (Accessed: September 5, 2011).

Jaffe, D., Prestbo, E., Swartzendruber, P., Weiss-Penzias, P., Kato, S., Takami, A., Hatakeyama, S., Kajii, Y., 2005. Export of atmospheric mercury from Asia. Atmospheric Environment 39, 3029-3038.

Jaffe, D., Strode, S., 2008. Sources, fate and transport of atmospheric mercury from Asia. Environmental Chemistry 5, 121-126.

Jenkins, B.M., Jones, A.D., Turn, S.Q., Williams, R.B., 1996. Emission factors for polycyclic aromatic hydrocarbons from biomass burning. Environmental Science & Technology 30, 2462-2469.

Kamman, N.C., Engstrom, D.R., 2002. Historical and present fluxes of mercury to Vermont and New Hampshire lakes inferred from Pb-210 dated sediment cores. Atmospheric Environment 36, 1599-1609.

Kannan, K., Johnson-Restrepo, B., Yohn, S.S., Giesy, J.P., Long, D.T., 2005. Spatial and temporal distribution of polycyclic aromatic hydrocarbons in sediments from Michigan inland lakes. Environmental Science & Technology 39, 4700-4706.

Keeler, G.J., Landis, M.S., Norris, G.A., Christianson, E.M., Dvonch, J.T., 2006. Sources of mercury wet deposition in Eastern Ohio, USA. Environmental Science & Technology 40, 5874-5881.

Killin, R.K., Simonich, S.L., Jaffe, D.A., DeForest, C.L., Wilson, G.R., 2004. Transpacific and regional atmospheric transport of anthropogenic semivolatile organic compounds to Cheeka Peak Observatory during the spring of 2002. Journal of Geophysical Research-Atmospheres 109.

Landis, M.S., Vette, A.F., Keeler, G.J., 2002. Atmospheric mercury in the Lake Michigan basin: Influence of the Chicago/Gary urban area. Environmental Science and Technology 36, 4508-4517.

Lima, A.L.C., Eglinton, T.I., Reddy, C.M., 2003. High-resolution record of pyrogenic polycyclic aromatic hydrocarbon deposition during the 20th century. Environmental Science & Technology 37, 53-61.

Lindberg, S., Bullock, R., Ebinghaus, R., Engstrom, D., Feng, X.B., Fitzgerald, W., Pirrone, N., Prestbo, E., Seigneur, C., 2007. A synthesis of progress and uncertainties in attributing the sources of mercury in deposition. Ambio 36, 19-32.

Lipiatou, E., Saliot, A., 1991. Fluxes and Transport of Anthropogenic and Natural Polycyclic Aromatic-Hydrocarbons in the Western Mediterranean-Sea. Marine Chemistry 32, 51-71.

Lockhart, W.L., Macdonald, R.W., Outridge, P.M., Wilkinson, P., DeLaronde, J.B., Rudd, J.W.M., 2000. Tests of the fidelity of lake sediment core records of mercury deposition to known histories of mercury contamination. Science of the Total Environment 260, 171-180.

Long, D.T., Eisenreich, S.J., Swackhammer, D.L. *Volume III - Metal Concentrations in Sediments of the Great Lakes*; Government Printing Office, 1995.

Long, D.T., Parsons, M.J., Yansa, C.H., Yohn, S.S., McLean, C.E., Vannier, R.G., 2010. Assessing the response of watersheds to catastrophic (logging) and possible secular (global temperature change) perturbations using sediment-chemical chronologies. Applied Geochemistry 25, 143-158.

Masclet, P., Cachier, H., Liousse, C., Wortham, H., 1995. Emissions of Polycyclic Aromatic-Hydrocarbons by Savanna Fires. Journal of Atmospheric Chemistry 22, 41-54.

Menounou, N., Presley, B.J., 2003. Mercury and other trace elements in sediment cores from central texas lakes. Archives of Environmental Contamination and Toxicology 45, 11-29.

State Of MIchigan, 2011. About Fayette Historic Townsite, Garden, Available online at www.michigan.gov/dnr. (Accessed: September 5, 2011).

State of Michigan, 2011. Sediment Chemistry, Available online at http://www.michigan.gov/deq/0,4561,7-135-3313_3686_3728-32365--,00.html. (Accessed: September 5, 2011).

Morrison, P.C., 1945. Cement Plant Migration in Michigan. Economic Geography 21, 1-16.

Munthe, J., Bodaly, R.A., Branfireun, B.A., Driscoll, C.T., Gilmour, C.C., Harris, R., Horvat, M., Lucotte, M., Malm, O., 2007. Recovery of mercury-contaminated fisheries. Ambio 36, 33-44.

Mzoughi, N., Chouba, L., 2011. Distribution of trace metals, aliphatic hydrocarbons and polycyclic aromatic hydrocarbons in sediment cores from the Sicily Channel and the Gulf of Tunis (south-western Mediterranean Sea). Environmental Technology 32, 43-54.

NOAA, 2011. Thunder Bay National Marine Sanctuary, Available online at http://thunderbay.noaa.gov. (Accessed: September 5, 2011).

Obrist, D., Hallar, A.G., McCubbin, I., Stephens, B.B., Rahn, T., 2008. Atmospheric mercury concentrations at Storm Peak Laboratory in the Rocky Mountains: Evidence for long-range transport from Asia, boundary layer contributions, and plant mercury uptake. Atmospheric Environment 42, 7579-7589.

Oros, D.R., Simoneit, B.R.T., 2000. Identification and emission rates of molecular tracers in coal smoke particulate matter. Fuel 79, 515-536.

Pacyna, E.G., Pacyna, J.M., Fudala, J., Strzelecka-Jastrzab, E., Hlawiczka, S., Panasiuk, D., 2006. Mercury emissions to the atmosphere from anthropogenic sources in Europe in 2000 and their scenarios until 2020. Science of the Total Environment 370, 147-156.

Parsons, M.J., Long, D.T., Yohn, S.S., Giesy, J.P., 2007. Spatial and Temporal Trends of Mercury Loadings to Michigan Inland Lakes. Environmental Science and Technology 41, 5634-5640.

Reidmiller, D.R., Jaffe, D.A., Chand, D., Strode, S., Swartzendruber, P., Wolfe, G.M., Thornton, J.A., 2009. Interannual variability of long-range transport as seen at the Mt. Bachelor observatory. Atmospheric Chemistry and Physics 9, 557-572.

Wisconsin Department of Natural Resources, 2011. Climate Change Guide e-Appendix, Available online at http://dnr.wi.gov. (Accessed: September 5, 2011).

Rogge, W.F., Hildemann, L.M., Mazurek, M.A., Cass, G.R., Simoneit, B.R.T., 1993. Sources of Fine Organic Aerosol 2. Noncatalyst and Catalyst-Equipped Automobiles and Heavy-Duty Diesel Trucks. Environmental Science & Technology 27, 636-651.

Schuster, P.F., Krabbenhoft, D.P., Naftz, D.L., Cecil, L.D., Olson, M.L., Dewild, J.F., Susong, D.D., Green, J.R., Abbott, M.L., 2002. Atmospheric mercury deposition during the last 270 years: A glacial ice core record of natural and anthropogenic sources. Environmental Science & Technology 36, 2303-2310.

Simcik, M.F., Eisenreich, S.J., Lioy, P.J., 1999. Source apportionment and source/sink relationships of PAHs in the coastal atmosphere of Chicago and Lake Michigan. Atmospheric Environment 33, 5071-5079.

Sofowote, U.M., Allan, L.M., McCarry, B.E., 2010. Evaluation of PAH diagnostic ratios as source apportionment tools for air particulates collected in an urban-industrial environment. Journal of Environmental Monitoring 12, 417-424.

Sofowote, U.M., Hung, H., Rastogi, A.K., Westgate, J.N., Deluca, P.F., Su, Y.S., McCarry, B.E., 2011. Assessing the long-range transport of PAH to a sub-Arctic site using positive matrix factorization and potential source contribution function. Atmospheric Environment 45, 967-976.

R version 2.6.2, 2008. R version 2.6.2

US EPA, 2011. Proposed Rule: National Emission Standards for Hazardous Air Pollutants From Coal- and Oil-Fired Electric Utility Steam Generating Units and Standards of Performance for Fossil-Fuel-Fired Electric Utility, Industrial-Commercial-Institutional, and Small Industrial-Commercial-Institutional Steam Generating Units. US EPA.Government Printing Office, Washington, D.C. 40 CFR Parts 60 and 63.

Usenko, S., Smonich, S.L.M., Hageman, K.J., Schrlau, J.E., Geiser, L., Campbell, D.H., Appleby, P.G., Landers, D.H., 2010. Sources and Deposition of Polycyclic Aromatic Hydrocarbons to Western US National Parks. Environmental Science & Technology 44, 4512-4518.

Valente, R.J., Shea, C., Humes, K.L., Tanner, R.L., 2007. Atmospheric mercury in the Great Smoky Mountains compared to regional and global levels. Atmospheric Environment 41, 1861-1873.

Wakeham, S.G., Schaffner, C., Giger, W., 1980. Polycyclic Aromatic-Hydrocarbons in Recent Lake-Sediments 1. Compounds Having Anthropogenic Origins. Geochimica et Cosmochimica Acta 44, 403-413.

Wang, G.D., Mielke, H.W., Quach, V., Gonzales, C., Mang, Q., 2004. Determination of polycyclic aromatic hydrocarbons and trace metals in New Orleans soils and Sediments. Soil & Sediment Contamination 13, 313-327.

Wang, Z.D., Fingas, M., Shu, Y.Y., Sigouin, L., Landriault, M., Lambert, P., Turpin, R., Campagna, P., Mullin, J., 1999. Quantitative characterization of PAHs in burn residue and soot samples and differentiation of pyrogenic PAHs from petrogenic PAHs - The 1994 Mobile Burn Study. Environmental Science & Technology 33, 3100-3109.

Watras, C.J., Bloom, N.S., Hudson, J.M., Gherini, S., Munson, R., Claas, S.A., Marrison, K.A., Hurely, J., Wiener, J.G., Fitzgerald, W.F., Mason, R., Vandal, G., Powell, D., Rada, R., Rislov, L., Winfrey, M., Elder, J., Krabbenhoft, D., Andren, A.W., Babiarz, C., Porcella, D.B., Huckabee, J.W., 1994. Sources and fates of mercury and methylmercury in Wisconsin lakes. In: C.J. Watras, J.W. Huckabee (Eds.), Mercury Pollution: Intergration and Synthesis. CRC Press, Ann Arbor, pp. 153-179.

Yohn, S., Long, D., Fett, J., Patino, L., 2004. Regional versus local influences on lead and cadmium loading to the Great Lakes region. Applied Geochemistry 19, 1157-1175.

Yunker, M.B., Macdonald, R.W., 2003. Alkane and PAH depositional history, sources and fluxes in sediments from the Fraser River Basin and Strait of Georgia, Canada. Organic Geochemistry 34, 1429-1454.

Yunker, M.B., Macdonald, R.W., 1995. Composition and Origins of Polycyclic Aromatic-Hydrocarbons in the Mackenzie River and on the Beaufort Sea Shelf. Arctic 48, 118-129.

Yunker, M.B., Macdonald, R.W., Cretney, W.J., Fowler, B.R., McLaughlin, F.A., 1993. Alkane, Terpene, and Polycyclic Aromatic Hydrocarbon Geochemistry of the Mackenzie River and Mackenzie Shelf - Riverine Contributions to Beaufort Sea Coastal Sediment. Geochimica et Cosmochimica Acta 57, 3041-3061.

Yunker, M.B., Macdonald, R.W., Goyette, D., Paton, D.W., Fowler, B.R., Sullivan, D., Boyd, J., 1999. Natural and anthropogenic inputs of hydrocarbons to the Strait of Georgia. Science of the Total Environment 225, 181-209.

Yunker, M.B., Macdonald, R.W., Vingarzan, R., Mitchell, R.H., Goyette, D., Sylvestre, S., 2002. PAHs in the Fraser River basin: a critical appraisal of PAH ratios as indicators of PAH source and composition. Organic Geochemistry 33, 489-515.

Zechmeister, H.G., Dullinger, S., Hohenwallner, D., Riss, A., Hanus-Illnar, A., Scharf, S., 2006. Pilot study on road traffic emissions (PAHs, heavy metals) measured by using mosses in a tunnel experiment in Vienna, Austria. Environmental Science and Pollution Research 13, 398-405.

Zhang, X.L., Tao, S., Liu, W.X., Yang, Y., Zuo, Q., Liu, S.Z., 2005. Source diagnostics of polycyclic aromatic hydrocarbons based on species ratios: A multimedia approach. Environmental Science & Technology 39, 9109-9114.

Zheng, W., Lichwa, J., Yan, T., 2011. Impact of different land uses on polycyclic aromatic hydrocarbon contamination in coastal stream sediments. Chemosphere 84, 376-382.

CHAPTER 5
ASSESSING THE NATURAL RECOVERY OF A LAKE CONTAMINATED WITH HG USING ESTIMATED RECOVERY RATES DETERMINED BY SEDIMENT CHRONOLOGIES.

Abstract

Deer Lake is an impoundment located near Ishpeming, MI, USA. Iron mining assay laboratories located in Ishpeming disposed of Hg salts to the city sewer whose outfall was located along an inlet to Deer Lake. An effort to remediate the system in the mid 1980s which consisted of drawing down water in the impoundment in order to volatize Hg from the sediments did not result in recovery of the system. Since the mid 1990s, the remediation strategy has been to allow the continual burial of the contaminated sediments, i.e., natural recovery. The goal of this study was to assess the effectiveness of this strategy. This was accomplished by investigating the state of the system in terms of its recovery and estimating the time frame for recovery. Sediment cores were collected in 2000 to determine historical trends in accumulation rates and concentrations of Hg and other metals. Sedimentation rates and sediment ages were estimated using ^{210}Pb. Event based dating (e.g., peak of ^{137}Cs in 1963) was used to supplement ^{210}Pb data due to non-monotonic features in the ^{210}Pb profile and activities that were not at supported levels at the base of the core. Selected results are that 1) drawdown significantly influenced sedimentation patterns causing slopes for ^{210}Pb profiles that reflected the influx of older sediment, 2) periods of iron production correlate to Hg loading indicating the point source for contamination, a relationship not previously identified, 3) Hg:Al ratios indicate a recent change to a watershed pathway for Hg loading and 4) Hg concentrations had decreased from their peak, remain elevated, and were increasing after 1997. The cause of the recent Hg concentrations may be related to influx of contaminated watershed soils or sediments. Estimating the time frame for

recovery is challenging in this system because the process of natural recovery seems to have been arrested and deeper, uncontaminated sediments, were not recovered as a basis for reference. However, a recovery to background conditions is likely not achievable since rates of Hg loading to nearby lakes and the current rate of atmospheric deposition are greater than an estimate of background conditions for Deer Lake. Assuming recovery continued after 2000, estimates of the time required for recovery varied based on the system state used to define it (e.g., recent rates of wet Hg deposition or Hg surface concentrations/fluxes from similar systems), but were less than 12 y. However, the recent increasing values of recovery indicators (e.g., Hg concentrations) suggests that these estimates are conservative and will be longer if recovery remains arrested, which may in part be due to the legacy of Hg contamination on the landscape. This study shows that estimates of recovery of highly disturbed lake systems can be made in the absence of within lake reference conditions by using comparisons to reference systems and challenges of estimating ages from atypical ^{210}Pb activity profiles can be overcome in part using event-based dating techniques.

Introduction.

Deer Lake is an impoundment located in the western Upper Peninsula of Michigan within the Marquette Iron Range (Figure 5.1). An ecological assessment of the lake in 1979 determined that fish and sediments were contaminated with Hg (MDNR, 1987). In 1981 a Michigan Department of Natural Resources (MDNR) fish survey determined that fish contained up to 1.38 mg Hg/kg wet weight greatly exceeding the 1981 US average of 0.2 mg Hg/kg and the State of Michigan Fish Consumption Advisory level (MDNR, 1987). Past gold and iron mining related activities were considered to have led to the contamination of the system (MDNR, 1987). As a result of the widespread contamination and threats to ecosystem and human health, the Deer

Lake area, including a portion of the Carp River (Figure 5.1), was designated an Area of Concern (AOC) by the International Joint Commission in 1985 (USEPA, 2007b).

The first steps in the remediation of Deer Lake consisted of lake-level drawdown, fish eradication, and then water level stabilization. In the fall of 1984 Deer Lake was drawn down to its lowest level to facilitate Hg degassing from the sediments and to assist with fish eradication (D'Itri *et al.*, 1992, USEPA, 2007b). Fish eradication efforts included addition of a sharp grate on the dam exiting Deer Lake (killing any fish that might pass through), net-and-kill, and rotenone application; fish were not removed from the system. Prior to 1984 lake levels in Deer Lake were allowed to fluctuate in order to control spring floods and flow through the Cliffs Electric Service Company hydroelectric dam. Fluctuating lake levels might have led to increased rates of Hg methylation in the sediments (D'Itri *et al.*, 1992). Therefore, maintaining a constant water level was included as part of the remediation strategy. In 1987 the lake was refilled and restocked with yellow perch and walleye. It was thought that water level stabilization would reduce the potential for the sediments to act as a source of methyl-Hg to the water column, and reduce Hg burdens in fish. However, in 1999 Hg burdens in large fish were still elevated with respect to other local lakes (USEPA, 2007b)

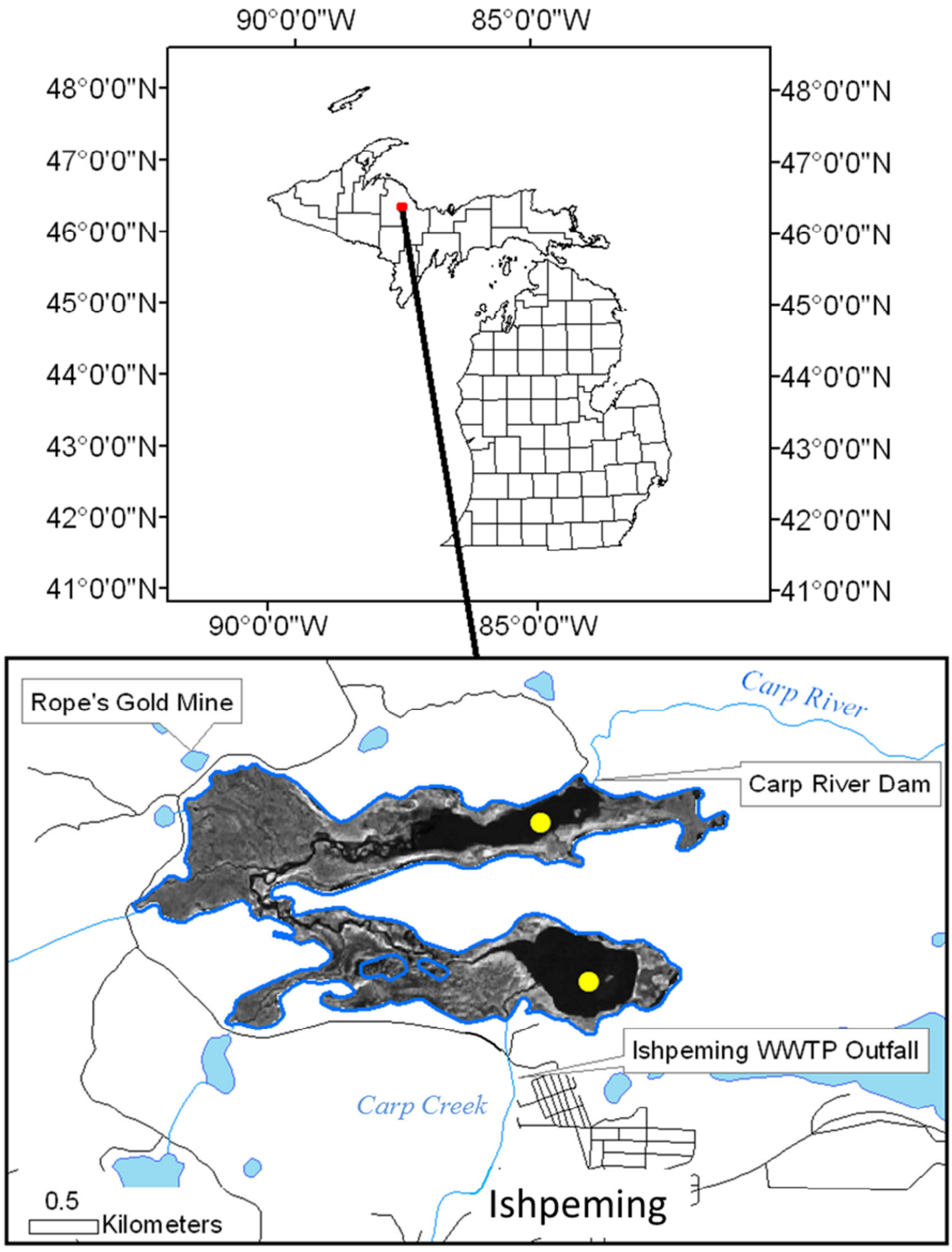

Figure 5.1. Deer Lake study area. Expanded view shows an areal photograph of the study area clipped to the Deer Lake shoreline during the major drawdown. Yellow circles indicate sampling locations. Also shown are the approximate locations of the Rope's Gold Mine, Carp River Dam and the City of Ishpeming WWTP Outfall.

Since initial remediation efforts failed, three alternative remediation strategies were proposed: 1) dredging to remove the most contaminated sediments, 2) installing a gel-cap to isolate the contaminated sediments from newly deposited sediments or 3) allowing new sediment to accumulate and bury the contaminated sediment (natural recovery). To gain insight into the feasibility of natural recovery, sediment cores were taken from the lake to assess current conditions and if temporal trends of Hg loadings and concentrations indicated natural recovery. Natural recovery processes would be indicated by Hg loadings showing a decreasing trend. If recovery is occurring then the time to recovery could be estimated as the time required for the surface sediments to have concentrations or fluxes similar to geochemical background. In addition when the major pathway for contaminant is atmospheric transport as it is for Hg, then another indicator for the state of recovery would be current atmospheric deposition rates.

History and Site Description

A complete history of the Deer Lake AOC is described in the 1987 Remedial Action Plan (RAP) available from the U.S. Environmental Protection Agency (USEPA) AOC website (USEPA, 2007a). Key dates for this study are highlighted in Table 1.

Deer Lake was directly impacted by two mining operations, the Rope's Gold Mine (RGM) and Cleveland Cliffs Incorporated (CCI). The RGM operated on the western shore of Deer Lake from 1882-1899; Hg was used to amalgamate gold during this period. Tailings piles from the mine still exist along the northwestern shoreline of Deer Lake (Figure 5.1); however, most of these tailings are covered by sediments or the road way that separates Causeway Pond from Deer Lake. CCI operated iron mines in the region and maintained analytical laboratories in

the City of Ishpeming. From 1929 to 1981 CCI used mercuric chloride to assay iron ore and discharged the wastes into the City of Ishpeming sewer system. The sewer outfall for the City of Ishpeming was located on Carp Creek (Figure 5.1), approximately 1 km upstream of Deer Lake. CCI ceased this activity in 1981 after an ecological survey of the area determined that the sediments and fish of Deer Lake were contaminated with Hg.

Deer Lake has undergone significant hydrologic changes over time. Prior to the installation of a series of dams between 1912 and 1942 on the Carp River, Deer Lake was much smaller (36 ha) than present day (367 ha). The first dam was installed by the RGM, near the present dam site, to satisfy water needs for the mining process. The present dam was installed by the Cliffs Electric Service Company. Between 1979 and 1984, the water level of Deer Lake was regulated for flood control of spring run-off and power generation, resulting in annual water level changes of approximately 2 m. It has been estimated that 52% of Deer Lake sediments were exposed to the atmosphere during these annual water level fluctuations (MDNR, 1987).

The City of Ishpeming waste water treatment plant (WWTP) prior to 1986 consisted of only primary treatment of the incoming waste stream and therefore did not remove dissolved heavy metals or nutrients (D'Itri, 2008). Mercury wastes from CCI were in particulate form and did, for the most part, settle out during treatment; however, heavy rains would cause flooding of the treatment plant resulting in solid waste flowing into Carp Creek (D'Itri, 2008). Excess nutrient load from the WWTP resulted in the eutrophication of Deer Lake with dissolved oxygen supersaturation of the epilimnion and hypolimentic anoxia (MDNR, 1987). This has important implications for the cycling of Hg in the water column and sediments of the lake. Methyl-Hg

production is favored and methyl-Hg bioaccumulation is significantly enhanced under anoxic conditions (Eckley *et al.*, 2005, Munthe *et al.*, 2007, Watras *et al.*, 1994). Therefore, anthropogenic eutrophication may have lead to the increased rate of Hg methylation in Deer Lake and consequently higher Hg burdens in fish. A new WWTP, serving the City of Ishpeming, which has the capability of removing nitrogen and phosphorus, was put on-line in 1986. Reduced nutrient input should result in a reduced rate of eutrophication; this should also result in decreased rates of Hg methylation by reducing the periods of anoxia in bottom waters.

Although it cannot be shown that the water level stabilization in Deer Lake resulted in reduced rates of Hg methylation, recent work has shown that methyl-Hg production may be enhanced during sediment resuspension (Sunderland *et al.*, 2004, Tseng *et al.*, 2001) and drying/re-wetting cycles (Rumbold and Fink, 2006). The fluctuation in water level would also expose areas of the lake bottom to periods of higher energy regimes that would lead to movement of more sediment into depositional zones. Under stable water level conditions these sediment would not otherwise be transported (Shotbolt *et al.*, 2005). Thus, higher energy regimes could result in the transport of Hg contaminated sediments from the littoral zone to the profundal zone in Deer Lake, increasing the burden of sediments exposed to anoxic bottom waters. The increased mass of Hg-contaminated sediments exposed to anoxic bottom waters may have led to increased rates of methyl-Hg production and increased fish Hg burdens.

Sampling and Analytical Methods

In the summer of 2000 sediment cores were retrieved from the deepest portion of the North and South basins of Deer Lake. Aerial photography indicated these sites had remained under water during the major drawdown period (1984-1987). Sediment cores were collected using an Ocean Instrument MC-400 Multicorer (www.oceaninstruments.com) deployed from the US EPA *R/V Mudpuppy*. The MC-400 collects four simultaneous cores which were used for porewater metals analyses, radiometric dating, and sediment metals analyses; the fourth core was kept as an archive core. Polypropylene jars and polyethylene bottles used to collect and/or store samples for trace metal analyses were thoroughly acid cleaned, using trace metal grades hydrochloric (HCl) and nitric (HNO_3) acids, using one of three procedures: 1) cold-acid washing; cold 24hr 10% hydrochloric acid (HCl) cycle followed by a 24hr pure water (≥18 μS-cm) rinse; 2) hot acid washing, hot 24hr 15% HCl cycle followed by a 24hr pure water rinse; 3) clean-acid washing, cold 24hr 1:1 HCl cycle followed by a hot 24hr 1:1 HNO_3 cycle followed by a 24hr pure water rinse. Cores intended for radiometric dating and sediment metals analyses were sectioned on-shore immediately after retrieval at 0.5 cm increments for the first 8 cm and at 1 cm increments for the remainder of the core. The effects of core smearing during extrusion were reduced by discarding those sediments in contact with the walls of the core tube (metals core only). Sediment samples were placed in cold-acid-washed polypropylene jars and stored on ice until return to the laboratory.

In the laboratory, sediment samples for elemental analysis were stored frozen until being freeze-dried prior to microwave-assisted nitric acid digestion using EPA Method 3051 (USEPA, 2007c). Samples for radiochemical dating were shipped to the Freshwater Institute, Winnipeg, Canada. Reference material NIST 8704 Buffalo River Sediment (RM8704) and procedural

blanks were analyzed with each digestion batch. Precision of the digestion procedure was evaluated with NIST RM8704, Buffalo River Sediment, %RSD for 10 replicates was 9.0% and 6.0% for Al and Hg, respectively. Concentrations of metals in procedural blanks were consistently lower than the quantification limit (MDL) of the analytical method (Hg_{MDL} = 1.27 ng/mL, Al_{MDL} = 91.93 ng/mL). Digestates were diluted to 100 mL with pure water (≥18 μS-cm) prior to filtration with acid-cleaned, cold 10% HNO_3 followed by a 24hr pure water rinse, 0.40 μm Nucleopore filters. Total metal and Hg samples were filtered into separate hot acid washed 60 mL polyethylene bottles. Samples for Hg analysis were preserved by adding 200 μL of a 100 ppm gold chloride solution. All samples were stored in the dark at 4ºC prior to analysis. Sediment iron and calcium concentrations were determined using atomic absorption spectrophotometry (Yohn *et al.*, 2002). All other sediment metal concentrations were determined using a Micromass Platform (now Thermo) ICP-MS with hexapole collision cell technology. A 2% HNO_3 rinse solution was used for all sediment metals analyses, except for Hg which used a 2.5% HNO_3 + 2.5%HCl + 10 ppm gold chloride rinse solution. The HNO_3/HCl + gold solution was used to prevent memory effects of Hg in the mass spectrometer (Allibone *et al.*, 1999).

The radionuclide ^{210}Pb was used to determine sedimentation rates and assign dates to the sediment cores and cesium-137 (^{137}Cs) was measured in select slices of sediment from the North Basin to determine the peak value in ^{137}Cs activity. Detailed methods of analysis for ^{210}Pb and ^{137}Cs can be found elsewhere (Wilkinson and Simpson, 2003). Cs-137, was determined by direct counting of 5-10 g of sediment on a γ-spectrometer (Ge-Li) semiconductor detector.

Samples of 1-3 g were analyzed for ^{210}Pb and radium-226 by leaching in 6 N HCl in the presence of a ^{209}Po tracer, autoplating Po onto a silver disk, and counting the disk on an α-spectrometer to determine ^{210}Pb via its ^{210}Po daughter. Sediment slice ages were estimated using the constant rate of supply (CRS) model (Appelby and Oldfield, 1978) or the regression equation of excess ^{210}Pb activity versus total accumulated sediment dry mass using the constant flux:constant sedimentation (CF:CS) (Golden *et al.*, 1993) and segmented CF:CS models (Heyvaert *et al.*, 2000).

Results and Discussion

Effects of Lake Level Drawdown on ^{210}Pb Profiles. Vertical changes in the slope of excess ^{210}Pb versus depth are used to identify changes in sedimentation rates caused by natural (Appleby *et al.*, 1998) or anthropogenic processes (Heyvaert *et al.*, 2000) and were used here to investigate the effects of the major drawdown period in the mid to late 1980s on sedimentation rates in Deer Lake. Higher sedimentation rates are indicated by more vertical slopes of the excess ^{210}Pb profile. It was anticipated that during the drawdown period more material from the littoral areas would be focused into the deeper portions of the lake because of the increased energy regimes (Shotbolt *et al.*, 2005). Such focusing would be reflected by an increase in slope during the drawdown.

Vertical profiles of excess ^{210}Pb activities, in general, increased to the surface in both sediment cores (Figure 5.2). However, in the South Basin ^{210}Pb activities increased until about 17 cm depth. Then between 17 and 10 cm there was a large deviation from the log-linear trend.

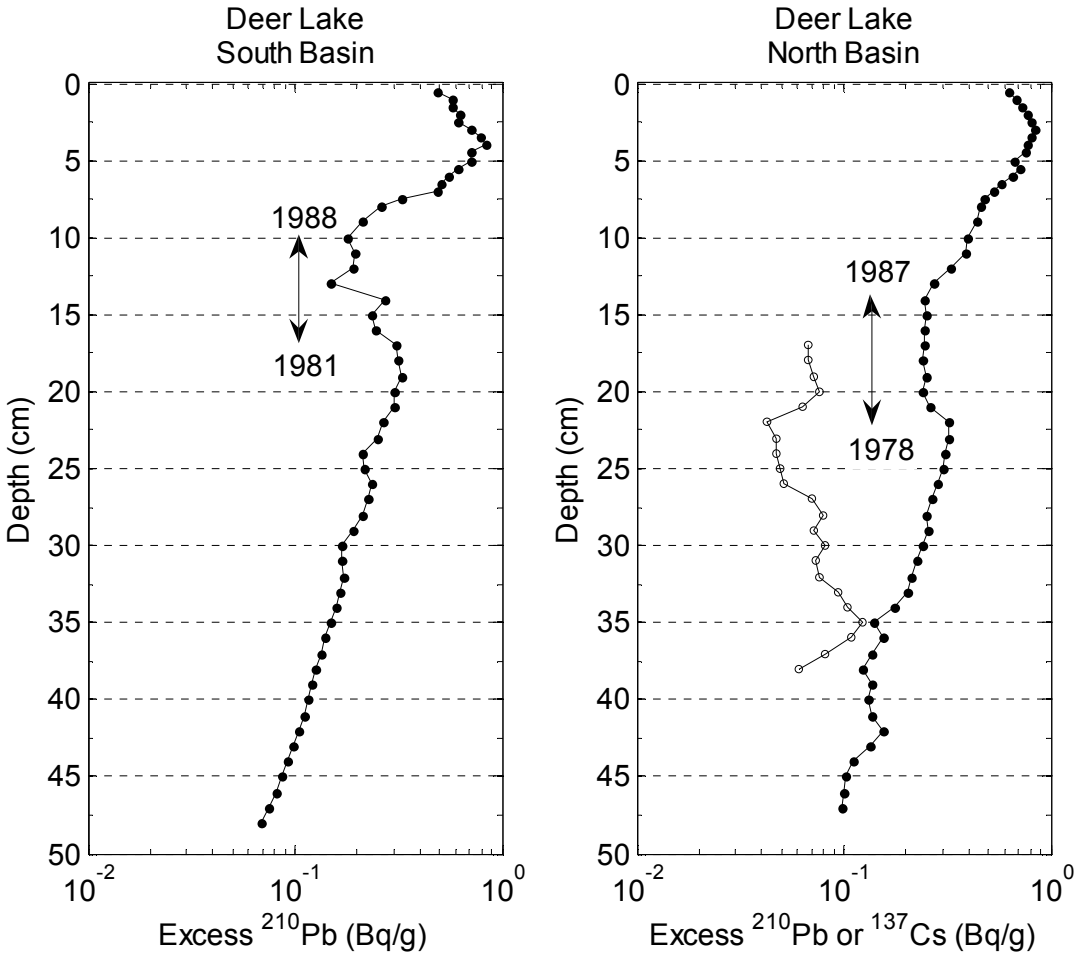

Figure 5.2. Excess ^{210}Pb profiles (solid circles) from the South and North Basins and the ^{137}Cs profile (open circles) from the North Basin of Deer Lake. Double arrows indicate the large deviation in the excess ^{210}Pb profile; CRS model dates were assigned to the beginning and end of the large deviation for their associated mass depths.

Maximum ^{210}Pb activity was at approximately 4 cm and then decreased towards the sediment-water interface. In the North Basin ^{210}Pb activities generally increased until around 22 cm depth. From 20 to 14 cm activities were lower and constant. Above 14 cm ^{210}Pb activities increased and peaked at 3 cm and then decreased to the surface.

From our past work (Parsons *et al.*, 2007, Yohn *et al.*, 2004, Yohn *et al.*, 2002) the CF:CS and CRS models were considered the most appropriate methods of estimating dates for sediment cores collected from inland lakes of Michigan. The CF:CS model assumes a constant flux of ^{210}Pb and a constant sedimentation rate and more appropriately models core profiles that exhibit a log-linear trend (Appleby *et al.*, 1998, Robbins and Edgington, 1975). The CRS model also assumes a constant flux of ^{210}Pb to the sediment surface but allows for changes in sedimentation rate to account for the inventory of excess ^{210}Pb activity, where the inventory is the product of sediment dry mass and excess ^{210}Pb summed for the entire core. This model would be useful for interpretations of small scale deviations in the ^{210}Pb profile, such as those above 15 cm in the South Basin. However, to calculate the CRS model unsupported ^{210}Pb must reach 99% equilibrium with the supporting ^{226}Ra which occurs in approximately 150 y (Appelby and Oldfield, 1978, Krishnaswamy *et al.*, 1971, Robbins, 1978) which was not observed in either sediment core.

Cesium-137 is a radionuclide introduced to the environment during the atmospheric testing of nuclear weapons. Testing of these weapons peaked in 1963 thus supplying a chronostratigraphic marker in lake sediments (for a review of chronostratigraphic markers see (Appleby, 2001)). When the CF:CS model was used to estimate dates the peak in ^{137}Cs activity from the North Basin core was assigned a date of 1956, almost a decade early. Furthermore, the deviation in ^{210}Pb activity at 22 cm depth, which we assume to be a result of lake level management or draw down occurred in 1973, five years before the active water level management of the lake. It appears that the CF:CS model did not assign appropriate dates to these events, and it would be useful to date the core with an alternative method. Since excess ^{210}Pb was detected in the bottom slices of the South and North basin sediment cores use of the CRS model might be considered limited because the ^{210}Pb inventory could not be calculated directly (Appelby and Oldfield, 1978). However, in an effort to more appropriately reflect the changes in the trajectories observed in the excess ^{210}Pb profile a modified approach to the CRS model was used. First, activities of excess ^{210}Pb for the North Basin were extrapolated to equilibrium with supported ^{210}Pb. Resultant dates were then adjusted by adding ^{210}Pb inventory (less than 1%) to the last core sample so that the peak of ^{137}Cs occurred in 1963. Using this approach the deviation in the ^{210}Pb profile that occurred at 22 cm dated to 1978, the start of the active water level management period. Activities of excess ^{210}Pb between 20 and 14 cm were constant indicating a zone where sediments have been mixed. Both the modified CRS

approach and the CF:CS model assigned a date of 1987, the year the lake was refilled, to the upper portion of this zone.

Since the CRS dates for the North Basin more appropriately reflected the period of active water level management period (1979-1984, Table 1) and the major drawdown and lake refilling (1984-1987, Table 1) a similar modified CRS model approach was used to assign dates to the South Basin core. The South Basin core was not submitted for ^{137}Cs analysis so the trajectory change in excess ^{210}Pb at 17 cm was used to adjust dates with the assumption that the change occurred in the late 1970s or early 1980s coincident with the start of active water-level management of Deer Lake. Similarly to the North Basin, excess ^{210}Pb inventory (~1%) was added to the last core sample so that the 17 cm transition to lower ^{210}Pb activities occurred in 1981. Doing so placed the upper limit of the mixing zone, at 10 cm, in 1988. This is similar to the procedure used to correct for old date error (Binford, 1990). The CF:CS model assigned dates of 1979 and 1993 to the 17 and 10 cm depths, respectively. Although the former date appears to reflect the beginning of the water-level stabilization period the latter does not correspond to the refilling of Deer Lake as might be expected and found for the North Basin. Since the ^{137}Cs profile could not be used to verify the dates assigned by the CRS model, the peak in stable Pb concentration was used to assess the accuracy of the assigned dates (Figure 5.3) Stable Pb concentrations in sediment cores should peak in the mid 1970s consistent with the removal of Pb from gasoline and this approach has been used to confirm sediment ages (Alfaro-De la Torre and Tessier, 2002, Yohn *et al.*, 2004, Yohn *et al.*, 2002). The Pb concentration profile from the South Basin had two peaks: the first in the early 1960s and the second in the

early 1970s using the CRS model (Figure 5.3). The older peak had concentrations that were greater, but following the more recent peak concentrations steadily decreased. We consider the latter peak, occurring in 1973 (1971 using the CF:CS model), followed by the decline to be indicative of the removal of leaded gasoline and therefore useful as a event-based dating tool. In the North Basin the peak in Pb concentration occurred in the late 1970s (1974 using the CF:CS model) (Figure 5.3) The approach of using a modified CRS model resulted in a more appropriate reflection of age information obtained from the peak in stable Pb as well as events influencing sedimentation rates in Deer Lake. Thus, the dates from the modified CRS approach will be used here.

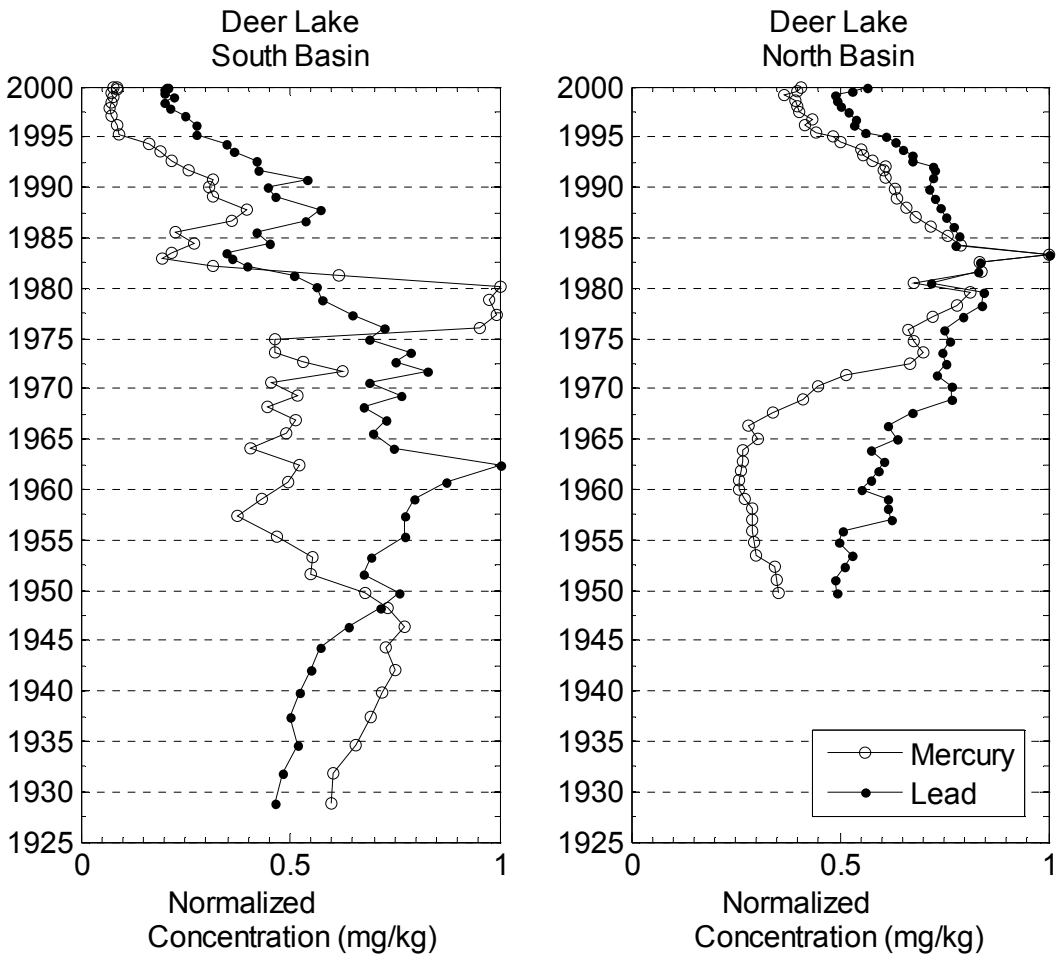

Figure 5.3. Profiles of mercury (open markers) and lead (solid markers) normalized to their respective maximums to highlight similarities between the profiles.

Trends of ^{210}Pb activities that are steep or approaching vertical would be anticipated as a result of increased sediment fluxes and mixing during the draw down (e.g., (Appleby *et al.*, 1998, Robbins, 1982); however, the negative slopes were not. Sediment dry mass was higher during this period consistent with an increased flux of sandy sediment from the littoral zones of the lake (Figure 5.4), evidenced by sediment color and texture change. The negative slopes indicate that sediments were diluted with older (i.e., lower ^{210}Pb activities) sediment. Dates corresponding to the 17 and 22 cm depths were 1981 and 1978 in the South and North basins,

respectively, which is just prior to the active water level management period of Deer Lake (Table 1). It is highly probable that, during the water level management period and major drawdown, older sediment from shallower non-depositional zones of the lake as well as shoreline sediments were focused to the deeper areas where the samples were taken. The prolonged exposure of lake-bottom sediments would 1) allow wind erosion of exposed sediments and 2) create zones of higher energy at lake locations that would otherwise be at lower energy regimes (Shotbolt *et al.*, 2005). These processes could result in the transport of older sediment into the depositional zone diluting the activity of ^{210}Pb. Lead can be influenced by post depositional mobility (Benoit and Rozan, 2001); however, vertical patterns of ^{210}Pb activities would not be expected if this processes were occurring and the correlation of ^{210}Pb deviations with human activities provides strong evidence against the mobility of Pb in the sediment column.

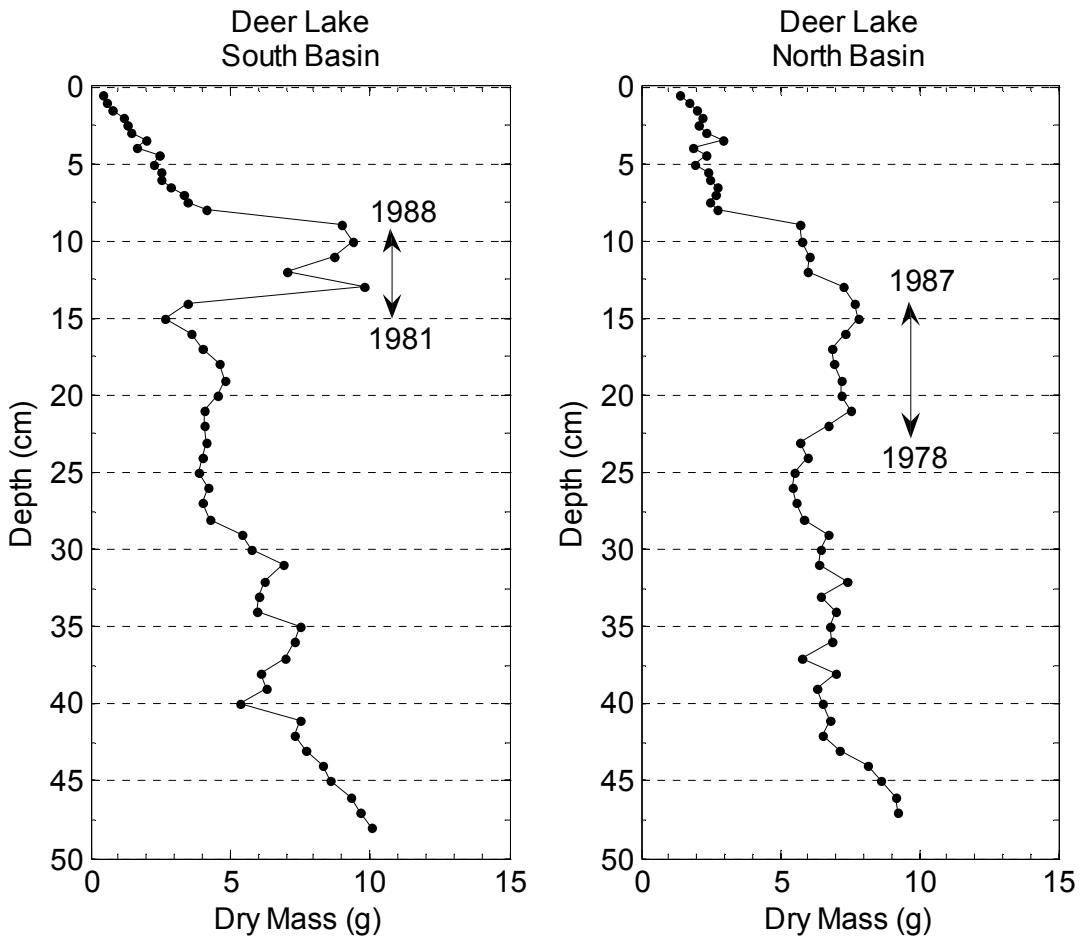

Figure 5.4. Dry mass profiles from the South and North basins of Deer Lake. Double arrows indicate the large deviation in the excess ^{210}Pb profile; dates are assigned to the beginning and end of the large deviation for their associated mass depths.

The peak in excess ^{210}Pb activities occurred at about 4 and 3 cm depths in the South and North basins, respectively. Near the surface ^{210}Pb activity values are often homogenized because of biotubation and currents resulting in near vertical slopes (Robbins, 1982). Again, the negative slopes imply that older sediment was deposited over and perhaps mixed with newer material. However, lake levels have not been intentionally lowered as was interpreted to be the cause for the negative slopes down core. Thus a possible explanation might be explained by drought conditions that existed in the study area during the 1990s.

The Palmer modified drought index (PMDI) indicated that there was a period of prolonged drought (PMDI < 0) between June 1997 and June 1999 (National Oceanic and Atmospheric Administration, 2007). This was followed by a brief, four month, recovery (PMDI between 0 and 2) between July 1999 and October 1999. Drought conditions then persisted until January 2001. This prolonged drought may have resulted in lake level lowering and exposure of lake-bottom sediment and the influx of older sediment, similar to what may have occurred during the major draw down.

Impact of mining activities on mercury concentration in Deer Lake. In the South Basin, temporal changes in sediment Hg concentrations were more variable and concentrations higher than in the North Basin (Figure 5.5). This is most likely due to the proximity of this basin to Carp Creek, the discharge location for the City of Ishpeming WWTP (Figure 5.1). Recently, sediment Hg concentrations from both basins have remained constant albeit elevated above background concentrations from other Upper Peninsula of Michigan lakes (Parsons *et al.*, 2007). Prior to this, in the South Basin, sediment Hg concentrations increased steadily from the late 1920s until the mid 1940s, declined until the late 1950s, and then slowly increased until the mid 1970s. During the mid to late 1970s sediment Hg concentration increased, remained elevated and then rapidly declined until the early 1980s, consistent with the removal of the point source of Hg contamination. Concentrations then increased until the late 1980s followed by decreased concentrations until the late 1990s. In the North Basin, sediment Hg concentrations slowly declined from the 1950s until the mid 1960s, then increased until the early 1980s. Since then,

sediment concentrations declined until the late 1990s.

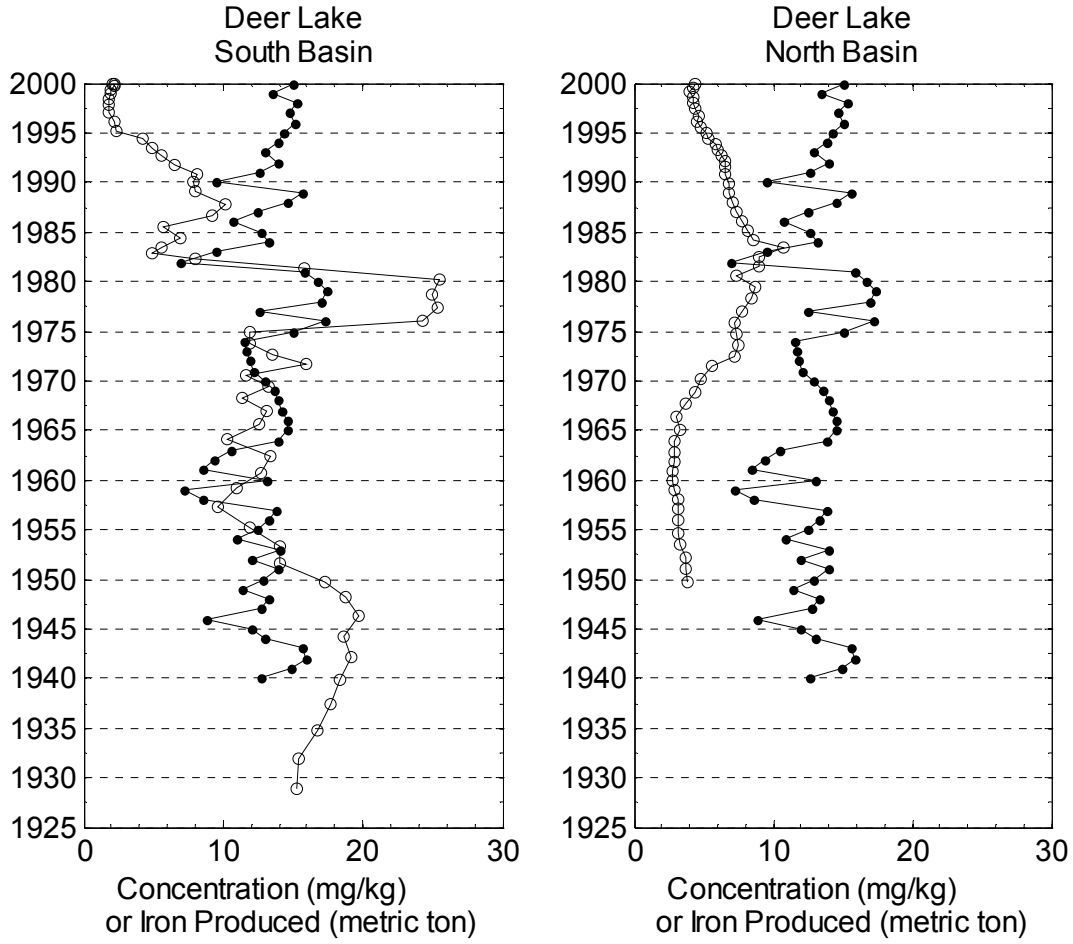

Figure 5.5. Hg concentration (mg/kg) profiles from the South and North basins of Deer Lake (open circles) and production of usable iron ore from Michigan (closed circles, metric ton(x1000)).

Because of the long history of base-metal mining in Michigan's Upper Peninsula the impact of mining activities has been well documented (Kerfoot *et al.*, 1999, Kerfoot *et al.*, 2004, Kerfoot and Lauster, 1994, Kolak *et al.*, 1998, Kolak *et al.*, 1999) and although CCI was eventually found liable for the contamination of Deer Lake the RAP (MDNR, 1987) does not provide geochemical evidence to link CCI's mining activities to Hg accumulation in Deer Lake. The role of the abandoned RGM, specifically the mine tailings on the northwestern shore of the lake, to mercury contamination has been unclear. Since our sediment records can not provide

information about the potential contribution of the mine tailings to mercury contamination (i.e., do not contain sediment of adequate age), profiles of Hg concentrations were compared to production of iron ore from the Upper Peninsula of Michigan (USGS, 2009). The assumption is that an estimate of CCI's activities can be deduced from these production records. In other words, when production of CCI was producing more iron they would in turn being assaying more iron resulting in an increased load of Hg to Deer Lake. Therefore, if the sediment Hg profiles can be correlated to the production records of iron ore then this would tend to indicate CCI's activities as the primary source of contamination Deer Lake Hg concentration profiles and usable iron ore production from the Marquette Range of Michigan's Upper Peninsula (1940-2000) (USGS, 2009) are shown in Figure 5.5. Production of iron ore from the State of Michigan was greatest in the 1940s, when iron was needed for wartime manufacturing, and 1970s, when monetary inflation and other economic forces created renewed interest in mining iron ore (Fenton, 1998).

In the South Basin, sediment Hg concentrations exhibited high concentrations in the mid 1940s coincident with higher iron production during the 1940s and Hg concentration generally tracks the production of iron ore between 1950 and 1980 (Pearson's $r = 0.59$, $p = 0.001$) (Figure 5.5) providing further evidence for a mining related source for the Hg contamination of Deer Lake. Mercury concentrations and iron ore production appeared to be correlated after the early 1980s to 1990, but their trends become decoupled after 1990. In the North Basin, iron ore production and sediment Hg concentration did not correlate as well as in the South Basin between 1950 and 1980 (Pearson's $r = 0.52$, $p = 0.006$) (Figure 5.5). A general decrease in iron ore production corresponds to the decrease in Hg concentration between 1950 and 1965 and the

peak in Hg concentration in the late 1970s correlates with the peak in iron ore production during this period providing evidence for an iron-mining related source. Mercury concentration and iron ore production become decoupled after ca. 1985, slightly earlier than what was observed in the South Basin but more consistent with the removal of the point source of Hg contamination. The smoother North Basin Hg concentration profile and poorer correlation to iron ore production are suggestive of a slow bleed of Hg contaminated sediments from the South Basin. This evidence coupled with the decreasing concentrations of Hg after removal of the point source indicate that the Hg in the North Basin were also related to the CCI mining activities rather than contributions from the RGM mine tailings. The reason for the later decoupling in the South Basin is unclear, but may be related to watershed disturbance and is discussed below.

The influence of watershed processes on mercury concentrations in Deer Lake. If the City of Ishpeming sewer were the sole pathway of Hg to Deer Lake via Carp Creek then Hg concentrations should have decreased after CCI stopped the disposal of mercuric chloride into the sewer in 1981. In both basins Hg concentrations clearly declined after 1981 (Figure 5.5); however, the decrease in the South Basin was rapid while in the North Basin more gradual. The more rapid decline of Hg concentrations in the South Basin is likely due to the response of this basin to the removal of the point source and the proximity of this Basin to the WWTP discharge location. The gradual decline observed in the North Basin could then be interpreted as a muted response to the point source removal combined with inter-basin mixing of contaminated sediments.

Since watershed soils are known to be significant sinks of metals (Mason and Sheu, 2002), when disturbed by human activities or climatic changes they can be significant sources of metals to aquatic ecosystems. Metal/aluminum concentration ratio and aluminum concentration profiles are often used to infer and quantify the contribution of chemicals derived from terrestrial material (i.e., watershed soils) into a lake (Bruland *et al.*, 1974, Koelmans, 1998, Tuncer *et al.*, 2001, Yohn *et al.*, 2002). Ratios of Hg:Al were calculated for both basins and are shown in Figure 5.6 along with aluminum concentrations. In the South Basin Al concentrations steadily decreased from the late 1920s until the early 1980s, increased rapidly until the late 1980s and have since decreased (Figure 5.6). The Hg/Al ratio was relatively constant prior to 1935 then increased until the mid 1940s, decreased until the mid 1950s and generally increased again until the mid 1970s (Figure 5.6). After the mid 1970s the ratio rapidly increases, peaking in the late 1970s, then rapidly decreases until the mid 1980s. Ratio values then generally decline until the mid 1990s and increase thereafter. The above trends are interesting in that they can be interpreted to indicate two different pathways of Hg to the South Basin. Between 1930 and the early 1980s the Hg/Al ratio and Al concentration profiles were not correlated, which clearly indicates a point source for Hg, i.e., mercuric chloride from CCI, to Deer Lake during this period. During the major draw down period Al concentrations increased while the Hg/Al profile decreased suggesting a dilution of Hg concentration due to increased sediment focusing, which is the likely reason for the sharp decline in Hg concentrations at the beginning of the draw down (Figure 5.5). After the late 1980s, about the time Deer Lake was refilled, and until the mid 1990s Al concentrations once again start to decline and appear coupled to the Hg/Al ratio which suggests a terrestrial pathway for Hg. After 1995 the two profiles are again decoupled, indicating an additional source for Hg to the lake. The profile of Pb was similar to that of Hg

between 1983 and 1995 suggesting a watershed pathway for Pb as well (Figure 5.3), the profiles prior the early 1980s were not as similar indicating unique sources for each chemical.

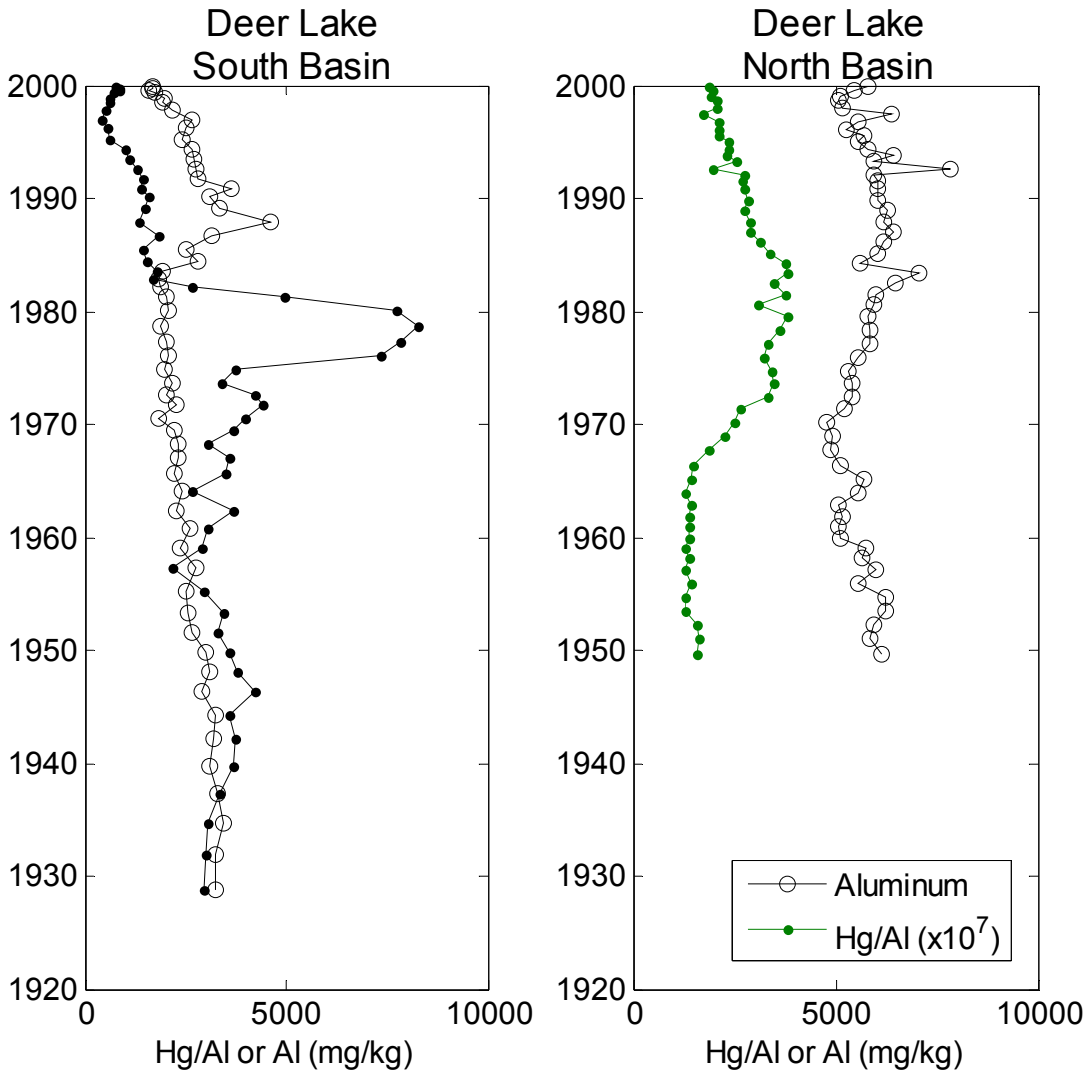

Figure 5.6. Profiles of Al (open circles) and Hg:Al ratio (solid circles) for the South and North basins of Deer Lake.

In the North Basin Al concentrations, in general, decreased between 1950 until 1970, increased until ca. 1983, decreased rapidly then slowly increased between 1983 and 1987 and had since been generally declining until the late 1990s (Figure 5.6). The ratio of Hg/Al was relatively constant between the 1950s and mid 1960s, increased from 1965 until the early 1970s,

remained relatively constant or increased slowly until 1985, and had since declined. The trends in Al and Hg:Al ratio of the North Basin differ from those of the South Basin. The most apparent difference is the broad nature of the trends compared to the more abrupt changes observed in the South Basin. The effects of the direct addition of mercuric chloride are most evident between 1965 and 1972. From 1972 to 1985 both the Hg/Al ratios and Al concentrations were high which might indicate a contribution to Hg levels from South Basin contaminated sediment as well as direct inputs. The correlated decrease in Hg/Al ratio and Al concentrations between 1985 and 1997 can be interpreted as burial of contaminated sediments by less contaminated sediment. The profile of Pb in the North Basin was more similar to Hg than the South Basin throughout the entire sediment core. This is indicative of the processes leading to deposition of chemical to the North Basin i.e., transport of sediment from the South Basin.

These patterns are interpreted to indicate that the pathway for Hg has changed from being a point source to that of a terrestrial source (i.e., Hg laden soils/sediment from the watershed or Carp Creek sediments). The possibility of the Carp Creek sediments as a source/pathway has important implications for the recovery of Deer Lake in that total recovery may not take place until the sediments of Carp Creek have been remediated.

Estimating Recovery using Hg Accumulation Rates and Sediment Concentrations. The recovery of a system is often defined as the condition when contaminant loading rates or concentrations reach a specified threshold or reference value (Magar, 2001). Threshold values are concentrations or fluxes of contaminants to the environment usually defined by state and federal agencies as above which there are adverse effects on ecological and human health.

Because threshold values are defined independent of system processes, they cannot be used to indicate recovery of disturbed watershed-lake systems. Reference values are estimates of the geochemical background flux or concentration of a contaminant prior to human perturbation. However, recovery to a reference value may not be achievable when current loading rates are greater than pre-disturbance conditions. For example, 1999 wet deposition rates of Hg along the border between Wisconsin and Michigan's Upper Peninsula varied between 9.0 and 13.3 μg Hg m^{-2} y^{-1} (Illinois State Water Survey, 2008) compared to the background flux of about 8.3 μg Hg m^{-2} y^{-1} for 5 Upper Peninsula lakes (Parsons *et al.*, 2007). Total deposition would be greater due to dry deposition of Hg (Lindberg *et al.*, 2007) which can equal that of wet deposition for this region (Landis and Keeler, 2002). A more reasonable recovery condition would then be that of similar systems, in this case surface concentrations/fluxes of nearby inland lakes or equal to the atmospheric deposition rate of a contaminant. In this way the recovery of a system could then be defined as when the system comes into balance (steady-state and equilibrium processes) with current inputs (e.g., atmospheric and watershed inputs) (Long et al., 2010).

To estimate the effects of the natural recovery remediation strategy for Deer Lake focusing corrected accumulation rates (FCAR) of Hg were calculated as:

$$Hg\ Acc\ Rate(\mu g\ m^{-2}\ y^{-1}) = \frac{Hg\ (mg\ kg^{-1}) \times Sed\ Rate(g\ m^{-2}\ y^{-1})}{FF} \quad (1)$$

where *FF* is the focusing factor and is calculated as the ratio of the actual ^{210}Pb inventory to that which is expected and *Sed Rate* is the sedimentation rate calculated from the profiles of excess ^{210}Pb. The expected inventory of excess ^{210}Pb for this region is 0.574 Bq cm^{-1} (Golden *et al.*,

1993). Since neither core was deep enough to observe ^{210}Pb equilibrium with 226-Radium, the excess ^{210}Pb inventory was estimated by extrapolation (Parsons *et al.*, 2007). The FF's were approximately 1.7 and 2.7 for the South and North basins, respectively and were similar to other Michigan lakes which range from 1 - 3 (Parsons *et al.*, 2007, Yohn *et al.*, 2004).

On average, focusing corrected accumulation rates (FCAR) for Hg were higher in the South Basin than the North Basin (Figure 5.7) and are higher than other Upper Peninsula lakes (Parsons *et al.*, 2007) consistent with the pollution history of Deer Lake. Mercury FCAR showed only small changes in the North or South basin since 1997, and may have started to increase, suggesting that natural recovery had ceased. Surficial FCAR were greater for the North Basin (1167 μg Hg m^{-2} y^{-1}) than the South Basin (719 μg Hg m^{-2} y^{-1}) and both are much higher than what would be expected for wet Hg deposition to this region (Illinois State Water Survey, 2008). The reasons for the cessation of recovery are unclear but may be due to watershed disturbance or leaching of Hg from the RGM tailings piles. Surficial Hg FCAR for other Upper Peninsula lakes vary between 14 and 63 μg Hg m^{-2} y^{-1} (Parsons *et al.*, 2007) and would be expected for Deer Lake in the absence of point-source Hg pollution. To estimate the time required for surficial sediment Hg FCAR in Deer Lake to achieve a flux of 20 μg Hg m^{-2} y^{-1}, the median surficial Hg flux for 5 Upper Peninsula lakes (Parsons *et al.*, 2007), a linear regression was made on Hg FCAR starting in 1993 and 1991 in the South Basin and North Basin, respectively (Figure 5.8). These dates were chosen because they represent the most recent peaks or slope changes in Hg FCAR. It is assumed here that the regions of relatively constant FCAR represent a brief period of arrested recovery and were not included in the regression and that the processes resulting in

clean sediment being deposited on top of the more contaminated sediment continue at the same rate. Regression equations calculated from the FCAR profile were shifted to the most recent sediment slice to calculate a rate of recovery, that is, if recovery were to begin again how long would it take for fluxes/concentrations to be in the new system state. However, it is not certain if or when recovery will resume since the initial recovery was arrested, indicated by relatively constant or increasing FCAR since 1997 (Figure 5.8). Results of this regression suggest that recovery in the South and North Basins would be approximately 3 and 7 years, respectively. Using the average of the 1999 wet deposition for the four Wisconsin and the northeast Minnesota Mercury Deposition Network sites (9.1 μg $Hg/m^2/y$, Illinois State Water Survey, 2008), chosen for their proximity to Deer Lake, as the system state the same results were found. This indicates that the rate of recovery for Deer Lake is rapid and that natural recovery appears to be a proper remediation strategy for this system. However, there is no guarantee that the loading of Hg to Deer Lake will remain constant and a longer term monitoring strategy should be adopted.

Calculating fluxes of contaminants permits comparisons among lakes and comparisons to atmospheric deposition rates. However, fluxes do not provide direct information about potential exposure of benthos to sediment contaminants. The concentrations of Hg in the surficial sediments were about one order of magnitude greater than most Upper Peninsula lakes (Parsons *et al.*, 2006). Thus, it would be helpful to know when concentrations of Hg in the surficial sediment of Deer Lake would be more reflective of other Upper Peninsula lakes. Similar to the flux regression analysis above, a linear regression on concentration was made to determine the

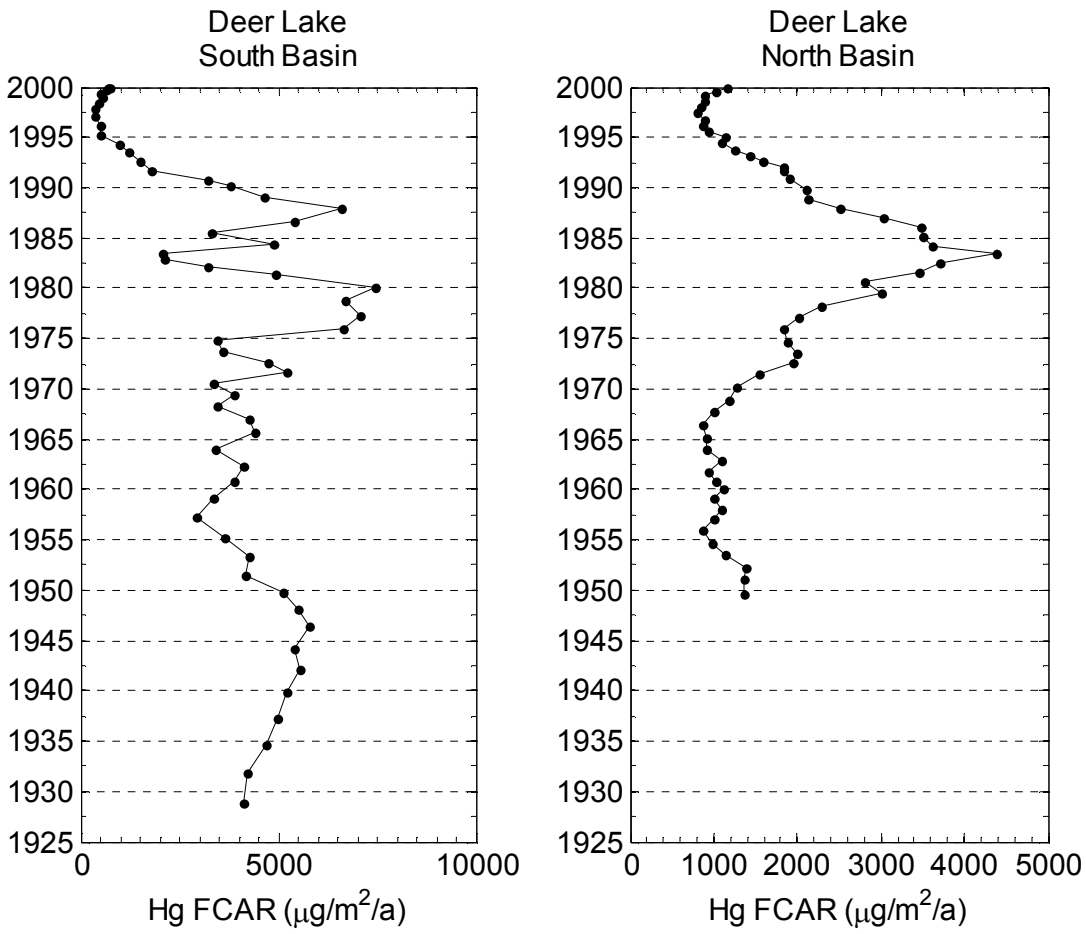

Figure 5.7. Focusing corrected Hg accumulation (μg/m2/y) rates for the South and North basins of Deer Lake.

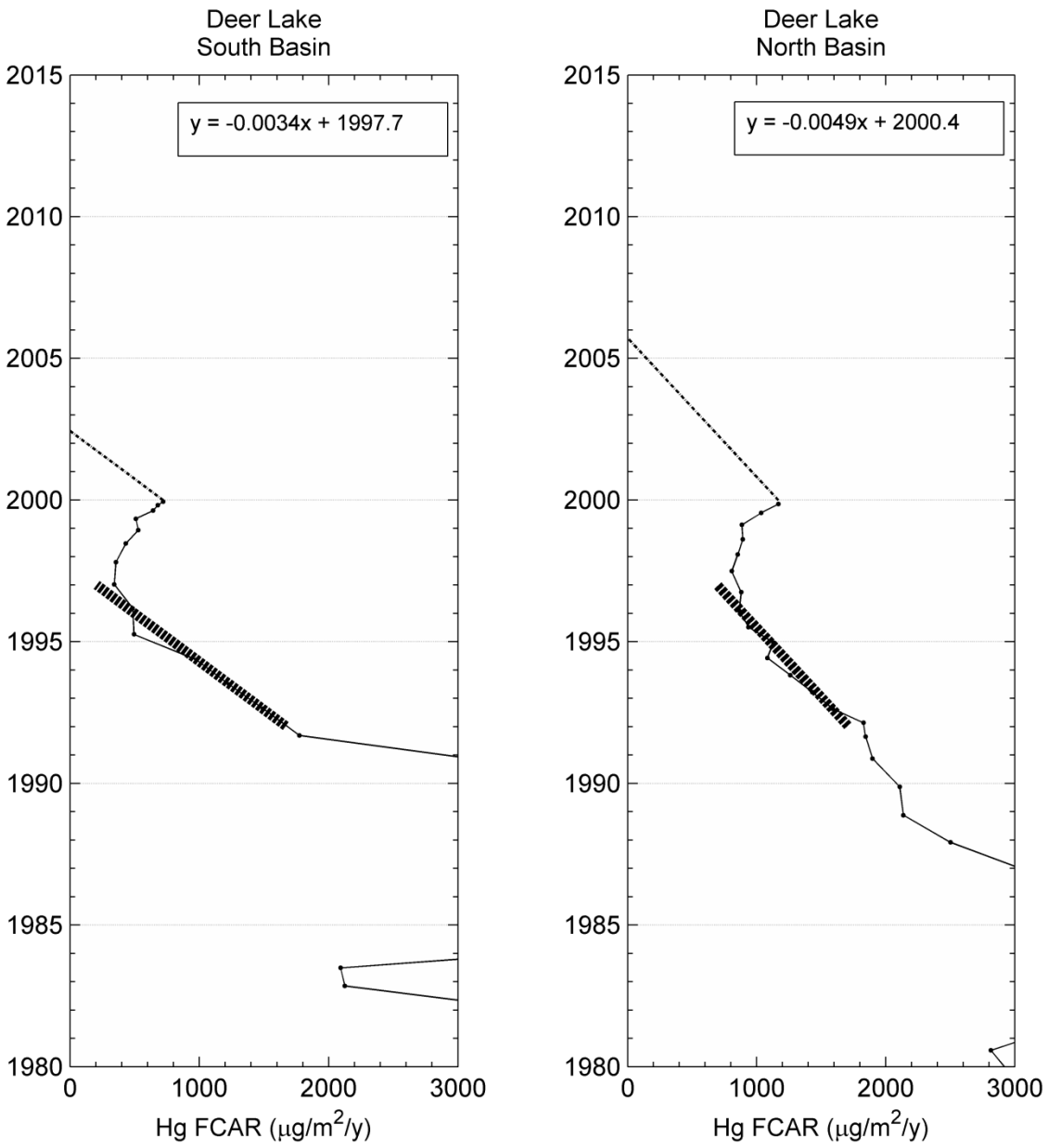

Figure 5.8. Hg FCAR profiles for the South and North basins of Deer Lake, 1980 to present. The dashed line shows the linear model used to determine the time to recovery, equations used are also shown. The dash-dot-dash line shows the model applied to predict the year of recovery.

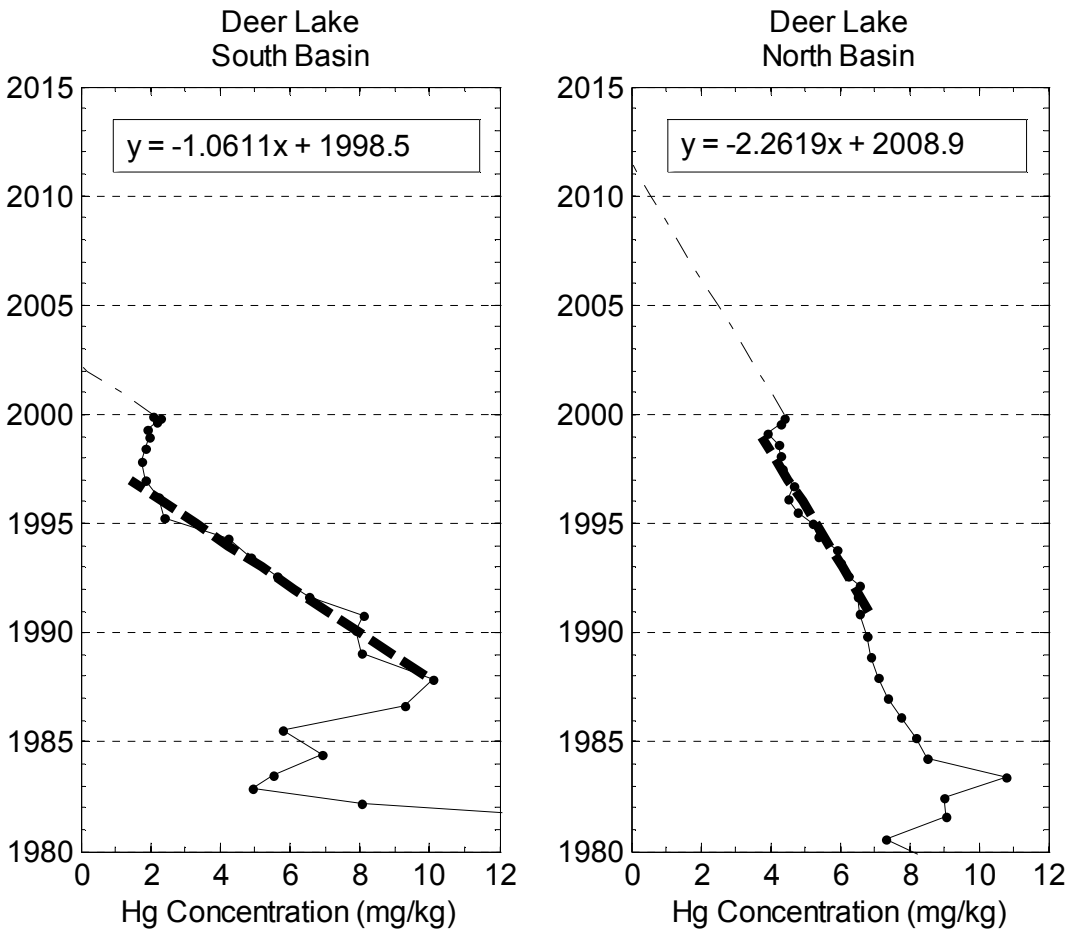

Figure 5.9. Hg concentration profiles for the South and North basins of Deer Lake, 1980 to present. The dashed line shows the linear model used to determine the time to recovery, equations used are also shown. The dash-dot-dash line shows the model applied to predict the year of recovery.

time it would take for Deer Lake sediments to have Hg concentrations similar to surficial sediments of other Upper Peninsula lakes (Figure 5.9). Assuming that sedimentation rates remained constant, to be similar to current Hg concentrations (0.16 mg Hg/kg; average of 5 Upper Peninsula lakes (Parsons *et al.*, 2007)) the South Basin would require at least 3 y, whereas the North Basin would require 12 y. Again this analysis points out the connection between the two basins of the lake. That is, the estimated recovery to current concentration, wet deposition and surficial fluxes were the same for the South Basin, while those recovery estimates for

concentration in the North Basin were longer than the other two system states. This suggests that the recovery of the North Basin is coupled to the recovery of the South Basin due to the transport of sediment from the South to the North basin.

Conclusions

The goal of this study was to assess the state of recovery of a Hg contaminated lake in which remediation is through the natural burial of contaminated sediments. The results revealed two previously undocumented assumptions 1) a correlation between iron ore production from the Marquette Range of Michigan's Upper Peninsula and Hg concentrations in the profiles clearly demonstrates the influence of mining related activities on Deer Lake and 2) Al concentration and Hg:Al ratio profiles show a change in pathway for Hg from a point source to a non-point source (atmospheric deposition and watershed runoff) with cessation of mining activities.

This study also shows the challenges in interpreting the states of highly disturbed systems. In this case, atypical ^{210}Pb profiles and lack of within lake historic uncontaminated sediments posed challenges to age determination and a reference condition for recovery assessment comparison. These problems were caused by human and climatically induced water-level fluctuations which introduced older sediments into the profundal areas of the lake and the depth of contaminated sediment. Sedimentation rates and sediment ages were determined via modifications to the constant rate of supply (CRS) model, combined with event-based dating techniques. Several definitions of system state (e.g., flux and concentrations) were used to estimate the time required for recovery.

Although recovery to background conditions is often one of the types of goals for a remediation program it could not be used here because current rates of atmospheric Hg deposition for the region are greater than an estimate of background conditions for Deer Lake. Thus, Hg loadings can only recover to atmospheric loading rates. Considering this and using the most recently measured surface sediment as a starting condition once recovery begins, and remains uninterrupted, it will take between 3 and 7 y for the South and North Basin, respectively, for recovery based on a flux reference and 3 y and 12 y, respectively, based on a concentrations reference. However, the recently increasing values of recovery indicators (e.g., Hg concentration) suggest that these estimates are conservative and will be longer if recovery remains arrested. This may be due in part to the legacy of Hg contamination on the landscape.

REFERENCES

REFERENCES

Alfaro-De la Torre, M.C., Tessier, A., 2002. Cadmium deposition and mobility in the sediments of an acidic oligotrophic lake. Geochimica et Cosmochimica Acta 66, 3549-3562.

Allibone, J., Fatemian, E., Walker, P.J., 1999. Determination of mercury in potable water by ICP-MS using gold as a stabilising agent. Journal of Analytical Atomic Spectrometry 14, 235-239.

Appelby, P.G., Oldfield, F., 1978. The calculation of ^{210}Pb dates assuming a constant rate of supply of unsupported ^{210}Pb to the sediment. Catena 5, 1-8.

Appleby, P.G., 2001. Chronostratigraphic Techniques in Recent Sediments. In: W. M. Last, J. P. Smol (Eds.), Tracking Environmental Change Using Lake Sediments. Kluwer Academic Publishers, Boston, pp. 171-205.

Appleby, P.G., Flower, R.J., Mackay, A.W., Rose, N.L., 1998. Paleolimnological assessment of recent environmental change in Lake Baikal: sediment chronology. Journal of Paleolimnology 20, 119-133.

Benoit, G., Rozan, T.F., 2001. Pb-210 and Cs-137 dating methods in lakes: a retrospective study. Journal of Paleolimnology 25, 455-465.

Binford, M.W., 1990. Calculation and uncertainty analysis of ^{210}Pb dates for PIRLA project lake sediment cores. Journal of Paleolimnology 3, 253-267.

Bruland, K.W., Bertine, K., Koide, M., Goldberg, E.D., 1974. History of Metal Pollution in Southern-California Coastal Zone. Environmental Science & Technology 8, 425-432.

D'Itri, F., 2008. Personal Communication.

D'Itri, F.M., Evans, E.D., Kubitz, J.A., Ushikubo, A., Kurita-Matsuba, H., 1992. The remediation of mercury contaminated fish in an artificial reservoir. International Journal of Limnology 52, 301-317.

Eckley, C.S., Watras, C.J., Hintelmann, H., Morrison, K., Kent, A.D., Regnell, O., 2005. Mercury methylation in the hypolimnetic waters of lakes with and without connection to wetlands in northern Wisconsin. Canadian Journal of Fisheries and Aquatic Sciences 62, 400-411.

Fenton, M., 1998. Iron and Steel. In: U.S. Geological Survey Metal Prices in the United States Through 1998. pp. 61-64.

Golden, K.A., Wong, C.S., Jeremiason, J.D., Eisenreich, S.J., Sanders, M.G., Hallgren, J., Swackhammer, D.L., Engstrom, D.R., Long, D.T., 1993. Accumulation and preliminary inventory of organochlorines in Great Lakes sediments. Water Science and Technology 28, 19-31.

Heyvaert, A.C., Reuter, J.E., Slotton, D.G., Goldman, C.R., 2000. Paleolimnological reconstruction of historical atmospheric lead and mercury deposition at Lake Tahoe, California-Nevada. Environmental Science and Technology 34, 3588-3597.

National Atmospheric Deposition Program (NRSP-3), Illinois State Water Survey, NADP Program Office, 2204 Griffith Drive, Champaign, IL 61820, Available online at http://nadp.sws.uiuc.edu/mdn/. (Accessed: February 5, 1998).

Kerfoot, W.C., Harting, S., Rossmann, R., Robbins, J.A., 1999. Anthropogenic copper inventories and mercury profiles from Lake Superior: Evidence for mining impacts. Journal of Great Lakes Research 25, 663-682.

Kerfoot, W.C., Harting, S.L., Jeong, J., Robbins, J.A., Rossmann, R., 2004. Local, regional, and global implications of elemental mercury in metal (copper, silver, gold, and zinc) ores: Insights from Lake Superior sediments. Journal of Great Lakes Research 30, 162-184.

Kerfoot, W.C., Lauster, G., 1994. Paleolimnological study of copper mining around Lake Superior: Artificial varves from Portage Lake provide a high resolution record. Limnology and Oceanography 39, 649-669.

Koelmans, A.A., 1998. Geochemistry of suspended and settling solids in two freshwater lakes. Hydrobiologia 364, 15-29.

Kolak, J.J., Long, D.T., Beals, T.M., Eisenreich, S.J., Swackhamer, D.L., 1998. Anthropogenic inventories and historical and present accumulation rates of copper in Great Lakes sediments. Applied Geochemistry 13, 59-75.

Kolak, J.J., Long, D.T., Kerfoot, W.C., Beals, T.M., Eisenreich, S.J., 1999. Nearshore versus offshore copper loading in Lake Superior sediments: Implications for transport and cycling. Journal of Great Lakes Research 25, 611-624.

Krishnaswamy, S., Lal, D., Martin, J.M., Meybeck, M., 1971. Geochronology of Lake Sediments. Earth and Planetary Science Letters 11, 407.

Landis, M.S., Keeler, G.J., 2002. Atmospheric mercury deposition to Lake Michigan during the Lake Michigan Mass Balance Study. Environmental Science and Technology 36, 4518-4524.

Lindberg, S., Bullock, R., Ebinghaus, R., Engstrom, D., Feng, X.B., Fitzgerald, W., Pirrone, N., Prestbo, E., Seigneur, C., 2007. A synthesis of progress and uncertainties in attributing the sources of mercury in deposition. Ambio 36, 19-32.

Magar, V.S., 2001. Natural recovery of contaminated sediments. Journal of Environmental Engineering-Asce 127, 473-474.

Mason, R.P., Sheu, G.R., 2002. Role of the ocean in the global mercury cycle. Global Biogeochemical Cycles 16.

MDNR, M.D.o.N.R. Surface Water Quality Division. *Remedial Action Plan for Deer Lake Area of Concern*; Government Printing Office, 1987.

Munthe, J., Bodaly, R.A., Branfireun, B.A., Driscoll, C.T., Gilmour, C.C., Harris, R., Horvat, M., Lucotte, M., Malm, O., 2007. Recovery of mercury-contaminated fisheries. Ambio 36, 33-44.

National Oceanic and Atmospheric Administration, 2008. NNDC Climate Online, Available online at http://www7.ncdc.noaa.gov/. (Accessed: October 27, 2008).

Parsons, M.J., Long, D.T., Yohn, S.S., Giesy, J.P., 2007. Spatial and Temporal Trends of Mercury Loadings to Michigan Inland Lakes. Environmental Science and Technology 41, 5634-5640.

Parsons, M.J., Yohn, S.S., Long, D.T., Patino, L.C., Stone, K.A., 2006. Inland Lakes Sediment Trends: Mercury Sediment Analysis Results for 27 Michigan Lakes. Lansing, MI. 47 pages. Available from:

Robbins, J.A., 1978. Geochemical and geophysical applications of radioactive lead. In: J. O. Nriagu (Ed.), The Biogeochemistry of Lead in the Environment. Elsevier, New York, pp. 285-393.

Robbins, J.A., 1982. Stratigraphic and dynamic effects of sediment reworking by Great Lakes zoobenthos. Hydrobiologia 92, 611-622.

Robbins, J.A., Edgington, D.N., 1975. Determination of recent sedimentation rates in Lake Michigan using Pb-210 and Cs-137. Geochimica et Cosmochimica Acta 39, 285-304.

Rumbold, D.G., Fink, L.E., 2006. Extreme spatial variability and unprecedented methylmercury concentrations within a constructed wetland. Environmental Monitoring and Assessment 112, 115-135.

Shotbolt, L.A., Thomas, A.D., Hutchinson, S.M., 2005. The use of reservoir sediments as environmental archives of catchment inputs and atmospheric pollution. Progress in Physical Geography 29, 337-361.

Sunderland, E.M., Gobas, F., Heyes, A., Branfireun, B.A., Bayer, A.K., Cranston, R.E., Parsons, M.B., 2004. Speciation and bioavailability of mercury in well-mixed estuarine sediments. Marine Chemistry 90, 91-105.

Tseng, C.M., Amouroux, D., Abril, G., Tessier, E., Etcheber, H., Donard, O.F.X., 2001. Speciation of mercury in a fluid mud profile of a highly turbid macrotidal estuary (Gironde, France). Environmental Science & Technology 35, 2627-2633.

Tuncer, G., Tuncel, G., Balkas, T.I., 2001. Evolution of metal pollution in the Golden Horn (Turkey) sediments between 1912 and 1987. Marine Pollution Bulletin 42, 350-360.

Deer Lake River Area of Concern, Available online at http://www.epa.gov/glnpo/aoc/drlake.html. (Accessed: January 30, 2008).

US EPA, 2007. Great Lakes Areas of Concern, Available online at http://www.epa.gov/glnpo/aoc/. (Accessed: January 31, 2008).

USEPA. Office of Solid Waste and Emergency Response. *Test Methods for Evaluating Solid Waste, Physical/Chemical Methods*; Government Printing Office, 2007c.

United States Geological Survey, 2009. Minerals Yearbook, Available online at http://minerals.usgs.gov/minerals/pubs/myb.html. (Accessed: July 9).

Watras, C.J., Bloom, N.S., Hudson, J.M., Gherini, S., Munson, R., Claas, S.A., Marrison, K.A., Hurely, J., Wiener, J.G., Fitzgerald, W.F., Mason, R., Vandal, G., Powell, D., Rada, R., Rislov, L., Winfrey, M., Elder, J., Krabbenhoft, D., Andren, A.W., Babiarz, C., Porcella, D.B., Huckabee, J.W., 1994. Sources and fates of mercury and methylmercury in Wisconsin lakes. In: C.J. Watras, J.W. Huckabee (Eds.), Mercury Pollution: Intergration and Synthesis. CRC Press, Ann Arbor, pp. 153-179.

Wilkinson, P., Simpson, S.L. Geological Survey of Canada. *Radiochemical analysis of Lake Winnipeg 99-900 cores 4 and 8*; Ottawa, Ontario: Government Printing Office, 2003.

Yohn, S., Long, D., Fett, J., Patino, L., 2004. Regional versus local influences on lead and cadmium loading to the Great Lakes region. Applied Geochemistry 19, 1157-1175.

Yohn, S.S., Long, D.T., Fett, J.D., Patino, L., Giesy, J.P., Kannan, K., 2002. Assessing environmental change through chemical-sediment chronologies from inland lakes. Lakes Reserv Res Manage 7, 217-230.

CHAPTER 6
SUMMARY AND RECOMMENDATIONS

Summary

The working hypothesis of this research is: local scale sources and watershed scale processes have more impact on the rate of Hg accumulation in the aquatic environment than regional to global scale sources. The hypothesis was investigated using the following approaches: 1) local scale sources are reflected in the sediment record as discontinuities in spatial scale analysis of anthropogenic inventories and Hg profiles should be unique to a lake or sub-region, 2) watershed scale processes will impact the rate of modern recovery from Hg contamination and variations in the recovery rate between watersheds can be correlated to differences in watershed attributes and 3) diagnostic ratios of PAHs infer sources of Hg since they share a common source and pathway.

Spatial analysis of anthropogenic inventories amongst Michigan inland lakes were indicative of a regional source for Hg assuming the inventories found for Lakes Michigan and Superior are representative of a regional source. However, there were notable exceptions to this generalization, specifically lakes Houghton, Higgins, Gull. Additionally, lakes that are in close proximity should have anthropogenic inventories that are similar if a regional source were present. Elk and Torch and Higgins and Houghton share watershed boundaries, but have quite different anthropogenic inventories more consistent with watershed scale sources or processes. Inventories from Upper Peninsula lakes were consistent with those found for Lake Superior, but were varied suggesting the influence of watershed scale processes.

In general anthropogenic accumulation of Hg in the study lakes first occurred in the late 1800s consistent with the habitation of the lower Great Lakes region by European settlers. Increased anthropogenic accumulation continues until the middle or latter part of the previous

century. Lakes from sub-regions of the study area had similar profiles of anthropogenic Hg accumulation suggesting sources that were common to these lakes. Episodic accumulation events common among those lakes provide further evidence of more local scale processes. Recent trend analysis showed that several lakes had increasing Hg accumulation none of which were located near coal-fired power plants, a predominant source for Hg, providing further verification for local-scale or watershed process influence for these lakes.

To examine the impacts of watershed attributes on the modern recovery of lakes from Hg contamination slopes of recent declines in Hg concentration and accumulation were calculated and compared to GIS delineated watershed attributes. Strong correlations were found for agriculture, forest and wetland attributes. However, those attributes along highly conductive flowpaths or within close proximity to the lake had the strongest relationships. Though relationships between the accumulation of Hg to the environment and watershed attributes have been studied previously, the relationship between watershed attributes and dynamic flowpaths was unique to this study. What may be a more important finding of this study is the lack of relationship between recovery rate and measures of atmospheric Hg such as sulfate deposition and Hg emissions. This lack of relationship suggests that local scale sources and watershed processes determine the recovery of lakes from Hg enrichment rather than regional decreases in Hg emission. However, the lack of relationship may also be related to "legacy Hg" deposited to the landscape and the lag time required for that Hg to reach the aquatic ecosystem. The implications of this are it is then those activities that disturb the landscape that control accumulation of Hg in inland lakes.

Diagnostic ratios of PAHs can often be used to differentiate sources of these contaminants. Mercury and PAHs share common sources and pathways allowing these

diagnostic ratios to infer sources of Hg to the environment. Modern ratios of PAH showed that combustion sources predominate across the State. The prevalence of combustion sources prior to 1900 in Avalon and Round lakes may be indicative of early industrial activity near these lakes, i.e., cement manufacturing and iron smelting, respectively. Coincident with the ratios of An/178 and Fl/Fl+Py a coal combustion source was potentially identified for Birch Lake, i.e., coal fired power plants in the Chicago/Gary industrial complex. A coal combustion source was also presumed to cause the increase in Hg in Sand Lake, which was coincident with the commissioning of power plants in southeast Michigan. In Muskegon Lake where a coal-fired power plant resides on the lakes' shoreline no coal combustion source was identified. Rather a source consistent with fossil fuels was observed. This could have two explanations either a vehicular or natural gas power plant source. The lake is in a highly urbanized area of the state and lies due east of a natural gas fired power plant in Wisconsin. The latter is more likely due to the elevated Hg levels observed in the sediment of Muskegon Lake and the geochemical cycle of Hg. Furthermore, the lack of evidence of a biomass combustion source may be indicative of the long range transport of Hg due to the height of power plant smokestacks. Unlike Muskegon Lake, Otter Lake showed evidence of influence by biomass combustion throughout the entire core, likely coal fired power plants due to its proximity to power plants fired with coal to the north and east. Crystal Lake showed a varied response between fossil fuel and biomass combustion, evidence of mixed sources to the lake.

Burial in deep sediments is often the fate of Hg emitted to the environment. This was the case for Deer Lake where Hg was used to assay iron ore in the Cleveland Cliffs Laboratory and dumped to the City of Ishpeming municipal sewer system. Deer Lake became an Area of Concern when it was determined that fish in the lake had concentrations of mercury that

exceeded health limits along with other beneficial use impairments. A high concentration of Hg in the sediments was suspected to be the primary cause of fish Hg. When the original remediation attempt failed to lower fish tissue concentrations it was determined to allow the lake to recover naturally by the accumulation of clean sediments. Although the point source had been removed Hg concentrations were still not reflective of a recovering system. Using Hg:Al ratios it was determined that a watershed or erosional source for Hg could be an important contemporary source which could be contaminated sediments upstream or in the floodplain of the creek used for wastewater discharge. Calculations based on the slope of modern concentrations and accumulation rates indicate a quick, ~10 y, recovery to those concentrations and accumulation rates of nearby Upper Peninsula lakes even though surficial concentrations are an order of magnitude greater than nearby lakes. This has important implications for the use of natural recovery as a remediation strategy.

This is the first research to show strong correlations between watershed attributes and the recovery of inland lake systems and the first to use ratios of PAHs to infer sources of Hg. Much of the previous work investigating watershed attributes has focused on the impact of specific land cover types, investigated a narrow time period or used a limited number of lakes. The high correlation between Hg recovery and watershed attributes gives promise to this approach when choosing sediment archives for contaminant trend monitoring. It also has implications for watershed managers attempting to manage daily loads of contaminants to environmental systems. Inferring source of Hg using PAHs showed great promise in the elucidation of source and source areas for these contaminants to the environment. Though several studies have presented PAHs and heavy metal data, few have attempted to correlate the two measures of

environmental state. The powerful potential insight into sources of Hg using diagnostic ratios of PAHs should not be overlooked in future Hg studies.

Recommendations

Below are suggestions for future work based on the outcome of this study.

1) The statistical outcomes shown in Chapter 3 demonstrate the effectiveness of this approach; however, ground truth studies would be useful in determining the transport mechanics in these systems. Highly dynamic flowpaths of a watershed can easily be determined using GIS techniques. In depth mechanistic studies of Hg release and transport from these flowpaths should be identified.
2) Apply the lake recovery models to more lakes. Based on the results of Chapter 2 there were a limited number of lakes that could be used to investigate the impact of watershed attributes on recovery. The correlations should have widespread applicability and should be tested using a larger sample size of lakes and potentially a larger range of watershed attributes. A larger sample size may also allow us of more powerful multivariate statistics.
3) Increase the number of organic tracers measured in the sediment core. The results of using diagnostic tracers of PAHs was effectively demonstrated, but could be made even more powerful by measuring those organics that are more discerning of source including: alkyl PAHs, simonellite and retene. These organics have been used successfully to delineate combustion and vegetation sources of PAHs to the environment.
4) Ground truth the relationship between PAHs and Hg, i.e., correlation is not causation. The high correlation observed between PAHs and Hg combined with knowledge of

their geochemical cycles provides confidence in stating that they share common sources and pathways to the environment. However, a more detailed atmospheric based study of the relationship between these contaminants and their sources and pathways would provide further discriminating power to this approach.

5) Extend the use of diagnostic PAHs and recovery models to other metals. Mercury is not the only metal of concern in the Great Lakes region and with the vast body of data available the approach taken here for Hg could easily be extended to lead, and to a lesser extent zinc, cadmium and copper.
6) Return to resample Deer Lake to evaluate the system state and verify predictions made based on the linear models of recovery.

This research has many practical benefits that may extend beyond the research community. The use of inland lake sediment chronologies to determine areas of increased contaminant loading in a region cannot be overstated. They also provide important information regarding the potential for exposure to recreational users of the lake. Atmospheric deposition monitors are expensive to maintain and require a long-term commitment for meaningful data. In addition, they do not incorporate information concerning the overland transport of contaminants. Sediment chronologies provide a long term and relatively inexpensive method for determining system state; however, identifying the source or ratio of sources is difficult at best. The potential of an organic tracer to help elucidate source is unique, but still may have difficulty determining proportions of mixed sources. Watershed managers will find useful the contributions of dynamic flowpaths to Hg recovery since reduction of loads to aquatic systems is the goal of many of their programs. The costs of remediating contaminated sediment systems can

often soar into the hundreds of millions of dollars. A less costly alternative would be natural recovery if the system can be managed in such a way to the make the strategy feasible. Here we have demonstrated how sediment chronologies can be used to monitor such a strategy.

The approach taken here has identified the importance of local sources and determined the watershed processes that impact Hg accumulation in inland lakes. The techniques used here can easily be translated to other regions, that is to say, to the extent that a significant amount of lakes exist in the area to sample.

APPENDICIES

APPENDIX A

SEDIMENT CHEMICAL DATA

APPENDIX A. SEDIMENT CHEMICAL DATA

Sediment concentration, ^{210}Pb activities and dates, and core desciptions can be found in Michigan Department of Environmental Quality reports including:

Cass, Gratiot, Gull, Elk and Higgins lakes:
Simpson, S.J., Long, D.T., Geisy, J.P., and Fett, J.D., 2000. Inland lakes sediment trends: sediment analysis results for five Michigan Lakes (MI/DEQ/SWQ-01/030), Department of Environmental Quality, Lansing, MI.
http://www.michigan.gov/deq/0,1607,7-135-3313_3686_3728-32365--,00.html

Crystal M and Littlefield lakes:
Yohn, S.S., Long, D.T., Giesy, J.P., Fett, J.D., and Kannan, K., 2001. Inland lakes sediment trends: sediment analysis results for two Michigan Lakes (MI/DEQ/WD-02/115), Department of Environment Quality, Lansing, MI.

Cadillac, Crystal B, Mullett, Paw Paw, and Whitmore lakes:
Yohn, S.S., Long, D.T., Giesy, J.P., Scholle, L.K., Patino, L.C., Fett, J.D., and Kannan, K., 2002. Inland lakes sediment trends: sediment analysis results for five Michigan Lakes (MI/DEQ/WD-03/052). Department of Environmental Quality, Lansing, MI.

Houghton, Hubbard, Imp, Round, Torch and Witch lakes:
Yohn, S.S., Parsons, M.J., Long, D.T., Giesy, J.P., Scholle, L.K., and Patino, L.C., 2003. Inland lakes sediment trends: sediment analysis results for six Michigan lakes (MI/DEQ/WB-04/066). Department of Environmental Quality, Lansing, MI.

Avalon, Birch, Muskegon, Sand and Shupac lakes:
Parsons, M. J.; Yohn, S. S.; Long, D. T.; Giesy, J. P.; Bradley, P. W., 2004. Inland Lakes Sediment Trends: Sediment Analysis Results for Five Michigan Lakes (MI/DEQ/WB-06/003). Michigan Department of Environmental Quality: Lansing, MI.

Crystal M04, George, Hackert, Otter and Round lakes:
Parsons, M. J.; Yohn, S. S.; Long, D. T.; Giesy, J. P.; Patino, L.C., 2005. Inland Lakes Sediment Trends: Sediment Analysis Results for Five Michigan Lakes (MI/DEQ/WB-07/078). Michigan Department of Environmental Quality: Lansing, MI.

Mercury analysis for all lakes above:
Parsons, M. J.; Yohn, S. S.; Long, D. T.; Patino, L. C.; Stone, K. A., 2006. Inland Lakes Sediment Trends: Mercury Sediment Analysis Results for 27 Michigan Lakes (MI/DEQ/WB-06/090). Michigan Department of Environmental Quality, Water Bureau: Lansing, MI.

Charlevoix, Cadillac05, Gull05, Nichols, Campau, Muskegon06 and White lakes:

Parsons, M. J.; Yohn, S. S.; Long, D. T.; Giesy, J. P.; Patino, L.C., 2005. Inland Lakes Sediment Trends: Sediment Analysis Results for Seven Michigan Lakes (MI/DEQ/WB-09/069). Michigan Department of Environmental Quality: Lansing, MI.

Table A1. ^{210}Pb activities for Deer Lake South sediment core.

SAMPLE	DRY WT (g)	ACCUMULATED DRY WT (gm./sq.cm.)	POROSITY	Thickness (cm)	WATER (%)	Excess Pb-210 (Bq/g)	ACTIVITY Pb-210 (Bq/g)	ERROR (+/- 1 SD) (Bq/g)
DEER1-1	0.44	0.0062	1.00	0.44	98.6	4.88E-01	5.28E-01	1.64E-02
2	0.55	0.0140	0.99	0.32	97.6	5.73E-01	6.13E-01	1.64E-02
3	0.78	0.0250	0.99	0.40	97.3	5.77E-01	6.17E-01	1.44E-02
4	1.20	0.0419	0.99	0.52	96.8	6.28E-01	6.68E-01	1.22E-02
5	1.34	0.0608	0.99	0.50	96.3	6.18E-01	6.58E-01	1.16E-02
6	1.45	0.0813	0.98	0.46	95.6	7.13E-01	7.53E-01	1.36E-02
7	1.98	0.1092	0.98	0.45	94.1	7.91E-01	8.31E-01	1.41E-02
8	1.68	0.1329	0.98	0.40	94.2	8.44E-01	8.84E-01	1.63E-02
9	2.44	0.1673	0.97	0.46	92.9	7.12E-01	7.52E-01	1.29E-02
10	2.22	0.1986	0.98	0.44	93.2	7.14E-01	7.54E-01	1.47E-02
11	2.55	0.2346	0.97	0.45	92.4	6.19E-01	6.59E-01	1.23E-02
12	2.51	0.2700	0.97	0.42	92.0	5.54E-01	5.94E-01	1.05E-02
13	2.83	0.3100	0.97	0.45	91.7	5.12E-01	5.52E-01	1.06E-02
14	3.36	0.3574	0.97	0.51	91.2	4.87E-01	5.27E-01	9.55E-03
15	3.47	0.4063	0.96	0.45	89.9	3.25E-01	3.65E-01	7.91E-03
16	4.14	0.4647	0.95	0.42	87.4	2.61E-01	3.01E-01	7.25E-03
17	8.95	0.5910	0.95	0.93	87.5	2.12E-01	2.52E-01	6.84E-03
18	9.35	0.7229	0.95	0.91	86.8	1.80E-01	2.20E-01	6.05E-03
19	8.68	0.8454	0.96	0.95	88.1	1.94E-01	2.34E-01	6.46E-03
20	7.03	0.9446	0.96	0.93	90.1	1.91E-01	2.31E-01	5.24E-03
21	9.77	1.0824	0.95	0.95	86.8	1.49E-01	1.89E-01	4.27E-03
22	3.45	1.1311	0.98	0.92	94.9	2.71E-01	3.11E-01	6.72E-03
23	2.69	1.1690	0.99	0.96	96.1	2.33E-01	2.73E-01	5.77E-03
24	3.60	1.2198	0.98	0.91	94.6	2.45E-01	2.85E-01	7.13E-03
25	3.99	1.2761	0.98	0.98	94.4	3.06E-01	3.46E-01	9.38E-03

Table A1 (cont'd)

SAMPLE	DRY WT (g)	ACCUMULATED DRY WT (gm./sq.cm.)	POROSITY	Thickness (cm)	WATER (%)	Excess Pb-210 (Bq/g)	ACTIVITY Pb-210 (Bq/g)	ERROR (+/- 1 SD) (Bq/g)
26	4.62	1.3413	0.97	0.88	93.0	3.16E-01	3.56E-01	1.04E-02
27	4.78	1.4087	0.97	0.92	93.0	3.29E-01	3.69E-01	9.00E-03
28	4.57	1.4732	0.98	0.90	93.1	3.04E-01	3.44E-01	7.92E-03
29	4.10	1.5310	0.98	0.86	93.6	2.99E-01	3.39E-01	8.55E-03
30	4.07	1.5885	0.98	0.90	93.9	2.68E-01	3.08E-01	7.62E-03
31	4.16	1.6472	0.98	0.84	93.3	2.48E-01	2.88E-01	7.22E-03
32	4.02	1.7039	0.98	0.81	93.3	2.10E-01	2.50E-01	8.57E-03
33	3.89	1.7587	0.98	0.82	93.6	2.17E-01	2.57E-01	7.03E-03
34	4.20	1.8180	0.98	0.90	93.7	2.36E-01	2.76E-01	8.34E-03
35	4.03	1.8749	0.98	0.85	93.6	2.25E-01	2.65E-01	7.19E-03
36	4.30	1.9355	0.97	0.81	92.9	2.10E-01	2.50E-01	8.23E-03
37	5.44	2.0123	0.97	0.87	91.6	1.89E-01	2.29E-01	7.74E-03
38	5.72	2.0930	0.97	0.88	91.4	1.67E-01	2.07E-01	6.03E-03
39	6.89	2.1902	0.96	0.91	90.0	1.69E-01	2.09E-01	6.70E-03
40	6.19	2.2775	0.97	0.87	90.6	1.72E-01	2.12E-01	
41	5.99	2.3620	0.97	0.88	90.9	1.64E-01	2.04E-01	
42	5.97	2.4462	0.97	0.90	91.2	1.57E-01	1.97E-01	
43	7.47	2.5516	0.96	0.99	90.0	1.48E-01	1.88E-01	
44	7.27	2.6542	0.96	0.89	89.3	1.40E-01	1.80E-01	
45	6.95	2.7523	0.96	0.90	89.8	1.33E-01	1.73E-01	
46	6.11	2.8385	0.96	0.81	90.1	1.27E-01	1.67E-01	
47	6.29	2.9272	0.97	0.90	90.7	1.21E-01	1.61E-01	
48	5.33	3.0024	0.97	0.86	91.7	1.16E-01	1.56E-01	
49	7.51	3.1084	0.96	0.88	88.9	1.10E-01	1.50E-01	
50	7.29	3.2112	0.96	0.92	89.6	1.04E-01	1.44E-01	

Table A1 (cont'd)

SAMPLE	DRY WT (g)	ACCUMULATED DRY WT (gm./sq.cm.)	POROSITY	Thickness (cm)	WATER (%)	Excess Pb-210 (Bq/g)	ACTIVITY Pb-210 (Bq/g)	ERROR (+/- 1 SD) (Bq/g)
51	7.71	3.3200	0.96	0.91	88.9	9.81E-02	1.38E-01	
52	8.32	3.4374	0.96	0.91	88.1	9.21E-02	1.32E-01	
53	8.55	3.5580	0.95	0.86	87.1	8.64E-02	1.26E-01	
54	9.32	3.6895	0.95	0.91	86.7	8.05E-02	1.20E-01	
55	9.65	3.8256	0.95	0.90	86.3	7.48E-02	1.15E-01	
56	10.03	3.9671	0.95	0.91	85.9	6.93E-02	1.09E-01	
57	10.22	4.1113	0.94	0.90	85.4	6.42E-02	1.04E-01	
58	11.43	4.2726	0.94	0.93	84.5	5.42E-02	9.42E-02	2.88E-03
59	12.37	4.4471	0.94	0.96	83.8	5.37E-02	9.37E-02	3.37E-03

Table A2. ^{210}Pb activities for Deer Lake North sediment core.

SAMPLE	DRY WT (g)	ACCUMULATED DRY WT (gm./sq.cm.)	POROSITY	Thickness (cm)	WATER (%)	Excess Pb-210 (Bq/g)	ACTIVITY Pb-210 (Bq/g)	ERROR (+/- 1 SD) (Bq/g)
DEER2-1	1.38	0.0195	0.99	0.60	96.8	4.88E-01	6.71E-01	1.38E-02
2	1.69	0.0433	0.97	0.31	92.7	5.73E-01	7.26E-01	1.66E-02
3	2.02	0.0718	0.98	0.40	93.3	5.77E-01	7.70E-01	1.65E-02
4	2.18	0.1026	0.98	0.44	93.3	6.28E-01	8.05E-01	1.65E-02
5	2.06	0.1316	0.97	0.40	93.1	6.18E-01	8.39E-01	1.35E-02
6	2.30	0.1641	0.97	0.42	92.7	7.13E-01	8.82E-01	1.47E-02
7	2.94	0.2056	0.97	0.56	92.9	7.91E-01	8.48E-01	1.48E-02
8	1.88	0.2321	0.97	0.33	92.3	8.44E-01	8.16E-01	1.44E-02
9	2.36	0.2654	0.97	0.37	91.5	7.12E-01	7.88E-01	1.46E-02
10	1.90	0.2922	0.97	0.31	91.9	7.14E-01	7.09E-01	1.51E-02
11	2.38	0.3258	0.97	0.35	91.1	6.19E-01	7.47E-01	1.43E-02
12	2.45	0.3603	0.97	0.43	92.3	5.54E-01	6.95E-01	1.24E-02
13	2.74	0.3990	0.97	0.47	92.1	5.12E-01	6.12E-01	1.17E-02
14	2.69	0.4369	0.96	0.35	90.0	4.87E-01	5.65E-01	1.01E-02
15	2.46	0.4716	0.97	0.34	90.5	3.25E-01	5.15E-01	9.49E-03
16	2.77	0.5107	0.97	0.42	91.3	2.61E-01	4.99E-01	9.20E-03
17	5.69	0.5910	0.97	0.86	91.2	2.12E-01	4.79E-01	1.19E-02
18	5.78	0.6725	0.97	0.84	90.9	1.80E-01	4.36E-01	1.38E-02
19	6.06	0.7580	0.97	0.87	90.7	1.94E-01	4.24E-01	1.15E-02
20	5.96	0.8421	0.97	1.02	92.2	1.91E-01	3.70E-01	9.30E-03
21	7.24	0.9443	0.96	0.88	89.2	1.49E-01	3.14E-01	6.58E-03
22	7.66	1.0523	0.96	0.94	89.3	2.71E-01	2.83E-01	6.45E-03
23	7.81	1.1625	0.96	0.97	89.4	2.33E-01	2.89E-01	6.64E-03
24	7.34	1.2661	0.96	0.94	89.7	2.45E-01	2.83E-01	6.59E-03
25	6.87	1.3630	0.96	0.89	89.8	3.06E-01	2.87E-01	5.87E-03

Table A2. (cont'd)

SAMPLE	DRY WT (g)	ACCUMULATED DRY WT (gm./sq.cm.)	POROSITY	Thickness (cm)	WATER (%)	Excess Pb-210 (Bq/g)	ACTIVITY Pb-210 (Bq/g)	ERROR (+/- 1 SD) (Bq/g)
26	6.92	1.4606	0.96	0.88	89.7	3.16E-01	2.78E-01	6.02E-03
27	7.17	1.5618	0.97	1.01	90.6	3.29E-01	2.88E-01	6.92E-03
28	7.19	1.6632	0.96	0.94	89.9	3.04E-01	2.79E-01	6.23E-03
29	7.55	1.7698	0.96	0.92	89.3	2.99E-01	3.00E-01	6.42E-03
30	6.75	1.8650	0.97	0.97	90.8	2.68E-01	3.58E-01	7.52E-03
31	5.68	1.9451	0.97	0.90	91.6	2.48E-01	3.58E-01	7.37E-03
32	5.98	2.0295	0.97	0.97	91.8	2.10E-01	3.50E-01	7.36E-03
34	5.53	2.1075	0.97	0.94	92.1	2.17E-01	3.39E-01	7.02E-03
35	5.45	2.1844	0.97	0.94	92.3	2.36E-01	3.21E-01	7.24E-03
36	5.60	2.2634	0.97	0.94	92.0	2.25E-01	3.04E-01	6.40E-03
37	5.84	2.3458	0.97	0.88	91.2	2.10E-01	2.89E-01	6.13E-03
38	6.73	2.4407	0.97	0.99	91.0	1.89E-01	2.93E-01	5.15E-03
39	6.47	2.5320	0.97	0.94	90.8	1.67E-01	2.81E-01	5.14E-03
40	6.37	2.6219	0.97	0.90	90.6	1.69E-01	2.64E-01	5.11E-03
41	7.38	2.7260	0.96	1.00	90.2	1.72E-01	2.50E-01	4.82E-03
42	6.42	2.8166	0.96	0.89	90.4	1.64E-01	2.43E-01	7.45E-03
43	6.99	2.9152	0.96	0.96	90.4	1.57E-01	2.15E-01	6.63E-03
44	6.82	3.0114	0.96	0.94	90.4	1.48E-01	1.81E-01	6.62E-03
45	6.84	3.1079	0.97	0.96	90.5	1.40E-01	1.96E-01	6.63E-03
46	5.79	3.1896	0.97	0.83	90.8	1.33E-01	1.78E-01	5.71E-03
47	6.97	3.2880	0.97	0.98	90.6	1.27E-01	1.62E-01	5.56E-03
48	6.35	3.3775	0.97	0.89	90.5	1.21E-01	1.77E-01	6.12E-03
49	6.53	3.4697	0.96	0.90	90.4	1.16E-01	1.71E-01	5.67E-03
50	6.82	3.5659	0.96	0.91	90.2	1.10E-01	1.77E-01	4.03E-03

Table A2. (cont'd)

SAMPLE	DRY WT (g)	ACCUMULATED DRY WT (gm./sq.cm.)	POROSITY	Thickness (cm)	WATER (%)	Excess Pb-210 (Bq/g)	ACTIVITY Pb-210 (Bq/g)	ERROR (+/- 1 SD) (Bq/g)
51	6.53	3.6580	0.96	0.88	90.2	9.81E-02	1.94E-01	4.22E-03
52	7.10	3.7582	0.96	0.90	89.6	9.21E-02	1.73E-01	4.43E-03
53	8.14	3.8730	0.96	0.95	88.8	8.64E-02	1.52E-01	3.67E-03
54	8.63	3.9948	0.95	0.87	87.1	8.05E-02	1.42E-01	3.33E-03
55	9.17	4.1242	0.95	0.93	87.3	7.48E-02	1.41E-01	3.68E-03
56	9.23	4.2544	0.95	0.91	86.9	6.93E-02	1.38E-01	3.45E-03
57	9.33	4.3860	0.95	0.93	87.0	6.42E-02	1.27E-01	3.12E-03
58	9.69	4.5227	0.95	0.93	86.6	5.42E-02	1.09E-01	3.91E-03
59	9.25	4.6532	0.95	0.92	87.0	5.37E-02	1.10E-01	3.55E-03

Table A3. Metal concentrations for Deer Lake south core (mg/kg).

Sample	Depth	Sc	Ti	V	Cr	Co	Ni	Cu	As	Mo	Cd	Pb
Deer 1-1	0.5	2.19	161.03	27.71	36.96	7.04	29.11	151	31.85	1.66	1.03	46.67
Deer 2-1	1.0	2.21	165.55	30.05	45.22	6.90	27.21	155	32.45	1.54	1.03	47.64
Deer 3-1	1.5	2.10	131.55	27.36	42.00	7.92	29.52	110	34.52	2.08	0.95	45.77
Deer 4-1	2.0	2.26	156.33	26.65	40.68	8.04	32.02	76	35.03	2.04	1.00	45.77
Deer 5-1	2.5	2.57	51.43	30.89	47.88	8.50	32.23	68	33.06	1.90	1.01	50.89
Deer 6-1	3.0	2.43	33.28	30.66	45.53	9.59	33.48	54	39.92	2.16	0.93	46.02
Deer 7-1	3.5	2.93	41.14	35.42	53.98	9.86	36.06	74	41.61	1.81	1.06	49.30
Deer 8-1	4.0	3.36	37.85	39.11	64.73	11.48	43.39	79	33.54	2.14	1.37	57.68
Deer 9-1	4.5	3.23	26.30	37.14	64.06	11.92	44.40	59	35.94	2.97	1.24	62.95
Deer 10-1	5.0	3.13	24.92	35.93	60.41	10.43	41.48	64	37.60	2.99	1.26	63.52
Deer 11-1	5.5	3.18	47.08	36.96	62.73	9.67	36.88	66	38.82	2.94	1.51	80.29
Deer 12-1	6.0	3.01	38.57	36.11	56.76	9.75	31.43	220	36.64	2.89	1.43	84.26
Deer 13-1	6.5	3.14	28.35	37.45	60.73	10.20	32.30	48	36.11	2.83	1.77	96.58
Deer 14-1	7.0	3.07	29.06	35.24	58.71	11.10	32.99	76	43.29	3.64	2.11	97.51
Deer 15-1	7.5	3.94	55.46	41.69	74.88	12.29	41.82	78	40.51	3.17	2.61	123.88
Deer 16-1	8.0	3.22	226.63	32.99	60.56	9.20	30.73	87	28.43	2.02	2.35	103.11
Deer 17-1	9.0	3.45	235.10	34.85	68.37	9.64	32.90	117	27.10	1.98	2.43	106.32
Deer 18-1	10.0	3.72	251.76	36.30	71.15	9.83	35.07	104	26.92	1.76	2.53	131.30
Deer 19-1	11.0	3.25	184.31	34.15	72.99	8.92	31.28	86	24.25	1.96	2.14	123.37
Deer 20-1	12.0	2.65	158.05	28.69	49.88	6.94	24.67	79	16.68	1.74	1.65	96.34
Deer 21-1	13.0	2.71	170.00	28.47	55.06	6.55	24.67	161	21.14	2.57	1.86	103.96
Deer 22-1	14.0	2.21	169.31	21.37	42.90	5.36	21.85	77	21.76	3.70	1.32	79.96
Deer 23-1	15.0	2.18	131.25	20.96	43.16	4.82	21.68	103	23.70	3.95	1.58	83.08
Deer 24-1	16.0	2.09	130.39	21.09	46.33	5.26	20.88	114	24.74	3.76	1.65	91.66
Deer 25-1	17.0	2.41	141.63	23.44	57.03	5.72	21.27	156	27.96	4.60	2.30	117.50

Table A3. (cont'd)

Sample	Depth	Sc	Ti	V	Cr	Co	Ni	Cu	As	Mo	Cd	Pb
Deer 26-1	18.0	2.37	138.38	23.83	54.50	5.88	21.54	149	25.62	4.20	2.33	129.76
Deer 27-1	19.0	2.29	141.41	22.29	54.55	5.94	20.89	120	22.86	4.29	2.21	133.00
Deer 28-1	20.0	2.56	165.85	22.79	56.20	6.28	22.54	126	23.51	6.47	2.60	148.91
Deer 29-1	21.0	2.46	55.95	23.36	55.44	6.26	24.47	38	17.17	7.15	2.61	166.19
Deer 30-1	22.0	2.38	213.98	23.16	53.03	6.04	21.98	157	23.62	4.11	2.36	158.17
Deer 31-1	23.0	2.54	209.94	25.48	57.62	5.82	24.14	199	25.08	3.88	2.48	180.90
Deer 32-1	24.0	2.28	190.86	22.46	61.65	5.01	19.67	167	23.54	3.63	2.48	172.28
Deer 33-1	25.0	2.56	64.13	24.78	76.24	7.70	26.65	45	20.98	4.96	2.72	189.76
Deer 34-1	26.0	2.22	161.77	21.18	70.55	5.49	19.56	108	22.26	2.72	2.36	158.63
Deer 35-1	27.0	2.63	182.13	25.76	121.67	7.31	24.50	181	26.47	3.82	3.03	176.04
Deer 36-1	28.0	2.48	163.73	25.42	119.79	8.23	23.06	168	22.58	3.02	2.60	155.10
Deer 37-1	29.0	2.53	156.32	26.26	101.81	8.56	23.91	155	23.25	3.50	2.80	167.28
Deer 38-1	30.0	2.52	155.26	24.85	79.73	8.19	21.15	141	20.02	3.77	2.74	160.25
Deer 39-1	31.0	2.76	194.58	27.00	98.35	8.31	23.42	112	18.67	3.57	2.53	172.11
Deer 40-1	32.0	2.54	70.51	25.42	70.81	8.56	17.86	90	19.83	4.09	2.71	229.96
Deer 41-1	33.0	2.70	39.10	28.62	54.49	9.71	19.64	99	18.89	2.62	2.43	200.27
Deer 42-1	34.0	2.39	55.34	25.84	50.27	8.77	15.93	103	17.65	2.47	2.24	183.45
Deer 43-1	35.0	3.04	81.90	30.73	54.15	10.00	30.49	207	24.92	2.77	2.15	177.87
Deer 44-1	36.0	2.91	40.39	29.44	50.27	9.71	28.89	170	23.53	3.01	2.06	178.14
Deer 45-1	37.0	2.77	100.22	28.02	47.76	9.44	27.62	120	22.30	3.35	2.00	159.60
Deer 46-1	38.0	2.78	199.46	28.70	48.83	9.54	29.75	158	20.86	2.74	2.26	155.48
Deer 47-1	39.0	3.21	68.08	32.44	57.67	11.28	33.74	103	20.04	4.27	2.14	174.71
Deer 48-1	40.0	3.20	85.72	32.77	57.97	11.37	33.61	98	20.57	6.19	2.23	164.61
Deer 49-1	41.0	3.10	95.19	32.70	52.21	11.23	32.43	103	22.56	5.83	2.09	146.60
Deer 50-1	42.0	3.37	173.52	35.78	53.96	11.89	35.36	116	23.35	4.66	2.03	131.89

Table A3. (cont'd)

Sample	Depth	Sc	Ti	V	Cr	Co	Ni	Cu	As	Mo	Cd	Pb
Deer 51-1	43.0	3.28	181.19	34.43	52.06	11.82	35.32	90	25.67	4.15	2.15	126.03
Deer 52-1	44.0	3.22	199.47	34.84	51.35	11.41	33.55	104	24.57	3.53	2.12	120.12
Deer 53-1	45.0	3.37	200.77	35.68	50.47	11.87	34.20	116	25.03	2.82	2.13	114.52
Deer 54-1	46.0	3.56	242.82	38.51	52.82	12.49	36.48	134	26.58	2.97	2.27	118.71
Deer 55-1	47.0	3.28	246.18	35.80	46.53	11.60	33.56	103	25.97	2.81	2.29	111.10
Deer 56-1	48.0	3.33	215.27	35.55	46.81	11.47	49.88	100	25.30	2.48	1.99	107.23

Table A3. (cont'd)

Sample	Depth	Al	Zn	Se	Sr	Mg	K	Mn	Ba	U	Fe	Ca	Hg
Deer 1-1	0.5	6686	172	3.08	40.18	3344	1065	3098	337	2.23	554	185	2.05
Deer 2-1	1.0	6828	168	3.25	41.20	3280	857	3603	415	2.28	601	226	2.28
Deer 3-1	1.5	6357	160	2.98	36.47	3165	837	3110	297	2.18	547	210	2.18
Deer 4-1	2.0	6873	175	3.15	33.79	3350	845	2570	225	2.14	533	203	1.90
Deer 5-1	2.5	7838	197	3.26	35.69	3839	856	2601	152	2.36	618	239	1.96
Deer 6-1	3.0	7652	187	3.17	34.23	3598	717	2728	85	2.39	613	228	1.88
Deer 7-1	3.5	8690	218	3.17	34.26	4396	765	3187	136	2.75	708	270	1.75
Deer 8-1	4.0	10612	251	3.07	36.08	5433	931	2994	121	2.94	782	324	1.84
Deer 9-1	4.5	10124	251	3.23	37.95	4903	929	2840	93	2.61	743	320	2.26
Deer 10-1	5.0	9651	240	3.07	38.01	4704	955	2633	87	2.54	719	302	2.38
Deer 11-1	5.5	10553	282	3.27	39.04	4555	861	2451	136	2.71	739	314	4.20
Deer 12-1	6.0	10921	267	3.20	39.57	4238	763	2320	129	2.56	722	284	4.86
Deer 13-1	6.5	10957	319	3.03	40.26	4701	871	2435	97	2.73	749	304	5.60
Deer 14-1	7.0	11140	406	3.35	43.66	4735	824	2233	98	2.70	705	294	6.52
Deer 15-1	7.5	14544	471	3.53	53.62	6421	1104	2017	170	2.70	834	374	8.09
Deer 16-1	8.0	12392	342	2.70	43.10	5616	796	1386	210	2.13	660	303	7.87
Deer 17-1	9.0	13376	358	2.81	49.11	5997	845	1338	281	2.23	697	342	8.02
Deer 18-1	10.0	18516	370	2.96	48.36	6102	968	1640	261	2.16	726	356	10.09
Deer 19-1	11.0	12592	323	2.99	48.38	5787	711	1454	244	2.34	683	365	9.26
Deer 20-1	12.0	10142	237	1.99	40.34	5480	567	1228	223	2.22	574	249	5.77
Deer 21-1	13.0	11169	249	3.31	61.65	4968	606	1700	358	2.20	569	275	6.90
Deer 22-1	14.0	7797	184	3.30	75.52	3762	581	1091	280	1.79	427	215	5.52
Deer 23-1	15.0	7388	232	3.83	63.37	3212	490	1307	301	2.43	419	216	4.93
Deer 24-1	16.0	7582	233	3.86	64.36	3110	469	1135	348	2.81	422	232	8.03
Deer 25-1	17.0	8007	290	4.24	65.81	3339	499	1426	411	3.55	469	285	15.78

Table A3. (cont'd)

Sample	Depth	Al	Zn	Se	Sr	Mg	K	Mn	Ba	U	Fe	Ca	Hg
Deer 26-1	18.0	8247	300	4.42	66.51	3376	501	1185	416	3.51	477	273	25.50
Deer 27-1	19.0	7536	267	4.27	65.73	3276	481	781	373	3.12	446	273	24.89
Deer 28-1	20.0	8105	317	5.39	72.31	3712	543	791	380	3.45	456	281	25.35
Deer 29-1	21.0	8308	405	4.98	64.32	3622	712	798	50	4.67	467	277	24.34
Deer 30-1	22.0	7942	310	5.79	70.21	3419	632	857	395	3.98	463	265	11.87
Deer 31-1	23.0	8728	334	3.56	77.84	3930	663	1040	472	3.90	510	288	11.86
Deer 32-1	24.0	8014	331	3.12	77.43	3433	599	971	453	3.73	449	308	13.58
Deer 33-1	25.0	9011	427	2.85	81.61	4178	686	1002	64	4.13	496	381	15.96
Deer 34-1	26.0	7300	299	3.00	67.72	3549	494	1077	349	4.24	424	353	11.62
Deer 35-1	27.0	8946	447	3.76	75.14	4623	599	1563	398	4.36	515	608	13.23
Deer 36-1	28.0	9277	415	3.65	70.23	4765	594	2212	405	4.33	508	599	11.40
Deer 37-1	29.0	9175	376	4.49	73.77	4872	578	2246	409	4.63	525	509	13.13
Deer 38-1	30.0	8955	331	4.19	67.90	5166	628	1592	380	4.45	497	399	12.56
Deer 39-1	31.0	9678	394	4.13	65.15	6106	759	1352	351	4.33	540	492	10.30
Deer 40-1	32.0	9087	383	5.55	71.08	4771	676	1945	300	5.19	508	354	13.33
Deer 41-1	33.0	10406	349	4.40	68.60	4899	775	2050	252	4.82	572	272	12.66
Deer 42-1	34.0	9403	320	4.35	63.35	4438	669	1880	271	4.39	517	251	10.98
Deer 43-1	35.0	11060	348	4.39	73.89	5064	1394	2423	319	5.69	615	271	9.60
Deer 44-1	36.0	10145	358	4.10	78.83	5040	1259	2642	308	5.51	589	251	11.92
Deer 45-1	37.0	10177	359	4.77	74.91	5203	1256	1868	274	4.69	560	239	14.09
Deer 46-1	38.0	10561	437	3.77	76.23	5501	1238	1916	305	4.29	574	244	14.00
Deer 47-1	39.0	12086	428	4.03	75.71	6583	1312	1892	179	4.58	649	288	17.31
Deer 48-1	40.0	12329	435	4.51	75.45	6632	1373	1655	118	4.55	655	290	18.71
Deer 49-1	41.0	11658	407	3.62	72.58	6597	1280	1866	127	4.33	654	261	19.72
Deer 50-1	42.0	12911	377	3.79	71.36	7434	1451	1822	197	3.96	716	270	18.62

Table A3. (cont'd)

Sample	Depth	Al	Zn	Se	Sr	Mg	K	Mn	Ba	U	Fe	Ca	Hg
Deer 51-1	43.0	12833	382	3.28	75.22	6763	1289	1687	224	3.79	689	260	19.21
Deer 52-1	44.0	12461	349	3.20	71.90	6152	1239	1774	221	3.29	697	257	18.31
Deer 53-1	45.0	13160	347	3.18	70.08	6307	1294	1985	232	3.00	714	252	17.63
Deer 54-1	46.0	13791	364	3.19	72.72	6870	1311	1994	233	2.74	770	264	16.73
Deer 55-1	47.0	12928	393	2.81	63.74	6339	1168	1883	202	2.35	716	233	15.39
Deer 56-1	48.0	13024	384	2.62	62.68	5804	1151	1721	183	2.27	711	234	15.25

Table A4. Metal concentrations for Deer Lake north core (mg/kg).

Sample	Depth	Sc	Ti	V	Cr	Co	Ni	Cu	As	Mo	Cd	Pb
Deer 1-2	0.5	2.68	232.1	35.57	62.07	14.55	68.27	0.00	23.52	2.52	1.73	58.93
Deer 2-2	1.0	2.55	230.9	34.81	59.88	14.44	65.01	0.00	24.11	2.42	1.73	55.34
Deer 3-2	1.5	2.34	223.6	32.03	54.13	13.22	59.78	0.00	20.33	2.04	1.56	51.13
Deer 4-2	2.0	2.29	205.4	31.74	54.68	12.23	59.78	0.00	17.85	1.84	1.55	51.21
Deer 5-2	2.5	2.43	203.9	33.37	55.67	13.30	63.65	0.00	18.27	2.24	1.49	52.30
Deer 6-2	3.0	2.51	226.7	34.38	59.59	13.88	65.17	0.00	18.76	2.32	1.54	54.32
Deer 7-2	3.5	2.58	229.6	34.16	58.64	14.40	66.84	0.00	20.14	2.54	1.68	56.17
Deer 8-2	4.0	2.54	210.7	32.58	56.06	13.32	61.39	0.00	19.46	2.25	1.59	55.75
Deer 9-2	4.5	2.50	217.0	32.37	58.38	13.85	64.24	0.00	20.46	2.62	1.71	58.34
Deer 10-2	5.0	2.54	207.7	32.72	61.47	15.89	68.38	0.00	24.21	3.15	1.82	63.68
Deer 11-2	5.5	2.58	218.0	31.77	55.24	15.78	67.78	0.00	24.29	3.31	1.85	66.12
Deer 12-2	6.0	2.49	198.4	30.92	58.41	16.71	64.73	0.00	24.96	3.31	1.98	68.06
Deer 13-2	6.5	2.52	222.2	31.31	57.69	16.80	64.81	0.00	26.00	3.52	2.11	70.07
Deer 14-2	7.0	2.41	195.9	30.22	53.74	17.07	62.48	0.00	26.87	3.59	2.09	70.26
Deer 15-2	7.5	2.48	200.1	31.01	55.13	18.63	66.48	0.00	29.17	3.85	2.24	75.32
Deer 16-2	8.0	2.56	217.0	30.85	56.33	18.69	69.56	0.00	29.98	3.94	2.23	75.67
Deer 17-2	9.0	2.52	196.7	30.45	55.54	19.92	66.25	0.00	30.79	3.92	2.34	75.57
Deer 18-2	10.0	2.46	206.3	30.20	55.58	19.84	69.65	0.00	30.39	3.95	2.28	74.62
Deer 19-2	11.0	2.56	228.5	31.17	54.34	20.72	63.65	0.00	31.74	3.95	2.30	75.64
Deer 20-2	12.0	2.63	230.4	30.84	57.17	19.62	65.30	0.00	30.36	3.96	2.27	77.17
Deer 21-2	13.0	2.73	257.5	32.12	60.00	18.23	63.87	0.00	29.71	4.06	2.13	78.87
Deer 22-2	14.0	2.73	259.2	31.40	60.36	14.19	59.41	0.00	26.34	4.23	1.99	80.55
Deer 23-2	15.0	2.70	252.0	31.95	62.74	12.15	59.46	0.00	23.14	4.35	1.77	81.77
Deer 24-2	16.0	2.51	214.3	29.64	57.92	10.71	56.88	0.00	21.78	4.09	1.70	81.01
Deer 25-2	17.0	3.16	254.3	36.70	73.96	12.60	71.37	0.00	24.87	5.29	2.15	104.27

Table A4. (cont'd)

Sample	Depth	Sc	Ti	V	Cr	Co	Ni	Cu	As	Mo	Cd	Pb
Deer 26-2	18.0	2.62	229.2	31.18	58.76	10.51	58.54	0.00	19.96	4.38	1.83	86.98
Deer 27-2	19.0	2.83	232.1	31.16	62.25	11.09	65.35	74.98	21.98	4.21	1.86	86.74
Deer 28-2	20.0	2.41	203.6	29.84	53.27	10.73	59.45	45.18	22.45	3.88	1.67	74.76
Deer 29-2	21.0	2.73	238.1	30.99	64.67	9.34	61.72	56.71	20.60	4.42	1.72	88.26
Deer 30-2	22.0	2.72	246.5	30.33	59.64	9.12	61.05	53.71	19.94	4.28	1.63	87.42
Deer 31-2	23.0	2.67	274.0	30.92	56.25	9.12	61.93	55.08	19.64	4.08	1.61	83.09
Deer 32-2	24.0	2.55	245.6	30.22	54.38	8.64	59.96	40.88	19.63	4.09	1.47	78.09
Deer 33-2	25.0	2.48	228.8	27.96	58.60	8.19	57.50	51.58	17.63	4.13	1.50	79.42
Deer 34-2	26.0	2.50	249.6	31.72	52.84	8.75	60.45	52.59	19.36	3.91	1.57	77.86
Deer 35-2	27.0	2.46	246.2	32.08	55.07	10.69	62.50	57.37	20.99	4.37	1.52	78.46
Deer 36-2	28.0	2.46	261.6	29.84	54.15	7.90	57.86	50.36	18.32	3.77	1.44	76.29
Deer 37-2	29.0	2.31	136.6	26.13	46.20	6.39	53.37	43.04	18.63	4.02	1.17	79.96
Deer 38-2	30.0	2.22	222.4	25.95	47.72	5.58	54.44	51.39	18.99	3.91	1.15	79.98
Deer 39-2	31.0	2.22	237.8	26.94	50.73	5.47	49.86	56.27	19.96	3.69	1.02	70.18
Deer 40-2	32.0	2.26	234.0	29.48	54.83	6.07	50.02	52.34	20.72	3.41	1.04	64.11
Deer 41-2	33.0	2.47	257.8	32.41	59.35	6.73	52.22	46.92	22.25	3.59	1.02	66.33
Deer 42-2	34.0	2.44	247.9	31.63	48.65	6.29	50.97	53.61	19.92	3.49	0.93	59.98
Deer 43-2	35.0	2.27	169.7	29.22	50.20	6.40	50.60	40.76	18.25	3.38	1.05	62.94
Deer 44-2	36.0	2.21	167.1	28.18	41.02	5.90	47.40	53.20	16.70	3.59	1.29	61.91
Deer 45-2	37.0	2.27	177.6	27.37	44.03	5.60	47.50	41.51	15.61	3.40	0.98	59.66
Deer 46-2	38.0	2.22	175.7	26.97	43.66	5.49	47.56	53.50	14.55	2.97	0.91	57.40
Deer 47-2	39.0	2.35	208.7	28.52	42.35	5.26	47.59	48.23	16.99	3.22	0.94	64.10
Deer 48-2	40.0	2.45	212.0	30.70	44.05	5.95	48.92	44.28	16.51	2.79	0.95	64.23
Deer 49-2	41.0	2.55	239.5	31.33	48.84	6.16	50.81	58.73	16.87	2.93	0.95	65.17
Deer 50-2	42.0	2.30	192.1	28.19	42.30	5.49	46.36	45.43	15.76	2.84	0.82	52.70

Table A4. (cont'd)

Sample	Depth	Sc	Ti	V	Cr	Co	Ni	Cu	As	Mo	Cd	Pb
Deer 51-2	43.0	2.50	247.4	30.29	44.00	5.55	47.27	47.21	15.82	3.24	0.88	51.86
Deer 52-2	44.0	2.49	208.3	28.97	43.82	5.36	49.03	61.44	15.38	3.06	0.84	55.21
Deer 53-2	45.0	2.43	211.3	31.38	46.80	5.83	47.14	41.94	17.18	3.23	1.03	53.51
Deer 54-2	46.0	2.36	233.7	32.01	43.87	6.02	46.99	43.89	17.85	3.22	1.00	51.13
Deer 55-2	47.0	3.11	275.9	32.81	42.29	6.19	48.38	57.40	17.38	3.18	1.00	51.64

Table A4. (cont'd)

Sample	Depth	Al	Zn	Se	Sr	Mg	K	Mn	Ba	U	Fe	Ca	Hg
Deer 1-2	0.5	11616	272	4.29	42.09	4653	924	1491	110.42	3.62	67515	16879	4.39
Deer 2-2	1.0	10966	255	4.32	40.02	4171	903	1604	118.66	3.69	69470	17367	4.28
Deer 3-2	1.5	10289	233	4.11	37.86	3879	919	1572	120.17	3.33	64758	16190	3.94
Deer 4-2	2.0	10144	232	4.31	36.97	3910	868	1334	110.86	3.27	63405	15851	4.23
Deer 5-2	2.5	10312	238	4.93	37.29	3947	864	918	103.90	3.71	63028	15757	4.29
Deer 6-2	3.0	12743	250	4.65	36.39	4091	879	789	96.24	3.92	63444	15861	4.36
Deer 7-2	3.5	11153	260	4.69	35.90	4217	884	853	91.05	3.96	67870	16968	4.67
Deer 8-2	4.0	10528	249	4.71	33.76	4010	807	948	79.09	3.52	70258	17565	4.49
Deer 9-2	4.5	11436	263	4.78	35.11	4139	900	981	76.07	3.68	68015	17004	4.78
Deer 10-2	5.0	11158	291	5.03	36.14	4272	857	822	74.23	3.89	58787	14697	5.24
Deer 11-2	5.5	11587	304	4.52	35.74	4388	910	781	78.72	3.56	53258	13315	5.40
Deer 12-2	6.0	12838	319	5.02	35.59	4374	867	817	78.75	3.61	54471	13618	5.94
Deer 13-2	6.5	11876	336	4.39	36.48	4381	927	803	81.44	3.61	54852	13713	6.00
Deer 14-2	7.0	15683	339	4.91	36.07	4231	853	801	84.78	3.54	54593	13648	6.22
Deer 15-2	7.5	11934	378	5.22	38.96	4447	908	868	84.37	3.56	56149	14037	6.58
Deer 16-2	8.0	12082	376	4.79	39.19	4431	945	947	84.25	3.60	57615	14404	6.52
Deer 17-2	9.0	12084	407	5.03	40.85	4439	893	1107	85.86	3.63	56271	14068	6.57
Deer 18-2	10.0	12053	407	4.70	48.31	4406	930	1346	95.01	3.63	56090	14022	6.80
Deer 19-2	11.0	12607	400	4.62	43.34	4523	977	1303	89.50	3.62	54879	13720	6.88
Deer 20-2	12.0	12387	393	4.54	46.06	4593	1020	1250	92.87	3.67	52231	13058	7.13
Deer 21-2	13.0	12825	357	4.65	46.52	4775	1106	1042	94.77	3.75	52154	13038	7.38
Deer 22-2	14.0	12393	301	4.33	45.03	4870	1090	688	95.64	3.97	49981	12495	7.74
Deer 23-2	15.0	12114	263	4.69	45.61	4928	1080	561	93.90	4.12	47968	11992	8.19
Deer 24-2	16.0	11260	240	4.76	45.30	4906	944	528	90.67	4.13	45494	11374	8.52
Deer 25-2	17.0	14167	289	6.22	57.77	6141	1122	623	112.70	5.37	56539	14135	10.78

Table A4. (cont'd)

Sample	Depth	Al	Zn	Se	Sr	Mg	K	Mn	Ba	U	Fe	Ca	Hg
Deer 26-2	18.0	12997	240	5.21	48.11	5141	1023	550	95.05	4.38	47179	11795	9.01
Deer 27-2	19.0	12032	260	5.35	50.23	5077	801	644	97.46	4.34	48450	12112	9.05
Deer 28-2	20.0	11936	222	5.20	55.10	4205	650	616	88.73	4.00	44824	11206	7.31
Deer 29-2	21.0	11589	227	4.98	49.46	4969	835	585	89.61	4.53	47984	11996	8.78
Deer 30-2	22.0	11679	218	4.84	48.41	4850	856	580	86.12	4.53	48069	12017	8.43
Deer 31-2	23.0	11718	202	4.88	47.89	4639	938	512	79.76	4.32	49482	12371	7.81
Deer 32-2	24.0	11145	183	5.05	49.12	4269	839	460	73.03	4.20	46837	11709	7.17
Deer 33-2	25.0	10660	188	4.81	46.69	4303	799	486	75.62	4.31	42423	10606	7.31
Deer 34-2	26.0	10840	195	4.84	58.02	4501	834	520	84.99	4.25	41890	10473	7.54
Deer 35-2	27.0	10806	195	5.03	55.10	4261	809	465	76.70	4.56	49006	12251	7.20
Deer 36-2	28.0	10477	176	4.85	53.21	4099	859	474	79.92	4.15	45230	11307	5.57
Deer 37-2	29.0	9571	168	4.39	68.31	3560	777	580	83.78	4.02	40630	10157	4.81
Deer 38-2	30.0	9847	141	4.31	47.86	3160	741	325	76.31	4.07	43492	6524	4.42
Deer 39-2	31.0	9759	122	4.12	50.16	2992	773	327	77.31	4.22	47020	7053	3.67
Deer 40-2	32.0	10253	123	4.55	52.63	3201	799	343	80.26	4.21	42164	6325	3.05
Deer 41-2	33.0	11398	128	4.98	58.29	3554	899	383	84.16	4.39	44196	6629	3.27
Deer 42-2	34.0	11155	107	4.80	58.25	3470	875	406	78.53	4.23	40806	6121	2.90
Deer 43-2	35.0	10101	108	5.19	59.88	3481	653	391	79.18	4.27	40040	6006	2.90
Deer 44-2	36.0	10311	104	5.25	60.70	3479	657	353	77.52	4.02	39057	5859	2.85
Deer 45-2	37.0	10186	97	5.22	60.64	3535	697	344	77.54	3.93	37391	5609	2.80
Deer 46-2	38.0	10234	95	4.74	60.69	3528	704	338	78.31	3.82	33898	5085	2.80
Deer 47-2	39.0	11540	101	4.76	62.74	3799	825	347	83.06	4.35	37148	5572	2.93
Deer 48-2	40.0	11265	105	4.42	65.83	3820	825	351	86.13	3.99	36475	5471	3.11
Deer 49-2	41.0	12026	108	4.54	68.88	3965	1708	362	90.08	3.96	37529	5629	3.11
Deer 50-2	42.0	11116	95	4.16	67.90	3724	817	350	85.04	3.48	35720	5358	3.13

Table A4. (cont'd)

Sample	Depth	Al	Zn	Se	Sr	Mg	K	Mn	Ba	U	Fe	Ca	Hg
Deer 51-2	43.0	12454	96	4.24	72.11	4011	997	357	91.11	3.48	38789	5818	3.20
Deer 52-2	44.0	12483	92	4.20	74.98	4096	904	359	97.53	3.27	38099	5715	3.25
Deer 53-2	45.0	11865	102	4.13	74.07	3667	851	345	93.03	3.48	39028	5854	3.70
Deer 54-2	46.0	11678	100	3.81	73.24	3483	876	337	90.86	3.38	40287	6043	3.75
Deer 55-2	47.0	12243	103	3.93	73.20	3636	1024	342	93.36	3.24	38359	5754	3.81

APPENDIX B

SUPPORTING INFORMATION FOR CHAPTER 2

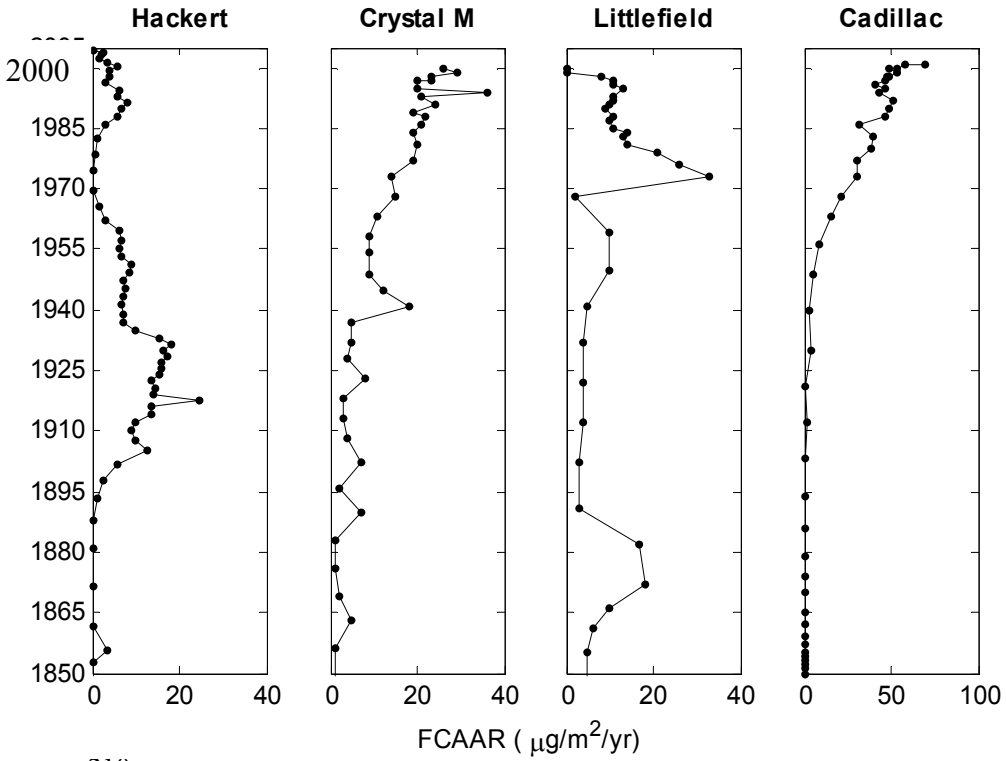

Figure S1. ^{210}Pb dated focusing-corrected anthropogenic accumulation rates for four Michigan lakes, dates older than 1850 were truncated to highlight more recent loading. Note the change in scale on the x-axis.

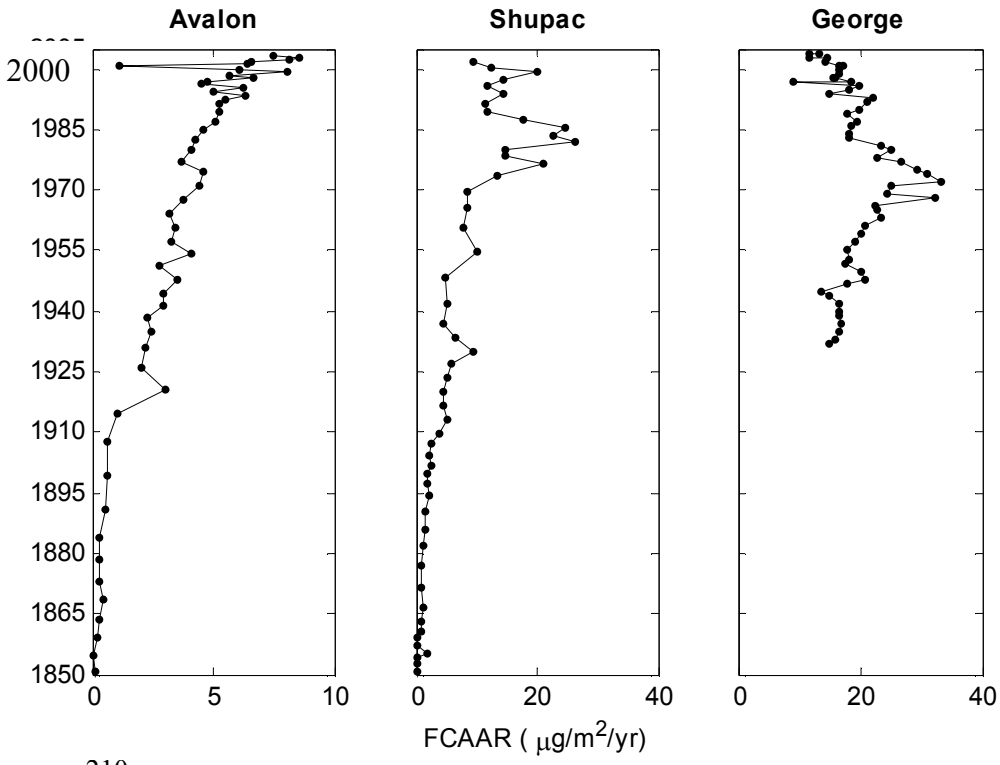

Figure S2. ^{210}Pb dated focusing-corrected anthropogenic accumulation rates for three Michigan lakes, dates older than 1850 were truncated to highlight more recent loading. Note the change in scale on the x-axis.

Dating Methodology

Methods for determining appropriate sediment ages for these cores were adapted from a decade of work in the Great Lakes region (Golden *et al.*, 1993, Kolak *et al.*, 1998, Kolak *et al.*, 1999, Pearson *et al.*, 1998, Pearson *et al.*, 1997a, Pearson *et al.*, 1997b, Simick *et al.*, 1996, Wong *et al.*, 1995). Four different ^{210}Pb dating models were compared to determine accurate dates for sediment cores collected in this study (Table S1). The constant flux: constant sedimentation (CF:CS) model assumes a constant flux of ^{210}Pb to the sediment and a constant rate of sedimentation (Golden *et al.*, 1993). However, if clear sedimentation rate changes occurred within the core indicated by changes in slope of the accumulated dry mass versus excess ^{210}Pb plot then a segmented CF:CS (SCF:CS) model was used (Heyvaert *et*

al., 2000). If a mixing zone was present, appearing as a vertical straight line in the accumulated dry mass versus excess ^{210}Pb plot, then the rapid steady state mixing model (RSSM) (Robbins, 1982) may be used. When excess ^{210}Pb inventories could be calculated the constant rate of supply model (CRS) was also evaluated (Oldfield *et al.*, 1978). The most appropriate dating model was chosen based on three separate qualifiers: date of peak ^{137}Cs activity (ca. 1963) (Walling and Qingping, 1992), age of oldest sediment containing excess ^{210}Pb (ca. 1850), and stable Pb peak concentration (ca. 1970) (Alfaro-De la Torre and Tessier, 2002) (Table S1). Maximum stable Pb concentration not placed in the mid-1970s does not conclude an incorrectly dated sediment core if significant local watershed sources exist. However, if the maximum stable Pb concentration does occur in the mid-1970s then the age dating model was appropriate. Only core sections containing excess ^{210}Pb can be dated, therefore core sections without excess ^{210}Pb were dated by assuming that sedimentation rates remained constant below this depth. For the CF:CS, SCF:CS and RSSM model the sedimentation rate for the lowest excess ^{210}Pb-containing sections was used. For the CRS model the average of the last five excess ^{210}Pb-containing core sections was used.

Focusing factors were calculated for all lakes. When ^{210}Pb was present in all core sections inventories of ^{210}Pb were estimated by extrapolating the regression equation of excess ^{210}Pb vs. accumulated dry mass (g/cm^2). For lakes dated with the CF:CS model the entire core section was used. Only the bottom core sections were used to determine the equation

when the SCF:CS was applied. Dry mass was estimated as the average dry mass for the bottom two to twelve core sections. The final focusing factor was deemed appropriate when additional core sections did not result in an appreciable change.

Dating in Littlefield Lake was difficult due to a disturbed ^{210}Pb profile; however, stable Pb concentrations appeared to reach background concentrations when compared to other study lakes. In order to date this sediment core, the core section containing the greatest stable Pb concentration was assigned a median year of deposition of 1972. The total mass of sediment was determined for core sections above the greatest stable Pb concentration and divided by 28 y (2000-1972) to determine the sedimentation rate, 693 g/m^2/yr. However, applying this sedimentation rate to the entire core placed background concentrations of Pb much earlier than other lakes. Therefore, a SCF:CS model was used to date this core with a sedimentation rate of 693 g/m^2/y for core sections younger than 1972 and a sedimentation rate of 252 g/m^2/y in core sections older than 1972. The focusing factor for Littlefield Lake was determined as the average of Elk, Gull, Crystal M, and Higgins lakes.

Table S1: ^{210}Pb data for 26 Michigan lakes

Lake	Model	^{137}Cs Date	Stable Pb Date	Excess ^{210}Pb Range (Bq/g)	Sedimentation Rate Range[e] ($g/m^2/y$)
Avalon	CRS	1957	1974	0.0152-0.461	100-637
Birch	CRS	1969	1982	0.00162-1.10	235-1871
Cadillac	CRS	Disturb[a]	1973	0.00357-0.764	76-398
Cass	CF:CS	NM[b]	1981	0.128-0.309	3480
Crystal B	CRS	1966	1966	0.0213-0.636	421-796
Crystal M	CRS	1977	1977	0.00382-0.536	351-548
Elk	SCF:CS	1966	1972	0.000489-0.637	450, 980, 220
George	CF:CS	1968	1971	0.101-0.931	417
Gratiot	CF:CS	NM[b]	1968	0.000612-1.27	255
Gull	SCF:CS	NM[b]	1977	0.00147-0.372	190,535
Hackert	CRS	1966	1988	0.0133-3.12	87-1116
Higgins	CF:CS	NM[b]	1984	0.00368-0.988	232
Houghton	SCF:CS	1971	1969	0.000489-0.795	59,490,152
Imp	CRS	1978	1974	0.00201-2.52	51-431
Littlefield	Pb	NM[b]	assigned	0.199-0.250[d]	252,693
Mullett	SCF:CS	1965	1973	0.000893-0.426	980, 1550, 420
Muskegon	CF:CS	Unclear[c]	1968	0.0911-0.329	1711
Otter	CF:CS	1963	1961	0.0768-1.02	933
Paw Paw	CF:CS	1963	1974	0.0741-0.581	828
Round	CRS	1971	1971	0.00486-1.01	154-442
Round D	CRS	1968	1937	0.00280-1.20	137-1439
Sand	CRS	Disturb[a]	1997	0.00834-0.905	110-2173
Shupac	CRS	1961	1983	0.00296-3.38	99-1134
Torch	SCF:CS	1969	1983	0.000149-0.922	390, 1108, 329, 1280, 1504
Whitmore	SCF:CS	1967	1976	0.0198-0.822	552, 2188, 202
Witch	CRS	1961	1961	0.0822-1.18	44-590

[a]Indicates that the ^{137}Cs profile was disturbed and a clear peak in activity was not identified.

[b]^{137}Cs was not measured in these lakes.

[c]The ^{137}Cs was not disturbed but a peak was not readily identifiable.

[d]Excess ^{210}Pb values for Littlefield Lake were estimated

[e]In the case of the CF:CS model the sedimentation rate applies to the entire core. The range of sedimentation rates are provided for the CRS model. Sedimentation rates for cores dated with the SCF:CS model are read from left to right representing sedimentation rates from the top to the bottom of the core.

REFERENCES

REFERENCES

Alfaro-De la Torre, M.C., Tessier, A., 2002. Cadmium deposition and mobility in the sediments of an acidic oligotrophic lake. Geochimica et Cosmochimica Acta 66, 3549-3562.

Golden, K.A., Wong, C.S., Jeremiason, J.D., Eisenreich, S.J., Sanders, M.G., Hallgren, J., Swackhammer, D.L., Engstrom, D.R., Long, D.T., 1993. Accumulation and preliminary inventory of organochlorines in Great Lakes sediments. Water Science and Technology 28, 19-31.

Heyvaert, A.C., Reuter, J.E., Slotton, D.G., Goldman, C.R., 2000. Paleolimnological reconstruction of historical atmospheric lead and mercury deposition at Lake Tahoe, California-Nevada. Environmental Science and Technology 34, 3588-3597.

Kolak, J.J., Long, D.T., Beals, T.M., Eisenreich, S.J., Swackhamer, D.L., 1998. Anthropogenic inventories and historical and present accumulation rates of copper in Great Lakes sediments. Applied Geochemistry 13, 59-75.

Kolak, J.J., Long, D.T., Kerfoot, W.C., Beals, T.M., Eisenreich, S.J., 1999. Nearshore versus offshore copper loading in Lake Superior sediments: Implications for transport and cycling. Journal of Great Lakes Research 25, 611-624.

Oldfield, F., Appleby, P.G., Battarbee, R.W., 1978. Alternative Pb-210 Dating - Results from New-Guinea Highlands and Lough Erne. Nature 271, 339-342.

Pearson, R.F., Swackhamer, D.L., Eisenreich, S.J., Long, D.T., 1998. Atmospheric inputs of polychlorinated dibenzo-p-dioxins and dibenzofurans in sediments of the Great Lakes: compositional comparison of PCDD and PCDF in sediments. Journal of Great Lakes Research 24, 65-82.

Pearson, R.F., Swackhamer, D.L., Eisenreich, S.J., Long, D.T., 1997a. Concentrations, accumulations, and inventories of polychlorinated dibenzo-p-dioxins and dibenzofurans in sediments of the Great Lakes. Environmental Science and Technology 31, 2903-2909.

Pearson, R.F., Swackhamer, D.L., Eisenreich, S.J., Long, D.T., 1997b. Concentrations, accumulations, and inventories of toxaphene in sediments of the Great Lakes. Environmental Science and Technology 31, 3523-3520.

Robbins, J.A., 1982. Stratigraphic and dynamic effects of sediment reworking by Great Lakes zoobenthos. Hydrobiologia 92, 611-622.

Simick, M.F., Eisenreich, S.J., Golden, K.A., Liu, S., Lipiatou, E., Swackhammer, D.H., Long, D.T., 1996. Atmospheric loading of polycyclic aromatic hydrocarbons to Lake

Michigan as recorded in sediments. Environmental Science and Technology 30, 3039-3046.

Walling, D.E., Qingping, H., 1992. Interpretation of caesium-137 profiles in lacustrine and other sediments: the role of catchment-derived inputs. Hydrobiologia 235, 219-230.

Wong, C.S., Sanders, G., Engstrom, D.R., Long, D.T., Swackhammer, D.L., Eisenreich, S.J., 1995. Accumulation, inventory, and diagenesis of chlorinated hydrocarbons in Lake Ontario sediments. Environmental Science and Technology 29, 2661-2672.

APPENDIX C

METHODS FOR ACQUISITION OF WATERSHED CHARACTERISTIC DATA

APPENDIX C. METHODS FOR ACQUISITION OF WATERSHED CHARACTERISTICS DATA

The following methods supplement those prepared by Sharon S. Yohn and were used in the acquisition of the watershed characteristics used in Chapter 3. ArcGIS run on a Windows platform was used for all GIS work.

Calculating Land Use in Watershed and Buffers

First, reclassifying the land use makes the process a bit easier. A reclass file has been saved to the C:\Workspace file for both the IFMAP (C:\Workspace\ifmap_class) and 1978 MIRIS (C:\Workspace\78_class) land use databases. To reclassify the data follow the steps below.

IFMAP

1. Add the buffer polygon file and the watershed land use raster to the active layer
2. In the ArcToolbox→Spatial Analyst→Reclass→Reclassify toolbox
3. Input Raster: The watershed land use raster
4. Reclass Field: Use the Value field
5. Press the Load.. button and find the proper reclassification table (IFMAP or MIRIS)
6. Run the Tool
7. Now you have a reclassified landuse raster. The table below defines how the raster was reclassified.

Table C1. IFMAP Reclassification Scheme

Land Use Type	Old Classification	New Classification
Urban	1-4	100
Agriculture	5,6,7,9	200
Upland Openland	10,12,13	300
Forest	14-22,24-26	400
Water	23	500
Wetland	27-30	600
Barren	31,32,35	700

   a. *Note the Forest classification includes lowland forest which by IFMAP classifcations is defined as wetland. Following the methods of Yohn S. S. 2004 it will be defined as forest here.

8. Now that the land use has been reclassified we need to clip the watershed land use raster with the buffer polygon. For this we shall set the analysis mask of the spatial

analyst. Setting the mask in spatial analyst will force all operations to be constrained to the mask and thus must be reset or turned off in order to complete new mask operations.

9. In the Spatial Analyst Toolbar choose Options

10. In the General Tab:
    a. Working directory: Set this to the directory in which to save the files
    b. Analysis Mask: Set this to the buffer polygon in the drop down menu
    c. Analysis Coordinate System: Set this to the coordinate system of the active data layer (Be sure to change the active data layer to the Michigan GEOREF projection)

11. In the Extent Tab:
    a. Analysis Extent: In the pulldown menu specify the buffer polygon

12. In the Cell Size Tab:
    a. Analysis cell size: In the pulldown menu specify the reclassified watershed landuse raster
    b. Specify the cell size, generally you want to use the lowest cell size possible to capture all of the detail, 1m is generally works well. 1m will not work well with large watersheds due to restrictions in space and computing time.

13. Press Ok to exit the Options Window.

14. In the Spatial Analyst toolbar click on the Raster Calculator and double-click on the reclassified watershed landuse raster and press Evaluate

15. Now a temporary file called "Calculation" has been created. To create a permanent file right click on the Calculation file and press Make Permanent. This does not have to be done in able to calculate areas but may be convienent if you want to revisit the data. Instead of making the raster "Calculation" permanent you can join the results of the Calculation to the watershed land use raster.
    a. Create a file name and save it in the directory

16. Add the file you created when you made the Calculation data file permanent. Right click on the file and open the attribute table.

a. The Value represents the land use classification scheme described above and the count is the number of cells making up the land use. Multiplying the count times the square of the cell size will result in the area in square meters of land use. The attribute file can be exported to Excel for ease of calculation.

17. With the attribute table open, click on the Options.. menu and click on Export.
    a. Export: All records
    b. Output Table: Specify the directory and name.
    c. Click on the folder button to browse and change the file type to text.
    d. Click Save

18. Open the new land cover file in Excel and multiply the count column times the square of the cell size specified above (generally 30^2). These are the areas of land use in the buffer around the lake.

MIRIS Land Use

The method for calculating 1978 MIRIS land use is different because the values assigned to the land use classifications change from lake to lake.

1. Add the 1978 land use shapefile clipped to the watershed to the active layer
2. Convert the shapefile to a raster dataset in the ArcToolbox→Conversion Tools→To Raster→Feature to Raster
    a. Input Features: Select the 1978 land use shapefile
    b. Field: Select the LABEL1 field
    c. Output Raster: Specify the file name and location
    d. Output Cell Size: Specify the cell size (1m generally works well for our watersheds and simplifies the calculation of land use)

3. Follow step 9-14 from the IFMAP area calculations to create a raster of the land use in the buffer.
4. Right click on the newly created raster and open the attribute table.
    a. You will notice that the counts and label name are not preserved in the buffer raster attribute file we need to join the fields in the buffer raster with the fields in the 1978 land use watershed raster
5. A join can be made between the 1978 watershed land use file and the buffer file to preserve the labels
    a. Right click on the 1978 land use buffer raster and click on Joins and Relates→Join…
        i. You want to join attributes from a table
        ii. Choose the Value Field in the 1. Drop down box
        iii. Choose the 1978 watershed land use raster from the 2. drop down box
        iv. Choose the Value Field in the 3. drop down box
        v. Click OK

6. Now right click on the buffer raster file and the labels are now included in the file.
    a. Export the attribute file to a text file
7. Open the newly created text file in Excel and multiply the counts times the square of the cell size you specified when creating the raster.
8. These are the areas of 1978 land use categorized by the most general level of detail
    a. Urban, Agriculture, Nonforested, Forested, Water, Wetlands, and Barren

*Note: Barren in the MIRIS database has a different meaning than Barren in the IFMAP. Barren in MIRIS is defined as beaches and riverbanks or sand covered beaches.

Calculating Land Use/Land Cover Using the Inland Lakes Toolbox in ArcGIS 9.2

This method requires that the Proj_Fill_Fdir_Facc and Watershed_No_Lake_Polygon models have been run.

Make sure that the ArcINFO license is installed and that the Spatial Analyst Extension is activated

Details for installing the ArcINFO license can be found at: http://support.esri.com/index.cfm?fa=knowledgebase.techarticles.articleShow&d=24741, it requires changes to the registry, so be sure that you understand the implications of this and make a backup of the current registry if necessary.

This methodology will

1. Calculate the LULC attributes of a watershed based on the 1978 MIRIS database and the 2001 IFMAP
2. Calculate the LULC attributes within a 100m buffer of the lake based on the 1978 MIRIS database and the 2001 IFMAP
3. Calculate the Flow weighted LULC attributes of a watershed based on the 1978 MIRIS database and the 2001 IFMAP
4. Calculate the Flow weighted LULC attributes within a 100m buffer of the lake based on the 1978 MIRIS database and the 2001 IFMAP

Land Use/Land Cover delineated are:

Urban
Agriculture
Forest
Barren
Rangeland/Upland
Water
Wetlands

1978 MIRIS Land Use/ Land Cover

Open up the 1978_Landuse model in the Inland Lakes Toolbox

A dialog box similar to the one below will appear.

The following datasets will be needed:

1. County Land Use
    a. These files are available from the MiDL website for each county. If the watershed spans multiple counties the individual county landuse files will need to be merged.
        i. The merge tool can be found in ArcToolbox→Data Management→General→Merge

2. No Lake Polygon

    a. This is the watershed no lake polygon that was created using the WS_NL_Polygon model, e.g., lakeshed_nl

3. Lake Shapefile
    a. This is the lake shapefile created using the Proj_Fill_Fdir_Facc model, e.g., lakes_rivers_select.

4. Field
    a. Select Level 1. This is the top level Anderson LULC codes for the MIRIS database

5. Flow Length Raster
    a. This is the flow length raster calculated using the WS_NL_Polygon model, e.g., lakeshed_fl

6. Extent
    a. Browse to the lake_elev file in the NED geodatabase.

7. Environments
    a. Click on the Environments button and open up the General Settings drop-down box.
        i. Change the current workspace to the lu1978 geodatabase.

2001 Land Use / Land Cover

Open the 2001_Landuse model in the Inland Lakes Toolbox

A dialog box will appear similar to the one above.

Four datasets will be required

1. Flow length Raster
    a. The flow length raster calculated using the WS_NL_Polygon model, e.g., lakeshed_fl

2. WS_NL_Polygon
    a. The watershed no lake polygon calculated using the WS_NL_Polygon model, e.g., lakeshed_nl

3. Lake Shapefile
    a. The lake shapefile calculated using the Proj_Fill_Fdir_Facc model, e.g., lakes_rivers_select. It will be located in the Scratch folder.

4. Lakename

    a. The name of the lake, an abbreviation of the lake works best, e.g., cad for Cadillac.

5. Environments
    a. Change the current workspace to the lu2001 geodatabase.

Creating buffers around lake:

1. Open lake only file – polygon or shape in the lake layer
2. In ArcToolbox open Analysis Tools→Proximity→Buffer
3. Input Features: Select lake only file from drop down menu or browse
4. Output Features: New file name
5. Select Distance: Be sure that a coordinate system is specified
6. Dissolve Type: Select All (This will force the new file to only contain one polygon)
7. Run the Tool

This creates a buffer extending to the specified distance around the lake but also includes the lake itself. The lake now needs to be removed, accomplished by creating the union of the lake and buffer file just created.

8. In ArcToolbox→Analysis Tools→Overlay→Union
9. Input Features: Select the lake only file and the buffer file created above
10. Output Features: The new file name
11. Run the Tool

Creating the Watershed No Lake Shapefile Using the Inland Lakes Toolbox in ArcGIS 9.2

The watershed no lake file is required to calculate the land use/land cover within the watershed, it erases the lake from the watershed.

Make sure that the ArcINFO license is installed and that the Spatial Analyst Extension is activated

Details for installing the ArcINFO license can be found at: http://support.esri.com/index.cfm?fa=knowledgebase.techarticles.articleShow&d=24741, it requires changes to the registry, so be sure that you understand the implications of this and make a backup of the current registry if necessary.

This methodology will:

1. Create a watershed with the lake removed
2. Calculate the flow length clipped to the watershed

Open the Watershed_No_Lake_Polygon model in the Inland Lakes Toolbox

A dialog box will appear similar to the one shown above.

The following datasets will be needed

1. Watershed raster
    a. The watershed calculated by the Proj_Fill_Facc_FDir model, e.g., lake_shed
2. FDIR Raster
    a. The flow direction raster calculated by the Proj_Fill_Facc_FDir model, e.g., FlowDir_Fill1
3. Lake Shapefile
    a. The lake shapefile, found in the scratch geodatabase, that was created using the Proj_Fill_Facc_FDir model, e.g., lakes_rivers_select
4. Directory
    a. Browse to the NED geodatabase, this is where all of the output will be stored.
        i. Two files are created:
            1. Lakeshed_nl – the watershed with the lake removed
            2. Lakeshed_fl – the calculated flow length clipped to the watershed
5. Extent
    a. Browse the the lake_elev file, this is the original file that was projected, e.g., lake_elev.

Creating the watershed_nl file in ArcMap 9.2

For many of the analyses it is desirable to have a coverage or shape file of the watershed without the lake present (e.g., soils in the watershed, land cover, or slope). The watershed_nl file will also be used to clip grids for flow weighted land cover and average slope calculations.

This method will do the following:
Create a lake_shapefile from the county TIGER lakes dataset
Convert the lake_shapefile to a raster dataset to use for clipping grids

Open up the county TIGER shapefile dataset, these can be downloaded from the MiGDL website (http://www.mcgi.state.mi.us/mgdl/) making sure that the projection has been defined for the lakes file, this may be necessary using **Data Management Tools Toolbox→Define Projection**
Open the watershed file
Open the attribute table of the TIGER lakes file and record the FID for the lake of interest
From the ArcToolbox navigate to Analysis Tools→Extract→Select
Input Features: TIGER lakes file
Output Features: create a name and location for the new lake file (e.g., white_lake)
Expression: click on the SQL box to the right
Double click on "FID"
Click the "=" button
Type in the expression for the FID for the lake, recorded above
From the ArcToolbox navigate to Conversion Tools→From Raster→Raster to Polygon
Input Raster: watershed raster (e.g., white_shed)
Field: ID
Output polygon features: Create a name and location for the new file (e.g., white_shedp)
From the ArcToolbox navigate to Analysis Tools→Overlay→Union
Input Features: watershed polygon file (e.g., white_shedp from above) and the lake file (e.g., white_lake from above)
Output Feature Class: Create a name and location for the new union file (e.g., whiteshed_nl)
Keep the defaults for the remaining selections
Right click on the watershed_nl file (e.g., whiteshed_nl from above) and open the attribute table
In the Editor Toolbar select Start Editing
Select the rows in the watershed_nl file and press delete
In the Editor Toolbar select Stop Editing and save changes
From the ArcToolbox navigate to Conversion Tools→To Raster→Feature to Raster
Input Features: select the watershed_nl file (e.g., whiteshed_nl from above)
Field: ID
Output Raster: create a name and location for the output (e.g., whiteshed_nl)
Output cell size: navigate to the flowaccumulation file for the lake of interest (e.g., white_facc)

Delineating Watershed (Long Method) in ArcMap 9.2

This method uses NED elevation data available from the US Geological Survey. It compliments the ArcINFO method but benefits in its GUI interface which is more easily used by traditionally non-GIS users.

This method will

1. Project the NED elevation data set from the WGS_1983 standard to Michigan GeoRef 1983 (meters)
2. Fill any sinks in the data set
3. Calculate flow direction
4. Calculate flow accumulation
5. Create "pour-points" for watershed delineation
6. Delineate a watershed

Methodology

1. Obtain 1 arc second NED elevation data from USGS website http://seamless.usgs.gov
2. Open ArcMap and add the NED elevation data
3. Open the ArcToolbox if not already open
4. Navigate to the **Data Management Toolbox → Projections and Transformation → Raster → Project Raster**
    a. Input Raster: Select the NED elevation data set
    b. Output Raster: Create a name (e.g., white_elev) and location for your new projected elevation data set
    c. Output coordinate system: click on the box to the right
        i. In the new *Spatial Reference Properties* dialog box click **Select**
            1. **Choose the 1983 Michigan GeoRef (meters) projection from: Projected Coordinate Systems→State Systems**
    d. Geographic Transformation: NAD 1983 to WGS 1984_5 (if necessary)
    e. Resampling Technique: Cubic
    f. Output cell size: 30.86 for 1 arc second DEM data
5. Navigate to **Spatial Analyst Toolbox→Hydrology→Fill**
    a. Provide the input raster (e.g., white_elev from above)
    b. Create a name and location for your new filled elevation data set (e.g., white_elevf)
    c. Provide a Z-limit if appropriate (usually no Z-limit is required)
6. Navigate to **Spatial Analyst Toolbox→Hydrology→Flow Direction**
    a. Select the filled elevation dataset (e.g., white_elevf from above)
    b. Create a name and location for the flow direction raster data set (e.g., white_fdir)
7. Navigate to **Spatial Analyst Toolbox→Hydrology→Flow Accumulation**
    a. Select the flow direction raster data set (e.g., white_facc from above)
    b. Create a name and location for the flow accumulation raster data set (e.g., white_facc)
8. Double-click on the newly created flow accumulation raster data set
    a. Click on the Symbology tab

b. In the Show: frame at left click on classified
c. Click on the classify button at the right
d. Change the classification to the standard deviation and change the Interval Size to ¼ Std Dev
e. Apply the changes (you may need to invert the colors or choose an appropriate color ramp to see the output)
f. You should now see several lines of flow accumulation in the data frame, zoom into the lake of interest and find the output (i.e., where flow accumulation is the highest, can be found using the identity tool)

9. Open ArcCatalog and navigate to the folder where the raster files are saved.
    a. Right click in the right most open pane
    b. Click on New
        i. Click on Shapefile
            1. In the *Create New Shapefile* dialog box
                a. Create a name for the shapefile (e.g., whiteout)
                b. Make sure Feature Type: is point
                c. Click **EDIT** and select the Michigan GeoRef 1983 (meters) projection
10. Change the Spatial Analyst and Environment Settings to reflect the extent and cell size of the flow accumulation raster data set
    a. Click on the Spatial Analyst Toolbar→Options
        i. click on the Extent Tab
            1. Change the Analysis Extent: to the flow accumulation raster (e.g., white_facc)
        ii. Click on the Cell Size tab
            1. Change the Analysis cell size: to the flow accumulation raster (e.g., white_facc)
    b. In the Tools menu navigate to Options and click on the Geoprocessing tab, open Environments…
        i. In the General Settings drop down specify the Extent: to the flow accumulation raster (e.g., white_facc)
        ii. In the Raster Analysis Settings drop down box specify the Cell Size: to the flow accumulation raster (e.g., white_facc)
    c. Record the cell size, you will need this number in Step 11 below.
11. In ArcMap add the newly created shapefile (e.g., whiteout from above)
    a. In the Tools Menu click on the Editor Menu if not already open
    b. In the Editor Tools click start editing
        i. In the dialog box select the file that contains the newly created shapefile (e.g., whiteout from above)
    c. Using the sketch tool place the newly created shapefile in the flow accumulation line where it exits the lake
    d. In the Editor Tools click stop editing and save the changes
    e. Navigate to the Conversion Tools Toolbox→To Raster→Feature to Raster
    f. Select the newly created and positioned shapefile
    g. Create a new name for the raster (e.g., white_out)

h. Make sure the output cell size is the same size as the flow accumulation raster data set, recorded in step 10 above

12. Navigate to the Spatial Analyst Tools Toolbox→Hydrology→Watershed
    a. Select the flow direction raster (e.g., white_fdir)
    b. Select the raster pour point (e.g., white_out)
    c. Pour point field should be Value
    d. Create a name for the output (e.g., white_shed)

Delineating Watersheds using the Inland Lake Toolbox in ArcGIS 9.2

Make sure that the ArcINFO license is installed and that the Spatial Analyst Extension is activated

Details for installing the ArcINFO license can be found at: http://support.esri.com/index.cfm?fa=knowledgebase.techarticles.articleShow&d=24741, it requires changes to the registry, so be sure that you understand the implications of this and make a backup of the current registry if necessary.

This methodology will:

7. Project the NED elevation data set from the WGS_1983 standard to Michigan GeoRef 1983 (meters)
8. Fill any sinks in the data set
9. Calculate flow direction
10. Calculate flow accumulation
11. Convert the lake shapefile to a raster dataset
12. Calculate the watershed using the lake as the pour point

In ArcCatalog create a new lake folder in the lakes_ned file folder found in the C:\Workspace directory

In the new lake folder create four new file geodatabases

1. ned - for all of the elevation, filled elevation, flow direction, flow accumulation, lake rasters, and watershed files
2. scratch – necessary for future landuse toolboxes
3. lu2001 – will contain all of the output from the 2001 landuse toolbox
4. lu1978 – will contain all of the output from the 1978 landuse toolbox

Methodology

Obtaining and projecting the NED data from USGS

13. Obtain 1 arc second NED elevation data from USGS website http://seamless.usgs.gov
14. Open ArcMap and add the NED elevation data
15. Open the ArcToolbox if not already open
16. Navigate to the **Data Management Toolbox → Projections and Transformation → Raster → Project Raster**
    a. Input Raster: Select the NED elevation data set
    b. Output Raster: Create a name (e.g., white_elev) and location for your new projected elevation data set (i.e., the ned geodatabase in the lake folder created above)
    c. Output coordinate system: click on the box to the right
        i. In the new *Spatial Reference Properties* dialog box click **Select**
            1. **Choose the 1983 Michigan GeoRef (meters) projection from: Projected Coordinate Systems→State Systems**
    d. Geographic Transformation: NAD 1983 to WGS 1984_5 (if necessary)

e. Resampling Technique: Cubic
f. Output cell size: 30 for 1 arc second DEM data

Using the Proj_Fill_Fdir_Facc toolbox

1. Double-click on the Proj_Fill_Fdir_Facc model in the Inland_Lakes toolbox and a dialog box will appear.

    a. Input the necessary features
        i. Projected NED Raster is the raster downloaded and projected above
        ii. Input Features is the county lakes_rivers TIGER95 shapefile, this may be a problem since it appears that MiGDL has discontinued the use of the TIGER95 files
        iii. Expression – this input relates to the lakes_rivers input that you selected in the Input Features input line
        iv. Click on the SQL button to the right
        v. In the new dialog box
            a. Scroll to "Name" in the menu to the left and double click on it
            b. Press the equals sign
            c. Scroll to the Lake Name in the menu to the left and double click on it
            d. Press OK
    b. In the Field input, scroll down to AREA
    c. In the Extent input, browse to the projected lake_elev file you created in the steps above
    d. In the Directory input, browse to the NED geodatabase that was created in the steps above
    e. This steps insures that all data created are put into the NED folder
        1. The lake_shapefile that is created is put into the scratch folder
        2. All other datasets are put into the NED folder
    f. Click OK

    Depending upon the size of the elevation dataset, the tool may take up to ½ hour before completing.

Determining Land Use in Watershed (ArcMap 9.2)

Land use for Michigan comes from two sources the IFMAP (Landsat 2001) and the MRBIS 1978 land use data. The ifmap data should be available on the local machine in C:\Workspace\ifmap. There are two IFMAP rasters, lp and up, for the Lower Peninsula and Upper Peninsula, respectively. The 1978 land use must be obtained from MiGDL by county at the following website http://www.mcgi.state.mi.us/mgdl/ . This method assumes that you have already created the watershed_nl file.

This method will:

1. Clip the land use data file to the watershed
2. Reclassify data to the highest level, needed to compare land use among datasets.
3. Create tables for export into Excel for data analysis

2001 land use IFMAP

1. In the ArcToolbox navigate to **Spatial Analyst Tools→Extraction→Extract by Mask**
    a. Input Raster: IFMAP raster
    b. Input Raster or feature mask data: watershed_nl raster
    c. Output Raster: Create a name and location for the file (e.g., white_2001)
2. In the ArcToolbox navigate to **Spatial Analyst Tools→Reclass→Reclassify**
    a. Input Raster the watershed landuse file (e.g., white_2001 from above)
    b. Reclass field: Value
    c. Reclassification: follow the reclassification scheme in the table below. The reclassification can be saved and used for other lakes

Table C2. Landuse reclassification scheme

Land Use Type	Old Classification	New Classification
Urban	1-4	100
Agriculture	5,6,7,9	200
Upland Openland	10,12,13	300
Forest	14-22,24-26	400
Water	23	500
Wetland	27-30	600
Barren	31,32,35	700

    d. Output raster: create a name and location for the new file (e.g., white_2001rc)
3. Right click in the newly created reclassified watershed land use file and open the attribute table
    a. The VALUE corresponds to the reclassified land use in the table above
    b. The COUNT column is the number of cells in the watershed with a specific land use
        i. The product of COUNT and area of the cell is the total land use in the watershed
    c. Click Options: in the lower right hand corner of the attribute table and select Export…

i. Export: All records
ii. Output Table: create a name and location for the file (e.g., white_2001) the file can be saved as ".dbf" or ".txt"

4. Right click in the newly created reclassified watershed land use file and open Properties…
    a. Click on the Source tab
    b. Note the cell size, this value squared will be the area of one raster cell
5. Open the exported table in Excel
    a. Multiply the COUNT column by the area of the raster cell
    b. Sum all of the areas
    c. Compare the calculated land use to the area of watershed_nl file by calculating the product of COUNT and the cell area for the watershed_nl file. COUNT can be found in the attribute table of the watershed_nl file.
    d. Area of the total land use in the watershed and the watershed should be comparable
    e. Save the file as an Excel worksheet

1978 MIRIS Land use

1. Download the 1978 MIRIS land use data from MiGDL
    a. If multiple the watershed spans several counties it will require the individual county files to be merged
2. From the ArcToolbox navigate to Data Management Tools→General→Merge
    a. Input Datasets: select all of the county 1978 land use files
    b. Output Dataset: create a name and location for the output (e.g., 1978 lulc)
3. From the ArcToolbox navigate to the Analysis Tools→Overlay→Intersect
    a. Input Features: select the watershed_nl (e.g., whiteshed_nl) and merged land use files (e.g., 1978 lulc from above)
    b. Output Feature Class: create a name and location for the output (e.g., white_1978)
    c. keep all of remaining selection at default values
4. From the ArcToolbox navigate to the Conversion Tools→To Raster→Feature to Raster
    a. Input features: select the watershed landuse file (e.g., white_1978 from above)
    b. Field: Select Level 1
    c. Output Raster: create a name and location for the file (e.g., white_1978)
    d. Output cell size: either enter the cell size desired (usually the same as the original DEM) or navigate to the original projected DEM
5. Right click on the newly created watershed land use raster (e.g., white_1978 from step 4) and open the attribute table
    a. Export the data to a text file following step 3 from the IFMAP watershed land use methodology above
6. Open the exported table in Excel
    a. Multiply the COUNT column by the area of the raster cell
    b. Sum all of the areas
    c. Compare the calculated land use to the area of watershed_nl file by calculating the product of COUNT and the cell area for the watershed_nl file. COUNT can be found in the attribute table of the watershed_nl file.

d. Area of the total land use in the watershed and the watershed should be comparable
e. Land use codes for 1978 land use

Table C3. Land use classifcations for the 1978 MIRIS dataset

Land Use	Level 1 Code
Urban	1
Agriculture	2
Rangeland	3
Forest	4
Water	5
Wetlands	6
Barren	7

f. Save the file as an Excel worksheet

APPENDIX D

ERROR ANALYSIS

APPENDIX D. Error Analysis

Absolute error in analytical methods can be derived from both random and systematic sources. Sources of random errors are operationally unknown. They appear as spread in the data during the analysis of a known analyte concentration and can often be described using Gaussian statistics. Sources of systematic error are known and include: instrumental, personal and method. Instrumental error occurs due to the wear, corrosion, or drift in electrical circuits over time; it is usually overcome by the calibration of instruments prior to analysis. Personal error can include such things as number bias and prejudice. Method errors occur due to non-ideal chemical and physical behavior of reactants during analysis. Analysis of NIST standards, of similar matrix to the samples of interest, can aid in determining method error. This report shall outline the error in sediment mercury analysis from six sampling seasons (1999-2004) and sediment major and trace element analysis from two sampling seasons (2003-2004).

Systematic errors will be assumed to instrumental in this analysis. Personal errors are limited due to computer interfaces but still exist due to pipeting or weighing errors. Pipeting and weighing errors generally considered gross errors and can be eliminated utilizing outlier analysis. Outliers will be defined, by box plots, as . Method errors are generally minimized by calibration curves which are run during each set of analyses.

Descriptive Statistics

The definitions and equations described below shall be utilized in the examination of error in both mercury and major and trace element analysis. Equations presented below can be found in

any instrumental analysis chemistry textbook such as Skoog and Leary (1992). Absolute error, E_a, is defined as the deviation of the sample mean, $\bar{x}$ from the known analyte value, x_t,

$$E_a = \bar{x} - x_t \tag{1}$$

where the right hand side of the equation includes both random and systematic components. Random error, E_r, for a small set of data can be estimated using

$$E_r = \bar{x} - \mu \tag{2}$$

where μ is the population mean. In general the population mean is determined, and assumed to be free of random error, by replicating the measurement 20 to 30 times and is calculated by

$$\mu = \lim_{N \to \infty} \frac{\sum_{i=1}^{N} x_i}{N} \tag{3}$$

where x_i is the value for the i^{th} measurement and N is the number of measurements. The standard deviation, σ, of the population is calculated

$$\sigma = \sqrt{\lim_{N \to \infty} \frac{\sum_{i=1}^{N} (x_i - \mu)^2}{N}} \tag{4}$$

The standard deviation of a set of samples differs from the population standard deviation by replacing σ with s, μ with $\bar{x}$, and N by N-1.

$$s = \sqrt{\frac{\sum_{i=1}^{N} (x_i - \bar{x})^2}{N-1}} \tag{5}$$

The arithmetic mean, $\bar{x}$, will be used for sample means. The value of the population and sample mean may differ. The sample mean usually represents a subset of the population or a smaller set

of measurements intended for comparison to the population. Standard errors shall also be calculated to demonstrate the fluctuation in the standard deviation based upon the number of samples

$$s_m = \frac{s}{\sqrt{N}}. \tag{6}$$

The coefficient of variation, *CV*,

$$CV = \frac{s}{\bar{x}} \times 100\% \tag{7}$$

provides information on the magnitude of the standard deviation as a percentage of the mean and is generally more useful than the standard deviation alone.

95% confidence limits are quantified using a t-statistic as

$$95\%\ CL = \bar{x} \pm \frac{ts}{\sqrt{N}} \tag{8}$$

where t is obtained using a widely available statistical t-distribution table. Confidence limits can also be calculated using the z-distribution table where *z* replaces *t*, σ replaces *s* and μ replaces $\bar{x}$.

Systematic Error (Bias)

Bias in analytical methods is developed due to systematic errors and can be demonstrated using the t-statistic. The experimental difference between the sample mean and population mean is calculated as

$$\bar{x} - \mu \tag{9}$$

and compared to the calculated difference at a predetermined confidence level as

$$\pm \frac{ts}{\sqrt{N}}. \tag{10}$$

Bias is demonstrated if the experimental bias is greater than the calculated bias at a given confidence interval. A similar method can determine bias in a population where

$$x_t - \mu \tag{11}$$

and

$$\pm \frac{zs}{\sqrt{N}} \tag{12}$$

replace Equations 9 and 10 respectively.

Limit of Detection

The detection limit (LOD) of an analytical method, determined here as the minimum distinguishable signal, S_m, is a function of average signal of the blank, $\bar{S}_{bl}$, and a multiple, k, of the blank signal, s_{bl}

$$S_m = \bar{S}_{bl} + ks_{bl}. \tag{13}$$

Where blank data are available totaling a minimum of 20 to 30 measurements Equation 13 will result in the detection limit, $c_{m,}$ as

$$c_m = \frac{S_m - \bar{S}_{bl}}{m}. \tag{14}$$

where m is the slope of the calibration line at the concentration of interest. In the absence of reliable blank measurements the detection limit will be determined by linear regressions of calibration standard concentrations versus instrument response. In these cases the slope, intercept, and standard error of the estimate will be used to estimate the LOD.

Mercury

Mercury analysis was carried out on a Lumex Zeeman Corrected Atomic Absorption Spectrophotometer with Thermal Decomposition attachment (TD-AA). Calibration of the instrument was performed using either SRM 1633b (coal fly ash, Hg = 143.1 ng/g) or SRM 1515 (apple leaves, Hg = 44 ng/g) and the protocol outlined in Environmental Protection Agency (EPA) method 7473 was followed. EPA Method 7473 dictates that a SRM be run every 10 samples; descriptive statistics will be derived based upon these measurements.

Descriptive Statistics and Bias

Table D1 and Table D2 show the population means and standard deviation of SRM 1515 and SRM 1633b respectively. Based on the number of measurements for each SRM it is assumed that the standard deviation and means of these measurements represent the population. Bias for the population was determined using the z-distribution and was calculated using Equations 11 and 12; at 95% CL z is equal to 1.96.

Table D1 SRM 1515 Population Statistics

Population mean (ng/g)	43.9
Population standard deviation (ng/g)	2.13
CV (%)	4.85
s_m	0.23
N	87
NIST accepted value (ng/g)	44
Bias	No bias demonstrated at 95% CL

Table D2 SRM 1633b Population Statistics

Population mean (ng/g)	146.8
Population standard deviation (ng/g)	6.644
CV (%)	4.52
s_m	0.83
N	64
NIST accepted value (ng/g)	143.1
Bias	Presence of bias suggested at 95% CL

The presence of positive bias in SRM 1633b suggests that systematic errors influence the measurement.

Table D3 shows the descriptive statistics for each lake. Sample means and standard deviations are provided for each lake and are subsets of the population determined as subsets of the population. The SRM used during analysis of the lake sediment mercury is noted in column 2. Bias was calculated using Equations 9 and 10; the population mean was used to evaluate Equation 9. It is evident from this analysis that only three lakes exhibited bias at the 95% CL, Houghton, Littlefield, and Torch.

Table D3 Descriptive Sample Statistics and Bias

Lake	SRM	N	df	Average (ng/g)	Std. dev (ng/g)	CV (%)	s_m	Bias
Houghton	1633b	4	3	141.0	3.16	2.24	1.58	Bias
Round	1633b	6	5	142.0	5.90	4.15	2.41	-
Avalon	1633b	7	6	144.0	3.92	2.72	1.48	-
Birch	1633b	7	6	144.9	3.85	2.66	1.45	-
Muskegon	1633b	8	7	151.6	9.74	6.42	3.44	-
Sand	1633b	5	4	149.4	2.30	1.54	1.03	-
Crystal-M04	1633b	5	4	144.2	4.60	3.19	2.06	-
George	1633b	5	4	144.7	4.32	2.99	1.93	-
Hackert	1633b	6	5	148.0	5.33	3.60	2.18	-
Otter	1633b	4	3	154.0	10.8	7.01	5.40	-
Round_D	1633b	6	5	150.3	5.57	3.71	2.28	-
Gull	1515	3	2	47.0	1.66	3.54	0.96	-
Higgins	1515	11	10	43.5	1.86	4.29	0.56	-
Cass	1515	4	3	43.3	1.50	3.47	0.75	-
Crystal-M	1515	5	4	44.0	1.87	4.25	0.84	-
Littlefield	1515	9	8	46.6	2.55	5.49	0.85	Bias
Cadillac	1515	5	4	43.2	2.05	4.74	0.92	-
Crystal-B	1515	5	4	43.6	1.67	3.84	0.75	-
Hubbard	1515	5	4	43.8	1.30	2.98	0.58	-
Mullett	1515	6	5	44.3	1.75	3.95	0.71	-
Whitmore	1515	6	5	43.5	2.17	4.98	0.89	-
Houghton	1515	2	1	44.0	1.41	3.21	1.00	-
Imp	1515	7	6	42.4	1.62	3.81	0.61	-
Paw Paw	1515	7	6	43.0	2.08	4.84	0.79	-
Torch	1515	6	5	42.3	0.82	1.93	0.33	Bias
Witch	1515	6	5	44.3	2.07	4.66	0.84	-

Detection Limits

Detection limits, outlined in Table D4 and Table D5, were calculated using Equations 13 and 14 using the average blank signal obtained during sample runs. Slope was determined from plots of mass Hg vs. Area. In Equation 13, k was assigned a value of three (REF). Differences in the detection limit differed only slightly between the two SRMs. Detection limit concentrations are calculated using the population average (e.g. if 250 mg of sediment are used the LOD is 0.687 ng/g).

Table D4 SRM 1515 LOD

	Mass Hg (pg)	Hg (fmoles)	
Mean	141.8	706.9	
Standard Deviation	20.3	101.2	
	250 mg	125 mg	10 mg
Detection Limit (ng/g)	0.687	1.37	17.2

Table D5 SRM 1633b LOD

	Mass Hg (pg)	Hg (fmoles)	
Mean	133.5	665.5	
Standard Deviation	6.06	30.2	
	250 mg	125 mg	10 mg
Detection Limit (ng/g)	0.577	1.15	14.4

Discussion

Results of the mercury analysis indicate that, run to run, very little systematic error has been demonstrated and that detection limits are low. Population mean of SRM 1515 agreed well with the accepted value and did not demonstrate bias. Conversely SRM 1633b did demonstrate bias at a 95% CL. This may be an effect of improperly cleaned glassware. It is evident that during the analysis of high organic carbon sediments that lenses encasing the reaction cell can become contaminated. This reduces the amount of light penetrating the reaction cell which reduces signal and increases the amount of Zeeman correction (Lumex, personal communication). Otter, Sand, Muskegon, and Round_D lakes all visually appeared to contain high amounts of organic carbon and these lakes have higher average values. It may be necessary to implement a protocol for periodic lens cleaning during analysis of high organic carbon sediments. Individual runs indicate that only three lakes demonstrate bias and that none of the lakes demonstrating bias would be considered to have high organic carbon values. The test for bias by lake suffers from using t-statistics versus the z-statistic for the population. Detection limits are lower than those estimated by the manufacturer for this method (WWW.OHIOLUMEX.COM).

REFERENCES

REFERENCES

Skoog D. A. and Leary J. J. (1992) *Principles of Instrumental Analysis, Fourth Edition*. Saunders College Publishing.

SPSS. (2000) SYSTAT 10.

www.ohiolumex.com.

Yohn S. S. (2004) Natural and Anthropogenic Factors Influencing Spatial and Temporal Patterns of Metal Accumulation in Inland Lakes, Michigan State University.